Steroid receptor-dependent regulation of prostate-like secondary cells in *Drosophila*



Aashika Sekar
St. Hugh's College
University of Oxford

Thesis submitted for the degree of
Doctor of Philosophy in Physiology, Anatomy and Genetics

Supervised by:
Prof. Clive Wilson and Dr. Aaron Leiblich

Acknowledgments

The three years of my DPhil have been such an enriching experience, and I would like to thank my supervisor, Clive Wilson, for giving me this opportunity to work on a project which had the perfect blend of exploratory and application-oriented research. You have been so supportive and encouraging throughout my DPhil and I have constantly reminded myself of how lucky I am to have been pursuing my DPhil under your supervision. I appreciate you always having the time and patience to not only discuss ideas and quirky experiment results but also to guide me to become an independent scientist. I definitely value all the knowledge that I have gained and skills that I have gathered under your tutelage, but most importantly, I value our conversations, those "aha" moments of understanding, and opportunities to glean your scientific wisdom about work and life. You have been a guide, an inspiration for my professional ambitions and also, you have nurtured within me an intuition for scientific thought. By leading by example and showing me *how* to absorb science and cultivate disciplined thinking, I am finishing my DPhil grateful to you and ready to embrace new opportunities in science.

Aaron Leiblich, thank you for being my co-supervisor and bringing in the much-needed translational angle to my project. I enjoyed working with you on our PLoS Biology paper - thank you for the opportunity. You have been very kind and supportive throughout my DPhil, and every conversation with you has always uplifted my spirits and left me with hope that my DPhil and my ambitions were headed in the right direction. Cláudia Mendes, I am so thankful for your mentorship and friendship. I have learnt a great deal about *Drosophila* research and techniques from you. I admire your enthusiasm to discuss science with an open mind and your willingness to learn from everyone. Mark Wainwright, thank you for helping me with several of the day-to-day aspects of *Drosophila* research, most-importantly checking the eye colours while I was making the recombinants. I quite enjoyed working with you on some of the analytical aspects of the microcarrier project as well. Cláudia and Mark, thank you for often helping me solve the many roadblocks I encountered during my DPhil and I am indeed going to miss our long end-of-the-day chats. Pauline Marie, thank you for teaching me some of the techniques that I have widely used in my project and for being the force behind some much-needed fun social activities. Carina Gandy, thank you for getting me initiated into the lab, getting me acquainted with many important aspects of fly maintenance and most importantly for your friendship. I would like to thank Prof. Stephen Goodwin, Dr. Richard Bryant and Prof. Adrian Harris, for their insightful comments and suggestions during my transfer of status and confirmation milestones. I would like to thank the micron staff, Andrew Jefferson, Carina Monico and Nadia Halidi for helping me with the LSM880 and Deltavision microscopes. I would also like to thank Sarah Noujaim for helping me get through the administrative side of my DPhil and also for the lovely long conversations.

I would like to thank my parents and grandparents for always believing in me and being the pillar of strength throughout my life. This DPhil would not have been possible without my parents' constant support. I am indebted to you for all the sacrifices you have always made for me and, I am who I am because of the both of you. I know that a thank you does not begin to explain my boundless gratitude for you, but nevertheless thank you so much for everything- for IIT, for Oxford and for just being there for me regardless.

Another person I would like to thank from the bottom of my heart is Radhika aunty, for introducing me to the amazing world of science when I was six, which has infact led me to build a career in science.

I have also met some lovely people at Oxford, who have indeed become my close friends- Andrew Dhawan and Shreya Ramachandran, thank you for the lovely unwinding chai sessions.

Last but not the least, an enormous thank you to Shishir Rao. You have been a constant support throughout these past years – be it personal or professional downfalls, you have always had my back. You have been my home away from home and there is no way I would have gotten through my DPhil without you. You are such an inspiring person, who I learn from every single day. I am thankful for all the amazing conversations we have had, many of which have definitely sparked many ideas throughout my DPhil.

Abstract: Steroid receptor-dependent regulation of prostate-like secondary cells in *Drosophila*

The paired lobes of the male *Drosophila* accessory gland (AG) contain two epithelial cell types, main cells (MCs) and secondary cells (SCs). SCs are a useful *in vivo* genetic model system to study fundamental mechanisms regulating cell growth and secretion, and they share several properties with the human prostatic gland. The SCs in adult virgin males grow with age in a BMP-dependent manner, and this growth can be further enhanced upon mating. During my DPhil, I have developed the SC as a model to study steroid receptor-dependent growth regulation. The fly nuclear steroid receptor, the ecdysone receptor (EcR), and the human androgen receptor (AR) share similar structural and functional domains. I show that a complex interplay between the BMP and EcR signalling pathways is involved in the regulation of SC growth in both virgin and mated males, an interaction which may allow mated males to rapidly replenish the expelled contents of their AG. The growth that occurs after mating is partly accounted for by genome endoreplication which is BMP/EcR-dependent, as is the secretory activity of SCs. I show that SCs can synthesise the hormone ecdysone, much like the prostate gland which produces the most active form of androgen. Interestingly, SC growth that occurs in virgin males requires ecdysone, but in mated males, endoreplication-dependent growth occurs independently of this hormone. The switch from hormone-dependent steroid receptor signalling to hormone-independent signalling mirrors the transition from androgen-dependent prostate cancer to the more aggressive and incurable form of prostate cancer, androgen-independent 'castration-resistant prostate cancer' (CRPC). I demonstrate that the cell cycle regulators, Cyclin D (CycD), Cyclin E (CycE), Retinoblastoma (Rbf) and E2F1, which are all implicated in prostate cancer, are key regulators of SC growth and endoreplication both in virgin and mated males. Furthermore, CycD/Rbf/E2F1/CycE interacts with the BMP/EcR signalling axis to regulate the transition from hormone-dependent to hormone-independent steroid receptor signalling in SCs, mirroring some of the mechanisms associated with the transition to CRPC. Overall, my work suggests that there are parallels between the physiological roles of the EcR's switch to hormone-independence in SCs and the pathological changes seen in CRPC, and indicates that further genetic analyses in SCs may unravel the complex signalling mechanisms that mediate the transition to this lethal form of cancer.

List of abbreviations

Abbreviations	Description
20-HE	20-hydroxyecdysone
Acps	Accessory gland proteins
ADT	Androgen deprivation therapy
AF1	Activation function 1 domain of nuclear receptor
AF2	Activation function 2 domain of nuclear receptor
AG	Accessory gland
ANCE	Angiotensin-converting enzyme
AR	Androgen receptor
AR-Vs	Androgen recptor splice variants
BMP	Bone morphogenetic protein
Cdk 2/4/6	Cyclin-dependent kinase 2/4/6
CRPC	Castration-resistant prostate cancer
Cyc A/B/D/E	Cyclin A/B/D/E
DCG	Dense-core granule
DHEA	Dehydroepiandrosterone
DHT	Dihydrotestosterone
DIC	Differential inference contrast
E	Ecdysone
Ecdysone	Generically refers to E and 20-HE
EcR	Ecdysone receptor
EcRE	Ecdysone-response element
EdU	5-ethynyl-2'-deoxyuridine
ILE	Immature late endosomes
ILVs	Intraluminal vesicles
LBD	Ligand-binding domain
MC	Main cell
PMR	Post-mating responses (generally refers to females)
Pre-RC	Pre-replication complex
Rb	Retinoblastoma
Rbf	Drosophila Rb homologue
SC	Secondary cell
SP	Sex peptide
SRD5A	5-α reductase enzyme
Tkv	Thickveins
USP	Ultraspiracle
Wit	Wishful thinking

Acknowledgements i
Abstract ii
List of abbreviations iii
Table of contents iv
List of figures viii

Table of contents

Chapter-1: Introduction

1.1. Human prostate 1
1.2. Androgen signalling in normal prostate and prostate cancer 2
1.3. Castration-resistant prostate cancer (CRPC) 8
1.4. Role of Bone Morphogenetic Protein (BMP) signalling in prostate cancer 9
1.5. Role of Retinoblastoma signalling in prostate cancer 11
1.6. Mouse models for prostate cancer and CRPC 12
1.7. Contribution of Drosophila to the field of cancer biology 14
1.8. Drosophila accessory gland and its functions 15
1.9. Parallels between human prostate and Drosophila AG 17
1.10. Intracellular structure and cell biology of SCs 18
1.10.1. Types of SC compartments 18
1.10.2. Dense-core granule-containing compartments 19
1.10.3. Exosome secretion by SCs 19
1.11. BMP pathway in Drosophila 22
1.12. BMP signalling plays multiple roles in SCs 24
1.12.1. BMP signalling is essential for SC growth in virgin males 24
1.12.2. BMP signalling promotes SC delamination and migration 24
1.12.3. BMP signalling regulates SC secretory activity 25
1.12.4. BMP signalling modulates female PMR 25
1.13. Ecdysone signalling pathway in Drosophila 26
1.14. Endoreplication in post-mitotic growth regulation 29
1.15. Mechanisms of endoreplication in Drosophila 32
1.16. Relevant previous work by the Wilson group 34
1.16.1. EcR/USP signalling in Drosophila SCs 35
1.16.1.1. EcR-B1 is the major EcR isoform present in SCs 35
1.16.1.2. EcR regulates SC growth in virgin males independently of USP 35
1.16.1.3. EcR protein levels are regulated by BMP signalling in the SCs 36

1.16.2. The Rbf/E2F1 axis regulates EcR protein levels in SCs 37
1.17. Aims and Objectives 38

Chapter-2: Materials and Methods

2.1. Fly Husbandry 40
2.2. Fly Stocks 41
2.3. Fly genetics 45
2.4. Scheme for genetic combination generation 46
2.4.1. Scheme for combination of transgenes on different chromosomes 46
2.4.2. Scheme for combination of transgenes on same chromosome 47
2.5. Genomic DNA isolation 47
2.6. PCR to verify transgene recombination and combination stocks 48
2.7. Quantitative RT-PCR 49
2.8. Multiple mating experiments 50
2.9. Sample preparation for fixed confocal imaging 50
2.10. SC growth assay 51
2.11. SC DAPI intensity assay 51
2.12. EdU-containing food preparation and EdU incorporation assay 52
2.13. CD63-GFP pulse labelling assay 53
2.14. Sample preparation for live wide-field imaging 53
2.15. SC compartment and ILV analysis 54
2.16. Statistical Analysis 54

Chapter-3: Hormone-dependent and hormone-independent Ecdysone Receptor signalling in SCs

3.1. Introduction 56
3.2. Aims 57
3.3. Results 58
3.3.1. EcR isoforms A and B regulate SC nuclear growth in virgin males 58
3.3.2. EcR-A is essential for secondary cell growth that occurs after mating 60
3.3.3. BMP signalling appears to regulate EcR protein levels pre- and post-transcriptionally in secondary cells 62
3.3.4. The BMP signalling pathway interacts with EcR signalling to regulate mating-dependent SC growth 64
3.3.5. Hormone-dependent EcR signalling regulates secondary cell nuclear growth in virgin males 67
3.3.6. Hormone-independent EcR signalling promotes SC growth after mating 68
3.4. Summary and Discussion 71

3.4.1. EcR isoforms differentially regulate SC growth 71
3.4.2. USP-independent EcR signalling regulates SC growth 74
3.4.3. Autocrine BMP signalling promotes mating-dependent SC growth 74
3.4.4. SCs are a site for ecdysone synthesis in adult males 75
3.4.5. Ecdysone-dependent and -independent EcR signalling controls SC growth in virgin and mated males respectively 76

Chapter-4:BMP signalling and hormone-independent EcR signalling promote new DNA synthesis in SCs after mating

4.1. Introduction 77
4.2. Aims 78
4.3. Results 78
4.3.1. Genome endoreplication partially accounts for SC growth after mating 78
4.3.2. The BMP/EcR signalling axis also regulates mating-dependent SC endoreplication 79
4.3.3. EcR-A and USP regulate mating-dependent SC endoreplication 82
4.3.4. Mating-dependent SC endoreplication is under hormone-independent EcR regulation 84
4.3.5. Genome endoreplication leads to increased secretory biogenesis in SCs 85
4.3.6. Forkhead and torso regulate EcR-mediated endoreplication 87
4.4. Summary and Discussion 91
4.4.1. Mating promotes new DNA synthesis in SCs to deal with reproductive stress 91
4.4.2. Mating induces ecdysone production in the whole fly 93
4.4.3. An EcR-A/USP heterodimer promotes mating-induced, hormone-independent endoreplication in SCs 95
4.4.4. EcR-B1 is not essential for regulating SC growth in mated males 97
4.4.5. Modelling the CRPC switch in SCs 98

Chapter-5:Regulation of compartment formation and exosome secretion by BMP/EcR signalling axis

5.1. Introduction 100
5.2. Aims 100
5.3. Results 101
5.3.1. Regulation of Btl-labelled compartment formation and exosome biogenesis by EcR signalling 101
5.3.2. Regulation of Rab11-compartment maturation by EcR signalling 103
5.3.3. Regulation of Btl-, Rab6- and Rab11-compartment formation by BMP signalling 106
5.4. Summary and Discussion 111

Chapter 6: Cell cycle regulation of mating-dependent SC growth and genome endoreplication

6.1. Introduction 116

6.2. Aims 116

6.3. Results 117

6.3.1. EcR signalling regulates SC growth and endoreplication through CycE 117

6.3.2. CycD is vital for SC growth and endoreplication 120

6.3.3. p53/Rbf/E2F1 regulate nucleation state in adult SCs 120

6.3.4. Rbf negatively regulates SC growth and endoreplication 124

6.3.5. E2F1 is necessary and sufficient to promote SC endoreplication, but is not necessary to drive SC growth 125

6.3.6. Rbf/E2F1 functions upstream of EcR in a hormone-independent manner to regulate SC growth and endoreplication 129

6.3.7. BMP signalling is downstream of CycD/Rbf but upstream of E2F1 in the regulation of SC growth and endoreplication 133

6.4. Summary and Discussion 136

6.4.1. Activated Rbf reverses the binucleate state in adult SCs independently of its effects on growth and endoreplication 138

6.4.2. G1 cyclins promote the transition from ligand-dependent to ligand-independent EcR signalling upon mating 141

6.4.3. Multiple forms of Rbf signalling are involved in the regulation of SC growth and hormone-independent endoreplication 143

Chapter-7: Summary of findings, significance and concluding remarks

7.1. Summary of findings 145

7.2. *Drosophila* SCs as an *in vivo* model for studying the role of steroid receptor signalling on secretory activity 146

7.3. Physiological roles of SC signalling and cell biology 147

7.4. *Drosophila* SCs as an *in vivo* model for the transition of prostate cancer to CRPC 149

7.5. *Drosophila* SCs as an *in vivo* model to study the maintenance of binucleation 154

7.5 Concluding Remarks 156

Chapter-8: Bibliography 157

Appendix A: AR interacting transcription factors 166

Appendix B: Mammalian cell lines to study Rb regulation of nucleation state 167

Appendix C: Probable regulation of DCG formation by EcR 168

Appendix D: Miscellaneous exploratory experiments 169

D.1. Diffused expression of Asterless (Asl) in SCs 169
D.2. Mating decreases Putative Achaete Scute Target 1 (PAST1) expression 170
D.3. *Tdc2* is specifically expressed in SCs 171
D.4. Calcium reporter signalling increases after mating 172
Appendix E: Python Statistics Programme Code 173
Appendix F: Data Curation 178
Appendix References 179

Published Paper 180

List of figures

Chapter-1: Introduction

Figure 1.1 The human prostate 3
Figure 1.2 The androgen biosynthesis pathway in prostate cancer 4
Figure 1.3 Nuclear steroid receptor structure and function 7
Figure 1.4 Role of androgen signalling in prostate cancer progression 10
Figure 1.5 Cell cycle machinery 13
Figure 1.6 *Drosophila* accessory gland and cell types 18
Figure 1.7 SC intracellular structures 21
Figure 1.8 Ecdysteroid biosynthesis pathway 28
Figure 1.9 Cell cycle vs Endocycle 33
Figure 1.10 Rbf/E2F1 regulates EcR protein levels in SCs (Courtesy of Aaron Leiblich and Dhruv Sarma) 38

Chapter-3: Hormone-dependent and hormone-independent Ecdysone Receptor signalling in SCs

Figure 3.1 Mating-dependent SC growth 57
Figure 3.2 Role of EcR-A and EcR-B1 in regulating SC growth 59
Figure 3.3 The effects of EcR-C and USP on SC growth in virgin and mated males growth 61
Figure 3.4 Pre-translational mechanisms are partly involved in regulation of EcR protein levels by BMP signalling 63

Figure 3.5 Interaction of BMP and EcR signalling in regulation of SC growth 65
Figure 3.6 Interaction of BMP and EcR signalling in regulation of SC growth 66
Figure 3.7 Role of ecdysone in SC growth regulation 69
Figure 3.8 Role of ecdysone biosynthesis genes in SC growth regulation 70
Figure 3.9 Schematic depicting BMP/EcR growth regulation in SCs 72

Chapter-4:BMP signalling and hormone-independent EcR signalling promote new DNA synthesis in SCs after mating

Figure 4.1 Role of genome endoreplication in mating-dependent SC growth 80
Figure 4.2 Regulation of genome endoreplication by the BMP/EcR signalling axis 81
Figure 4.3 Interaction of BMP and EcR signalling pathways in the regulation of genome endoreplication 83
Figure 4.4 Role of EcR isoforms and USP in mating-dependent endoreplication 84
Figure 4.5 Role of EcR isoforms and USP in mating-dependent endoreplication 86
Figure 4.6 Role of EcR isoforms and USP in mating-dependent endoreplication 88
Figure 4.7 Role of FKH and Torso in SC growth and endoreplication 90
Figure 4.8 Schematic depicting regulation of growth and endoreplication in SCs 92

Chapter-5:Regulation of compartment formation and exosome secretion by BMP/EcR signalling axis

Figure 5.1 Role of EcR in Btl-GFP-labelled compartment formation and exosome synthesis 102
Figure 5.2 Role of EcR in Rab6-labelled compartment formation and exosome synthesis 104
Figure 5.3 Role of EcR in Rab11-labelled compartment formation and exosome synthesis 105
Figure 5.4 Role of EcR in Rab19-labelled compartment formation 107
Figure 5.5 Role of BMP signalling in Btl-labelled compartment formation and exosome synthesis 108
Figure 5.6 Role of BMP signalling in Rab6-labelled compartment formation and exosome synthesis 109
Figure 5.7 Role of BMP signalling in Rab11-labelled compartment formation and exosome synthesis 110
Figure 5.8 Schematic detailing the role of BMP and EcR signalling in the regulation of exosome biogenesis and compartment maturation 112

Chapter 6: Cell cycle regulation of mating-dependent SC growth and genome endoreplication

Figure 6.1 Role of cell cycle components in endoreplication 116

Figure 6.2 Role of CycE in the regulation of SC growth and endoreplication 118

Figure 6.3 EcR is not required for CycE-induced SC growth and endoreplication 119

Figure 6.4 Role of CycD in SC growth and endoreplication regulation 121

Figure 6.5 Role of p53/Rbf/E2F1 in SC nucleation state regulation 123

Figure 6.6 Role of Rbf in SC growth and endoreplication regulation 124

Figure 6.7 Role of E2F1 in SC growth and endoreplication regulation 127

Figure 6.8 Interaction between Rbf/E2F1 and EcR signalling in the regulation of SC growth and endoreplication 130

Figure 6.9 E2F1-mediated growth and endoreplication does not require ecdysone 132

Figure 6.10 Interaction between Rbf, E2F1 and BMP signalling in the regulation of SC growth and endoreplication 134

Figure 6.11 Schematic detailing cell cycle regulation of SC growth and genome endoreplication 135

Figure 6.12 Schematic detailing nucleation state regulation in adult SCs 139

Figure 6.13 Possible nuclear destabilisation upon Rbf^{CA} expression 141

Chapter-7: Summary of findings, significance and concluding remarks

Figure 7.1 Final schematic depicting key results presented in this thesis 118

Chapter-1:

Introduction

Prostate cancer is the second most common cause of cancer in the UK (Cancer Research UK, 2019). The majority of the deaths linked to prostate cancer is associated with its advanced and metastatic form, castration-resistant prostate cancer (CRPC). Androgenic steroid signalling plays a vital role in the development and progression of prostate cancer (Chandrasekar et al., 2015; Fujita and Nonomura 2019; Wilson et al., 2017). The broad goal of my DPhil was to better understand the various types of steroid receptor signalling observed in prostate cancer and CRPC.

During my DPhil I have focussed on studying steroid receptor-mediated growth regulation in the secondary cells of the male *Drosophila* accessory glands. I have extended this research to delineate the genetic interactions between the fly steroid receptor, the ecdysone receptor (EcR), the bone morphogenetic protein (BMP) pathway and cell cycle regulators in order to develop the SC as a model for prostate cancer and CRPC. In this Chapter, I initially discuss some important concepts that will form the background for this thesis. Later, in Section 1.16, I discuss some key results by previous lab members which laid the foundation for my DPhil research work.

1.1. Human prostate

The exocrine prostate gland is one of the male accessory glands in humans (Kumar and Majumder 1995). Anatomically, the prostate gland is divided into three zones: the central zone surrounding the ejaculatory duct, the transitional zone surrounding the urethra, and

the peripheral zone surrounding both (Fig 1.1). It lies above the neck of the bladder and below the urothelial diaphragm. The bilayered prostate epithelium has one layer of basal cells and another consisting of luminal cells (Henry et al., 2018). This epithelium is encased in a fibromuscular stroma, which upon contraction pumps the luminal contents of the prostate into the urethra. The prostatic fluid, which constitutes around 25% of the seminal fluid, is mixed with the sperm and is transferred to females during mating. Though the exact functions of the components of the prostatic fluid are not well understood, it is known that they are essential in aiding the maturation of sperm, inducing its motility, and promoting its capacitation prior to fertilisation (Costello and Franklin 2016; Wilson et al., 2017). Since, the prostate gland increases in size with age, older men over 50 years of age very commonly exhibit benign prostatic hyperplasia (Wilson et al., 2017).

1.2. Androgen signalling in normal prostate and prostate cancer

Androgenic steroids are necessary for the proper development and maintenance of homeostasis in males. These steroids are produced through a series of consecutive steps starting from cholesterol. The earlier steps of this cascade which result in the synthesis of testosterone and dehydroepiandrosterone (DHEA) primarily take place in the testes and the adrenal cortex respectively (Fig 1.2; White Background). The later anabolic reactions then occur in specific target peripheral tissues in order to synthesise the active forms of these androgenic steroids. 60% of androgens in the prostate is derived from the testes and is converted into a more active androgenic steroid, dihydrotestosterone (DHT). The remaining 40% of the steroids in the prostate comes from the adrenal glands, which synthesises DHEA, which then serves as a precursor for the production of more potent androgens within the prostate. This androgen steroidogenesis pathway is under the tight

regulation of the hypothalamic-pituitary-gonadal axis (Dai et al., 2017; Heinlein and Chang 2004; Pippione et al., 2017).

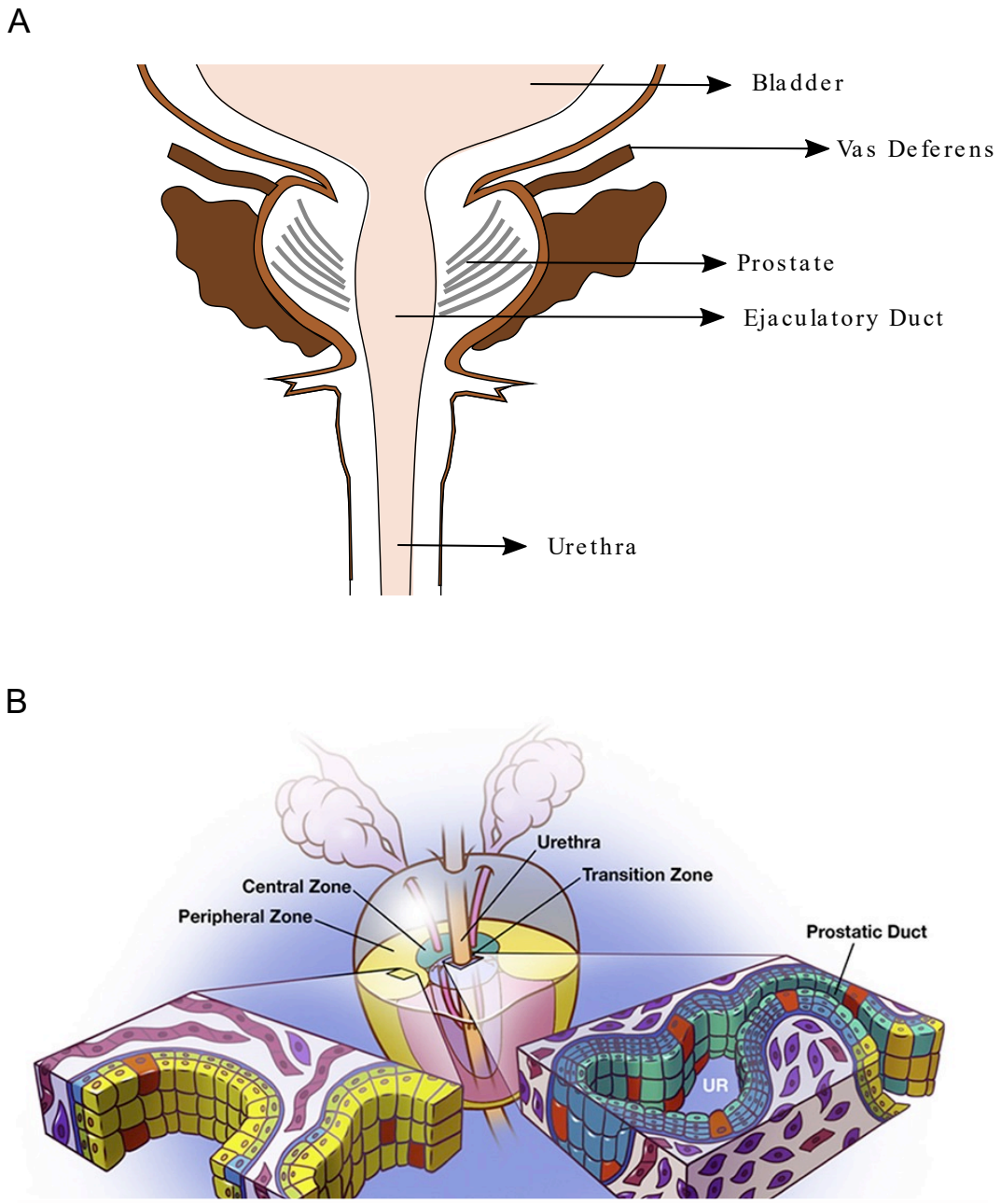

Figure 1.1 The human prostate
A: Schematic of the anatomy of the human prostate gland and surrounding structures
B: Schematic depicting the three zones of the prostate- Central zone, Transition zone and Peripheral zone (Adapted from Henry et al., 2018). Left-hand schematic shows bilayered epithelium in the peripheral zone.

Three methods of androgen synthesis have been speculated to occur in prostate cancer patients – the canonical pathway, backdoor pathway and 5α-dione pathway (Fig 1.2). Each of these methods represents a mechanism for the production of active androgenic steroids by the prostate either from cholesterol or other androgenic precursors (Stuchbery et al., 2017).

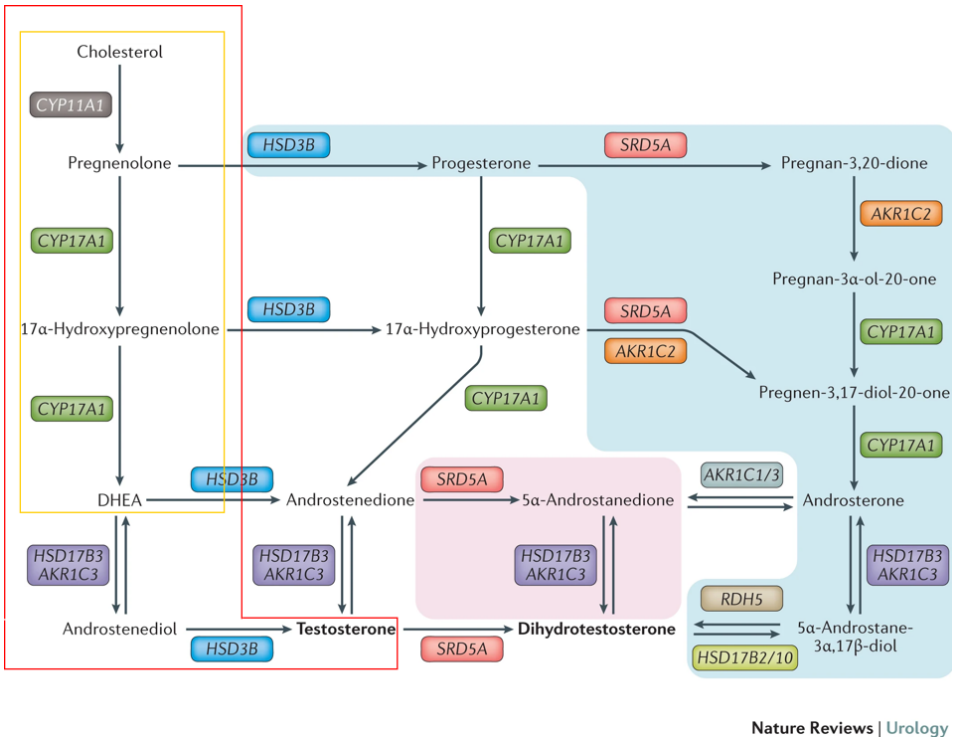

Figure 1.2 The androgen biosynthesis pathway in prostate cancer

Three proposed androgen biosynthesis pathways in prostate cancer: the canonical pathway (white background), backdoor pathway (blue background) and 5α-dione pathway (pink background). The canonical pathway refers to the physiological synthesis of androgens which requires testosterone produced from cholesterol in the testes (Red Box) and can presumably occur within the prostate in prostate cancer patients. DHEA, which is generally produced in the adrenal cortex (Yellow Box), is another precursor used by prostate cancer cells.The backdoor pathway refers to the production of androgens within the prostate, which does not require testosterone as a precursor. The 5α-dione pathway refers to an alternative canonical pathway that can directly lead to the production of intratumoral DHT. (Adapted from Stuchbery et al., 2017 (License issued))

Steroids generally enact their effect through their interaction with nuclear receptors. The androgenic steroids promote gene regulation via their steroid nuclear receptor, the androgen receptor (AR). Unlike the classical signal transduction pathways which initiate a cascade of signals to regulate transcription within the nucleus, the nuclear receptors

have the capacity to efficiently modulate transcription in a one-step process (King-Jones and Thummel 2005; Yamanaka et al., 2013). This is facilitated by their unique structural feature which houses both the ligand-binding domain (LBD) and the DNA-binding domain (DBD) within the receptor (Fig 1.3 A). The DBD, which binds to the regulatory regions (hormone-response elements (HREs)) of the hormone-responsive genes, and LBD are connected through a flexible hinge region. Apart from these domains, nuclear receptors have two activation surfaces: activation function 1 (AF1) in the N-terminal A/B region and AF2 in the LBD. These activation function regions recruit cofactors that facilitate transcriptional activity of the nuclear receptor. The family of nuclear receptor proteins is highly conserved and divided into six sub-families. The DBD at the N-terminus and AF2 domains are highly conserved, whereas the LBD, AF1 domains and the N-terminal region A/B are not conserved. It has been observed that the AF1 domain can regulate ligand-independent transactivation by the receptor, whereas AF2 acts in a ligand-dependent manner. Additionally, homodimerisation or heterodimerisation of the nuclear receptors is required for essential ligand binding activity (Cherbas et al., 2003; King-Jones and Thummel 2005; Yamanaka et al., 2013).

The nuclear receptors broadly function via two different mechanisms. Some nuclear receptors reside in the cytoplasm by binding to chaperone proteins, which helps maintain the steroid receptor in a conformation that promotes higher affinity to its ligands. Upon binding to the steroid, the receptor translocates to the nucleus as a homodimer or heterodimer (generally with retinoid X receptor) and initiates transcription of the hormone-responsive genes (Fig 1.3 B). The second mechanism involves a steroid receptor which is already present within the nucleus and has the capability to repress transcriptional activity while bound to the DNA, by associating with co-repressors in the

absence of the ligand. When this steroid receptor is activated by its steroid ligand, co-activator proteins replace co-repressors and promote transcription of hormone-responsive genes (Fig 1.3 C) (King-Jones and Thummel 2005).

Using the canonical androgenic biosynthesis pathway, prostate cancer cells convert testosterone to DHT irreversibly using the 5-α reductase enzyme (SRD5A). Both DHT and testosterone interact with the AR in the prostate and mediate prostate growth and physiology (Dai et al., 2017; Fujita and Nonomura 2019). In an unbound state, the AR is often bound to heat-shock proteins, such as Hsp70 and Hsp90, and is present in the cytosol. Testosterone or DHT activates the AR, which then translocates into the nucleus as a homodimer and binds to the androgen-responsive elements (ARE). The AR initiates the transcription of certain target genes that are essential for the development and growth of prostate cells (Fig 1.4 A) (Tan et al., 2015).

Huggins and Hodges were the first to show the role of hormones in regulating prostate cancer. They found that reducing the levels of androgenic steroids by castration or by neutralising the androgen hormone by injection of oestrogen resulted in a reduction in tumour growth (Huggins and Hodges 1941). Huggins went on to establish androgen deprivation therapy (ADT) based on these results and even now, ADT remains one of the frontline treatments for advanced prostate cancer (Zong and Goldstein 2013). ADT reduces the circulating androgen levels either by chemical or surgical castration (Fig 1.4 B). This treatment has an initial response rate of 80% in the first few years, but patients inevitably enter into a more aggressive and incurable state of prostate cancer, castration-resistant prostate cancer.

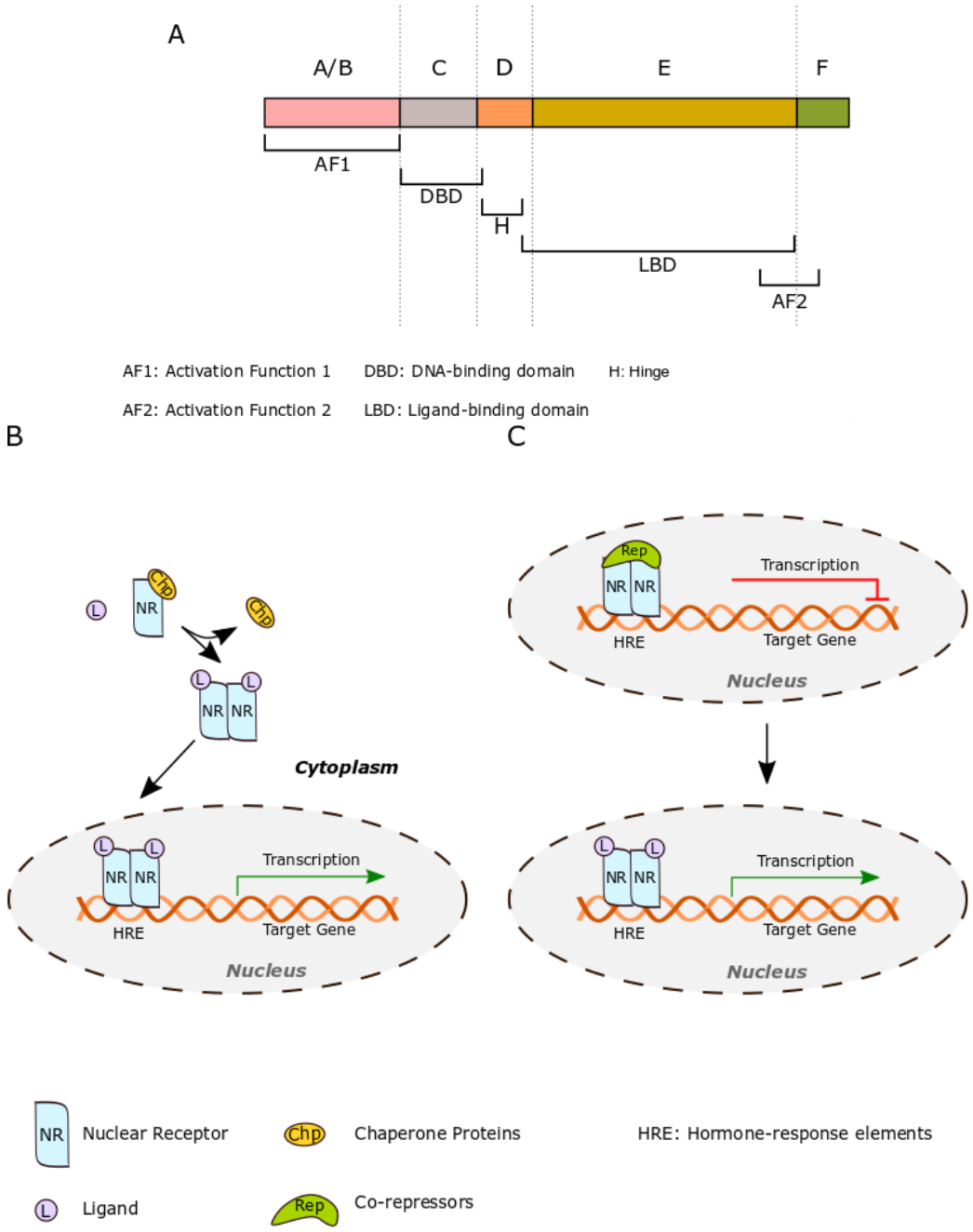

Figure 1.3 Nuclear steroid receptor structure and function
A: General structural domains of a canonical nuclear steroid receptor.
B: Nuclear receptor resides in the cytoplasm in association with chaperone proteins in an unliganded state. In the presence of the hormone, the nuclear receptor activates and translocates to the nucleus in order to transcribe the target genes.
C: Nuclear receptor is associated with co-repressors and is already present within the nucleus where it represses the expression of the target gene in the absence of the ligand. In the presence of the hormone, the nuclear receptor disassociates from the repressors and promotes the transcription of target genes.

1.3. Castration-resistant prostate cancer (CRPC)

As the term suggests, this advanced form of prostate cancer arises in the androgen-depleted tumour environment after ADT. It still remains unclear as to how exactly the transition to CRPC occurs. However, it has been found that in most cases androgen signalling is still active even in the absence of the androgenic steroids and that the androgen receptor is essential for CRPC to occur (Fig 1.4 C) (Zong and Goldstein 2013). This AR-dependent growth occurs mostly due to the activation of the AR independently of the ligand after ADT, though ligand-dependent activation is also possible. Following are some common mechanisms that are implicated in the transition to CRPC:

Intratumoural and alternate androgen synthesis: Conventional ADT does not completely eliminate the precursors of testosterone synthesised in the adrenal gland or the alternate androgen synthesis pathways, which are then able to reactivate the dormant AR signalling, thereby allowing prostate cancer to adapt to ADT (Huang et al., 2018; Zong and Goldstein 2013).

AR mutations and promiscuity: Mutations in the AR rarely occur in the early stages of prostate cancer, but approximately 20% of the hormone-refractory CRPC patients have gain-of-function mutations in the AR (Tilki et al., 2016), which can lead to transactivation of the AR and promiscuous binding of ligands other than androgens.

AR amplification : Around 80% of clinical CRPC cases have higher levels of AR mRNA and protein (Chandrasekar et al., 2015; Huang et al., 2018), which can hypersensitise the tumour to the low testosterone concentrations after ADT (Huang et al., 2018).

AR splice variants: Around 20 AR splice variants (AR-Vs) are associated with CRPC and most of the AR-Vs are either truncations or exon skipping of the LBD (Cao et al., 2016) . These AR-Vs can be activated in a ligand-independent manner (Cao et al., 2016; Huang et al., 2018; Zong and Goldstein 2013).

Altered activity of AR co-regulators: The AR interacts with around 150 different chaperone proteins that facilitate its transcriptional activation or repression activity thereby serving as co-activators or co-repressors respectively. Hence mutations that alter the function of these chaperone proteins can affect the activity of the AR (Huang et al., 2018).

The diverse mechanisms through which CRPC is inevitably achieved might suggest that this androgen-independence might reflect some part of a normal biological mechanism, but such a mechanism has not been identified to date.

1.4. Role of Bone Morphogenetic Protein (BMP) signalling in prostate cancer

BMPs form one of the largest subfamilies of the transforming growth factor beta (TGF-β) superfamily. The BMP-2, BMP-3, BMP-4, BMP-6 and BMP-7 proteins of the BMP subfamily are expressed in the prostate and are required for the maintenance of homeostasis (Bragdon et al., 2011). Several clinical studies have reported higher levels of BMP-6 and BMP-7 in metastasised prostate cancer (Hamdy et al., 1997; Lee et al., 2013). BMP-6 may play a vital role in regulating the osteoblastic changes that are required for the skeletal metastasis of advanced stages of prostate cancer. It has been shown that AR mRNA levels are positively regulated by the BMP-6 ligand in prostate cancer cell lines, thereby suggesting the possible interaction between the BMP signalling pathway and the AR to regulate prostate cancer progression and growth (Lee et al., 2013).

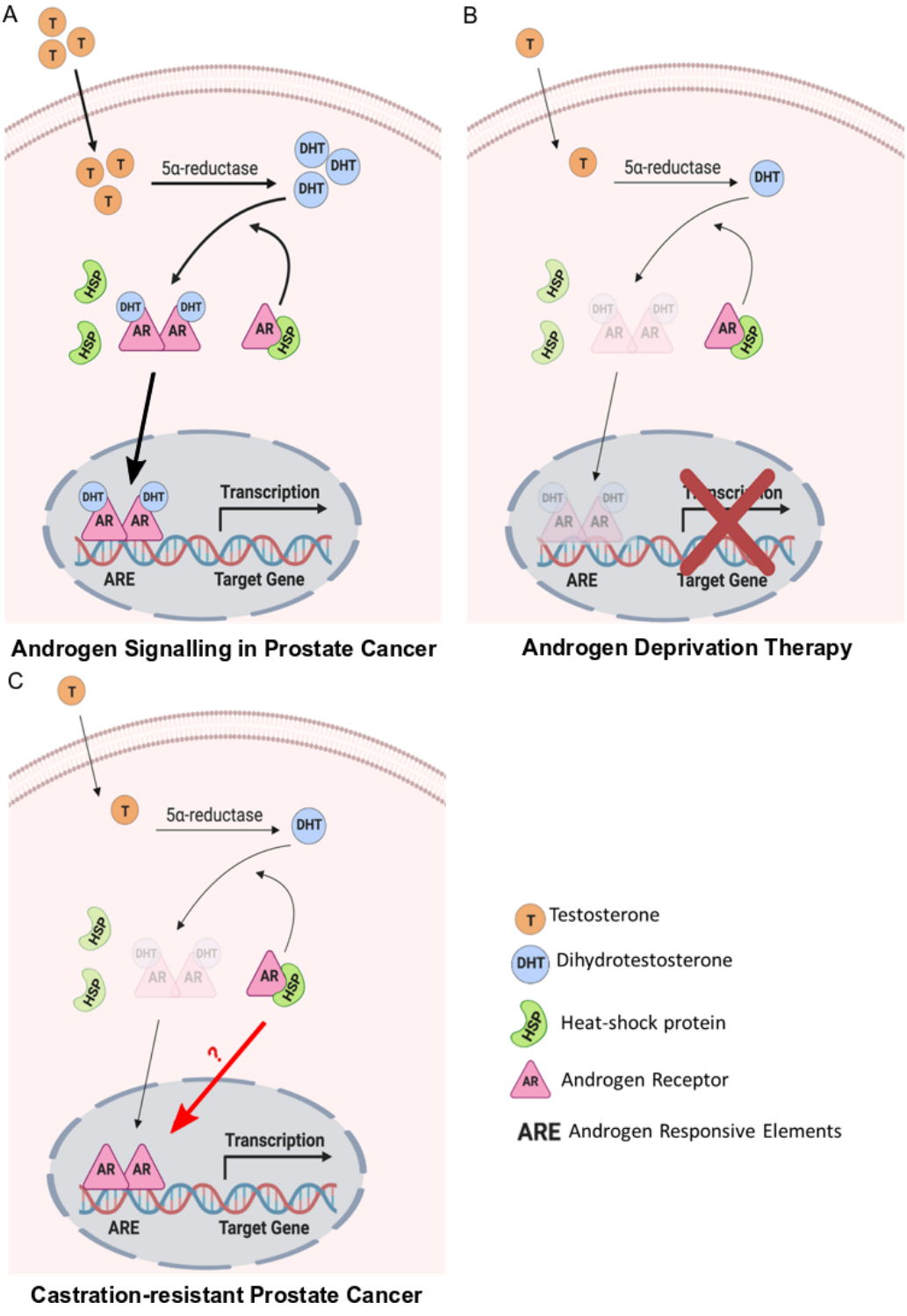

Figure 1.4 Role of androgen signalling in prostate cancer progression
A: Androgen signalling in prostate cancer cells initiates transcription of target genes that promotes tumour growth.
B: Androgen deprivation therapy (ADT) by chemical or surgical castration results in a reduction in androgen signalling which results in reduced transcription of target genes, thereby suppressing tumour growth.
C: Androgen-independent but AR-dependent signalling re-initiates transcription of target genes in the androgen-deprived tumour microenvironment and promotes prostate cancer growth in CRPC

1.5. Role of Retinoblastoma signalling in prostate cancer

Retinoblastoma (Rb) is a tumour-suppressor protein which is a major regulator of the cell cycle. Cell cycle progression is controlled by many cyclins and their partners, cyclin-dependent kinases (Cdks). Rb negatively regulates proteins from the E2F transcription factor family, when it is physically bound to their transactivation domains or by actively repressing them by recruiting certain epigenetic and chromosome remodelling factors such as HDACs, methyltransferases, SWI/SNF factors, and Polycomb proteins. E2F factors are involved in activating genes including Cyclin E (CycE), which are essential for the progression of the Synthesis (S)-phase of the cell cycle (Giacinti and Giordano 2006; Harbour and Dean 2000).

During the progression of the Gap 1 (G1)-phase, Rb is gradually phosphorylated by the Cyclin D1 (CycD1)/Cdk4/6 complex during early G1 and CycE/Cdk2 in late G1 and remains hyperphosphorylated until the Mitotic (M)-phase. The CycD1/Cdk4/6 complex transduces signals from mitogenic factors, which regulate cell cycle progression; CycE/Cdk2 is produced by the low concentration of free E2F produced during early G1. Hyperphosphorylation of Rb changes its conformation and releases E2F, thereby enabling E2F-dependent transcriptional activity (Fig 1.5) (Giacinti and Giordano 2006).

Loss of Rb is commonly observed in several cancer types and is considered to be essential for the early development of cancer. However, in prostate cancer, loss of Rb is associated with the progression of prostate cancer rather than its development. E2F1 regulates the expression levels of *AR*, therefore suggesting at least one interaction between the Rb/E2F signalling axis and the AR. In the early stages of prostate cancer, Rb tightly regulates E2F, which in turn regulates *AR* expression. However, with loss of Rb as the cancer

progresses further, an unsupervised activation of E2F occurs, thereby increasing the protein levels of AR. Therefore, even after hormone ablation therapy, loss of Rb results in higher protein levels of AR which promotes prostate cancer cellular growth and proliferation. Hence, loss of Rb is sufficient to induce the androgen-refractory form of prostate cancer. In accordance with these interactions, perturbation in the Rb/E2F/AR axis and loss of Rb are commonly observed in CRPC patients (A. Sharma et al., 2010; Thangavel et al., 2017).

1.6. Mouse models for prostate cancer and CRPC

The mouse prostate is anatomically and structurally very different from the human prostate. The prostate gland of the mouse is not a single organ but is composed of four distinct lobes, with different functions. There are still debates regarding which of these lobes can best capture the molecular and cellular mechanisms of prostate cancer and CRPC. Xenograft models, allograft models, genetically engineered mouse models and patient-derived models have been developed to study different aspects of prostate cancer. These models are generally derived from a single patient or a single cancer cell line thereby limiting the studies to determining only certain genetic modalities of this disease. There is no unified mouse model available to study the molecular mechanisms of prostate cancer and the transition to CPRC. Furthermore, prostate cancer rarely occurs in mice and once it has been induced in the above-mentioned models it does not resemble the human prostate cancer disease in several fundamental aspects (Grabowska et al., 2014; Maddison et al., 2004; Namekawa et al., 2019; Rea et al., 2016). Although these mouse models have provided insight into prostate cancer progression, there is a necessity to develop an *in vivo* model, which encapsulates various aspects of prostate cancer and allows for studying the genetic interaction of various signalling axes in regulating the

progression of this disease. In my DPhil, I have developed a plausible genetic model system to study prostate cancer and CRPC in *Drosophila melanogaster*.

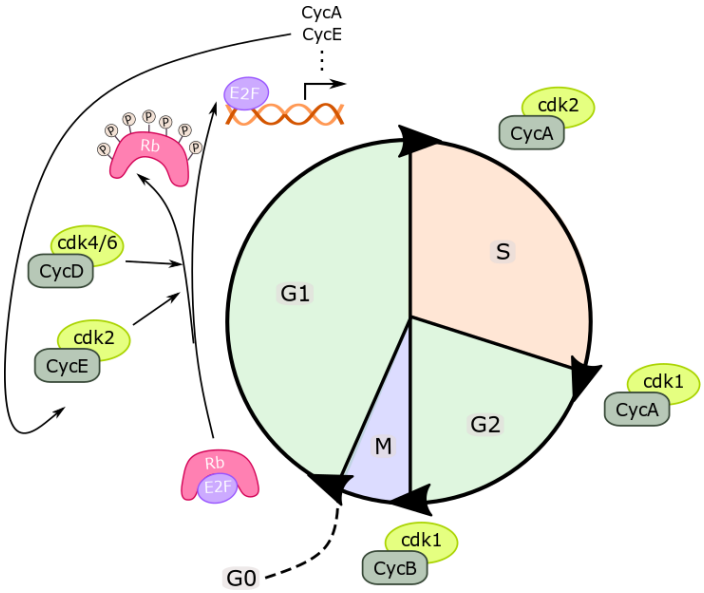

Figure 1.5 Cell cycle machinery
A brief graphical summary describing key features of the cell cycle transitions. The cell cycle can be divided into four distinct phases G1, S, G2 and M phases. The G0 phase represents those cells that are in a quiescent state, reached via G1, and not undergoing cell-division. Entry into the cell cycle is regulated by several extracellular mitogenic signals. Cdks can positively regulate the cell cycle when they are bound to the corresponding cyclin. The levels of Cdks remain constant throughout the cell cycle and their activity is controlled by the periodic oscillation in the levels of cyclins. Rb is one of the negative regulators of the cell cycle, which also include Cdk-inhibitors that are not shown in this figure. In its active form, Rb negatively regulates the E2F1 transcription factor. When it is inactivated by hyperphosphorylation it does not inhibit E2F1. CycD/cdk4/6 mediates events that occur in the early G1-phase (including Rb/E2F1 regulation), CycE/cdk2 is required for initiating the G1/S transition via a negative feedback loop that inhibits Rb activity, Cyclin A (CycA)/cdk2 and CycA/cdk1 are necessary for the progression of S-phase and Cyclin B (CycB)/cdk1 is required for the entry into the M-phase. G1-phase cyclins (CycD) generally regulate G1/S cyclins (CycE). The levels of G1/S cyclins increase at the start of G1-phase, peak at the G1/S transition and fall in S-phase. Levels of S-phase cyclins (CycA) increase from the start of G1-phase, but slower than G1/S-cyclins, peak throughout S-phase and G2-phase and fall during early M-phase. Levels of M-phase cyclins (CycB) increase from early G2-phase, peak during early M-phase and fall during metaphase/anaphase checkpoint of the M-phase. The molecular mechanisms described here are a general overview of classical cell cycle regulation. The cell cycle is complex and several variations from the classical cell cycle model have been reported

1.7. Contribution of *Drosophila* to the field of cancer biology

There are limitations associated with current methods of cancer investigation that depend on cell lines and mouse models. Studies in mammalian cell lines have limited clinical relevance as this system is not able to capture the complexity of cancer. Some limitations in the case of mouse models have been mentioned above for prostate cancer in Section 1.6 and apply to other types of cancer as well. Additionally, mouse models are expensive and time-consuming to develop and utilise for further studies. Studies with *Drosophila* have been able to provide us insight into the regulation of signal transduction, cell cycle and epithelial development, dysregulation of which results in cancer development and progression. Several research groups are now trying to tackle translational research questions in the realm of cancer biology by directly using flies (Rudrapatna et al., 2012; Sonoshita and Cagan 2017).

Two approaches are followed when developing the fruit fly as a model to study mammalian diseases and mechanisms: '*Drosophila to Mammals*' and '*Mammals to Drosophila to Mammals'*. The former approach has led to the identification of new signalling pathways, tumour suppressors and oncogenes which were shown to play a role in human cancers as well. This approach focusses on cellular mechanisms, which when disrupted, result in cancer phenotypes, such as defects in cell polarity, growth, apoptosis regulation and cell-cell competition, as well as invasiveness and activated oncogenic signalling pathways via molecules like Ras, epidermal growth factor receptor (EGFR) and c-Jun NH2-terminal kinase (JNK). The '*Mammals to Drosophila to Mammals*' approach has led to the development of several successful models that have helped delineate cancer mechanisms. The earlier models focussed on tumours that are dependent on mutations at a particular locus such as RET (rearranged during transformation)-based

tumours and Tuberous Sclerosis. These models primarily allowed for understanding the genetic interaction of various signalling pathways which proved to be relevant to their mammalian disease counterparts. However, in the past decade, models with higher complexity have been developed for glioblastoma multiforme and colorectal cancer (Rudrapatna, Cagan, and Das 2012; Sonoshita and Cagan 2017). Some models have been specifically developed to study the genetic heterogeneity that commonly occurs in tumours. Such studies have shown that cooperative interaction between oncogenic and tumour suppressor pathways regulate tumour induction, invasion and progression. For instance, these models have been pivotal in understanding the interaction between the oncogene Ras, tumour suppressor scribbled, JNK and JAK/STAT pathways which play a vital role in several cancer types (Wu et al., 2010).

1.8. *Drosophila* accessory gland and its functions

The *Drosophila* male reproductive system comprises the testes, seminal vesicles, paired accessory gland lobes, ejaculatory duct, and the ejaculatory bulb. The paired accessory glands (AGs) have a monolayer epithelium consisting of two distinct binucleate cell-types: main cells (MCs) (~1000 cells/AG) and secondary cells (SCs) (~40 cells/AG) (Fig 1.6). At 55 hours after puparium formation, both the MCs and SCs synchronously enter the mitotic phase and undergo nuclear division without cytoplasmic division. The *Drosophila* homologue of the microtubule binding protein NuMA (Mud), the mitotic aurora B kinase and the mitotic Cyclin inhibitor fizzy-related have been implicated in regulating the induction of binucleation in these cells during the pupal stage (Taniguchi et al., 2014). Additionally, this binucleation state of the cells in the AG is conserved in several other *Drosophila* species and has been implicated in facilitating AG contraction

for efficient seminal fluid secretion and transfer to females during mating (Taniguchi et al., 2012, 2018).

The squamous, hexagonal MCs are dispersed throughout the gland, whereas the cuboidal, spherical SCs are present at the distal tip of the AG (Bertram et al., 1992; Leiblich et al., 2019; Wilson et al., 2017). With age, the MCs become more squamous, while the SCs retain their apico-basal height and bulge into the AG lumen without losing contact with the basal membrane. Most of the SC apical surface is enveloped by a thin MC layer. Only the SCs increase in size with age and this growth is further enhanced upon mating (Leiblich et al., 2012). Apart from being morphologically different, both the MCs and SCs are also biochemically different as they each have unique gene expression patterns (Bertram et al., 1992; Sitnik et al., 2016). The AG epithelium is surrounded by a striated muscle layer, which contracts during mating, to empty about a third of the luminal contents into the ejaculatory duct, which is eventually transferred to the uterus of the female (Baumann 1974; Bertram et al., 1996). The serotonergic projection neurons which innervate the AG, are known to facilitate this muscle-induced AG contraction during mating (Tayler et al., 2012).

The AG produces at least 200 accessory gland proteins (Acps) that make up the seminal fluid. The Acps from both the MCs and SCs are essential in regulating post-mating responses (PMR) observed in females such as inducing female fertility, suppressing female immune response, and inducing several female behavioural changes, such as an increase in egg-laying rate, rejection of other males and alteration of diet (Bertram et al., 1992; Ravi Ram and Wolfner 2007; Wilson et al., 2017). The PMR is divided into short-term response (STR) and long-term response (LTR). The changes that occur within the

first 24 hours after mating are termed STR and the rest of the post-mating effects that usually lasts up to 10 days are considered as LTR (Gligorov et al., 2013; Sitnik et al., 2016; Wolfner 1997). The Acps secreted by the MCs play a major role in the regulation of female PMR. For instance, females mated with males that are unable to produce one of the MC Acps, Sex Peptide (SP), do not display any long-term PMR effects (Chapman et al., 2003; Liu and Kubli 2003). However, the secretory products of the SCs have been shown to glycosylate some of the MC products such as ovulin (Acp26Aa), CG1656, and CG1652; if SCs do not develop normally, the long-term PMR effects are not established in females (Gligorov et al., 2013). Additionally, SCs are also essential for the storage and release of SP in females after mating (Sitnik et al., 2016).

1.9. Parallels between human prostate and *Drosophila* AG

Both the mammalian prostate and the *Drosophila* AGs share several functional similarities. Both these secretory glands contribute to seminal fluid production. As mentioned above, transferred seminal fluid induces several behavioural and physiological changes in females in both humans and flies. Additionally, several human and *Drosophila* seminal fluid proteins fall into similar biochemical classes such as lectins, proteases and cysteine-rich secretory proteins (Ravi Ram and Wolfner 2009). The SCs of the male AG also share multiple cell biological properties with human prostate epithelial cells. Both the prostate gland and the SCs, unlike the MCs, increase in size with age (Leiblich et al., 2012). Besides secreting into seminal fluid, the SCs release tiny signalling nanovesicles called exosomes that fuse to sperm in the female reproductive tract and reprogramme females, so they reject other males. Human prostate exosomes (prostasomes) also fuse with sperm and affect their activities (Corrigan et al., 2014).

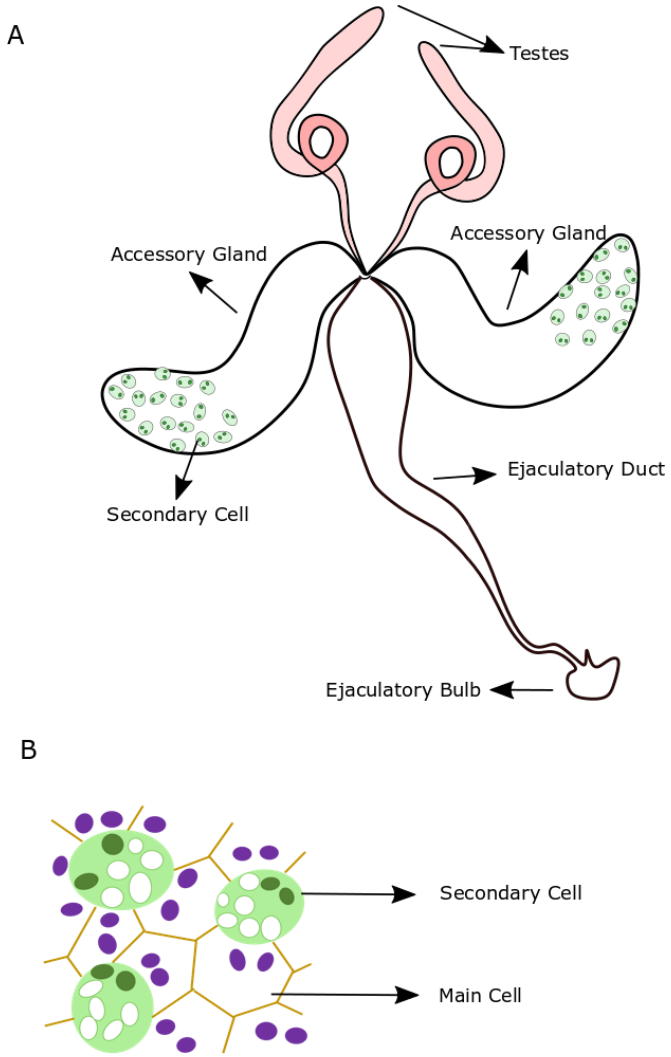

Figure 1.6 *Drosophila* accessory gland and cell types
A: Anatomy of the *Drosophila* male reproductive system (Not to scale; Testes are generally much longer).
B: Schematic of cellular arrangement of binucleate SCs and MCs within the AG epithelium. The cell boundaries are marked by yellow lines, nuclei in purple and the SC in green.

1.10. Intracellular structure and cell biology of SCs

1.10.1. Types of SC compartments

Each SC contains approximately thirteen non-acidic compartments (NACs; >2 µm in diameter), several smaller acidic immature late endosomes (ILEs; < 2 µm in diameter) and two or three large acidic maturing multivesicular bodies or lysosomes (MVBLs; > 2 µm in diameter) (Corrigan et al., 2014; Prince et al., 2019; Redhai et al., 2016). Approximately ten out of the thirteen NACs contain a central dense-core granule (DCG)

within them (Fig 1.7 A). The compartments and DCGs can be visualised using differential interference contrast (DIC) microscopy. Additionally, the limiting membrane of all the compartments can be observed by overexpressing a GFP-tagged human tetraspanin, CD63, an exosome marker (Corrigan et al., 2014). Another marker that is commonly used by the Wilson lab to label the non-acidic compartments is the overexpressed GFP-tagged Breathless (Btl), which is a *Drosophila* homologue of mammalian fibroblast growth factor receptors.

1.10.2. Dense-core granule-containing compartments

When the accessory gland is viewed through a wide-field microscope, the large intracellular compartments can be clearly visualised in SCs with DIC revealing the presence of DCGs in many of them. When viewed under an electron microscope, the central DCG can be clearly seen (Corrigan et al., 2014; Rylett et al., 2007). These DCGs, which are commonly present in exocrine and endocrine secretory cells, are unusually surrounded by tubular filamentous bodies in SCs. The DCGs contain tightly packed bioactive molecules such as protein precursors, proteases and hormones in a crystallised-like form and can be released or secreted by the cell upon receiving the necessary stimulus (Dikeakos et al., 2009). To date, the identity of only three proteins within the DCGs of SCs is known, Decapentaplegic (Dpp) (Redhai et al., 2016), Midline fasciclin (Mfas) (M. Wainwright, pers. comm) and angiotensin-converting enzyme (ANCE) (Rylett et al., 2007).

1.10.3. Exosome secretion by SCs

SCs secrete exosomes (Corrigan et al., 2014; Fan et al., 2020; Marie et al., 2020), which are nanovesicles that mediate intercellular signal transduction events (Gangoda et al.,

2015). Exosomes are known to carry a diverse range of cargoes, that assign specificity for target cells and determine their functions. They are initially formed as intraluminal vesicles (ILVs) in endosomal compartments, and are then secreted by compartment fusion with the plasma membrane. By overexpressing either CD63-GFP or Btl-GFP in SCs, secreted GFP-positive exosomes can be seen in the AG lumen (Corrigan et al., 2014; Fan et al., 2020). GFP-puncta are also present within some of the compartments. Super-resolution 3D-SIM microscopy has revealed that GFP marks the membranes of ILVs in these compartments from which the exosomes originate (Fan et al., 2020). When these constructs were expressed in MCs, no such puncta were observed either in the lumen or within the cell.

The Rab family of proteins consists of small GTPases which mediate intracellular membrane trafficking (Stenmark 2009). When the Rab proteins are bound to GTP, they are localised onto membranes of specific secretory, endosomal and lysosomal compartments within cells and recruit effector proteins to enable vesicle budding, vesicle movement and membrane fusion with other compartments or the plasma membrane. Using gene traps for different Rab proteins, it was demonstrated that the SC compartments have diverse Rab signatures (Fig. 1.7A) (Fan et al., 2020).

The late endosomal and lysosomal marker, Rab7, is present on the membranes of the acidic compartments; these compartments generally have a low pH, which is detected by the acidophilic dye LysoTracker. Rab6, which regulates trafficking to and from the Golgi complex, endosomes and, endoplasmic reticulum, is present on the limiting membranes of some of the non-acidic large compartments that lack a DCG. The recycling endosomal Rab marker, Rab11, primarily marks all the DCG-containing

compartments, which also contain most of the GFP-positive ILVs labelled by exosome markers. The large non-cored Rab6 compartments sometimes carry lower levels of YFP-Rab11 in subdomains around their limiting membrane. Rab19, whose function is unknown, marks only two or three DCG-containing compartments along with some smaller compartments.

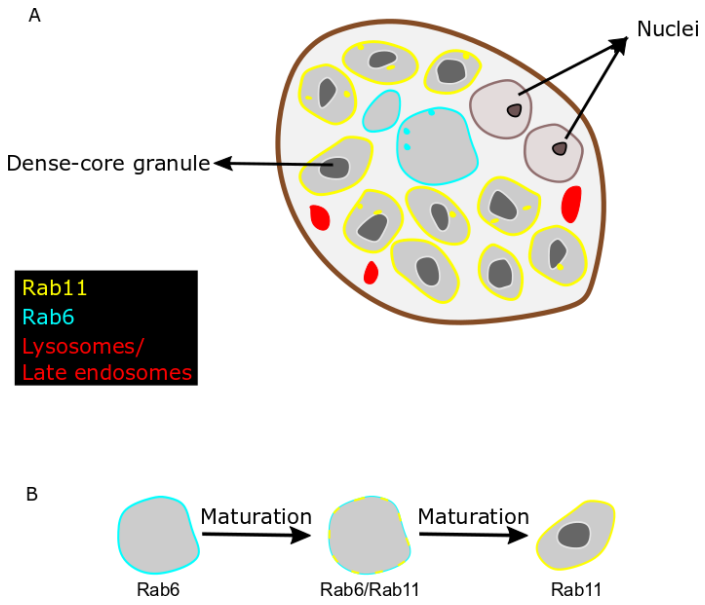

Figure 1.7 SC intracellular structures
A: Schematic of intracellular compartments of SCs. Rab11- and Rab6-compartments labelled in yellow and cyan respectively to mirror the reporter tag of the respective gene traps. The colour of the puncta represents the type of exosome subpopulation (Rab11 or Rab6).
B: Maturation process of SC compartments. Rab6-compartments mature into a DCG-containing Rab11-compartment over a period of a few hours. The transitionary compartment expresses both Rab6 and Rab11 which then results in the DCG-containing Rab11 compartment.

When gene traps for Rab6, Rab11 or Rab19 are expressed in the SCs, ILVs containing the respective Rab proteins, are found within the lumen of some of the large non-acidic compartments. Therefore, not only do the SC compartments have diversity in their Rab identity, but they also produce a diverse population of exosomes/ILVs. These exosomes could potentially play different functional roles depending on their Rab identity. Work by the Goberdhan lab has shown that under glutamine deprivation stress, cancer cells preferentially release Rab11-exosomes which alter tumour growth and blood vessel

formation in mouse tumour models. Collaborative studies with the Goberdhan lab have demonstrated that the mechanism of formation and secretion of Rab11 exosomes is conserved from flies to humans (Fan et al., 2020). Since the SC compartments are unusually large and can be easily studied using wide-field microscopy techniques, this system can be used as a model to study exosome biogenesis and secretion.

Time-course live-cell imaging experiments have allowed for visualising the transition of Rab6 compartments to Rab11 DCG-containing compartments, thereby suggesting a plausible maturation process (Fig 1.7 B) (Kroeger 2017). Apart from the above-mentioned Rab proteins, the localisation and function of several other Rab-GTPases in the SCs have also been studied (Prince et al., 2019).

1.11. BMP pathway in *Drosophila*

The BMPs were initially discovered for their role in promoting bone differentiation. However, later studies have implicated the BMP family in playing a multitude of roles such as insect and vertebrate dorso-ventral patterning (Kishigami and Mishina 2005; Lynch and Roth 2011), *Drosophila* wing development, cell proliferation and migration (Raftery and Umulis 2012; Tsuneizumi et al., 1997), stem cell maintenance (Chen et al., 2011; Xie and Spradling 1998), and regeneration (Li et al., 2013). Just like in mammals, the BMPs are a branch of the TGF- β signalling superfamily in *Drosophila*.

There are three extracellular BMP ligands in flies: Dpp, Glass-bottom boat, and ScrewB. These ligands heterodimerise or homodimerize to activate the BMP pathway by binding to a heterodimeric complex comprising of a BMP Type I receptor (BMPR-I) and a BMP Type II receptor (BMPR-II). The BMP receptors are transmembrane, serine/threonine

kinases that act as a bridge between the extracellular and intracellular environments (Hamaratoglu et al., 2014; Upadhyay et al., 2017).

The Type I and Type II receptor families each consist of only two members. The BMPR-I family includes Thickveins (Tkv) and Saxophone (Sax). These receptors have overlapping functions as Tkv can partially compensate for the loss of Sax (Brummel et al., 1994; Upadhyay et al., 2017). The BMPR-II family is comprised of Wishful thinking (Wit) and Punt. These are also receptors for the activin family of ligands (Upadhyay et al., 2017).

Upon binding with its ligands, BMPR-II activates its BMPR-I partner by phosphorylating it at the Glycine-Serine rich region, which in turn transduces the signal by phosphorylating Mothers against Dpp (Mad), the primary receptor-activated Smad. An inhibitory Smad, Daughters against Dpp (Dad), has been observed to regulate BMP signalling in *Drosophila*. Phospho-Mad (pMad), then complexes with Medea, the common-Smad (co-Smad), and translocates to the nucleus where it interacts with other cofactor molecules to regulate transcription (Hamaratoglu et al., 2014; Upadhyay et al., 2017). The BMP signalling pathway has a comprehensive feedback network which mostly occurs at the transcriptional level (Hamaratoglu et al., 2014). Recent studies have demonstrated that BMP signalling regulates several aspects of SC biology.

1.12. BMP signalling plays multiple roles in SCs

1.12.1. BMP signalling is essential for SC growth in virgin males

The lab has previously shown that the BMPR-I, Tkv, and the BMPR-II, Wit, are expressed in SCs (Redhai et al., 2016). Overexpressing an activated form of *Tkv* (Tkv^{act})

in SCs, results in an increase in SC growth and as expected, expression of *Dad*, leads to smaller SCs (Leiblich et al., 2012). Additionally, many of the other BMP pathway components such as Sax, Punt, and Med also regulate normal SC nuclear growth in virgin males (Leiblich et al., 2012; Redhai et al., 2016). SC growth generally appears to be reflected by SC nuclear growth, and hence, nuclear growth has been used to measure cellular growth of SCs (Leiblich et al., 2012).

1.12.2. BMP signalling promotes SC delamination and migration

Upon multiple mating, the AG epithelium becomes more cuboidal and a few SCs start to delaminate apically, by reducing their contact with the basement membrane (Leiblich et al., 2012).The spatial expression of the proteins required for apico-lateral cell-cell adhesion was maintained in these delaminating SCs. Therefore, this phenomenon does not compromise the AG epithelium. No such delamination is observed with MCs after mating. Additionally, the transcription of actin appears to be increased in migrating cells upon mating, which might facilitate SC delamination and migration. In approximately 4% of 3- and 10-day-old multiply-mated males, SCs were observed at the proximal end of the AG. These SCs were still attached to the apical surface of the epithelium. Similar to other migratory cells, asymmetrical accumulation of F-actin in lamellipodia-like structures was observed in SCs. Interestingly, some SCs and SC fragments are transferred to females upon mating (Leiblich et al., 2012).

Upregulation of BMP signalling in the SCs of virgin males by expressing Tkv^{act} leads to approximately 25% of SCs delaminating and migrating to the proximal end of the AG. However, males expressing *Dad* in the SCs, do not delaminate, migrate or transfer

to females after multiple matings. Hence, the BMP signalling pathway is necessary and sufficient for SC delamination and migration (Leiblich et al., 2012).

1.12.3. BMP signalling regulates SC secretory activity

A single mating stimulates the release of approximately four DCGs, which results in a Dpp-dependent autocrine positive feedback that regulates the replenishment of the lost DCGs (Corrigan et al., 2014; Redhai et al., 2016). This DCG release in SCs is facilitated by the membrane trafficking component, Soluble NSF Attachment Protein Receptor, SNAP24. Furthermore, BMP signalling regulates CD63 exosome secretion into the lumen although DCG compartments, which make these exosomes, are still formed (Corrigan et al., 2014). These results demonstrate that BMP signalling is involved in different aspects of SC secretory activity and as part of my DPhil, I have investigated its role in the regulation of compartment formation and Rab-marked ILV formation.

1.12.4. BMP signalling modulates female PMR

When females mate with males expressing Dad in SCs (‘Dad males’), they have higher receptivity to remating, unlike controls (Hopkins et al., 2019; Leiblich et al., 2012). Though the number of sperm transferred by mated Dad males is similar to controls, the proportion of sperm that enter the female sperm storage organs, the seminal receptacle and the spermathecae, and which are stored in these organs 5 h after mating, is significantly reduced. Interestingly, the reduced sperm that are stored specifically in the seminal receptacle of these females are retained for longer time-periods. No significant change in mating duration, egg-laying rate or fecundity was observed in these females. Therefore, females that mate with males that have aberrant BMP signalling in their SCs,

have uncoupled PMRs and also show disruptions in both SP-dependent (receptivity and sperm release) and -independent (sperm storage) mating responses.

Surprisingly, it was observed that when females mated with Dad males remate with a control male, they retain more sperm from the Dad males, which leads to a higher paternity share during competitive matings. This does not happen if the matings are performed in reverse order. Finally, the proteome of seminal fluid proteins is remodelled in males expressing Dad in their SCs with SC and MC proteins affected (Hopkins et al., 2019). Therefore, BMP signalling in SCs does not just affect several aspects of SC biology, it also regulates other aspects of male AG function and specific female PMRs.

1.13. Ecdysone signalling pathway in *Drosophila*

The ecdysteroid ecdysone (E) is the precursor to its active form 20-hydroxyecdysone (20-HE). Both E and 20-HE are often generically referred to as ecdysone and in this thesis, I will follow this convention (King-Jones and Thummel 2005). Ecdysone is a steroid hormone that regulates various aspects of *Drosophila* development and homeostasis. It is well known for co-ordinating the timing of the developmental transitions between the three larval instars. Although several other hormones are also essential for the transitions observed during moulting and metamorphosis, ecdysone is considered to be the master regulator that controls the other hormones in this process. This steroid hormone has also been implicated in playing similar roles in other arthropod species, including other insects (Bownes et al., 1984; Mykles 2011; Yamanaka et al., 2013).

Ecdysone regulates a wide range of several other physiological (e.g. puffing of salivary gland polytene chromosomes, growth, apoptosis, and tissue remodelling) (Ashburner

1990; King-Jones and Thummel 2005; Xu et al., 2020) and behavioural (e.g. germband retraction, head involution, mouth hook movements, feeding, and wandering) (King-Jones and Thummel 2005; Li et al., 2001; Truman 1996) changes that occur during moulting and metamorphosis. Though the ecdysone levels in adults are low as compared to the larval and pupal stages, recent studies have shown that the hormone regulates circadian clock, sleep, lifespan, courtship, reproduction, and memory in adults (Bownes et al., 1984; Ishimoto and Kitamoto 2010; Ishimoto et al., 2009; Schwedes and Carney 2012; Uryu et al., 2015). The concentration of the hormone in adults is very dynamic, but the Malphigian tubules and the male accessory gland have the highest ecdysone titres in 5- and 10-day old adults respectively (Bownes et al., 1984; Schwedes and Carney 2012).

Drosophila utilises cholesterol and other sterols that are acquired through food as a precursor for ecdysone synthesis. Six conserved P450 cytochrome enzymes, Neverland, Spook/Spookier, Phantom, Disembodied, Shadow, and Shade mediate the production of the ecdysone hormone in arthropods (Niwa and Niwa 2014). E produced after the first five steps in the prothoracic gland is secreted into the haemolymph during the larval stages. The terminal step catalysed by Shade that facilitates the final conversion of ecdysone to its active form, 20-HE, occurs in the peripheral tissues (Fig 1.8) (Niwa and Niwa 2014; Pankotai et al., 2010). The active form of ecdysone, 20-HE, typically functions via the heterodimeric complex of the nuclear receptors, Ecdysone Receptor (EcR) and Ultraspiracle (USP). The EcR has three isoforms, each of which can heterodimerise with USP: EcR-A, EcR-B1 and EcR-B2. The only difference between the isoforms is in the unconserved N-terminal region A/B (Cherbas et al., 2003; Lezzi et al., 1999; Mouillet et al., 2001).

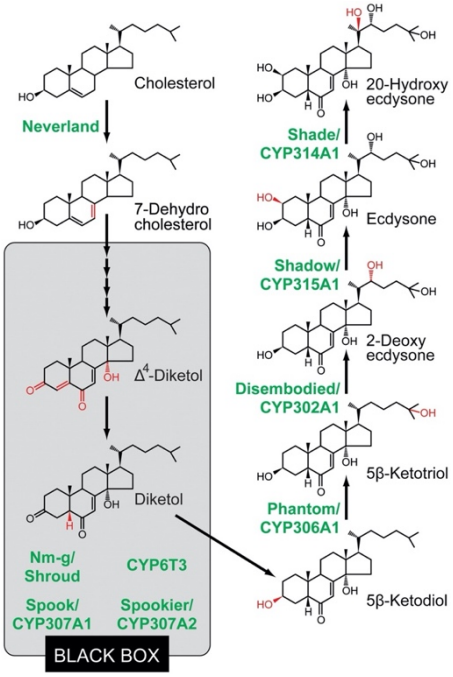

Figure 1.8 Ecdysteroid biosynthesis pathway
The six conserved enzymes of the ecdysone synthesis pathway are in green. Since the exact intermediates between 7-Dehydrocholestrol and 5β-Ketodiol have not been identified (might be attributed to the stability of these intermediates) these conversion steps are often referred to as the Black Box. Reused from Niwa and Niwa, 2014.

The EcR isoforms are temporally, spatially and, functionally distinct, thereby explaining the diverse activities undertaken by the ecdysone hormone (Cherbas et al., 2003; Mouillet et al., 2001; V. Sharma et al., 2017; Talbot et al., 1993). In the absence of the ligand, USP can bind to the ecdysone-response elements (EcREs) and repress the transcription of ecdysone-responsive genes. Upon 20-HE activation, EcR binds to USP, and EcR/USP along with other co-activators, promotes the activation of the previously repressed genes. Some studies have shown EcR and USP can form supramolecular complexes with chaperone proteins such as heat-shock proteins in the cytoplasm (Lezzi et al., 1999).

Therefore, it appears that EcR/USP can function via both the commonly described mechanisms that nuclear receptors utilise to enact their regulatory role (Section 1.2). Hence, it is important to note that EcR/USP has a dual role in regulating transcription of ecdysone-responsive genes.

Ecdysone and androgen hormones have similar functions in the development of the male reproductive system and maintenance of homeostasis in this system. Both these steroid hormones regulate cell and tissue growth and have been implicated in interacting with social and environmental cues such as nutrition and sexual activity. Additionally, the EcR and the AR are both nuclear receptors which share broad structural and functional similarities. Hence, in order to study cellular signalling mechanisms involved in human prostate biology using *Drosophila* SCs, it is imperative to study the role of the ecdysone signalling pathway in adult SCs.

1.14. Endoreplication in post-mitotic growth regulation

Since one overarching focus of my thesis is to understand SC growth regulation, in the coming sections I discuss endoreplication, an important driver of growth that is employed by various cells and tissues in *Drosophila* and other organisms. Interestingly, both the SCs and MCs of the *Drosophila* AG endoreplicate during pupal development and each nucleus is thought to be tetraploid at eclosion (Taniguchi et al., 2014). Furthermore, when I joined the Wilson group, new unpublished data from a previous DPhil student, Josephine Hellberg, was starting to suggest that genome endoreplication might be involved in mating-dependent SC growth (Hellberg 2018), which led me to conduct a detailed investigation into the role of endoreplication in the regulation of adult SC growth.

Some variations in the cell cycle result in a continuous alternation between the Gap (G) phases and the Synthesis (S) phase, thereby completely skipping the Mitotic (M) phase (Orr-Weaver 2015; Zielke, Edgar, and DePamphilis 2013). The cell undergoing this variation is referred to an endocycling cell and the result of the multiple rounds of

endocycles is a polyploid cell with no change in the number of cells and nuclei (Orr-Weaver 2015). Endocycles are generally referred to as endoreplication or endoreduplication cycles (Edgar et al., 2014). Although, all endocycling cells become polyploid, all polyploid cells have not endocycled as this can also arise from cell fusion, acytokinetic mitosis, endomitosis or other impaired cell cycle variants. Endomitosis includes a broader set of cell cycle variants which retain certain aspects of mitosis such as nuclear envelope breakdown, chromosome condensation, spindle formation and/or nuclear division without cytokinesis (Edgar and Orr-Weaver 2001; Orr-Weaver 2015). These variations are generally developmentally programmed or stress-induced and occur in terminally differentiated or post-mitotic cells (Zielke et al., 2013). In this thesis, I will be using the term endoreplication for cells undergoing multiple rounds of endocycling.

Endoreplication has been found to occur in a diverse range of organisms ranging from yeast to humans. Since cellular growth is generally proportional to genomic DNA content in the cell, the phenomenon of endoreplication plays important roles in regulating organ and tissue growth during development (Edgar and Orr-Weaver 2001; Orr-Weaver 2015). In mammals, trophoblast giant cells of the placenta, keratinocytes, megakaryocytes, hepatocytes and cardiomyocytes are some examples of cells that undergo endoreplication (Edgar and Orr-Weaver 2001; Orr-Weaver 2015). In *Drosophila,* endoreplication is commonly observed in many larval tissues, which are frequently highly secretory, such as the salivary gland, fat body, and gut. In adults, the intestinal rectal papillae, follicle and nurse cells of the ovary are known to undergo endoreplication (Orr-Weaver 2015; Shu et al., 2018). A primary function of endoreplication in these cell types is to regulate cell size and tissue organisation. However, there are some indications suggesting an increase in

metabolic activity due to the increase in the genomic DNA content and an increase in secretion (Orr-Weaver 2015).

Recently, endoreplication and polyploidy have been implicated to play a role in cancer development and progression. It has been observed that tumour samples from cancer patients have a higher percentage of polyploid cells. It is still unclear as to how endoreplication hijacks the cell cycle at the cellular level, but it has been reported that these polyploid cells have higher viability than diploid cells in colon cancer. It is speculated that aberrant endoreplication may also initiate genome instability which is a hallmark of cancer (Shu et al., 2018).

Though an initial therapeutic response is observed with Docetaxal, the only first-line treatment for CRPC patients, remission occurs through the development of multinucleated polyploid (MP) cells via endoreplication. Recently, it was suggested that this MP cell population is responsible for prostate cancer relapse in CRPC patients (Mittal et al., 2017). There are several studies that have shown that endoreplication is implicated in promoting cell proliferation using prostate cancer cell lines (Lanzi et al., 2001; Moon et al., 2011; Zekri et al., 2015). Therefore, endoreplication could be a mechanism through which development and progression of cancer occurs.

1.15. Mechanisms of endoreplication in *Drosophila*

Endoreplication is a very complex and diverse phenomenon which is differentially regulated in different cells and organisms. The core of what regulates endoreplication is still not well-understood. In *Drosophila*, the mechanistic aspect of endoreplication is generally studied in the proliferative phase of embryogenesis, larval salivary gland,

ovarian follicle cells and nurse cells (Edgar and Orr-Weaver 2001; Zielke, Edgar, and DePamphilis 2013).

The switch to a G-S endocycle (Fig 1.9) is achieved by reducing the levels of Cdksthat promote G2 to M phase transition (Cyc A and Cyc B) without affecting the Cdks that drive G1 to S phase progression (Edgar and Orr-Weaver 2001; Zielke et al., 2013). This reduction in M-phase Cdks (M-Cdks) has been observed in several organisms such as yeast, mice, flies and plants. Additionally, the levels of S-phase Cdks (S-Cdks) should fluctuate cyclically, as consistently high levels of S-Cdks can block endoreplication. In salivary glands, it was demonstrated that constitutive expression of the S-phase Cyclin, CycE, which activates its Cdk partner, Cdk2, blocks endoreplication after a single round of replication (Zielke et al., 2011). This is consistent with a model in which a reduction in S-Cdks is essential to allow for the pre-replication complex (pre-RC) to assemble on the origin of replication of the genomic DNA. The pre-RC complex consists of origin-replicating complex proteins, Cdc6, double parked (*Drosophila* orthologue of Cdt1), and mini-chromosome maintenance complex 2-7 and is responsible for initiation of DNA replication (Edgar et al., 2014; Zielke et al., 2011).

In mitotic cells, an E3 ubiquitin ligase, anaphase promoting complex Fzy (APC^{Fzy}), which is activated during M-phase, degrades the M-Cdks and the Cdt1 inhibitor, geminin (Gem), thereby allowing the pre-RC to be assembled and license DNA. Though this mechanism is not present in endoreplicating cells, a G1-specific variant of APC ($APC^{Fzr/Cdh1}$), has been shown to mediate the degradation of Gem and other cell cycle components, thereby inducing the required periodicity in the levels of the S-Cdks in larval salivary glands

(Zielke et al., 2011). However, the mechanisms involved in maintaining the cyclical levels of S-Cdks are very variable.

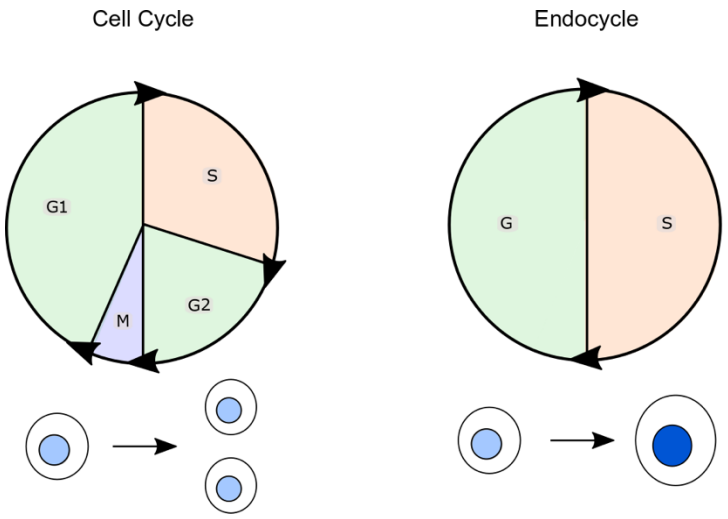

Figure 1.9 Cell cycle vs Endocycle
A diagrammatic representation of the general difference between the cell cycle and the endocycle. When a cell goes through the cell cycle it produces two smaller daughter cells with the same ploidy as the parent. When a cell goes through the endocycle it goes through only two phases - G-phase and S-phase - and this results in the same cell becoming bigger with a higher ploidy than before the start of the endocycle.

Studies in the salivary gland have explained how the periodicity in CycE/Cdk2 levels is maintained in endoreplication. It has been demonstrated that the E2F1 transcription factor promotes the transcription of *CycE* to initiate S-phase. Activation of an E3 ubiquitin ligase complex, $CRL4^{Cdt2}$, which targets substrates containing the proliferating cell nuclear antigen (PCNA)-interacting protein (PIP) domain, occurs during S-phase. These PIP-containing molecules bind to the PCNA, whose expression is promoted by CycE. During the progression of S-phase, $CRL4^{Cdt2}$ degrades the PIP-containing E2F1, thereby reducing the levels of E2F1 and CycE/Cdk2, which allows for the assembly of the pre-RC (Zielke et al., 2011). CycD/Cdk4, an upstream regulator of E2F1, has been shown to induce hyperploidy, thereby demonstrating the importance of E2F1 in regulating endoreplication. E2F1 has also been implicated to drive enteroblast/enterocyte growth via endoreplication. Several other growth signals (Notch/Delta and EGFR/Ras/MAPK)

(Edgar and Orr-Weaver 2001; Edgar et al., 2014; Xiang et al., 2017), stress signals (epithelial damage and injury) (Xiang et al., 2017), and differentiation signals (Orr-Weaver 2015; Zielke et al., 2013) are considered to be upstream of these cell cycle processes and help induce endoreplication.

1.16. Relevant previous work by the Wilson group

In this section I will discuss the key results of Aaron Leiblich - who fortunately was also my co-supervisor - which formed the basis for my DPhil thesis work. He was instrumental in developing the necessary tools for studying cell biology mechanisms in the SCs (Section 2.3). As discussed in Section 1.8, Leiblich observed that SCs grow further upon mating in a BMP-dependent manner. Leiblich and Josephine Hellberg also conducted some initial experiments on the control of SC growth by EcR signalling in both virgin and mated males. Additionally, as mentioned in Section 1.14, preliminary results from Hellberg showed that genome endoreplication might play a role in the regulation of mating-dependent growth. My DPhil work has significantly contributed towards our understanding of SC growth and endoreplication regulation by the BMP and EcR signalling pathways in virgin and mated males. Some of my data described in Chapters 3 and 4 have been included in Leiblich et al., 2019, on which I am a joint first-author. I am in the final stages of finishing another first-author manuscript which includes Leiblich's initial data discussed in 1.16.2 and my results described in Chapter 6. I also list a few outstanding questions that arise from the results presented in each subsection which piqued my interest, as I initiated my DPhil studies.

1.16.1. EcR/USP signalling in *Drosophila* SCs

1.16.1.1. EcR-B1 is the major EcR isoform present in SCs

In the AG, immunostaining with a pan-EcR antibody, showed that EcR is expressed in the nuclei of only the muscle cells and the SCs. No staining was observed in the MCs, therefore suggesting that the EcR plays a role in specifically regulating SC biology within the AG epithelium. The common EcR heterodimer partner, USP, is also expressed in the nuclei of the SCs. Since the isoform-specific EcR antibodies did not give a robust signal, the individual EcR isoforms were knocked down in SCs, and the AGs stained with the pan-EcR antibody. With this approach, it was determined that the EcR-B1 is the major isoform that is expressed in the SCs. When EcR-A was knocked down, no change in EcR expression patterns in the AG was observed (Leiblich et al., 2019); this does not eliminate the possibility that it is synthesised at relatively low levels compared to EcR-B1. One issue that arose during my DPhil was that the publicly available anti-pan-EcR monoclonal antibody used for this work ceased to stain consistently several years ago, so some experiments that I would have liked to have performed to assess EcR expression have not been possible.

1.16.1.2. EcR regulates SC growth in virgin males independently of USP

Apart from expression in the SCs, EcR was also shown to regulate SC growth in virgins. It was shown that knocking down EcR resulted in a reduced nuclear growth in SCs. Although USP is expressed in SCs, reduction in USP protein levels, had no effect on SC growth. Therefore, this suggests that an unconventional form of EcR signalling regulates SC growth in virgin males (Leiblich et al., 2019).

Outstanding questions:

- How does EcR signalling promote SC growth? What are the mechanisms that EcR regulates which leads to increase in growth in SCs?
- As the expression levels of different EcR isoforms vary significantly in SCs, is it possible that these isoforms play different roles in the regulation of growth?
- Does EcR signalling also regulate SC growth that occurs after mating, and if present, does a similar USP-independent EcR signalling axis also regulate this growth?
- Since USP is expressed in the SCs, does it have a functional role in the SCs?

1.16.1.3. EcR protein levels are regulated by BMP signalling in the SCs

Aaron Leiblich showed that overexpression of the EcR isoforms in the SCs did not increase EcR protein levels. However, when the EcR isoforms were co-overexpressed with Tkv^{act}, an increase in the EcR protein levels was observed. Overexpression of a synthetic isoform of the EcR that lacks the N-terminal domain, EcR-C, resulted in an increase in EcR protein levels, even with normal BMP signalling. Therefore, BMP signalling regulates EcR protein levels via a mechanism involving its N-terminal domain or the sequences encoding it (Leiblich et al., 2019).

Outstanding questions:

- How does the BMP pathway regulate EcR i.e. at a transcriptional, post-transcriptional, translational or post-translational level?
- Does BMP signalling mediate its effect on growth by only controlling the EcR protein levels or can it regulate growth independently of EcR as well?

1.16.2. The Rbf/E2F1 axis regulates EcR protein levels in SCs

Similar to AR regulation by Rb/E2F in prostate cancer (Section 1.5), unpublished work of Aaron Leiblich and Dhruv Sharma, showed that EcR protein levels were regulated by Rbf (*Drosophila* homologue of Rb) and E2F1 (*Drosophila* activating E2F protein) (Leiblich 2015). Using a pan-EcR antibody to stain the AG with SCs expressing an *Rbf*-RNAi (Section 2.3.2), they observed that EcR protein levels were highly increased as compared to controls, to the extent that EcR was also present in the cytoplasm of these cells. In order to determine the effects of upregulation of E2F1 activity, they overexpressed E2F1 with its binding partner, Dumpy (DP), which is essential for proper E2F1 activity. They observed that overexpression of E2F1/DP phenocopied all the effects observed with knocking down Rbf in SCs. Expressing a constitutively activated form of Rbf, Rbf^{CA} which cannot be phosphorylated, in SCs, was able to completely suppress EcR protein production, mirroring the phenotype observed with expression of *EcR*-RNAi. Interestingly, many SCs became mononucleate when Rbf^{CA} was expressed in SCs. However, *E2F1*-RNAi did not seem to have any effect on the EcR protein levels in SCs. As a negative control they expressed a combination genotype of E2F1/DP with EcR-RNAi in the SCs and no EcR expression was observed. Furthermore, the SCs and the SC nuclei in the *Rbf*-RNAi and E2F1/DP genetic backgrounds were extremely large, thereby suggesting that loss of Rbf results in an increase in cellular and nuclear growth in SCs (Fig 1.10). This parallels the observation that loss of Rbf results in prostate cancer progression.

Outstanding questions:

- How do the other cell cycle components interact with EcR to regulate SC growth?
- Do they also interact with BMP signalling to control SC growth?
- Do they differentially regulate SC growth in virgin males and mated males?

- Does Rbf and E2F1 affect nucleation state in MCs? Are there any other signalling pathways that control the nucleation state in SCs?

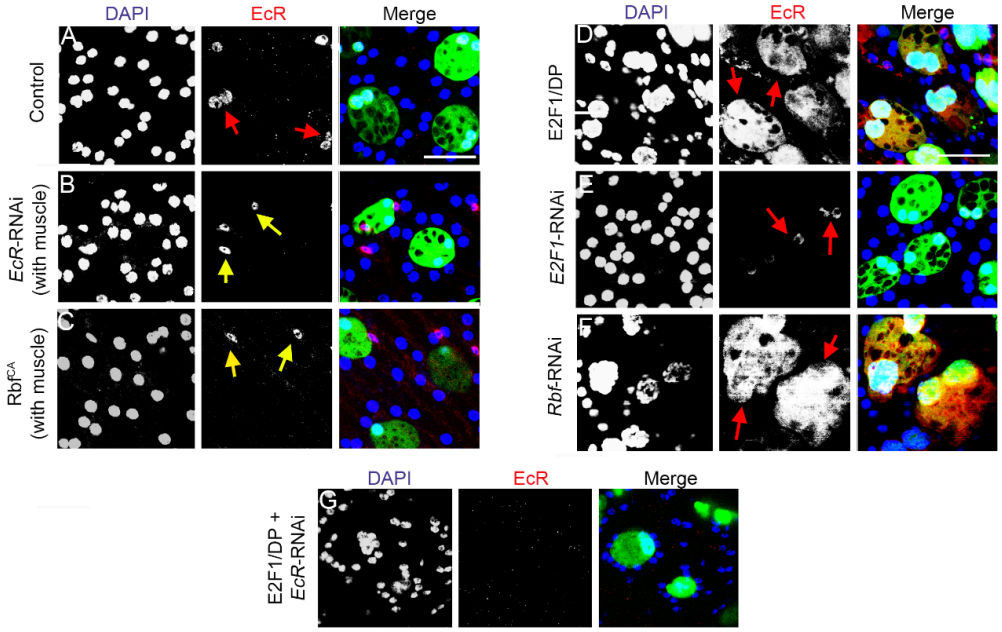

Figure 1.10 Rbf/E2F1 regulates EcR protein levels in SCs (Courtesy of Aaron Leiblich and Dhruv Sarma)
A-G: Images show distal tips of AGs dissected from 6-day-old males. Transgenes were specifically expressed in the SCs along with nuclear GFP (which also stains the cytosol) under esg^{ts}F/O control (refer to Section 2.3 for further details). Merge channel includes DAPI channel (nuclei staining; blue), GFP channel (SCs expressing nuclear GFP, which also stains cytoplasm; green) and Cy3 channel (pan-EcR antibody staining; red). Red arrows mark SCs expressing EcR. Yellow arrows mark muscle cells expressing EcR as a positive control (B,C). Scale bars correspond to 20 µm.

1.17. Aims and Objectives

To further the initial work on SC growth regulation by BMP and EcR signalling in the lab, I have explored the possibility of developing the SC as a model to study prostate cancer and CRPC. I employed the '*Mammals to Drosophila to Mammals*' approach to build this model. I have focussed on establishing parallels with the known prostate cancer and CRPC signalling signatures thereby fulfilling the '*Mammals to Drosophila'* part of the approach. By the end of my thesis, I hope to have convinced the reader of the

importance of pursuing the '*Drosophila to Mammals*' part of the approach with the SC model in order to investigate genetic mechanisms that might be involved in the progression of prostate cancer.

I was also interested in utilising the lab's pioneering research tools to study the role played by the BMP and EcR signalling in the regulation of the secretory activity of the SCs (Fan et al., 2020), as there is a growing interest in the possibility of using prostasomes as a possible biomarker for prostate cancer (Vlaeminck-Guillem 2018; Zijlstra and Stoorvogel 2016). Interestingly, a recent clinical trial by the Loudig lab at Hackensack University Medical Centre is focussing on validating the use of prostasome isolation techniques as a robust clinical diagnostic tool for prostate cancer. Another objective of this trial is to identify the molecular cargo of the isolated prostasomes and determine whether this information can be used to predict the stage of prostate cancer (Prostasomes as Diagnostic Tool for Prostate Cancer Detection 2018).

The overall objectives for my DPhil were as follows:

- To determine whether ecdysone-independent EcR activity is involved in adult SC growth, and if present, define the cellular functions of hormone-dependent and –independent signalling in SCs
- To investigate the role of BMP and EcR signalling in the regulation of SC secretory activity
- To study the role of cell cycle regulators such as Rbf/E2F and cyclins on SC growth and BMP-dependent EcR signalling
- To dissect out other roles of Rbf/E2F signalling in SCs, including the control of binucleation

Chapter-2:

Materials and Methods

2.1. Fly Husbandry

Flies were reared in vials or bottles containing standard cornmeal agar medium (Table 2.1) and no additional dried yeast was added to the vials or bottles except for the *ecd*^{1} mutant stocks. Fly stocks were maintained at 18°C and were transferred onto new food every 7-10 days. Experimental crosses were either kept at 18°C or 25°C and were flipped onto new food every 3-4 days.

For ecdysone feeding experiments, 20-HE-containing food was prepared by mixing standard medium with a 10 mM 20-HE (Selleckchem/Cambridge Biosciences) stock solution to a final concentration of 0.1 mM with or without 0.2 mM 5-ethynyl-2'-deoxyuridine (EdU; Section 2.12).

Table 2.1: Cornmeal Agar Medium Recipe

Reagents	Quantity	Source
Bacteriological agar	12.60 g/L	F Gutkind & Co. Ltd
Calcium chloride dihydrate	0.70 g/L	SigmaAldrich®
Potassium sodium tartrate	8.60 g/L	SigmaAldrich®
Methyl-4-hydroxybenzoate (Nipagen; diluted in ethanol)	2.50 g/L	SigmaAldrich®
Cornmeal	75.00 g/L	BTP Drewitt
Dried inactivated baker's yeast (Saccharomyces cerevisiae)	31.48 g/L	SigmaAldrich®
Ethanol	300 mL	SigmaAldrich®
Water	Up to 1L	

2.2. Fly Stocks

The following tables are a collection of *Drosophila* stocks that I have used during my DPhil. In these tables, I have also mentioned the source from where these fly stocks were obtained. Most of them were ordered from public stock centres - Bloomington *Drosophila* Stock Centre (Stock number mentioned with prefix BL) and Vienna *Drosophila* Stock Centre (Stock number mentioned with prefix VD). A few of the fly stocks were kindly gifted by other laboratories.

Table 2.2: GAL4 driver lines

Notation	Genotype	Source	Description
esg^{ts}F/O	*w; esg-GAL4 tub-GAL80^{ts} UAS-GFP$_{nls}$/CyO; UAS-flp act>CD2>GAL4/TM6*	B. Edgar (Jiang et al., 2009)	Temperature sensitive SC specific driver
CD63-GFP	*w; UAS-CD63-GFP, tub-GAL80^{ts}; dsxGAL4/SM5.TM6*	L.Corrigan (Corrigan et al., 2014)	SC-specific driver that expresses *UAS-CD63-GFP*
DTBtl	*w-; tub-GAL80^{ts}/CyO; dsx-GAL4, UAS-Btl-GFP/TM6B*	C. Mendes *tub-Gal80^{ts}* (BL 7108), *dsx-Gal4* (S. Goodwin), *Btl-GFP* (BL 41802)	SC-specific driver that expresses *UAS-Btl-GFP*
DTR6	*w-; Rab6-CFP, tub-GAL80^{ts}; dsx-GAL4*	C. Mendes *CFP-Rab6* (S.Eaton), *tubGal80^{ts}* (BL 7108), *dsx-Gal4* (S. Goodwin)	SC specific driver that expresses *UAS-CFP-Rab6*
DTR11	*w-; tub-GAL80^{ts}; Rab11-YFP, dsx-GAL4/Xa*	P. Marie *YFP-Rab11* (S. Eaton),*tubGal80^{ts}* (BL 7108),*dsx-Gal4* (S.Goodwin)	SC specific driver that expresses *UAS-YFP-Rab11*
DTR19	*w-; tub-GAL80^{ts}; dsx-GAL4, Rab19-YFP*	C. Mendes *YFP-Rab19* (S. Eaton), *tubGal80^{ts}* (BL 7108), *dsx-Gal4* (S. Goodwin)	SC specific driver that expresses *UAS-YFP-Rab19*

Acp26Aa^{ts}	*w Acp26Aa-GAL4; UAS-GFP$_{nls}$, tubGAL80^{ts}*	L. Corrigan	Temperature sensitive MC specific driver

Table 2.3: Control lines

Notation	Genotype	Source	Description
w^{1118}	*w^{1118}*;;	L. Partridge (Hazelrigg, Levis, and Rubin 1984)	Partial deletion of white locus; Considered controls as most of the stocks are in a w$^-$ background
Canton S	;;	H. Steller	Wild type

Table 2.4: Ecdysone signalling stocks

Notation	Genotype	Source	Description
ecd^1	*ecd^1 st^1 ca^1*	BL 218	Temperature-sensitive expression of *ecd^1* mutant allele in entire fly
spo-RNAi	y[1] sc[*] v[1]; P{y[+t7.7] v[+t1.8]=TRiP.HMC03251}attP2	BL 51496	Expression of *spo* dsRNA under *UAS* control
shd-RNAi	y[1] sc[*] v[1]; P{y[+t7.7] v[+t1.8]=TRiP.HMC06461}attP40	BL 67356	Expression of *shd* dsRNA under *UAS* control

Table 2.5: BMP and EcR signalling stocks

Notation	Genotype	Source	Description
Dad	*w-; P{w$^+$ UAS-Dad}*	D. Bennett (Tsuneizumi et al., 1997)	Expression of entire coding region of *Dad* under *UAS* control
Tkv^{act}	*w[*]; P{w[+mC]=UAS-Tkv^{Q253D}}3/TM3,Sb[1] Ser[1]*	Basler (Nellen et al., 1996)	Expression of construct that mimics activated phosphorylation state of *Tkv* receptor under *UAS* control
EcR-RNAi	*w[1118]; P{w[+mC]=UAS-EcR-RNAi}104*	BL 9327	Expression of *EcR* dsRNA common to all isoforms under *UAS* control
EcR-A-RNAi	*w[1118]; P{w[+mC]=UAS-EcR.A.dsRNA}91/TM3, P{w[+mC]=ActGFP}JMR2, Ser[1]*	BL 9328	Expression of *EcR-A* dsRNA under *UAS* control

EcR-B1-RNAi	*w[1118]; P{w[+mC]=UAS-EcR.B1.dsRNA}168*	BL 9329	Expression of *EcR-B1* dsRNA under *UAS* control
EcR-C	*w[1118];; P{w[+mC]=UAS-EcR.C}TP1-4*	BL 6868	Expression of N-terminal truncated form of *EcR* coding region under *UAS* control
EcR-C + Tkv^{act}	*w[*]; UAS-EcR.C, UAS-Tkv^{act}/TM6*	C. Wilson *EcR-C* (BL 6868), *Tkv^{act}* (Basler)	Co-expression of *EcR-C* and *Tkv^{act}* under *UAS* control
EcR-RNAi + Tkv^{act}	*w[*]; UAS-EcR-RNAi; UAS-Tkv^{act}/SM5.TM6*	C. Wilson *EcR*-RNAi (BL 9327), *Tkv^{act}* (Basler)	Co-expression of *EcR*-RNAi and Tkv^{act} under UAS control
Dad + EcR-C	*w[*]; UAS-Dad; UAS-EcR.C/SM5.TM6*	C. Wilson *Dad* (Daimark Bennett), *EcR-C* (BL 6868)	Co-expression of Dad and EcR-C under UAS control

Table 2.6: Cell cycle signalling and binucleation regulatory stocks

Notation	Genotype	Source	Description
Rbf^{CA}	*w[*]; P{w[+mC]=UAS-Rbf.280}3/TM3, Sb[1]*	BL 50748	Expression of constitutively active *Rbf* under *UAS* control
Rbf-RNAi (III)	*y[1] sc[*] v[1] sev[21]; P{y[+t7.7] v[+t1.8]=TRiP.HMS03004}attP2/TM3, Sb[1]*	BL 36744	Expression of *Rbf* dsRNA under *UAS* control
E2F1/DP (III)	*w[1118]; P{w[+mC]=UAS-E2f1.N}3B P{w[+mC]=UAS-Dp.D}1-4b/TM6B, Tb[1]*	BL 4770	Co-expression of *E2F1* and *Dp* under *UAS* control
E2F1/DP (II)	*w[1118]; P{w[+mC]=UAS-E2f1.N}5A P{w[+mC]=UAS-Dp.D}8C/CyO*	BL 4774	Co-expression of *E2F1* and *Dp* under *UAS* control
$E2F1^{PIP3A}$	*w[*]; P{w[+mC]=UASp-GFP-E2f1.PIP-3A}10*	BL 34059	Expression of an *E2F1* mutant lacking PIP domain (required for E2F1 degradation during S-phase) under *UAS* control
E2F1-RNAi	*y[1] v[1];; P{y[+t7.7] v[+t1.8]=TRiP.JF01741}attP*	BL 31214	Expression of *E2F1* dsRNA under *UAS* control

CycE	*w[*]; P{w[+mC]=UAS-CycE.L}ML1*	BL 4781	Expression of *CycE* under *UAS* control
CycE-RNAi (II)	*y[1] sc[*] v[1] sev[21]; P{y[+t7.7] v[+t1.8]=TRiP.GL00511}attP40* *(Chromosome: II)*	BL 36092	Expression of *CycE* dsRNA under *UAS* control
CycE-RNAi (III)	*y[1] sc[*] v[1] sev[21]; P{y[+t7.7] v[+t1.8]=TRiP.HMS00060}attP2 (Chromosome: III)*	BL 33654	Expression of *CycE* dsRNA under *UAS* control
CycD/cdk4	*w; UAS-cycD UAS-cdk4/CyO (J49)*	B. Edgar (Datar et al., 2000)	Co-expression of *CycD* and its kinase *cdk4* under *UAS* control
CycD-RNAi	*y[1] sc[*] v[1] sev[21]; P{y[+t7.7] v[+t1.8]=TRiP.HMS00059}attP2 (Chromosome: III)*	BL 33653	Co-expression of *CycD* dsRNA under *UAS* control
p53	*w; P[w+ UAS-p53]/TM6 Hu*	J.Abrams	Expression of p53 under UAS control
Mud-RNAi	*y[1] sc[*] v[1] sev[21]; P{y[+t7.7] v[+t1.8]=TRiP.HMS01458}attP2*	BL 35044	Expression of *Mud* dsRNA under *UAS* control

Table 2.7: BMP/EcR and cell cycle regulator combination lines

Notation	Genotype	Source	Description
EcR-RNAi + CycE	*w⁻; UAS-EcR-RNAi /CyO; UAS-CycE/TM6B*	A. Sekar *EcR*-RNAi (BL 9327), *CycE* (BL 4781)	Co-expression of *EcR*-RNAi and *CycE* under UAS control
EcR-RNAi + E2F1/DP	*w⁻; UAS-EcR-RNAi; UAS-E2F1, UAS-DP /SM5.TM6*	A. Sekar *EcR*-RNAi (BL 9327), *E2F1/DP* (III) (BL 4770)	Co-expression of *EcR*-RNAi and *E2F1/Dp* under *UAS* control
EcR-C + Rbf^{CA}	*w⁻; if/CyO;UAS-EcR.C ,UAS-Rbf^{CA} /TM6B*	A. Sekar *EcR-C* (BL 6868), *Rbf^{CA}*(BL 50748)	Co-expression of EcR-C and Rbf^{CA} under UAS control
Tkv^{act} + Rbf^{CA}	*w⁻; if/CyO; UAS-Tkv^{act}, UAS-Rbf^{CA}/TM6B*	A. Sekar *Tkv^{act}*(Basler), *Rbf^{CA}*(BL 50748)	Co-expression of *Tkv^{act}* and *Rbf^{CA}* under UAS control

Dad+ CycD/cdk4	*w⁻; UAS-CycD.cdk4, UAS-Dad/CyO*	A. Sekar *Dad* (Edgar), *CycD/cdk4* (Edgar)	Co-expression of *Dad* and *CycD/cdk4* under *UAS* control
Dad+ E2F1/DP	*w⁻; UAS-Dad /CyO; UAS-E2F1,UAS-DP /TM6B*	A. Sekar *Dad* (Edgar), *E2F1/DP* (III) (BL 4770)	Co-expression of Dad and *E2F1/Dp* under *UAS* control
E2F1/DP + *CycE*-RNAi	*w⁻; UCycE-RNAi (II)/CyO; UAS-E2F1, UAS-DP /TM6B*	A. Sekar *CycE*-RNAi (II) (BL 36092), *E2F1/DP* (III) (BL 4770)	Co-expression of *CycE* dsRNA and *E2F1/Dp* under *UAS* control
E2F1/DP + *shd*-RNAi	*w⁻; UAS-shd-RNAi; UAS-E2F1,UAS-DP /TM6B*	A. Sekar *shd*-RNAi (II) (BL 67356), *E2F1/DP* (III) (BL 4770)	Co-expression of *shd* dsRNA and *E2F1/Dp* under *UAS* control

Table 2.8: Balancer stocks

Notation	Genotype	Source	Description
DCDB	*w⁻;If /CyO; MKRS/TM6*	C.Mendes	Both arms of chromosomes II and III have either markers or balancers
FRT/SM5.TM6	*w; Df(2L)170B FRT 40A/SM5 TM6*	C.Wilson	*Df(2L)170B FRT 40A* is a recessive lethal mutant

2.3. Fly genetics

In Chapters 3, 4 and 6, I have extensively used the *esg^{ts}F/O* driver to express UAS-transgenes specifically in SCs under the control of *esg*-GAL4 and the temperature-sensitive GAL4 repressor, GAL80 (GAL80^{ts}). At 18˚C, the GAL80^{ts} actively represses GAL4 expression, but when switched to 28.5˚C GAL80^{ts} becomes inactive. This induces FLP-mediated recombination of the *act>CD2>GAL4* construct which then drives long-term, UAS-mediated expression of nuclear GFP, as well as other transgenes in the SCs (Leiblich et al., 2012). In Chapters 4 and 5, I use the SC-specific *dsx-GAL4* driver, under

the control of GAL80^{ts}, combined with *UAS-CD63-GFP*, *UAS-Btl-GFP*, *CFP-Rab6* (gene trap controlled by *Rab6* regulatory elements), *YFP-Rab11* (gene trap controlled by *Rab11* regulatory elements) or *YFP-Rab19* (gene trap controlled by *Rab19* regulatory elements), to express the required transgene along with the corresponding marker under investigation. Fly crosses were cultured at 18˚C or 25˚C to allow for normal development. Newly eclosed virgin males of the appropriate genotype were selected and transferred to 28.5˚C for 6-day expression either on normal food or EdU-containing food (Section 2.12).

2.4. Scheme for genetic combination generation

In Chapter 6, I use genetic combinations to study the interaction between the BMP and EcR signalling pathways, and cell cycle regulators. Below are mating schemes that I utilised to construct these combinations and recombinants.

2.4.1. Scheme for combination of transgenes on different chromosomes

UAS-A (referred to as A) on 2nd chromosome and UAS-B (referred to as B) on 3rd chromosome. Same coloured text refers to the same fly. If either A or B was a TRiP line, flies with coloured eyes were chosen and primers specific to the vector of the corresponding TRiP line (such as VALIUM 10/20/22) were used to test for the presence of the RNAi construct in the genomic DNA of male fly collected in Step 2 once larvae from Step 3 cross are visible (Section 2.6).

				Flies collected for use in next steps
1	;A; [♂]	X	w$^-$; $\frac{\text{If}}{\text{CyO}}$; $\frac{\text{MKRS}}{\text{TM6}}$ [♀^{v}]	w$^-$; $\frac{\text{A}}{\textit{If}}$; $\frac{+}{\text{TM6}}$ [♂/♀^{v}]
	;;B [♂]	X	w$^-$; $\frac{\text{If}}{\text{CyO}}$; $\frac{\text{MKRS}}{\text{TM6}}$ [♀^{v}]	w$^-$; $\frac{+}{\text{CyO}}$; $\frac{\text{B}}{\text{MKRS}}$ [♂/♀^{v}]
2	w$^-$; $\frac{\text{A}}{\textit{If}}$; $\frac{+}{\text{TM6}}$ [♂/♀^{v}]	X	w$^-$; $\frac{+}{\text{CyO}}$; $\frac{\text{B}}{\text{MKRS}}$ [♀^{v}/♂]	w$^-$; $\frac{\text{A}}{\text{CyO}}$; $\frac{\text{B}}{\text{TM6}}$ [♂]
3	w$^-$; $\frac{\text{A}}{\text{CyO}}$; $\frac{\text{B}}{\text{TM6}}$ [♂]	X	w$^-$; $\frac{\text{If}}{\text{CyO}}$; $\frac{\text{MKRS}}{\text{TM6}}$ [♀^{v}]	w$^-$; $\frac{\text{A}}{\text{CyO}}$; $\frac{\text{B}}{\text{TM6}}$ [♂/♀^{v}]

2.4.2. Scheme for combination of transgenes on same chromosome

UAS-A (referred to as A) on 2nd chromosome and UAS-B (referred to as B) on 2nd chromosome. Same coloured text refers to the same fly. A similar scheme was used when both the genes were on the 3rd chromosome. Primers specific to A and B (forward primer had some sequences specific to UAS to amplify only the transgene) were used to check if both the transgenes were present in the genomic DNA of the recombinant male fly collected in Step 3 once larvae from Step 4 cross are visible (Section 2.6).

				Flies collected for use in next steps
A	;A; [♂]	X	$w^-; \frac{If}{CyO}; \frac{MKRS}{TM6}$ [♀^{v}]	$w^-; \frac{A}{If}; \frac{+}{TM6}$ [♂/♀^{v}]
	;;B [♂]	X	$w^-; \frac{If}{CyO}; \frac{MKRS}{TM6}$ [♀^{v}]	$w^-; \frac{B}{CyO}; \frac{+}{MKRS}$ [♂/♀^{v}]
B	$w^-; \frac{A}{If}; \frac{+}{TM6}$ [♂/♀^{v}]	X	$w^-; \frac{B}{CyO}; \frac{+}{MKRS}$ [♀^{v}/♂]	$w^-; \frac{A}{B}; \frac{+/MKRS}{+/TM6}$ [♀^{v}]
C	$w^-; \frac{A}{B}; \frac{+/MKRS}{+/TM6}$ [♀^{v}]	X	$; \frac{FRT}{SM5.TM6};$ [♀^{v}]	$w^-; \frac{A,B}{SM5.TM6};$ [♂] *(Darkest eye colour)*
D	$w^-; \frac{A,B}{SM5.TM6};$ [♂]	X	$; \frac{FRT}{SM5.TM6};$ [♀^{v}]	$w^-; \frac{A,B}{SM5.TM6};$ [♂/♀^{v}]

2.5. Genomic DNA isolation

A single whole fly was frozen in a PCR tube at -20˚C for at least 1 hour. 50µL of squishing buffer with freshly added Proteinase-K (Table 2.10) to the PCR tube and the fly was squished using a sterile 10/20 µL pipette tip for 5-10 seconds. The genomic DNA was extracted using the Table 2.11 program on a 96-well Veriti thermocycler (Applied Biosystems), which was stored at -20˚C for 3-4 months.

Table 2.9: 100mM Tris-Cl Stock

Reagents	Quantity	Source
Trizma HCL	3.54 g	Sigma Aldrich
Trizma base	3.54 g	Sigma Aldrich
Deionised water (adjust pH to 8.2 with HCl)	Up to 500 mL	Sigma Aldrich

Table 2.10: Squishing Buffer Stock

Reagents	Final Concentration	Source
Tris-Cl (pH 8.2) [Table 2.9]	10 mM	Sigma Aldrich
EDTA	1mM	Sigma Aldrich
NaCl	25 mM	Sigma Aldrich
Proteinase-K (Added freshly)	200 µg/mL	Roche

Table 2.11: DNA extraction thermocycling conditions

Temperature	Time
37°C	30 min
95°C (inactivates Proteinase-K activity)	2 min
4°C	-

2.6. PCR to verify transgene recombination and combination stocks

The one-step REDTaq® ReadyMix™ PCR Reaction Mix was used for PCR amplification in order to verify the recombination stocks. The reagents in Table 2.12 were mixed in the order as listed on ice. A master mix was generally made when several PCR reactions were done simultaneously. Thermocycling conditions in Table 2.13 were used with transgene specific primers (Table 2.14).

Table 2.12: PCR Red-Taq reaction

Reagent	Quantity (12µL)
Deionised Water	3 µL
Forward Primer (1µM)	1 µL
Reverse Primer (1µM)	1 µL
RedTaq Ready Mix	6 µL
Genomic DNA (extracted according to Section 2.5)	1 µL

Table 2.13: PCR Red-Taq thermocycling conditions

Step	Temperature	Time
Initial Denaturation	94°C	5 min
30-35 cycles:		
	94°C	30 sec
	Tm	30 sec/kbp
	72°C	45 sec
Final Extension	72°C	5 min
Final Hold	4°C	-

Table 2.14: Primers for verification of recombination and combination stocks

Transgene	Forward Primer (5' to 3')	Reverse Primer (5' to 3')
Tkv^{act}	CTGGACCAGGATCAGAGGGA	GCGTCGCTTGTAGGTGAAAC
Rbf^{CA}	CAGGCGGAAATTCGGAACAA	CTTCTCGCACAGTGACAGC
shd-RNAi (VALIUM-20 vector)	CGCAGCTGAACAAGCTAAAC	TAATCGTGTGTGATGCCTACC

2.7. Quantitative RT-PCR

Total RNA was extracted using the RNAqueous™ Micro Total RNA Isolation Kit (Thermo Fisher) according to the manufacturer's protocol. RNA was quantified using the NanoDrop ND-1000 Spectrophotometer (New Brunswick) and then reverse transcribed into cDNA using the SuperScript™ IV VILO™ Reverse Transcription Master Mix Kit (Thermo Fisher). Gene expression was assessed via quantitative real-time PCR (qRT-PCR) using the TaqMan Universal Master Mix II (Thermo Fisher) and monitored using a StepOne™ Real-Time PCR system (Applied Biosystems). Each sample was analysed in triplicate and mRNA levels normalised to Actin-5C. Predesigned Taqman RT-PCR probes were used.

Table 2.15: Predesigned Taqman Gene Expression Assay IDs

Transgene	Assay ID
EcR	Dm01811602_g1
Act-5C	Dm02361909_s1

2.8. Multiple mating experiments

Newly eclosed virgin males (~10) of the required genotype were collected and each male was placed in individual vials with ten virgin w^{1118} females. w^{1118} females are visually impaired, which will affect mating success and frequency. However, since the males were allowed to mate with 10 females over a period of 6 days, these effects of w^{1118} are unlikely to dramatically affect overall mating frequency. Indeed, the frequency of SCs exhibiting endoreplication was consistently ~ 25% in control males, suggesting that they had all mated at similar levels. The protocol is slightly different from one used in Leiblich et al., 2012, as I consistently used 10 females instead of at least 6 females. It is also different from the experiments conducted by Josephine Hellberg for her thesis work, as she used two males and fifteen females. I did not follow this protocol as I wanted to control for any competition amongst the males. For virgin experiments for every genotype, approximately 10 males were placed together in a single vial. A similar setup was used for the nuclear size assay, DAPI intensity assay and EdU uptake assay. Adult males were kept at 28.5˚C for 6 days and the flies were then dissected on the sixth day. The experiments were performed for 6 days, primarily because SC nuclei continue to grow over this period in virgin males, but show little additional growth thereafter in controls in (Leiblich et al., 2012). Males have the ability to mate as early as 16 hours and are fully sexually mature about 3 days after eclosion (Ruhmann et al., 2016). The mating vials were checked for presence of larvae before dissection in order to ensure that mating had occurred.

2.9. Sample preparation for fixed confocal imaging

The protocol used for fixing the AG was based on previously published methods by our lab (Corrigan et al., 2014; Leiblich et al., 2012, 2019; Redhai et al., 2016). Flies were

briefly anaesthetised using CO_2. The whole male reproductive system was carefully pulled out of the body cavity, keeping accessory gland and the ejaculatory duct, with fine forceps in 4% paraformaldehyde (PFA) dissolved in PBS and were transferred to Eppendorf tubes containing PFA for 20 min at room temperature and then washed in 1 ml PBST (1 x PBS, 0.3% Triton X-100 (Sigma-Aldrich)) for 5 min. They were suspended in PBS and mounted onto slides using DAPI-containing Vectashield (Vector Laboratories). The glands were imaged using an upright Zeiss LSM 880 Airy Scan confocal microscope. The Zeiss Plan-Apochromat 63X/1.4 NA Oil objective (Carl Zeiss) was used for 63X magnification and Zeiss Plan-Apochromat 40X/1.3 NA Oil objective (Carl Zeiss) was used for 40X magnification (mainly used in Section 4.3.5 and 6.3.4). Immersion oil of refractive index 1.514 (Cargill labs) was used.

2.10. SC growth assay

Z-stack images of the whole SC (3 per gland) were acquired by confocal microscopy (Section 2.9). The sum of all stacked images was obtained and analysed using Fiji. For every z-stack to be analysed, three SCs with the highest nuclear GFP (nGFP of *esg^{ts}F/O* driver) intensities were selected, as this corresponds to the SCs with the highest transgene expression levels. For each selected binucleated SC, the sum of the maximum areas of both nuclei and the sum of the maximum areas of an adjacent MC were calculated. In the case of mononucleate cells (e.g. Rbf^{CA}), the area of the single nucleus was considered as the total SC nuclear area. Total SC Nuclear Area/ Total MC Nuclear Area was used as a measure of SC growth (Leiblich et al., 2012, 2019). Refer to Appendix F for detailed description on image and data curation.

2.11. SC DAPI intensity assay

The total quantity of DNA present in the nuclei was estimated by the intensity of DAPI staining. Using a similar setup as the SC growth assay, the sum of DAPI intensities of a complete z-stack of both nuclei from each selected SC and an MC adjacent to the SC were calculated and background intensity was subtracted. The SC Nuclear DAPI Intensity/MC Nuclear DAPI Intensity was used to quantify the relative amount of nuclear DNA in the SCs.

2.12. EdU-containing food preparation and EdU incorporation assay

The Click-iT™ Plus EdU Cell Proliferation Kit for Imaging (Invitrogen; Alexa Fluor™ 594 dye) was used to detect DNA replication. EdU is a synthetic analogue of thymidine. Flies were maintained on medium prepared by mixing standard yeast-cornmeal agar medium with a 80mM EdU (Cambridge Bioscience) stock solution after at 60°C (diluted in PBS, as per the manufacturer's instructions) to reach a final EdU concentration of 0.2mM; 750µL of the 80 mM EdU stock solution was used for every 300 mL of yeast-cornmeal agar. In order to detect EdU incorporation, flies fed on EdU-containing food were dissected, but the testes were kept intact as a positive control for EdU staining as the adult stem cell niches in the testes undergo DNA replication and incorporate EdU (de Cuevas and Matunis 2011). Once suspended in PBST, tissues were transferred to 200 µL PBSTG (PBST with 10% Goat Serum) and incubated for 45 minutes at RT to block, before being washed with 200 µL PBST. DNA was labelled by adding 200 µL of the Click-iT® reaction mix (prepared following manufacturer's instructions) to the vials and left to incubate for 30 min at RT, away from light. Glands were washed three times with

200 µL PBST and then re-suspended in 200 µL PBS. Only AGs from flies whose testes were positively stained for EdU staining were included for the analysis. The total number of SCs were quantified by counting the number of GFP-containing SCs (nGFP from $esg^{ts}F/O$ driver). Percentage of SCs which incorporated EdU was then used as a measure for endoreplication in the gland.

2.13. CD63-GFP pulse labelling assay

For the compartment pulse-labelling experiment, I used CD63-GFP (Corrigan et al., 2014) instead of GFP-GPI (Redhai et al., 2016) because GFP-GPI fluorescence is poorly preserved after paraformaldehyde fixation, which is necessary for EdU detection. w^{1118} males containing the UAS-CD63-GFP construct regulated by the temperature-sensitive dsx-GAL4 driver (Corrigan et al., 2014) were multiply mated for 6 days at 25˚C with 10 w^{1118} females on EdU-containing food (Section 2.12). On day 7, the males were mated with five new w^{1118} females on EdU-containing food for 24 hours at 25˚C, to ensure mating occurs on day 7. The males were isolated, and then a pulse of CD63-GFP expression was induced at 28.5˚C for 24 hours on normal food. The AGs were then dissected and stained for EdU using Click-iT™ Plus EdU kit. The number of CD63-GFP-labelled large compartments in each SC was counted in endoreplicated and non-endoreplicated cells.

2.14. Sample preparation for live wide-field imaging

The protocol used for preparation of the AG for live-imaging was based on previously published methods by our lab (Corrigan et al., 2014; Dar et al., 2020; Fan et al., 2020; Redhai et al., 2016). Flies were briefly anaesthetised using CO_2 and dissected in ice-cold PBS. The AGs along with the ejaculatory duct were then stained with ice-cold 500 nM

LysoTracker® Red DND-99 (Invitrogen®) diluted in PBS for 5 min, washed in ice-cold PBS for 1 min, then mounted onto High Precision microscope cover glasses (thickness No. 1.5H, Marienfeld-Superior). A custom-built holder was used to hold the specimen during imaging. To avoid dehydration and hypoxia, the glands were maintained in a small drop of 1 × PBS, surrounded by 10S Voltalef® (VWR Chemicals), held by a small cover glass (VWR). The living glands were imaged at room temperature using the inverted wide-field fluorescence system DeltaVision Core from Olympus AppliedPrecision (GE Healthcare Life Sciences) equipped with a 100×/1.4 UPlanSApo oil objective (Olympus) with an EM-CCD camera, applicable for fluorescence and interference contrast (DIC) microscopy. Immersion oil with refractive index of 1.514 (Cargill labs) was used. Z-sections were captured with 0.5 µm spacing using the Zen Blue suite software.

2.15. SC compartment and ILV analysis

Compartments were analysed from living SCs of 6-day-old Btl-GFP, CFP-Rab6, YFP-Rab11 or YFP-Rab19-expressing flies carrying no other transgene or a specific transgene or transgene combination. Total number of compartments expressing a given marker and the percentage of those compartments containing ILVs was counted following the methods described in (Fan et al., 2020), except all compartments with no limit on diameter size were included as certain manipulations with altered BMP or EcR signalling resulted in all compartments being smaller than 1µm. Since counting the compartments containing GFP/YFP/CFP puncta is undertaken manually by looking through the entire z-stack for every cell, in the future it would be important to verify some of these results by conducting the analyses by blinding the genotype of the cell being analysed.

2.16. Statistical Analysis

I developed an automated statistical analysis Python programme (Appendix E) incorporating the below pipeline.

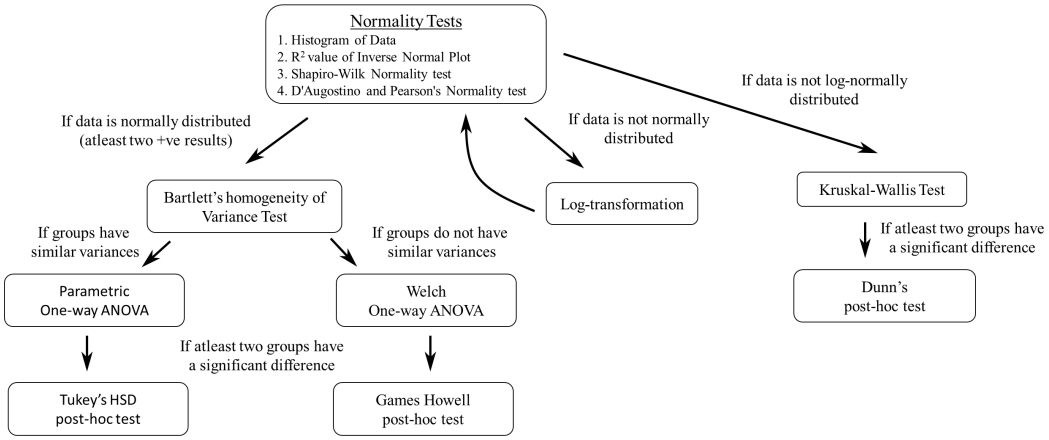

Since the parametric one-way ANOVA and the welch one-way ANOVA tests are robust and tolerate violations of the normality assumption to an extent, data that are considered to be normally distributed by atleast two of the four above-mentioned normality tests are treated as normal data. If data are not normally distributed, the normality of log-transformed data is checked. For data that are normally distributed, the Bartlett's test is used to determine whether the individual groups within the data have similar variances to determine the type of one-way ANOVA test to be used. The Tukey's HSD test is used as a post-hoc test for the parametric one-way ANOVA test as it computes all pairwise-comparisons and is robust with respect to unequal group sizes.

When the data are log-transformed, the analyses conducted compare the geometric means of the data rather than the arithmetic means (Equation 1). Therefore, when log-normal data are represented in a scatterplot graph, the geometric means and the corresponding geometric standard deviations are depicted.

Equation 1: $\frac{\sum_{i=1}^{N} \log(i)}{N} = \log\left(\sqrt[N]{\prod_{i=0}^{N} \mathrm{i}}\right)$; where $\frac{\sum_{i=1}^{N} \log(i)}{N}$ is the arithmetic mean of log-transformed values and $\sqrt[N]{\prod_{i=0}^{N} \mathrm{i}}$ is the geometric mean of actual data.

Chapter-3:

Hormone-dependent and hormone-independent Ecdysone Receptor signalling in SCs

3.1. Introduction

As described in Chapter 1, *Drosophila* SC growth is regulated by the BMP and EcR signalling pathways and this growth is further enhanced upon mating (Fig. 3.1) (Leiblich et al., 2012, 2019). Aaron Leiblich also showed that the BMP pathway interacts with the EcR signalling pathway by regulating EcR protein levels, most notably of the EcR-B1 isoform (Leiblich et al., 2019). These results revealed that the BMP/EcR signalling axis is critical for SC growth in virgin males, thereby establishing another parallel between the mechanisms underlying SC growth and prostate cancer development and progression, which involves BMP signalling and the AR (Ye et al., 2007). He also showed that although the common binding partner of EcR, Ultraspiracle (USP), was expressed in SCs, it was not necessary for the regulation of SC growth in virgins (Leiblich et al., 2012).

Preliminary work by Josephine Hellberg suggested that BMP and EcR signalling might also be involved in regulating SC growth that occurs after mating. In addition, there was some indication that the steroid hormone ecdysone might play a role in the regulation of growth in virgin males, but not in mated males. She used the absolute SC nuclear area as a measure for SC growth for all her experiments, which did not account for the variation between different AGs, which arises during sample preparation due to distortion of the specimens. Hence, I employed the method used by Leiblich et al., 2012, which used the ratio of SC nuclear area to its representative adjacent MC nuclear area, to validate, confirm and then extend some of the results regarding mating-dependent SC growth from her DPhil.

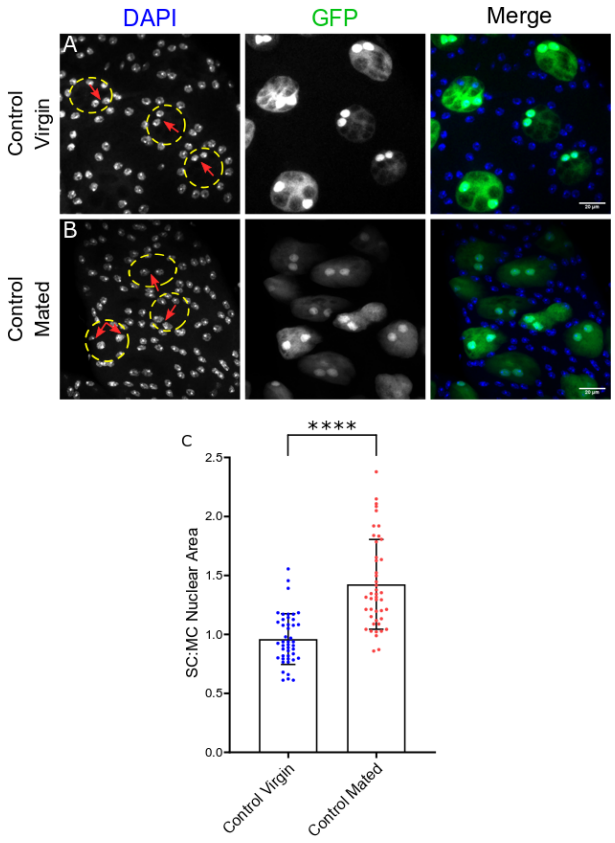

Figure 3.1 Mating-dependent SC growth
A-B: Dissected AGs from 6-day-old adult virgin males (A) and multiply mated males (B) switched to 28.5ºC at eclosion to activate GAL4 expression. Control represents w^{1118} flies specifically expressing nuclear GFP (which also stains the cytosol) in SCs under esg^{ts}F/O control. Nuclei are stained with DAPI (blue). Dashed yellow ellipses approximately outline SCs; red arrows points to pairs of SC nuclei. Scale bars correspond to 20 µm.
C: Bar chart depicting the geometric mean ratio of the size of the two SC nuclei relative to those of a neighbouring MC for control virgin and mated glands. The error bars show the geometric standard deviation within the sample. SC nuclear growth in mated males is significantly higher than in virgin males. Student's t-test on log-transformed data; ****$p \leq 0.0001$ (n=15 SCs ;5 males).

3.2. Aims

In this chapter, my broad aim was to study the role of the BMP/EcR signalling axis in regulating SC nuclear growth after mating. More specifically, I addressed the following research questions:

- Do the BMP and EcR signalling pathways regulate mating-dependent SC nuclear growth?
- How does the BMP pathway regulate EcR protein levels?

- Is there any difference between BMP/EcR-dependent regulation of SC growth in virgin and mated males?
- What is the role of the hormone ecdysone in regulating EcR signalling in both virgin and mated males?

Results from Sections 3.3.1-3.3.2 and 3.3.4-3.3.6 have been published in Leiblich et al., 2019, on which I am a joint co-first author.

3.3. Results

3.3.1. EcR isoforms A and B regulate SC nuclear growth in virgin males

Since EcR signalling plays a vital role in regulating SC growth in virgin males, I investigated the roles played by different EcR isoforms in this process. I used the esg^{ts}F/O system in which transgenes are expressed in SCs under the control of the yeast GAL4 transcription factor in a temperature–dependent fashion. Newly eclosed males were switched from 18°C to 28.5°C to activate SC transgene expression for 6 days. SC nuclear size relative to neighbouring MC nuclei was then measured to assess SC growth.

Aaron Leiblich previously showed that downregulating the levels of the highly expressed EcR-B1 protein in SCs, using an *EcR-B1*-RNAi, suppressed SC nuclear growth after 6 days (Leiblich et al., 2012). He had focused on this isoform, because knockdown experiments had suggested it was the major isoform expressed in SCs. Surprisingly, knocking down EcR-A levels in SCs also resulted in a major decrease in growth after 6 days, as compared to controls and even to SCs expressing pan-*EcR*-RNAi (Fig. 3.2 A, C, E, G), which suggests that *EcR-A* knockdown might be more efficient. These results show that both the EcR-B1 and EcR-A isoforms are essential in regulating the growth of SC nuclei in virgins.

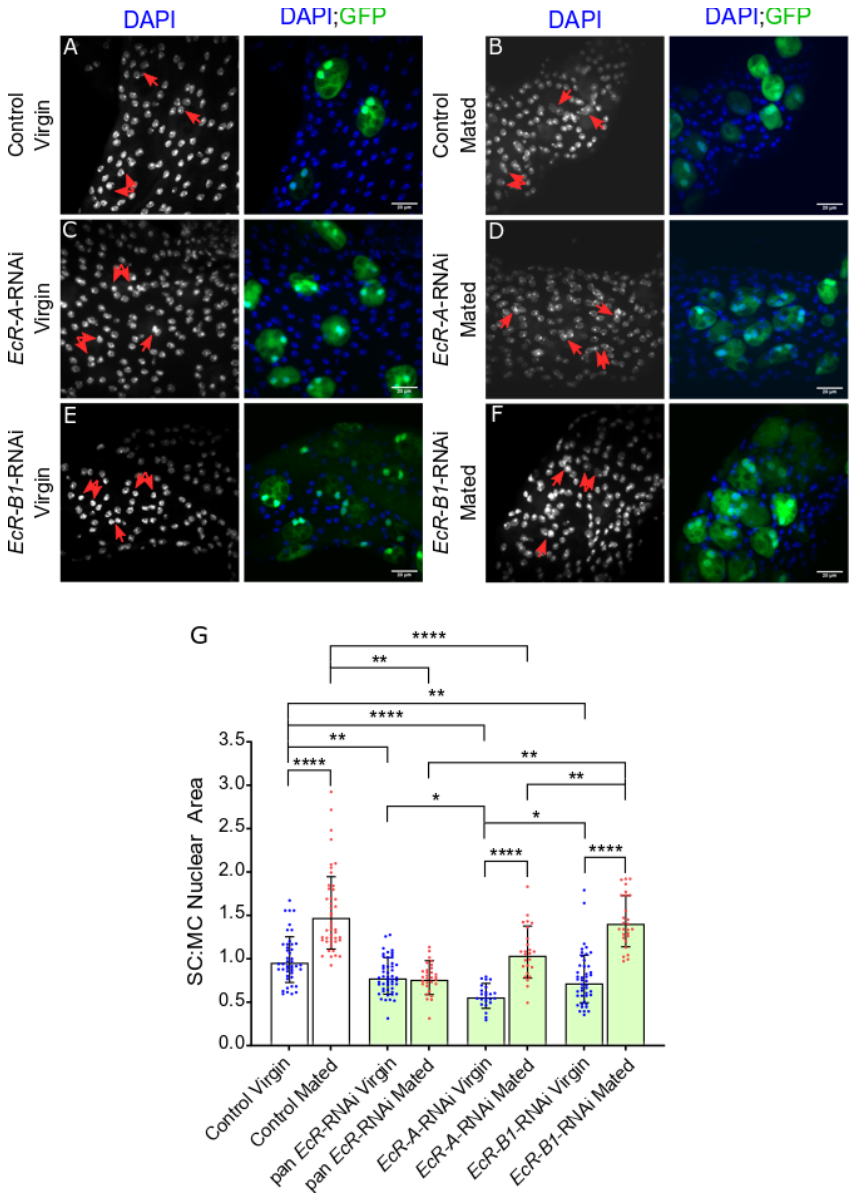

Figure 3.2 Role of EcR-A and EcR-B1 in regulating SC growth

A-F: Images show distal tip of AGs from 6-day-old adult virgin or mated males switched to 28.5°C at eclosion to express corresponding transgenes under the control of the esg^{ts}F/O driver. Control represents w^{1118} flies specifically expressing nuclear GFP (which also stains the cytosol) in SCs. Nuclei are stained with DAPI (blue). Red arrows point to representative SC nuclei for each transgene. In images D and E some SCs appear to be mononucleate, but this is because the other nucleus is in a different focal plane, which has not been included in the Z-projection of the images. Scale bars correspond to 20 µm.

D: Bar chart depicting the geometric mean ratio of the size of SC nuclei relative to neighbouring MC nuclei. The error bars show the geometric standard deviation within the sample. The graph includes SC growth assay data from virgin and mated flies expressing Control, pan-*EcR*-RNAi, *EcR-A*-RNAi or *EcR-B1*-RNAi in SCs. Expression of pan-*EcR*-RNAi, *EcR-A*-RNAi or *EcR-B1*-RNAi suppresses SC growth in virgin males. In mated males, expression of either pan-*EcR*-RNAi or *EcR-A*-RNAi results in a reduction in SC growth, but only pan-*EcR*-RNAi is able to suppress SC nuclear growth relative to virgin males. *EcR-B1*-RNAi expression does not appear to have any effect on SC nuclear growth in mated males. One-way ANOVA on log-transformed data; Tukey's HSD post hoc test,- $0.01<*p<0.05$; $0.001<**p\leq0.01$; $****p\leq0.0001$ ($n\geq24$ SCs; ≥8 males).

3.3.2. EcR-A is essential for secondary cell growth that occurs after mating

Preliminary experiments by Josephine Hellberg suggested that the EcR signalling pathway might be involved in the regulation of mating-dependent SC growth. In order to confirm this result, I knocked down all the EcR isoforms using a pan-*EcR*-RNAi line, which resulted in a suppression of SC growth in both virgin and mated males. Additionally, the SCs of these virgin and mated *EcR* knockdown flies had similar growth levels, therefore demonstrating the importance of EcR signalling in the regulation of mating-dependent growth. I was then interested in deciphering the precise roles of EcR signalling in this process.

Although, upon mating the SC nuclei of flies expressing *EcR-A*-RNAi grew relative to those of virgin males, this growth was restricted compared to mated controls. By contrast, expression of *EcR-B1*-RNAi in SCs did not block growth after mating (Fig 3.2 E-G). Knocking down the common binding partner of EcR, *USP*, in SCs also did not affect growth after mating, paralleling observations in virgin males (Fig 3.3 A-D, G). Overexpressing *EcR-C*, a synthetic EcR isoform that leads to EcR overexpression in SCs (Section 1.16.1.3), resulted in an increase in SC growth in virgins. Although an increase in SC nuclear growth was observed between virgin and mated males overexpressing EcR-C, the final growth in mated males was not significantly higher than control mated males (Fig 3.3 E-F, H). Therefore, taking these results together shows that EcR signalling is essential for SC nuclear growth after mating, but EcR-A, and not EcR-B1, is required. Since pan-*EcR*-RNAi completely suppresses any SC growth in mated males with respect to pan-*EcR*-RNAi virgin males, this suggests a possible role for EcR-B2 in growth regulation. Since the unique N-terminal domain of EcR-B2 is really small, there is no

available RNAi line which targets EcR-B2 specifically. The USP protein does not appear to be required for this EcR-mediated growth.

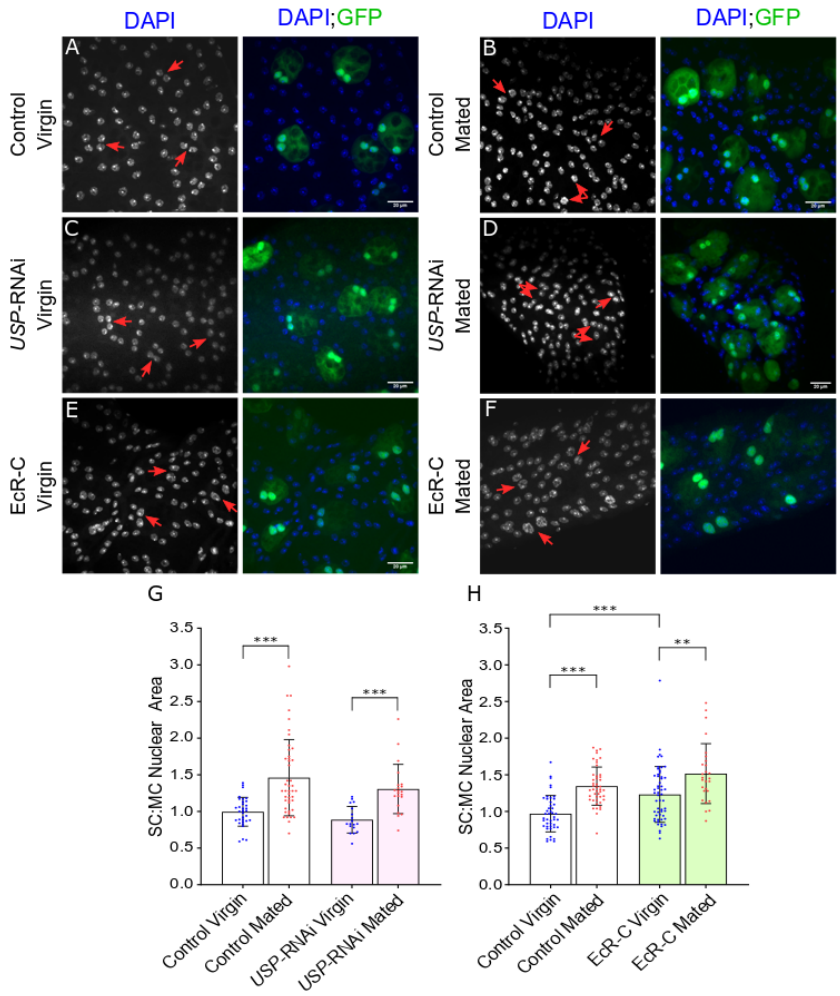

Figure 3.3 The effects of EcR-C and USP on SC growth in virgin and mated males
A-F: Images show distal tip of AGs from 6-day-old adult virgin or mated males switched to 28.5°C at eclosion to express corresponding transgenes under the control of the esg^{ts}F/O driver. Control represents w^{1118} flies specifically expressing nuclear GFP (which also stains the cytosol) in SCs. Nuclei are stained with DAPI (blue). Red arrows point to representative SC nuclei for each transgene. Scale bars correspond to 20 µm.
G: Bar chart depicting the mean ratio of the size of SC nuclei relative to neighbouring MC nuclei. The error bars show the standard deviation within the sample. The graph includes SC growth assay data from virgin and mated flies expressing either Control or *Usp*-RNAi in SCs. Suppression of *Usp* does not affect SC growth either in virgin or mated males. Welch ANOVA; Games-Howell post hoc test; 0.0001<***p≤0.001(n≥18 SCs; n≥6 males).
E: Bar chart depicting the geometric mean ratio of the size of SC nuclei relative to neighbouring MC nuclei. The error bars show the geometric standard deviation within the sample. The graph includes SC growth assay data from virgin and mated flies expressing either Control or EcR-C in SCs. EcR-C increases SC growth in virgin males. Although no significant difference is observed between EcR-C-expressing mated males and controls, a significant increase is observed with respect to EcR-C-expressing virgin males. One-way ANOVA on log-transformed data; Tukey HSD post hoc test; 0.001<**p≤0.01; ****p≤0.0001 (n≥27 SCs; ≥9 males).

3.3.3. BMP signalling appears to regulate EcR protein levels pre- and post-transcriptionally in secondary cells

Before investigating the role of BMP signalling in mating-dependent growth of SCs, I wanted to investigate its effects in virgin males in more detail. Following up on the results observed by Aaron Leiblich regarding the role of the BMP pathway in regulating EcR protein levels in SCs, I wanted to determine if this interaction occurred pre- or post-transcriptionally.

I employed the qRT-PCR technique to quantify *EcR* RNA levels in AGs containing SCs expressing the EcR-B1, EcR-B2 and EcR-C overexpression constructs with and without overexpression of the constitutively active form of the BMP Type I Thick veins receptor (Tkv^{act}). Since we did not have the EcR-A overexpression stock and hence its combination with Tkv^{act} in the lab, I was unable to determine the effects of BMP signalling on the EcR-A isoform. I undertook these experiments in triplicate, dissecting out AGs attached to the ejaculatory duct, and then confirming my findings with dissected samples containing only AGs.

It had previously been shown that activation of BMP signalling by expressing Tkv^{act} increased the protein levels of all EcR isoforms in SCs (Leiblich et al., 2019). No increase in relative *EcR* RNA levels was observed in adult AGs overexpressing EcR-B1 or EcR-B2 alone in SCs, which suggests either *EcR-B1* and *EcR-B2* gene transcription remains unchanged, or the *EcR-B1* and *EcR-B2* transcripts are unstable, or SC expression alone is insufficient to significantly increase AG levels of *EcR* RNA. Since the experiment with *EcR-B2* (and *EcR-B2* + Tkv^{act}) has been done only once, these results need to be validated (Fig. 3.4).

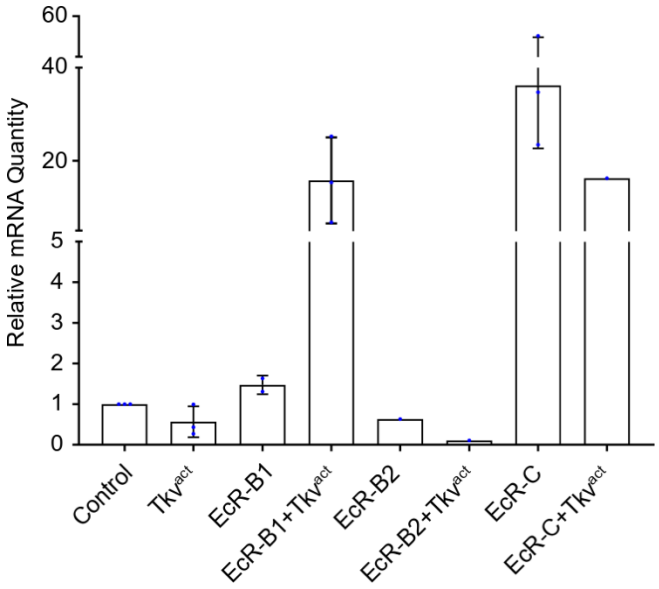

Figure 3.4 Pre-translational mechanisms are partly involved in regulation of EcR protein levels by BMP signalling
Bar graph depicts the relative mRNA levels of transgenes expressed in SCs under the control of esg^{ts}F/O with respect to the control genotype (w^{1118}). Each dot represents the mean of the relative mRNA levels of triplicates in one experiment. As the trends observed with dissecting out either the AG with the ejaculatory duct or just the AG were similar, I have included these data in the same graph. In the case of EcR-B2, EcR-B2 + Tkv^{act} and EcR-C + Tkv^{act}, I conducted this experiment only once by dissecting out just the AG. It appears that BMP signalling differentially regulates different EcR isoforms in an N-terminal-dependent manner.

However, when EcR-B1 was overexpressed with Tkv^{act}, *EcR* RNA levels increased drastically. Overexpression of just Tkv^{act} did not produce an obvious change in *EcR* RNA levels. Interestingly, when EcR-B2 was overexpressed with Tkv^{act}, no change in the levels of the *EcR* mRNA was observed. These results, along with immunohistochemical analysis from Leiblich, surprisingly suggest that the BMP signalling pathway can increase *EcR* gene expression to elevate EcR protein levels both pre- and post-transcriptionally, depending on the EcR isoform under study. When EcR-C, a synthetic isoform which is refractory to BMP pathway regulation, was overexpressed in SCs, an increase in *EcR* RNA levels was observed and this increase was reduced when this construct was co-expressed with Tkv^{act} (Fig 3.4). Therefore, the N-terminal domain of the EcR is vital for the normal regulation of EcR by the BMP pathway, although this regulation is multi-faceted, affecting different isoforms in different ways.

3.3.4. The BMP signalling pathway interacts with EcR signalling to regulate mating-dependent SC growth

In order to validate preliminary results from Josephine Hellberg that suggested a role for the BMP signalling pathway in controlling SC growth after mating, I overexpressed the BMP antagonist Dad in SCs. I observed that nuclei in these SCs did not grow after mating and were much smaller than in control mated males (Fig 3.5 A-D, G). Upregulation of BMP signalling by overexpressing the activated form of the Type I BMP receptor (Tkv), Tkv^{act}, resulted in an increase in SC growth in both virgin and mated males (Fig 3.6 A, C, G). These results stress the importance of the BMP pathway for SC growth after mating.

To understand how these pathways interact to regulate endoreplication in SCs, I generated combination UAS-genotypes with high BMP and low EcR signalling and vice versa. When Tkv^{act} (high BMP) was co-expressed with *EcR*-RNAi (low EcR) in the SCs of virgin and mated males, no change in the growth levels were observed with respect to controls (Fig 3.6). Expressing Dad (low BMP) along with EcR-C (high EcR) in SCs of virgin males gave similar results to those observed with *EcR*-RNAi + Tkv^{act} (Fig 3.5 A-F, H). Taking these results together, it appears that although the BMP and EcR signalling pathways interact with each other, they may also act partly independently in the regulation of SC growth and endoreplication. Alternatively, the genetic manipulations affecting EcR signalling do not fully suppress or dominantly activate signalling, so that they can still be modified by BMP signalling.

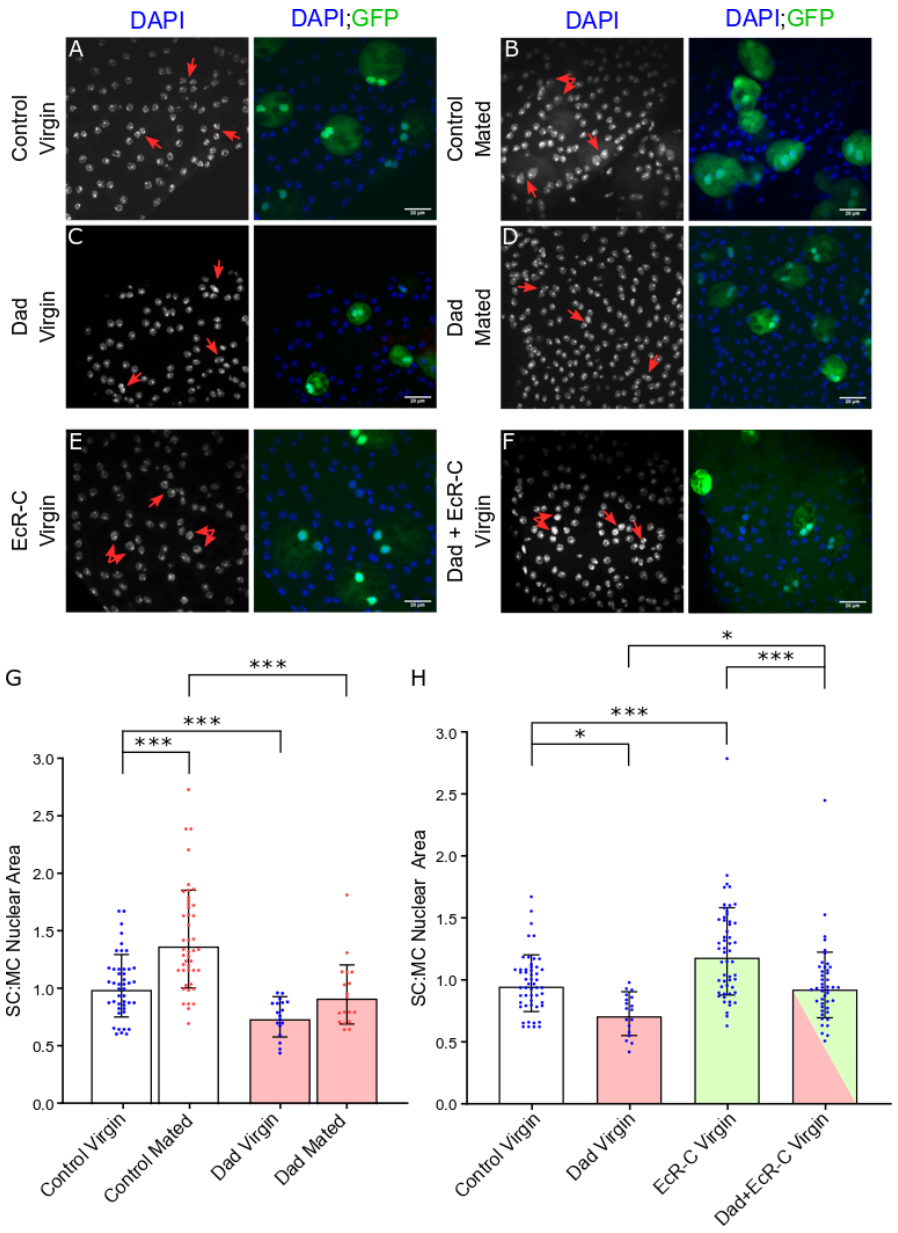

Figure 3.5 Interaction of BMP and EcR signalling in regulation of SC growth

A-F: Images show distal tip of AGs from 6-day-old adult virgin or mated males switched to 28.5°C at eclosion to express corresponding transgenes under the control of the esg^{ts}F/O driver. Control represents w^{1118} flies specifically expressing nuclear GFP (which also stains the cytosol) in SCs. Nuclei are stained with DAPI (blue). Red arrows point to representative SC nuclei for each transgene. Scale bars correspond to 20 µm.

G: Bar chart depicting the geometric mean ratio of the size of SC nuclei relative to neighbouring MC nuclei. The error bars show the geometric standard deviation within the sample. Downregulation of BMP signalling suppresses growth in both virgin and mated males. No difference in SC nuclear growth between Dad-expressing virgin and mated males is observed. One-way ANOVA on log-transformed data; Tukey HSD post hoc test; 0.0001<***p≤0.001 (n≥18 SCs; ≥6 males).

H: Bar chart depicting the geometric mean ratio of the size of SC nuclei relative to neighbouring MC nuclei. The error bars show the geometric standard deviation within the sample. Expression of Dad+EcR-C in SCs of virgin males produces an intermediate phenotype that has similar nuclear growth to controls. One-way ANOVA on log-transformed data; Tukey HSD post hoc test; 0.01<*p≤0.05; 0.0001<***p≤0.001 (n≥18 SCs; n≥6 males).

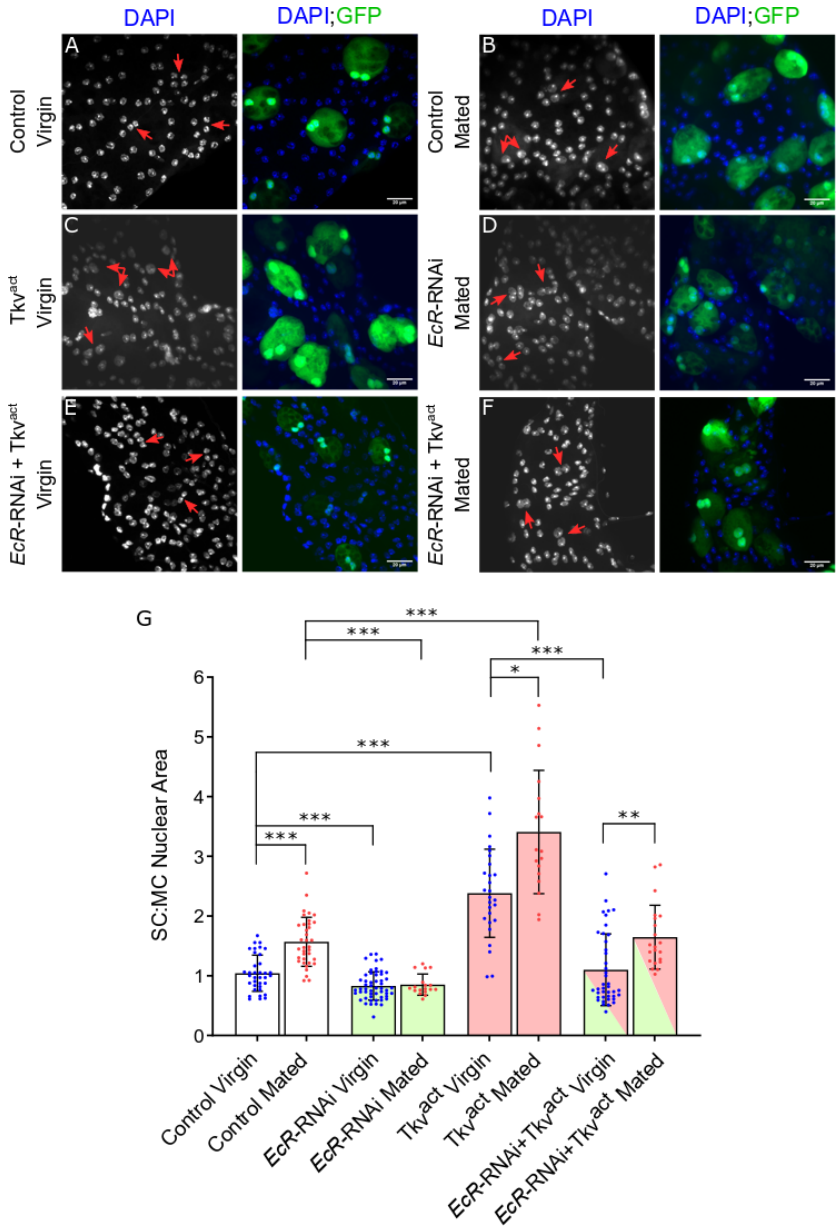

Figure 3.6 Interaction of BMP and EcR signalling in regulation of SC growth
A-F: Images show distal tip of AGs from 6-day-old adult virgin or mated males switched to 28.5°C at eclosion to express corresponding transgenes under the control of the esg^{ts}F/O driver. Control represents w^{1118} flies specifically expressing nuclear GFP (which also stains the cytosol) in SCs. Nuclei are stained with DAPI (blue). Red arrows point to representative SC nuclei for each transgene. Scale bars correspond to 20 µm.
G: Bar chart depicting the mean ratio of the size of SC nuclei relative to neighbouring MC nuclei. The error bars show the standard deviation within the sample. Upregulation of BMP signalling induces higher growth in both virgin and mated males. Expression of *EcR*-RNAi+Tkv^{act} in SCs results in an intermediate phenotype in both virgin and mated males. Welch ANOVA; Games-Howell post hoc test; 0.01<*p<0.05; 0.001<**p<0.01; 0.0001<***p<0.001 (n≥20 SCs; ≥7 males).

3.3.5. Hormone-dependent EcR signalling regulates secondary cell nuclear growth in virgin males

To study the role of the ecdysone hormone in EcR-dependent SC growth in virgin males, I used the temperature-sensitive mutant *ecdysoneless*^{1} (*ecd*^{1}), which inhibits the production of ecdysone in the whole animal when shifted to 29°C (Garen, Kauvar, and Lepesant 1977). Following a 6-day temperature shift after eclosion, SC nuclear growth in *ecd*^{1} males was significantly reduced compared to its respective control, suggesting that ecdysone plays a role in this process (Fig 3.7 A, C, G). Feeding virgin *ecd*^{1} males with food containing 10mM 20-hydroxyecdysone (20-HE) completely rescued the *ecd*^{1} phenotype in SCs, confirming the importance of ecdysone in SC nuclear growth (Fig 3.7 A, C, E, H).

ecd^{1} flies have several pleiotropic defects (Redfern and Bownes 1983). The mutation not only blocks the production of ecdysone, but also affects *EcR* pre-mRNA splicing, which results in a reduction in the *EcR* mRNA levels (Claudius et al., 2014). It was therefore essential to validate the results observed with this mutant by other means. In adults, it had previously been shown that the Torso receptor, which is essential for prothoracicotropic hormone (PTTH) to activate ecdysone synthesis in the larval prothoracic gland, is expressed specifically in the SCs of the AG (Hentze et al., 2013). This work suggested a possible role for SCs in synthesising ecdysone in the adult fly. Hence, I targeted two of the six conserved genes that are essential for the biosynthesis of ecdysone (Section 1.13), *spook* (*spo*; enzyme that acts earlier in the ecdysteroid biosynthesis pathway) and *shade* (*shd*; enzyme that acts later in the ecdysteroid biosynthesis pathway) (Hentze et al., 2013), using adult-induced knockdown in SCs. Although feeding 10mM 20-HE to SCs expressing *shd*-RNAi or *spo*-RNAi did not have a significant increase with respect to SCs

of unfed *shd*-RNAi or *spo*-RNAi flies, these flies had similar growth levels as controls (Fig 3.8 A, C, E, G-H). Therefore, not only do these results validate the important role of ecdysone in regulating EcR-dependent SC nuclear growth in virgin males, they also show that SCs are an ecdysone-producing hub in adults.

3.3.6. Hormone-independent EcR signalling promotes SC growth after mating

Since ecdysone is essential for SC growth in virgin males, I wanted to determine the role of the hormone in regulating mating-dependent SC growth. Remarkably, SC nuclei in ecd^{1} mutant mated males grew more than control mated males (Fig 3.7 A-D, G, I). However, feeding the control and ecd^{1} mated males with 10mM 20-HE throughout the 6 days of the experiment, did not have any effect on nuclear growth after mating (Fig 3.7 F, I). These results indicated that EcR-dependent growth after mating occurs independently of the ecdysone hormone, and that the effect of the ecd^{1} mutation on SC growth in mated males might not be due to changes in ecdysone levels. Expression of *shd*-RNAi or *spo*-RNAi in SCs did not affect nuclear growth after mating. Feeding 20-HE to these flies also had no effect on mating-dependent growth (Fig 3.8), thereby confirming that nuclear growth after mating is controlled by EcR signalling that is hormone-independent.

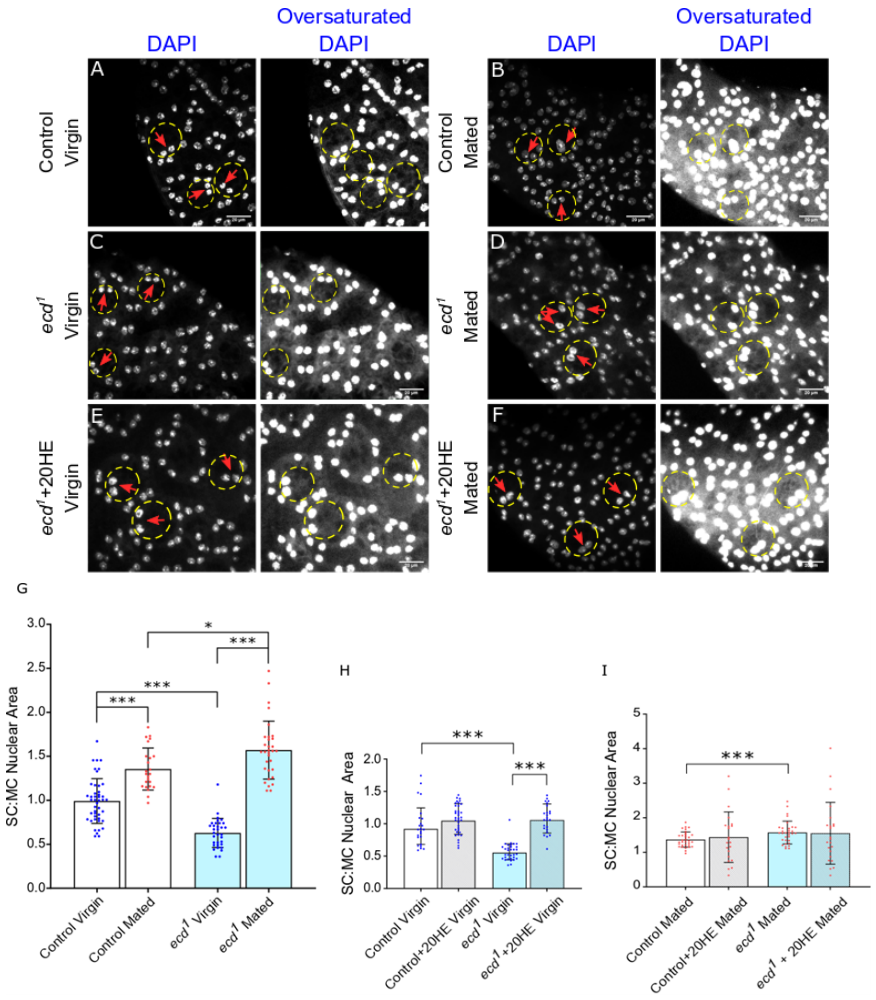

Figure 3.7 Role of ecdysone in SC growth regulation

A-F: Images show distal tip of AGs from 6-day old adult virgin or mated males were switched to 28.5°C at eclosion to express the *ecd*^{1} mutant allele either on normal food or 10mM 20-HE-containing food. DAPI stains nuclei. The DAPI channel is overexposed in order to see non-stained SC compartments and therefore identify SCs in the *ecd*^{1} flies. These compartments are not present in MCs. Yellow dashed ellipses mark the SCs identified as mentioned above. Red arrows point to representative nuclei for a given transgene. Scale bars correspond to 20 µm.

G: Bar chart depicting the mean ratio of the size of SC nuclei relative to neighbouring MC nuclei. The error bars show the standard deviation within the sample. The graph includes SC growth assay data from virgin and mated flies expressing either Control or *ecd*^{1}. Reduction in ecdysone synthesis in the whole animal suppresses SC nuclear growth in virgin males, in contrast to the slight increase in SC growth observed in mated males. Welch ANOVA; Games-Howell post hoc test; 0.01<*p<0.05; 0.0001<***p<0.001 (n≥24 SCs; ≥8 males).

H: Bar chart depicting the geometric mean ratio of the size of SC nuclei relative to neighbouring MC nuclei. The error bars show the geometric standard deviation within the sample. The graph includes SC growth assay data from virgin flies unfed or fed with 20-HE expressing either Control or *ecd*^{1}.Feeding *ecd*^{1} flies with 10mM 20-HE rescued SC growth in virgin males. One-way ANOVA on log-transformed data; Tukey HSD post hoc test; 0.0001<***p≤0.001 (n≥24).

I: Bar chart depicting the mean ratio of the size of SC nuclei relative to neighbouring MC nuclei. The error bars show the standard deviation within the sample. The graph includes SC growth assay data from mated flies unfed or fed with 20-HE expressing either Control or *ecd*^{1}.Feeding *ecd*^{1} flies with 10mM 20-HE did not affect SC growth in mated. Welch ANOVA; Games-Howell post hoc test; 0.0001<***p≤0.001 (n≥22 SCs; ≥8 males).

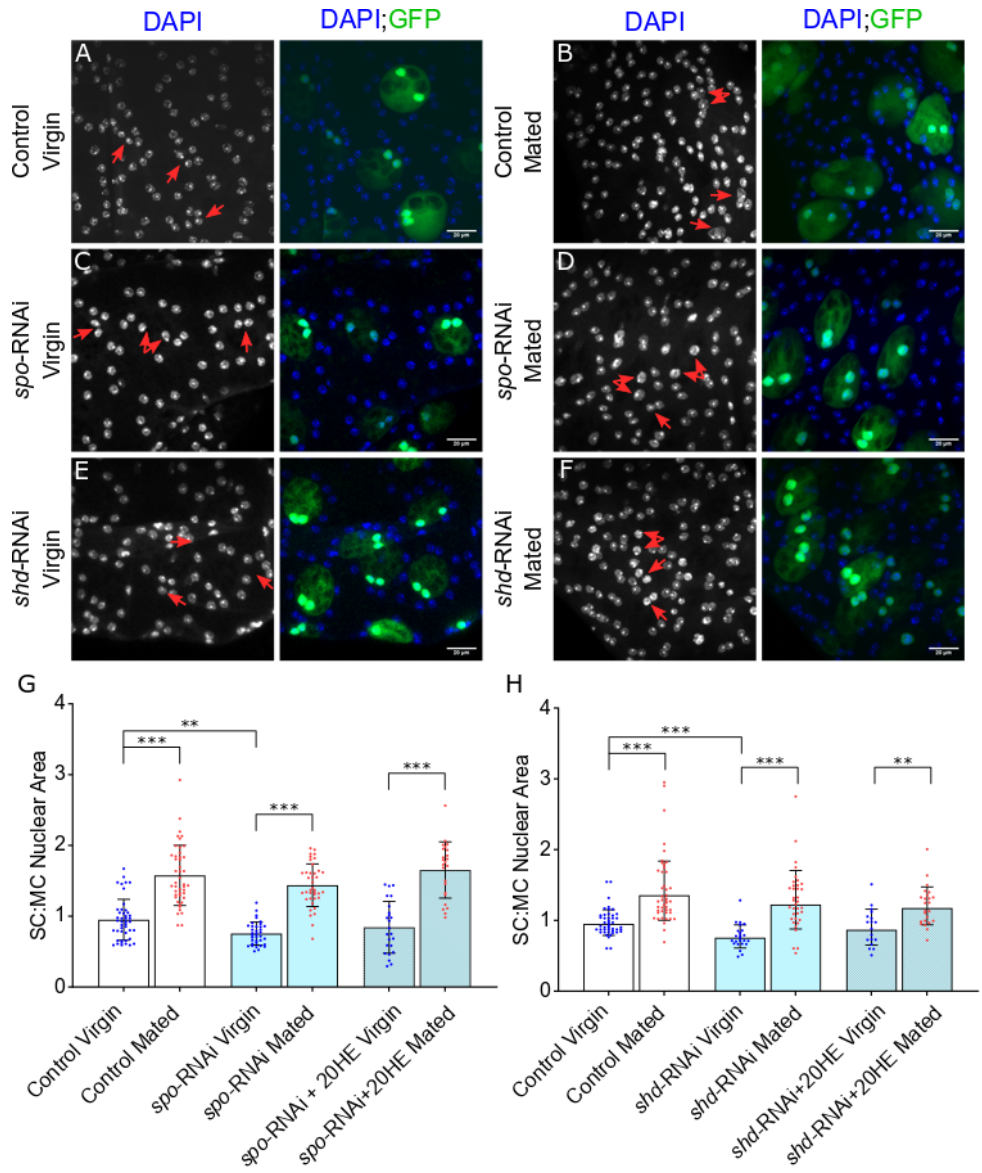

Figure 3.8 Role of ecdysone biosynthesis genes in SC growth regulation

A-F: Images show distal tip of AGs from 6-day-old adult virgin or mated males switched to 28.5°C at eclosion to express corresponding transgenes under the control of the esg^{ts}F/O driver. Control represents w^{1118} flies specifically expressing nuclear GFP (which also stains the cytosol) in SCs. Nuclei are stained with DAPI (blue). Red arrows point to representative SC nuclei for each transgene. Scale bars correspond to 20 µm.

G: Bar chart depicting the mean ratio of the size of SC nuclei relative to neighbouring MC nuclei. The error bars show the standard deviation within the sample. Knocking down spo in SCs results in a reduction in SC growth in virgin males which can be rescued by feeding 10mM 20-HE. In mated males, no effect is observed in SC growth with or without feeding 10mM 20-HE. Welch ANOVA; Games-Howell post hoc test; 0.001<**p<0.01; 0.0001<***p<0.001 (n≥24 SCs; n≥ 8 males).

H: Bar chart depicting the geometric mean ratio of the size of SC nuclei relative to neighbouring MC nuclei. The error bars show the geometric standard deviation within the sample. Knocking down *shd* in SCs phenocopies results observed with *spo*-RNAi. Welch ANOVA on log-transformed data; Games-Howell post hoc test; 0.001<**p<0.01; 0.0001<***p<0.001 (n≥18 SCs; ≥6 males).

3.4. Summary and Discussion

The SCs of the *Drosophila* accessory gland grow after mating. In this chapter, I show this mating-dependent nuclear growth, like secondary cell growth in virgins, is under the control of the BMP and EcR signalling axes. These pathways are connected, because BMP signalling regulates the levels of EcR via a mechanism at least partly involving the N-terminal AF1 domain of *EcR* or the sequences that encode it. I demonstrate that this appears to involve multiple mechanisms involving control of transcript and protein levels that is differentially imposed on different EcR isoforms.

I show that the different EcR isoforms play a specific role in regulation of SC growth. In virgins, both the EcR-A and EcR-B1 isoforms are essential for SC nuclear growth to occur. However, in mated males, only the EcR-A isoform is required. Interestingly, this dual control corresponds with different hormone-dependence. In virgins, the EcR functions in an ecdysone-dependent manner, whereas in mated males, the EcR functions in an ecdysone-independent fashion. Neither mechanism appears to involve EcR's common binding partner, USP, although as we will see later, specific aspects of the mating-dependent regulation are under USP control (Section 4.3.3).

3.4.1. EcR isoforms differentially regulate SC growth

It is interesting to note that even though EcR-B1 is the major isoform expressed in SCs of virgin males (Leiblich et al., 2019), SC growth regulation in these males is also dependent on EcR-A. Also, knocking down *EcR-A* results in SCs has a much stronger phenotype than knocking down all EcR isoforms or just EcR-B1. Although this must be

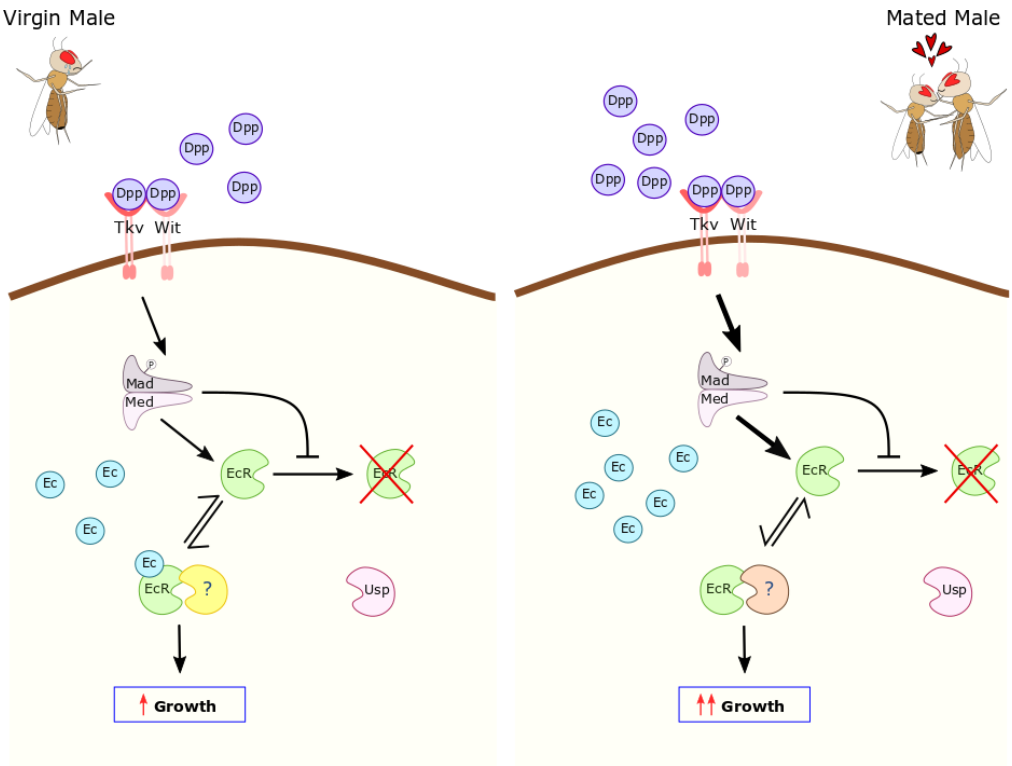

Figure 3.9 Schematic depicting BMP/EcR growth regulation in SCs
As previously shown, upon mating, BMP signalling activity increases (Redhai et al., 2016) and an increase in ecdysone titres are also observed (Leiblich et al., 2019). BMP signalling regulates EcR protein levels and both BMP and EcR regulate SC growth. In virgin males, EcR promotes growth in an ecdysone-dependent fashion and in mated males, EcR promotes growth in an ecdysone-independent manner. Dpp-Decapentaplegic; Ec-Ecdysone; EcR-Ec receptor; Med-Medea; Tkv-Thickveins; Usp-Ultraspiracle; Wit-Wishful thinking; ?-unknown EcR partners.

partly explained by a more efficient knockdown, this suggests the importance of the EcR-A isoform in the regulation of SC growth in virgin males. Furthermore, in mated males, only the EcR-A isoform has an effect on the final size of SCs. However, knocking down either *EcR-A* or *EcR-B1* in SCs results in an increase in growth after mating when compared to SCs from the equivalent virgin males, suggesting growth regulatory mechanisms independent of these isoforms may also be involved.

Different EcR isoforms have previously been reported to have diverse functions in different *Drosophila* tissues during development as well as having overlapping functions (Cherbas et al., 2003; Gradilla et al., 2011; Schubiger et al., 2003). EcR-A has been implicated as the predominant isoform in AG development (V. Sharma et al., 2017). The

authors also showed that *EcR-A* knockdown considerably reduced the levels of SC-specific proteins Abdominal-B (Abd-B) and angiotensin-converting enzyme (ANCE), suggesting that it might play an important role in regulating cellular processes in SCs before, as well as after, eclosion.

It is important to note that knocking down either of the EcR isoforms might result in a compensatory effect due to the functional redundancy between these isoforms (Schubiger et al., 2003). Therefore, it is possible that the increase in SC growth in mated males relative to virgin males observed when either *EcR-A* or *EcR-B1* is knocked down, could be attributed to the other isoforms in the SCs, EcR-B1 and EcR-B2 or EcR-A and EcR-B2 respectively, in promoting growth. Although it appears that EcR-A has a vital role in the regulation of SC growth, the difference in knockdown efficiency of the pan-*EcR*-RNAi, *EcR-B1*-RNAi and *EcR-A*-RNAi constructs needs to be considered while interpreting the effects observed with *EcR-A*-RNAi. Therefore, I can conservatively conclude that the EcR-A and EcR-B1 isoforms are essential for SC growth that occurs in virgin males and the EcR-A isoform is required for SC growth in mated males, but I cannot eliminate the possibility that EcR-B1 might have a function in the regulation of this mating-dependent growth. In the following chapter, I try to dissect out the molecular and genetic differences in SC growth in virgin and mated males that underpin these results. Furthermore, I also demonstrate that changes in growth observed in virgin and mated males expressing *EcR-A*-RNAi reflect mechanistically different EcR signalling pathways.

As reviewed in Section 1.3, similar differences in functions have been observed with the androgen receptor splice variants (AR-Vs). The AR-Vs have been implicated to play a

role in the progression of prostate cancer and development of resistance to therapies. AR-Vs have opposing roles in regulating prostate cancer progression. Although I have not identified opposing functions of EcR isoforms, it should be noted that the EcR-A isoform has a specific and unique function, which at least EcR-B1 does not perform.

3.4.2. USP-independent EcR signalling regulates SC growth

Although the USP protein is expressed specifically in the SCs of the male AG (Leiblich et al., 2019), it does not appear to regulate overall SC growth in either virgin or mated males. It was also observed that knocking down *Usp* in SCs did not affect EcR protein levels (Leiblich et al., 2019). EcR signalling independent of USP has been shown to be necessary for the proper morphological development of the male AG, and for its normal functions in fertility and post-mating response regulation (V. Sharma et al., 2017). Similarly, USP-independent EcR signalling is also observed in the induction of glue genes in the larval salivary glands (Costantino et al., 2008). Though the exact form of signalling has not been characterised, two possible mechanisms have been proposed: the EcR can homodimerize in an EcR-only complex or heterodimerize with another nuclear-hormone receptor. In this regard, it would be interesting to test whether any other *Drosophila* nuclear receptors are involved in SC growth regulation in the future.

3.4.3. Autocrine BMP signalling promotes mating-dependent SC growth

As discussed in Section 1.12.3, upon mating, it has been observed that SCs release approximately four Decapentaplegic- (Dpp-) containing dense-core granule (DCG) compartments (Redhai et al., 2016). The secreted ligand then activates BMP signalling in

SCs, through the interaction between Dpp and its receptor containing Tkv and Wit in an autocrine fashion. This mating-dependent increase in BMP signalling activity and the effect of BMP signalling on EcR levels at least partially explains the BMP-dependent regulation of SC nuclear growth after mating.

As mentioned in Section 1.4, altered BMP signalling has also been observed during the progression of prostate cancer. The regulatory mechanisms remain unclear due to the difficulty in recreating the tumour microenvironment in *in vitro* mammalian cell systems and the involvement of multiple BMPs with positive and negative effects. However, there are some indications that BMP signalling increases in advanced stages of prostate cancer (Ye et al., 2007), when AR signalling becomes hormone-independent, potentially paralleling the observations I have made in SCs, where BMP signalling is essential for the elevated growth seen after mating (Figure 3.5G).

3.4.4. SCs are a site for ecdysone synthesis in adult males

The ecdysone hormone plays a vital role during development and metamorphosis. It has also been shown that the ecdysone regulates various physiological mechanisms in adults as well. However, the sites of ecdysone production in adults are not well-defined. In adult females, it appears that the ovary is involved in the synthesis of ecdysteroids and in adult males, the AG has been suggested to be a site of ecdysone biogenesis (Hentze et al., 2013; Schwedes and Carney 2012). Here, I have demonstrated that the SCs in the AG are specifically responsible for the synthesis of ecdysone hormone in adult males, as knocking down the Halloween genes *shd* and *spo* phenocopied effects observed with ecd^{1}. Additionally, ecdysone synthesised by the SCs regulates growth in virgin males in a local,

potentially autocrine manner. However, in mated males, it appears that growth does not require this locally synthesised ecdysone hormone.

3.4.5. Ecdysone-dependent and -independent EcR signalling controls SC growth in virgin and mated males respectively

I have shown that two different EcR signalling mechanisms regulate SC growth: ecdysone-dependent in virgin males and ecdysone-independent in mated males (Figure 3.9). Interestingly, an ecdysone-independent EcR/USP complex is required for cell survival in a critical period before metamorphosis in the ecdysone-synthesising larval prothoracic gland (PG) before high levels of ecdysone are produced (Mansilla et al., 2016). Therefore, individual cells can switch between hormone-independent and -dependent states under normal conditions, as part of a physiological transition, in both cases, potentially involving EcR signalling at different ecdysone levels.

Interestingly, a comparable transition also appears to take place in CRPC (Section 1.3). Regulation via steroid receptors is complex and some studies have shown that the phosphorylation status of androgen receptor is linked to its ability to act in either a ligand-dependent or -independent manner in prostate cancer (Koryakina et al., 2014). Interestingly, in Chapter 4, I show that a tyrosine kinase receptor, torso, appears to regulate hormone-independent growth in SCs. Frequently steroid receptor signalling interacts with multiple other signalling pathways such as cell cycle and growth factor signalling, and this crosstalk has also been suggested to mediate ligand-independent receptor activity (Hill 1998; A. Sharma et al., 2010). In Chapter 6, I study the interaction between the cell cycle and the EcR in order to determine whether their interaction promotes the switch from hormone-dependent to -independent EcR signalling in SCs.

Chapter-4:

BMP signalling and hormone-independent EcR signalling promote new DNA synthesis in SCs after mating

4.1. Introduction

In Chapter 3, I showed that the BMP and EcR signalling pathway can interact with each other and also act independently to regulate SC growth in virgin and mated males. The EcR isoforms EcR-A and EcR-B1 are involved in the regulation of SC growth in virgin males and in mated males it appeared that EcR-A plays a role in mediating growth, but not EcR-B1. I also demonstrated that EcR-mediated growth in SCs is ecdysone-dependent in virgin males and ecdysone-independent in mated males. In this chapter, I delineate the processes through which the SCs grow after mating. Since certain tissues employ endoreplication as a mechanism to regulate size, I investigated the role of endoreplication in facilitating SC growth. As described in Section 1.14, endoreplication takes place when cells skip the mitotic phase and undergo multiple rounds of S-phase. More specifically, endoreplication is commonly associated with an increase in transcriptional and secretory activity in many cell types.

Previously, Aaron Leiblich was not able to detect any endoreplication in SCs after mating using bromodeoxyuridine (BrdU) (Leiblich et al., 2012). This might have occurred because the antibody for BrdU did not penetrate the AG epithelium. Josephine Hellberg repeated some of these experiments using another analogue of thymidine, ethynyl-2′-deoxyuridine (EdU). Preliminary results from Josephine, showed that endoreplication

occurs in SCs after mating. There was also some indication that the BMP/EcR signalling axis plays a role in this mating-dependent SC endoreplication.

4.2. Aims

In this chapter I describe the processes underlying SC growth in virgin and mated males. The specific research questions that I address in this chapter are:

- Is endoreplication involved in SC growth after mating?
- Does the BMP/EcR signalling axis regulate endoreplication after mating?
- What is the role of ecdysone in the control of endoreplicaton?
- What is the physiological output of mating-dependent SC growth and endoreplication?

Results from Sections 4.3.1- 4.3.5 data have been published in Leiblich et al., 2019.

4.3. Results

4.3.1. Genome endoreplication partially accounts for SC growth after mating

Using the EdU incorporation assay, which measures the proportion of SCs that undergo new DNA synthesis, I investigated the role of endoreplication in regulating adult SC growth after mating by feeding adult males with EdU. I observed that almost no SCs in virgin controls undergo endoreplication, but approximately 25% of SCs incorporate EdU after mating (Fig 4.1 A-C). To validate the role of endoreplication in regulating nuclear size, growth of SC nuclei that endoreplicated (EdU+) and nuclei that did not (EdU-) was measured in control mated males. EdU+ cells had significantly larger nuclei than EdU-

cells, but EdU- nuclei were still larger than those of SCs in virgin males (Fig 4.1 D). Similar trends were observed when total DAPI intensity was assessed, as a measure of nuclear DNA content (through a nuclear Z-stack), in SCs of virgin males and those with EdU (EdU+) and without EdU (EdU-) (Fig 4.1 E). This increase in DAPI intensity in EdU- SCs may occur due to chromatin decondensation, since it has been shown that dye intensity is inversely proportional to chromatin compaction (Carbonari, Tedesco, & Fiorilli, 2001), thereby limiting the use of DAPI intensity to gauge levels of endoreplication. Importantly, the EdU staining was distributed uniformly throughout the nucleus, thereby suggesting that in SCs the whole genome endoreplicates and not just certain regions of the genome as found in follicle cells where chorion genes are specifically amplified (Calvi et al., 1998). Therefore, two types of SC growth occur after mating: SC growth without endoreplication (75% of SCs) and SC growth with endoreplication (25% of SCs).

4.3.2. The BMP/EcR signalling axis also regulates mating-dependent SC endoreplication

I investigated whether SC endoreplication in mated males is under the control of the BMP/EcR regulatory axis, like SC growth. Downregulating BMP signalling by overexpressing Dad in SCs suppressed any endoreplication that occurs after mating (Fig. 4.2 C,G). Upregulation of the BMP pathway by overexpressing Tkv^{act} in SCs resulted in 75% SCs endoreplicating in virgin males and 98% in mated males (Fig. 4.2 D,G). Additionally, upregulating EcR levels by expressing EcR-C resulted in almost all SCs incorporating EdU in virgins and mated males, while knocking down EcR phenocopied the results that were observed by expressing Dad in the SCs, blocking endoreplication in

mated males (Fig 4.2 E-F, H). Hence, these results confirm the preliminary results from Josephine Hellberg that BMP and EcR signalling regulates endoreplication in SCs.

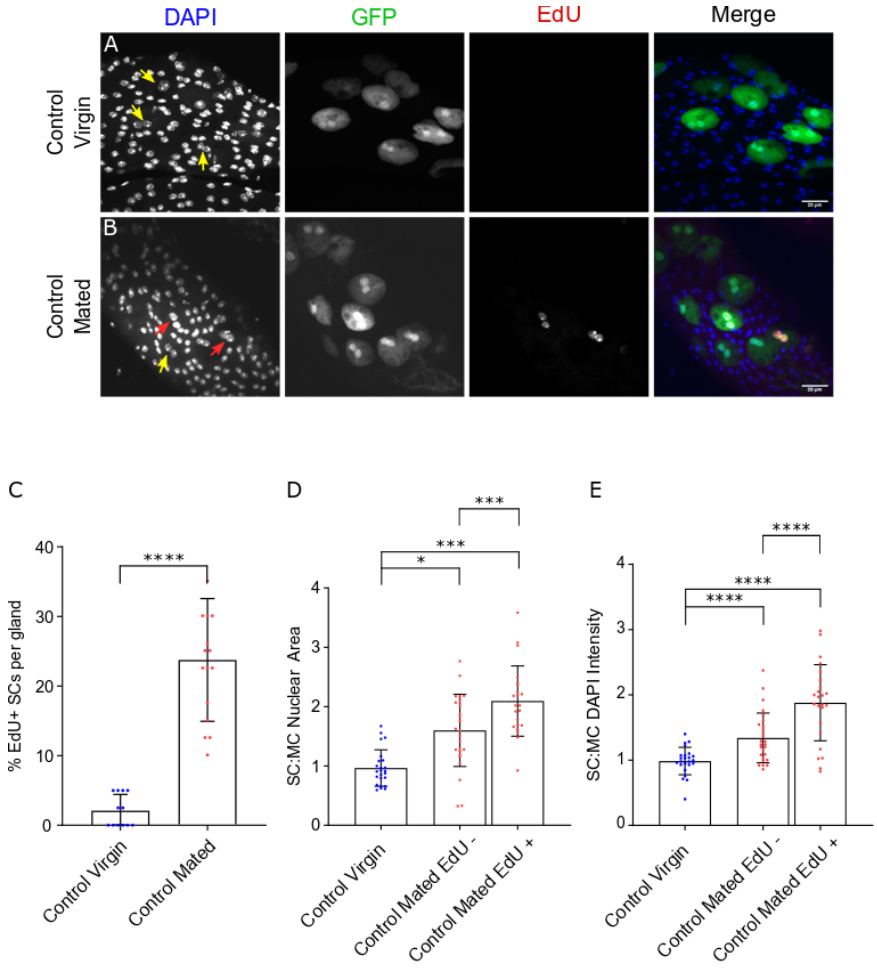

Figure 4.1 Role of genome endoreplication in mating-dependent SC growth
A-B: Images show distal tip of AGs from 6-day-old adult virgin and mated control males switched to 28.5ºC and on 0.2mM EdU-containing food at eclosion. Control represents w^{1118} flies specifically expressing nuclear GFP (which also stains the cytosol) under the control of the esg^{ts}F/O driver in SCs. Nuclei are stained with DAPI (blue). AGs are stained for EdU (red). Red arrow points to SC nuclei that have undergone endoreplication (EdU+) and yellow arrow points to SC nuclei that have not undergone endoreplication (EdU-). Scale bars correspond to 20 µm.
D: Bar chart depicting the mean ratio of the size of SC nuclei relative to neighbouring MC nuclei in control virgin males, control mated males that incorporated EdU (EdU +) and control mated males that did not incorporate EdU (EdU-). The error bars show the standard deviation within the sample. In mated males, SCs grow either by endoreplication or without endoreplication.Welch ANOVA; Games-Howell post hoc test; $0.01<*p\leq0.05$; $0.0001<***p\leq0.001$ ($n\geq7$ SCs; ≥4 males).
E: Bar chart depicting the mean ratio of the DAPI intensity of SC nuclei relative to neighbouring MC nuclei in control virgins, control mated males that incorporated EdU (EdU+) and control mated males that did not incorporate EdU (EdU-). The error bars show the standard deviation within the sample. Endoreplicated SCs have a higher DAPI intensity than non-endoreplicated SCs. However, EdU- SCs of mated males have a higher DAPI intensity than SCs of control virgin males. Brown-Forsythe and Welch ANOVA tests; Dunnett's T3 post hoc test; $****p\leq0.0001$ ($n\geq8$ SCs; ≥4 males).

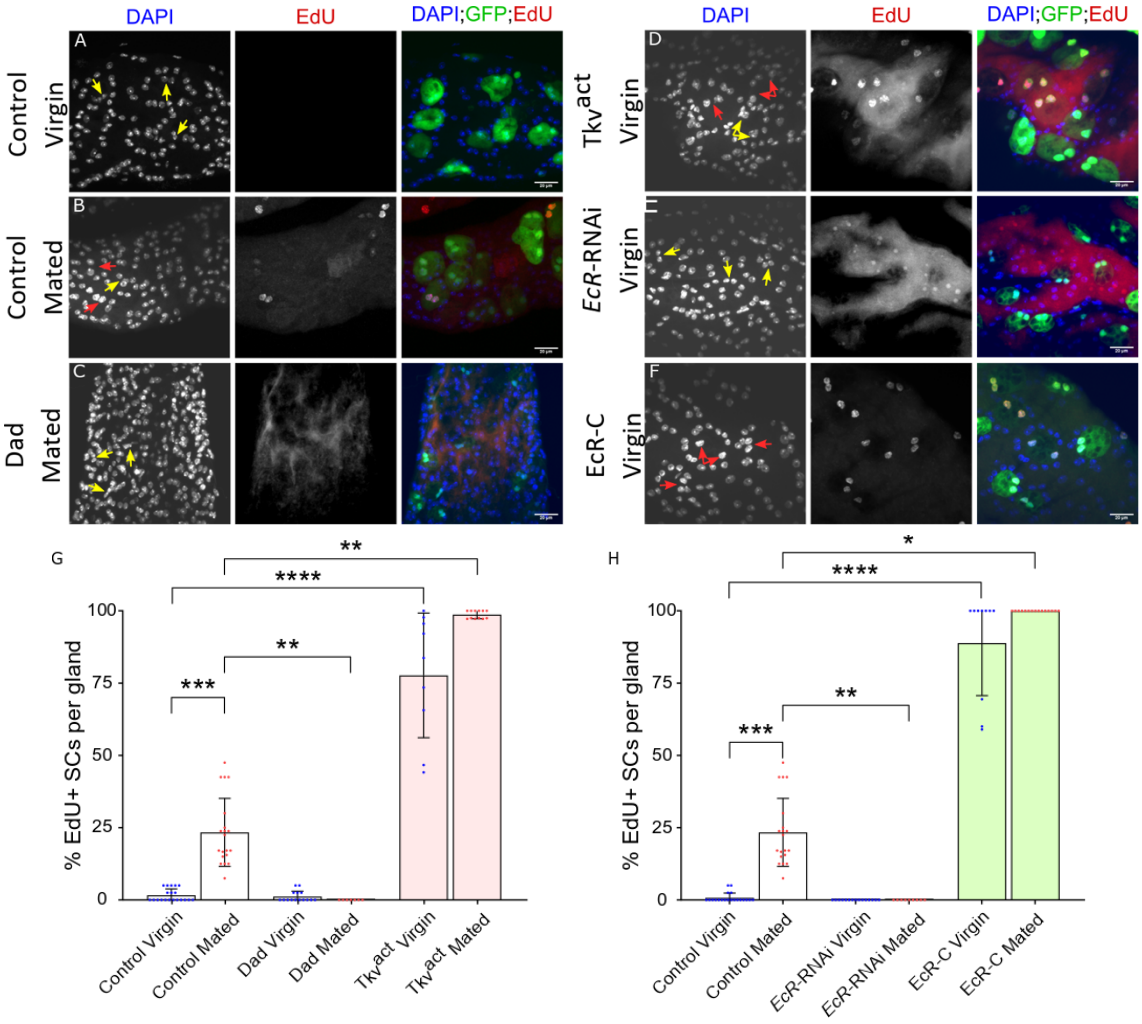

Figure 4.2 Regulation of genome endoreplication by the BMP/EcR signalling axis

A-F: Images show distal tip of AGs from 6-day-old adult virgin and mated males switched to 28.5°C and on 0.2mM EdU-containing food at eclosion to express the corresponding transgenes under the control of the esg^{ts}F/O driver in SCs. Control represents w^{1118} flies specifically expressing nuclear GFP (which also stains the cytosol) in SCs. Nuclei are stained with DAPI (blue). Endoreplicated SCs are stained with EdU (red). Red arrow points to SC nuclei that have undergone endoreplication (EdU+) and yellow arrow points to SC nuclei that have not undergone endoreplication (EdU-). Scale bars correspond to 20 µm.

G: Bar chart depicting the mean % of EdU+ SCs per gland. The error bars show the standard deviation within the sample. The graph includes EdU assay data from adult virgin or mated flies expressing Control, Dad or Tkv^{act} in SCs. BMP signalling is necessary for endoreplication to occur in SCs after mating and it is sufficient to induce endoreplication in virgin males. Kruskal Wallis test; Dunn's post hoc test; 0.001<**p≤0.01; 0.0001<***p≤0.001; ****p≤0.0001 (n≥7 males).

H: Bar chart depicting the mean % of EdU+ SCs per gland. The error bars show the standard deviation within the sample. The graph includes EdU assay data from adult virgin or mated flies expressing Control, *EcR*-RNAi or EcR-C in SCs. EcR signalling is necessary for endoreplication to occur in SCs after mating and it is sufficient to induce endoreplication in virgin males. Kruskal Wallis test; Dunn's post hoc test; 0.01<*p≤0.05; 0.001<**p≤0.01; 0.0001<***p≤0.001; ****p≤0.0001 (n≥9 males).

When either Tkv^{act} + *EcR*-RNAi (High BMP + Low EcR) or Dad + EcR.C (Low BMP + High EcR) were expressed in SCs approximately 20% of SCs in both of the genetic backgrounds endoreplicated (Fig 4.3). In Chapter 3, we had seen that SC growth in both these combinations was not significantly different from control levels. Therefore, these results suggest that like growth regulation, BMP and EcR signalling can mediate SC endoreplication independently as well as by interacting with each other. However, in subsequent genetic combinations (Section 6.3.6), I have been able to show that *EcR*-RNAi can fully suppress some of the effects of upstream cell cycle regulators on SCs.

4.3.3. EcR-A and USP regulate mating-dependent SC endoreplication

EcR-A, but not EcR-B1, regulates SC growth after mating (Section 3.3.2), I therefore examined the effects of reducing expression of these isoforms on mating-dependent endoreplication. Knocking down *EcR-A* abolished any endoreplication that occurred after mating, while silencing *EcR-B1* had no effect (Fig 4.4 A-C, E). Therefore, the expression of *EcR-A*-RNAi in SCs, completely inhibits growth directly resulting from endoreplication in mated males.

Since mating-dependent SC growth is controlled by endoreplication-dependent and -independent mechanisms and unlike SC growth in virgin males, these mechanisms appear to be differentially regulated by specific EcR isoforms, I tested if USP, the general EcR heterodimeric partner, played any role in regulating endoreplication in SCs. Surprisingly, knocking down *USP* suppressed mating-dependent endoreplication even though it had no effect on SC growth after mating. (Fig 4.4 D-E). Hence, I propose that the EcR-A isoform complexes with USP to regulate the endoreplication-dependent arm of SC growth after mating.

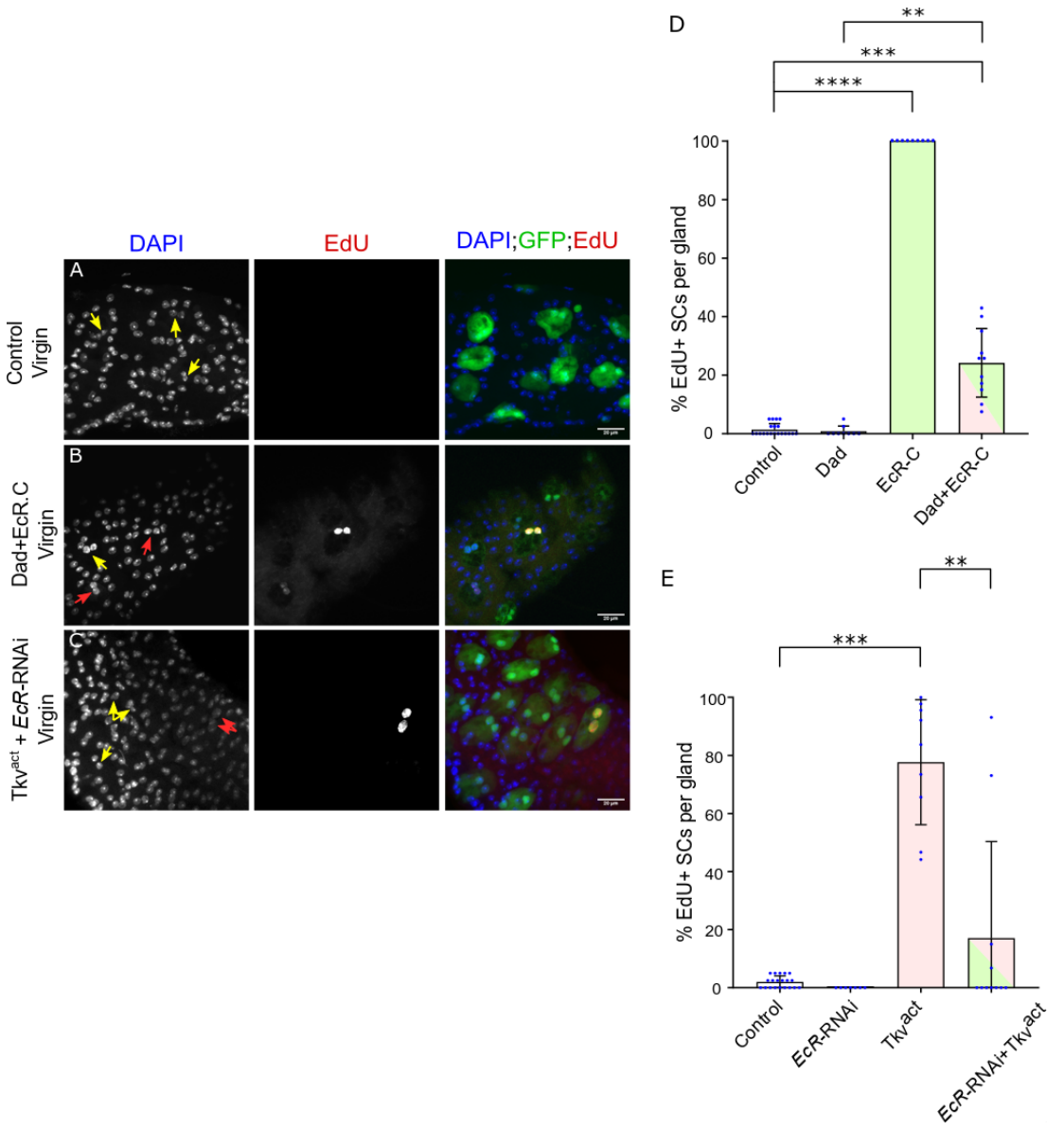

Figure 4.3 Interaction of BMP and EcR signalling pathways in the regulation of genome endoreplication

A-C: Images show distal tip of AGs from 6-day-old adult virgin and mated males switched to 28.5°C and on 0.2mM EdU-containing food at eclosion to express the corresponding transgenes under the control of the esg^{ts}F/O driver in SCs. Control represents w^{1118} flies specifically expressing nuclear GFP (which also stains the cytosol) in SCs. Nuclei are stained with DAPI (blue). Endoreplicated SCs are stained with EdU (red). Red arrow points to SC nuclei that have undergone endoreplication (EdU+) and yellow arrow points to SC nuclei that have not undergone endoreplication (EdU-). Scale bars correspond to 20 µm.

D: Bar chart depicting the mean % of EdU+ SCs per gland. The error bars show the standard deviation within the sample. The graph includes EdU assay data from adult virgin or mated flies expressing Control, Dad, EcR-C or Dad+EcR-C in SCs. Expression of Dad+EcR-C results in an intermediate phenotype in virgin males. Kruskal Wallis test; Dunn's post hoc test; 0.001<**p≤0.01; 0.0001<***p≤0.001; ****p≤0.0001 (n≥9 males).

E: Bar chart depicting the mean % of EdU+ SCs per gland. The error bars show the standard deviation within the sample. The graph includes EdU assay data from adult virgin or mated flies expressing Control, *EcR*-RNAi, Tkv^{act} or *EcR*-RNAi+Tkv^{act} in SCs. Expression of EcR-RNAi+Tkv^{act} results in an intermediate phenotype in virgin males. Kruskal Wallis test; Dunn's post hoc test; 0.001<**p≤0.01; 0.0001<***p≤0.001 (n≥9 males)

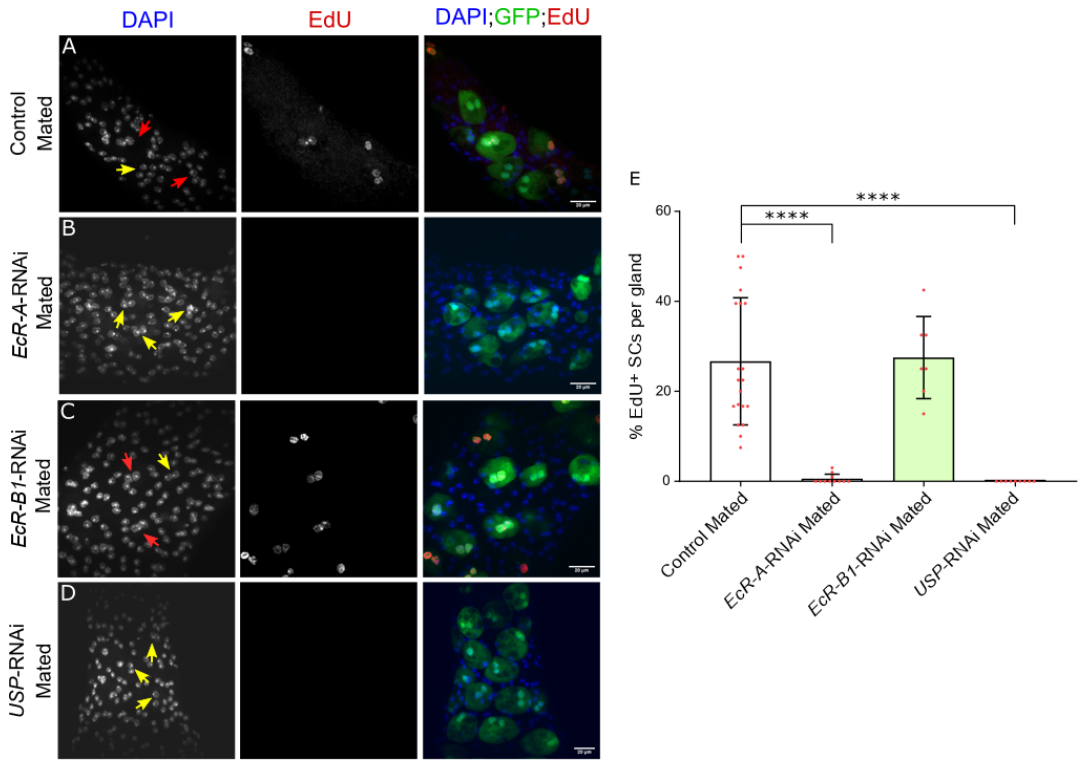

Figure 4.4 Role of EcR isoforms and USP in mating-dependent endoreplication
A-D: Images show distal tip of AGs from 6-day-old adult virgin and mated males switched to 28.5ºC and on 0.2mM EdU-containing food at eclosion to express the corresponding transgenes under the control of the esg^{ts}F/O driver in SCs. Control represents w^{1118} flies specifically expressing nuclear GFP (which also stains the cytosol) in SCs. Nuclei are stained with DAPI (blue). Endoreplicated SCs are stained with EdU (red). Red arrow points to SC nuclei that have undergone endoreplication (EdU+) and yellow arrow points to SC nuclei that have not undergone endoreplication (EdU-). Scale bars correspond to 20 µm.
E: Bar chart depicting the mean % of EdU+ SCs per gland. The error bars show the standard deviation within the sample. The graph includes EdU assay data from adult virgin or mated flies expressing Control, *EcR-A*-RNAi, *EcR-B1*-RNAi or *Usp*-RNAi in SCs. Suppressing *EcR-B1* expression has no effect on endoreplication in mated males. Kruskal Wallis test; Dunn's post hoc test; ****$p \leq 0.0001$ ($n \geq 7$ males).

4.3.4. Mating-dependent SC endoreplication is under hormone-independent EcR regulation

Since the SC growth that occurs after mating is independent of ecdysone, I determined whether mating-dependent endoreplication is independent of ecdysone as well. As expected, downregulating the levels of ecdysone hormone in the entire fly post-eclosion for 6 days by shifting the *ecd*^{1} males to the non-permissive temperature of 29°C resulted in no uptake of EdU in virgins. However, approximately 90% of SCs endoreplicated after

mating, providing a potential explanation for the drastic increase in SC growth seen in mated *ecd*^{1} males (Fig 4.5 A-B, E). Expressing *spo*-RNAi or *shd*-RNAi in the SCs resulted in only 30% of SCs undergoing endoreplication, much like in the control mated males (Fig 4.5 C-D,F). These results reveal the hormone-independent nature of mating-induced endoreplication, although the surprising result with the *ecd*^{1} mutant may reflect the pleiotropic effects of this mutant (Redfern and Bownes 1983), rather than a specific outcome of reducing ecdysone levels.

Consistent with the unusual behaviour of the *ecd*^{1} allele, when 20-HE was fed to virgin *ecd*^{1} males, 50% of the SCs underwent endoreplication. Feeding mated *ecd*^{1} males on 20-HE-containing food throughout adulthood revealed no significant reduction in the high level of endoreplication observed (Fig 4.5 E). By contrast, feeding 20-HE to *shd*-RNAi and *spo*-RNAi males had no effect on endoreplication levels either in virgin or mated animals (Fig 4.5 F-G), thereby confirming that endoreplication occurs in a hormone-independent manner. We also conclude that the unusual effects on endoreplication observed in *ecd*^{1} males do not result from changes in ecdysone levels.

4.3.5. Genome endoreplication leads to increased secretory biogenesis in SCs

Endoreplication often results in increased metabolic activity and protein synthesis which can be attributed to the increased DNA copy number. In order to test whether the hormone-independent genome replication after mating fulfilled a similar physiological role, I assessed the secretory trafficking in SCs after mating.

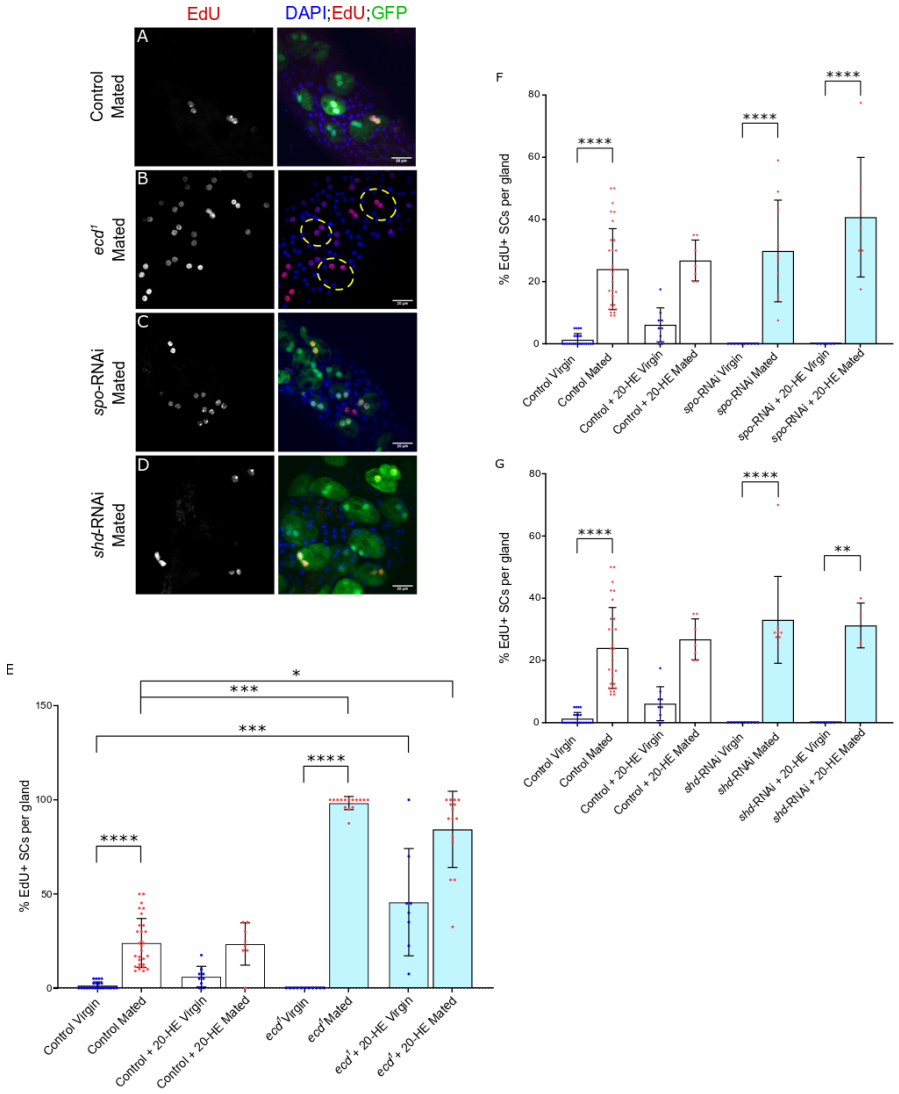

Figure 4.5 Role of EcR isoforms and USP in mating-dependent endoreplication

A-D: Images show distal tip of AGs from 6-day-old adult virgin and mated males switched to 28.5°C and on 0.2mM EdU-containing food at eclosion to express the corresponding transgenes under the control of the esg^{ts}F/O driver in SCs. Control represents w^{1118} flies specifically expressing nuclear GFP (which also stains the cytosol) in SCs. Nuclei are stained with DAPI (blue). Endoreplicated SCs are stained with EdU (red). Yellow ellipses outline the SCs in B. Scale bars correspond to 20 µm.

E: Bar chart depicting the mean % of EdU+ SCs per gland. The error bars show the standard deviation within the sample. The graph includes EdU assay data from adult virgin or mated flies expressing Control or *ecd*^{1} and maintained on normal food or 0.2mM 20-HE containing food. Upon feeding 10mM 20-HE, an increase in endoreplication is observed in virgin males, which probably occurs due to the pleiotropic effects of the mutant, and in mated males no change is observed. Kruskal Wallis test; Dunn's post hoc test; 0.01<*p≤0.05; 0.0001<***p≤0.001; ****p≤0.0001 (n≥7 males).

F-G: Bar chart depicting the mean % of EdU+ SCs per gland. The error bars show the standard deviation within the sample. The graph includes EdU assay data from adult virgin or mated flies expressing Control, *shd*-RNAi (F) or *spo*-RNAi (G) in SCs and maintained on normal food or 10 mM 20-HE containing food. Feeding 10mM 20-HE also did not have any effect on endoreplication in these backgrounds. Kruskal Wallis test; Dunn's post hoc test; 0.001<**p≤0.01; 0.0001<***p≤0.001; ****p≤0.0001 (F: n≥7 males; G: n≥7 males except for shd-RNAi+20HE mated (n=4 males)).

Previous work in the lab showed that the BMP pathway regulates the secretion of exosomes produced by SCs (Corrigan et al., 2014) and this secretory activity is increased after mating (Redhai et al., 2016). I combined the tools used to assess secretory activity with the EdU assay to see if these two processes are linked. I expressed a green fluorescent protein (GFP)-tagged form of the human exosome marker CD63-GFP in a 24-hour pulse (Corrigan et al., 2014) in multiply-mated males which were fed with EdU-containing food. The CD63 protein labels all large secretory compartments in SCs. Hence the rate of compartment formation could be measured by the number of compartments marked by GFP during a 24-hour pulse of expression of the CD63-GFP construct.

In virgin males one new compartment is labelled over 4 to 5 hours (Corrigan et al., 2014; Redhai et al., 2016). In mated males, I noticed that SCs that endoreplicated had a significantly higher number of GFP-positive compartments as compared to those that did not endoreplicate (Fig 4.6 A-B). Therefore, these results show that the rate of secretory trafficking is higher in endoreplicated SCs, and therefore indicate that these cells have greater secretory activity than their neighbours that do not endoreplicate.

4.3.6. Forkhead and torso regulate EcR-mediated endoreplication

Since SC growth and endoreplication regulation mirrors the signalling that occurs in CRPC, I was curious to determine whether other aspects of CRPC-associated signalling can also be observed in SCs. Some studies have shown that certain transcription factors that act alongside the AR are essential for sustaining active AR signalling in CRPC. I looked at one such transcription factor family that interacts with AR in prostate cancer, Forkhead box proteins A1 and A2 (FOXA1 and FOXA2). The Forkhead family contains pioneer factors that enable opening of compact chromatin.

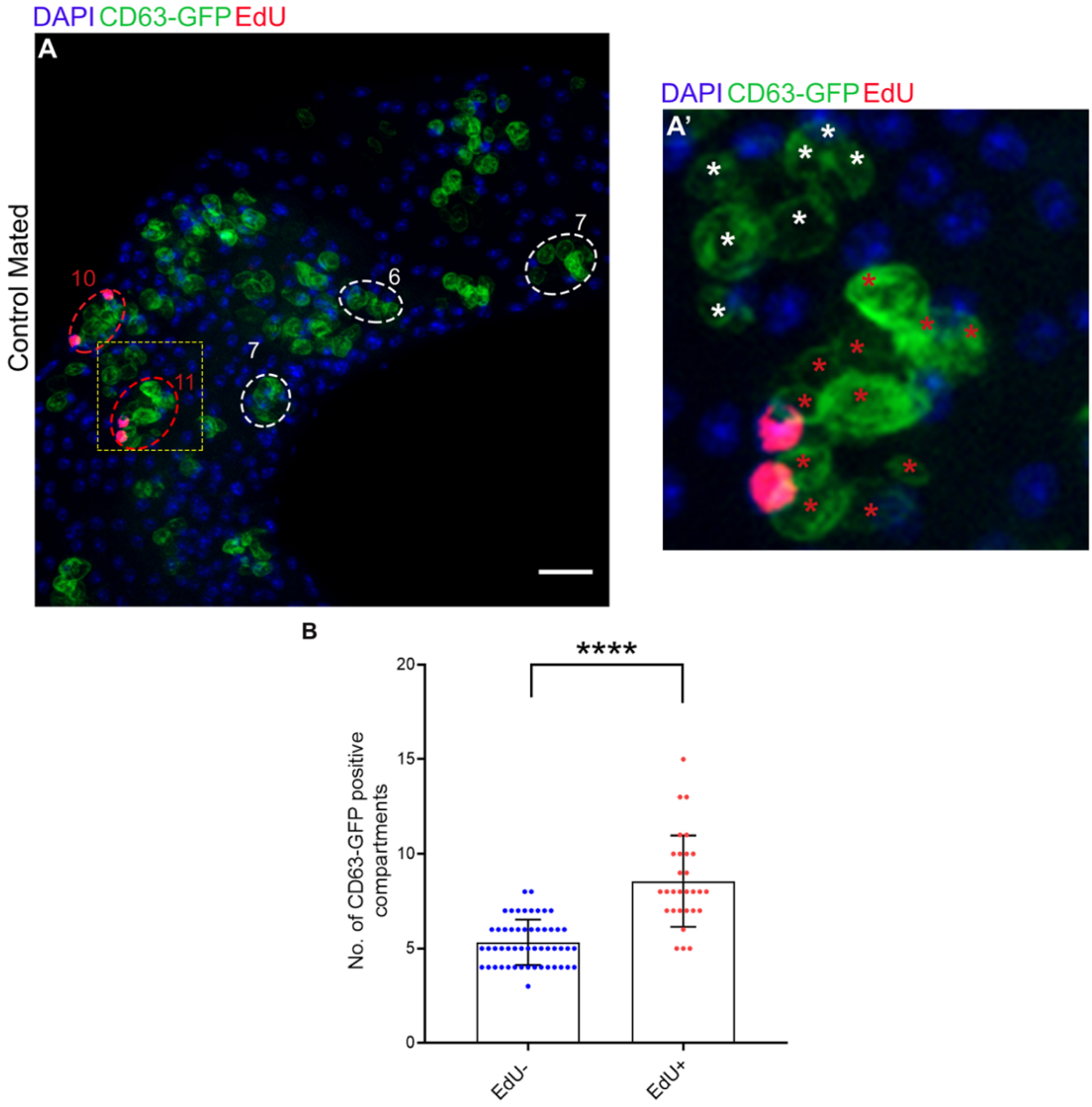

Figure 4.6 Role of EcR isoforms and USP in mating-dependent endoreplication

A: Image of AG of a 7-day-old male which was multiply mated for 6-days and was then shifted to 28.5°C for a 24-hour pulse of CD63-GFP expression to label newly formed SC compartments. Nuclei are stained with DAPI (blue). Endoreplicated SCs are stained with EdU (red). Dashed red ellipses outline EdU+ SCs and dashed white ellipses outline EdU- SCs. The numbers next to the marked SCs represent the total number of CD63-GFP compartments formed in one day. Scale bars correspond to 50 µm.

A': Inset image of boxed area in A containing one endoreplicated SC and one non-endoreplicated SC. Red stars label the compartments of EdU+ SCs and white stars label the compartments of EdU- SCs.

B: Bar chart depicting the total number of CD63-GFP-labelled compartments in EdU- and EdU+ SCs. Endoreplicated SCs produce a significantly higher number of new compartments as compared to non-endoreplicated SCs. Two-tailed Mann-Whitney test; ****$p<0.0001$ (n=14 SCs; ≥8 males).

They have been implicated in promoting hormone-dependent growth in early prostate cancer stages, but are not involved in some hormone-independent AR signalling in CRPC (Zhao et al., 2014). Knocking down the *Drosophila* homologue of *FOXA1* and *FOXA2*, *forkhead* (*fkh*), resulted in a reduction of SC growth in virgins. Expression of *fkh*-RNAi did not affect SC growth in mated males, but it increased the percentage of SCs that endoreplicated. Hence, FKH regulates the hormone-dependent EcR signalling in virgin males and it is not required for the hormone-independent EcR signalling that controls endoreplication in mated animals, though it may be involved in other aspects of hormone-independent growth. This broadly mirrors the activities of FOXA1 and FOXA2 in the regulation of prostate cancer progression.

Dysregulation of a class of receptor tyrosine kinases (RTKs) has also been implicated in mediating progression of prostate cancer to CRPC by promoting hormone-independent AR signalling (Brown et al., 2018; Chandrasekar et al., 2015). Hence, I studied the role of Torso, a *Drosophila* RTK, expressed in SCs (Hentze et al., 2013) in the regulation of SC growth and endoreplication. Knocking down *torso*, resulted in a reduction in growth in both virgin and mated males and it also completely suppressed mating-dependent endoreplication. Interestingly, SCs still exhibited increased growth after mating following *torso* knockdown, suggesting endoreplication-independent growth was not fully suppressed. Therefore, it appears that in virgin males, Torso is essential for hormone-dependent EcR signalling. In mated males, Torso seems to promote hormone-independent EcR signalling, thereby mirroring the effects observed in hormone-refractory prostate cancer. As mentioned in Section 3.4.5, it is possible that Torso regulates EcR signalling by controlling either the EcR's or USP's phosphorylation state.

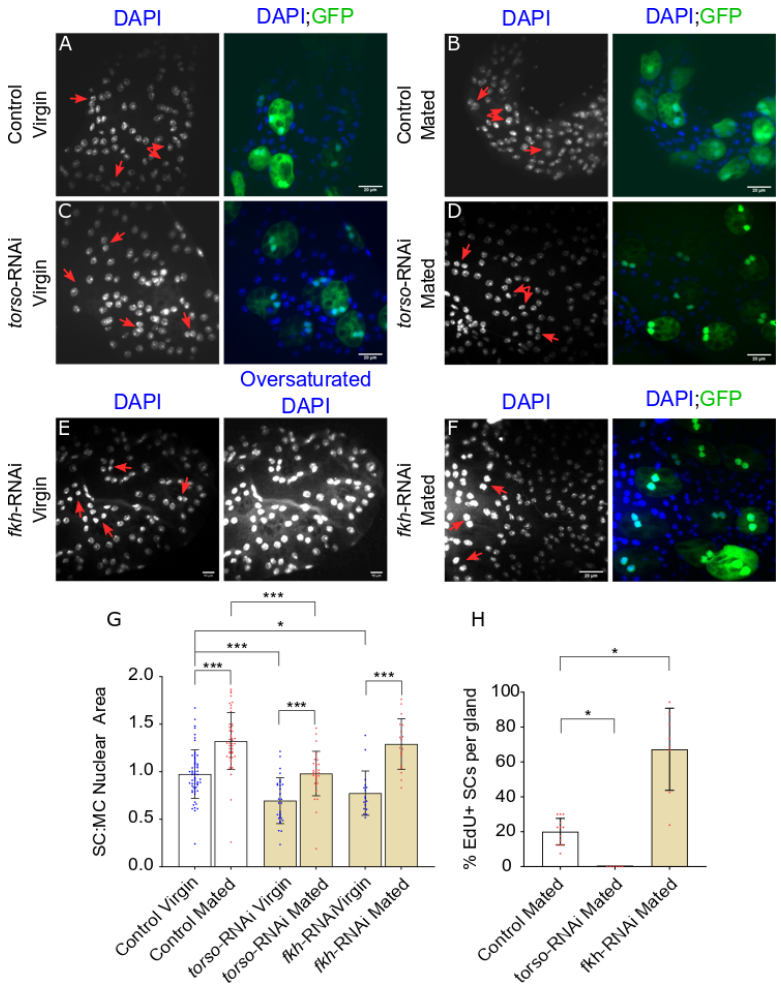

Figure 4.7 Role of FKH and Torso in SC growth and endoreplication

A-D: Images show distal tip of AGs from 6-day-old adult virgin and mated males switched to 28.5°C and on 0.2mM EdU-containing food at eclosion to express the corresponding transgenes under the control of the esg^{ts}F/O driver in SCs. Control represents w^{1118} flies specifically expressing nuclear GFP (which also stains the cytosol) in SCs. Nuclei are stained with DAPI (blue). Red arrows point to representative SC nuclei for each transgene. When the growth assay experiment was done with *fkh*-RNAi in virgin males, GFP expression was weak, for reasons we do not understand. Hence, the oversaturated DAPI channel is shown in order to identify the SCs.Scale bars correspond to 20 µm.

G: Bar chart depicting the mean ratio of the size of SC nuclei relative to neighbouring MC nuclei. The error bars show the standard deviation within the sample. The graph includes SC growth assay data for virgin and mated males expressing Control, *fkh*-RNAi or *torso*-RNAi in SCs. Expression of *torso*-RNAi in SCs suppresses SC growth in virgin and mated males. However, a difference between SC growth of *torso*-RNAi-expressing virgin and mated males is observed. Expression of *fkh*-RNAi in SCs inhibits SC growth in virgins and has no effect on mated males. One-way ANOVA; Tukey's HSD post hoc test; 0.01<*p≤0.05; ****p≤0.0001 (n≥21 SCs; 7 males).

H: Bar chart depicting the mean % of EdU+ SCs per gland. The error bars show the standard deviation within the sample. The graph includes EdU assay data for virgin and mated males expressing Control, *fkh*-RNAi or *torso*-RNAi in SCs. Expression of *torso*-RNAi in SCs completely suppresses mating-dependent endoreplication. Knocking down *fkh* in SCs results in an increase in the number of SCs that undergo endoreplication. As none of the SCs in virgin males in these background undergo endoreplication, these data have not been included in this graph. Kruskal Wallis test; Dunn's post hoc test; 0.01<*p<0.05; 0.0001<***p≤0.001; ****p≤0.0001 (n≥7 males).

4.4. Summary and Discussion

It is now well-established that adult secondary cells increase their rate of growth when males mate (Leiblich et al., 2012). In this chapter, I show that in multiply-mated males, 25% of SCs endoreplicate, a process that contributes to the increase in SC growth observed after mating. An unknown mechanism allows for the remaining non-endoreplicated SCs (75%) to also increase in size after mating. The growth that occurs in SCs of ageing virgin males does not involve endoreplication. Similar to the regulation of SC growth, both the BMP and EcR signalling pathways regulate SC endoreplication through a partially shared signalling pathway. Interestingly, an ecdysone-independent EcR-A/USP complex is essential for mating-dependent endoreplication in SCs, which correlates with an increase in biosynthetic secretory capacity. Furthermore, I have demonstrated that the SC model may capture other features of prostate cancer progression to CRPC such as regulation by homologues of AR-interacting transcription factors and RTKs (Fig. 4.8).

4.4.1. Mating promotes new DNA synthesis in SCs to deal with reproductive stress

Although BMP/EcR signalling plays a critical role in mating-induced endoreplication, only some cells endoreplicate, suggesting another signal is also required. The increased biosynthetic capacity of endoreplicated SCs is consistent with the idea that increased metabolic or secretory activity might be demanded of SCs after mating. Endoreplication has been observed to be initiated upon extreme stress conditions including genotoxic stress and DNA damage. For example, in the absence of light, *Arabidopsis* hypocotyls undergo an extra round of endoreplication in order to deal with the environmental stress (de Veylder et al., 2011).

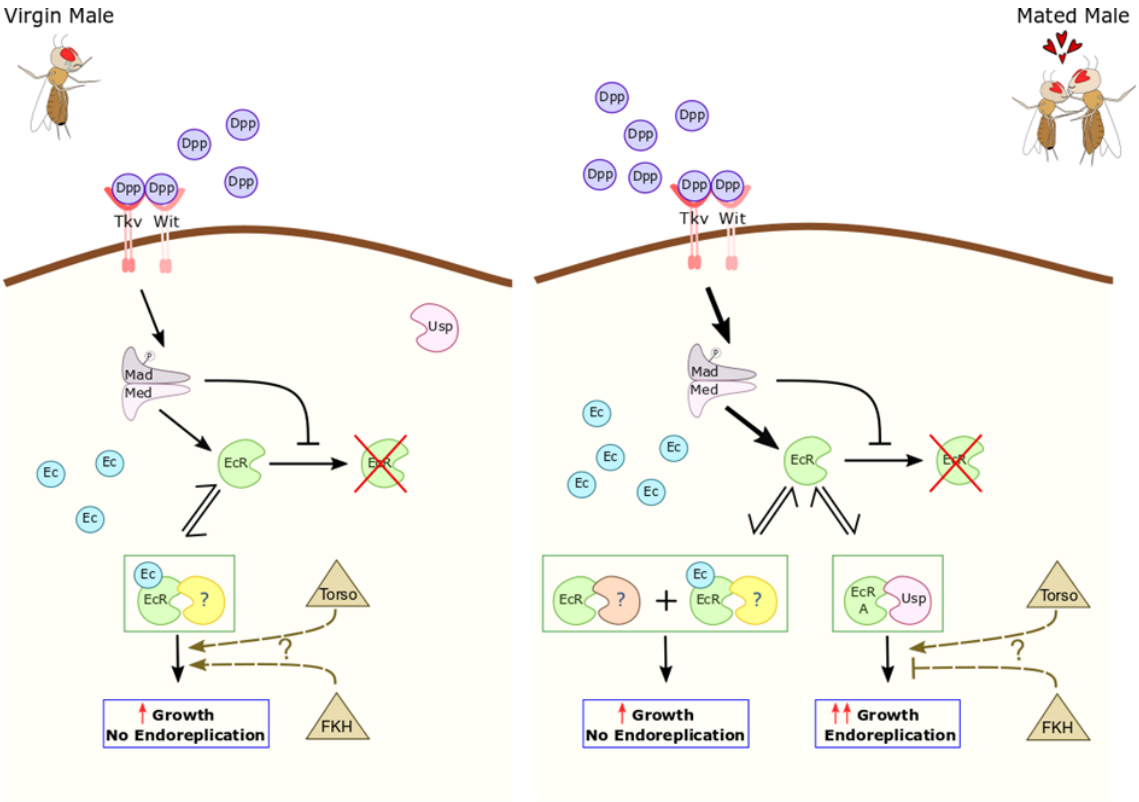

Figure 4.8 Schematic depicting regulation of growth and endoreplication in SCs
In mated males, 25% of SCs undergo endoreplication, which accounts for the increase in growth observed after mating. This endoreplication-dependent SC growth is regulated by an EcR-A/USP complex in an ecdysone-independent manner. However, there is no conclusive evidence on whether the non-endoreplication growth requires ecdysone hormone in mated males. No such endoreplication occurs in virgin males. Torso is required for SC growth in virgin males and it specifically regulates endoreplication-dependent SC growth in mated males. FKH promotes SC growth in virgin males, but it appears to inhibit endoreplication-dependent SC growth in mated males. It is not known whether Torso and FKH regulate SC growth by interacting with EcR in these scenarios. FKH-Forkhead; EcR A- EcR isoform A.

Similarly, *Pseudomonas entomophila*-induced gut damage in *Drosophila*, initiates the enterocytes to undergo approximately 5 rounds of endoreplication (Xiang et al., 2017). Hence, the act of mating might incur a stress at the cellular level in sporadic SCs, which could lead to the occurrence of endoreplication in these post-mitotic cells. The resulting increased secretion would contribute to the replenishment of seminal fluid proteins that were transferred to the females during mating. Hence, determining the mating-induced signal that triggers endoreplication in SCs is vital for understanding the physiological

basis of this phenomenon. Analysing the effect of hindering various aspects of courting and copulation might provide insight into the mating event that controls this process.

A study by Herndon et al., 1997 showed that seminal fluid transfer to females triggers expression of accessory gland proteins synthesised in MCs; a similar mechanism could also presumably stimulate SC endoreplication. This hypothesis could be tested by utilising the *Drosophila* premature ejaculation system, which activates *corazonin*-GAL4-(*crz*-Gal4-) expressing accessory gland neurons by synthesising dTRPA1, a temperature- and voltage-gated cation channel, to promote neuron action potential firing in a temperature-dependent manner (Berni et al., 2010; Tayler et al., 2012) in order to promote ejaculation. This system could be combined with the EdU assay in order to test whether the act of emptying the AG is sufficient to induce SC endoreplication. Since a male can mate approximately five times in one day (Douglas, Anderson, and Saltz 2020), promoting premature ejaculation by activating the *crz*-GAL4 neurons more than five times every day for 6 days, might be necessary for this experiment. This would be a first step towards understanding the mating signal that turns on endoreplication in SCs.

4.4.2. Mating induces ecdysone production in the whole fly

Collaborating with Aaron Leiblich, we found that mated males have higher ecdysone titres as compared to virgin males (Leiblich et al., 2019). Apart from showing that transfer of seminal fluid to females triggers the production of MC accessory gland proteins, authors of Herndon et al., 1997, also demonstrated that topical application of either 20-HE or juvenile hormone on virgin males simulates the changes in MC gene expression observed in mated males. This increase in ecdysone levels might be necessary for stimulating the production of accessory gland proteins in MCs. However, it appears that

some SC activities do not respond to ecdysone levels after mating. Ecdysone-independent growth and endoreplication in SCs might be mechanisms through which SCs compensate for their relatively small numbers during the replenishment of SC-specific accessory gland proteins in seminal fluid. This proposal is backed up by the fact that endoreplicated SCs have an increased biosynthesis activity. Since I have shown in Chapter 3 that SCs are an ecdysone biosynthesis hub in adult males, I think it would be interesting to determine whether suppressing ecdysone production in SCs has any effects on gene expression levels in MCs. Another method for testing this would be to assess whether an ecdysone reporter line, EcRE-GFP, which expresses GFP once ecdysone binds to EcRE regulatory elements, is activated in MCs, and if expressing *shd*-RNAi or *spo*-RNAi in SCs suppresses this. However, currently available reported constructs have not produced consistent signals in the accessory gland, and so these studies may require the analysis of genes of EcR targets in MCs.

Remarkably, it has been shown that in pupae, ecdysone secretion not only occurs via diffusion, but it also can occur through vesicle exocytosis, as dysregulating the trafficking machinery involved phenocopies results observed in ecdysone-deficient animals Yamanaka et al., 2015). Given that SCs are secretory cells that synthesise and secrete exosomes, it is possible that ecdysone produced by SCs can be secreted and transported to MCs, either via exosomes or through more conventional secretory pathways. Studying the MC gene expression in glands in which *Atet*, an ABC transporter implicated in regulating vesicle-mediating ecdysone secretion (Yamanaka et al., 2015), or an exosome regulator are knocked down in SCs might shed light on whether any observed hormone effects on MCs might be linked to secretory pathways rather than free diffusion.

4.4.3. An EcR-A/USP heterodimer promotes mating-induced, hormone-independent endoreplication in SCs

In Chapter 3, I showed that expression of *EcR-A*-RNAi in SCs of virgin and mated males reduces SC nuclear growth, and in this chapter, I have demonstrated that *EcR-A* knockdown blocks mating-dependent endoreplication. Since there is a significant increase in SC growth observed between virgin and mated males expressing *EcR-A*-RNAi, this suggests that some mating-dependent growth does not require EcR-A. The reduction in SC nuclear growth observed in mated males after *EcR-A* knockdown must be at least partially explained by the suppression of endoreplication-dependent SC growth. Although the fact that pan-*EcR* knockdown completely suppresses any growth that occurs after mating indicates that the rest of the growth not regulated by EcR-A is mediated by the other EcR isoforms. Therefore, genetic manipulation of EcR-A is important in decoupling endoreplication-dependent and endoreplication-independent growth that occurs after mating. Since knocking down *Usp* completely abolishes mating-dependent endoreplication, we propose that EcR-A heterodimerizes with USP to regulate SC endoreplication. Reinterpreting the nuclear growth data of *Usp*-RNAi in light of the role of USP in SC endoreplication, it appears that USP might inhibit endoreplication-independent SC growth after mating. One possible explanation is that its heterodimerisation with EcR-A or other EcR isoforms prevents the latter from interacting with other proteins to promote endoreplication-independent growth after mating. This form of EcR-A-dependent, but USP-independent, SC growth after mating would partially mirror the EcR-A-dependent, USP-independent, growth seen in virgin males, except that only the latter appears to be ecdysone-dependent. Since mating-dependent SC endoreplication does not require ecdysone, I propose that SC growth that occurs via endoreplication is regulated by an EcR-A/USP complex in an ecdysone-independent

manner. Although SC growth is not affected in the case of *shd*-RNAi and *spo*-RNAi mated flies, it cannot be concluded with certainty that endoreplication-independent SC growth does not require ecdysone.

As discussed in Section 3.4.5, an ecdysone-independent EcR/USP complex has been observed in the prothoracic gland (PG). It was shown that knocking down either EcR or USP resulted in cell-death which involved activation of the stress-sensing JNK signalling pathway, and this phenotype could be rescued by overexpressing a dominant negative form of the EcR-B1, EcR-B1^{W650A} (Cherbas et al., 2003), which does not bind to ecdysone (Mansilla et al., 2016). Therefore, it is possible that a similar ecdysone-independent EcR-A/USP complex regulates SC growth via endoreplication in the SCs, which like the PG also has the ability to synthesise ecdysone. Interestingly, several studies in prostate cancer cell lines have revealed that the AR and the apoptotic JNK signalling can interact either positively or negatively with each other in the regulation of prostate cancer progression. It appears that the AR can regulate JNK signalling and vice-versa but the molecular mechanisms underlying this have not been explained in detail yet (Lorenzo and Saatcioglu 2008; Xu and Hu 2020). Like in the *Drosophila* PG, knocking down AR in the androgen-sensitive LNCaP cell lines promotes JNK-mediated apoptosis (Lorenzo and Saatcioglu 2008). Furthermore, there is also some evidence suggesting that JNK deficiency promotes the development of the hormone refractory form of prostate cancer in mice (Hübner et al., 2012). Hence, it will be interesting to test whether the JNK pathway is suppressed by the ecdysone-independent, growth regulatory EcR-A/USP signalling in SCs of mated males, for example by using the JNK signalling reporter *puc-lacZ*. Additionally, studying the interaction between the EcR and JNK pathways in SCs, which appear to be particularly resistant to apoptotic signals, could help us better

understand the link between the AR and JNK signalling in androgen-dependent and -independent prostate cancer.

4.4.4. EcR-B1 is not essential for regulating SC growth in mated males

SC growth in virgin males requires the EcR-A and EcR-B1 isoforms. Knocking down all the EcR isoforms using the pan *EcR*-RNAi construct resulted in a reduction in both endoreplication-dependent and -independent growth in mated males. The EcR-A isoform appears to primarily regulate endoreplication-dependent growth and the EcR-B1 isoform does not play a role in either of the two types of mating-dependent growth. However, as discussed in Section 3.4.1, the effects observed with knockdown of *EcR-B1* might occur due to the functional redundancies of the EcR isoforms which might lead to a compensatory effect. In any case, these results suggest a possible role of EcR-B2 in the regulation of endoreplication-independent SC growth. One possible way to follow up this hypothesis would be to use the available EcR-B2 dominant negative flies. Interestingly, crossing any of the EcR isoform dominant negative flies with the esgF/O^{ts} driver line does not produce any progeny of the appropriate phenotype, for reasons we do not understand; *esg* is expressed in many stem cell populations and this might affect viability through leaky expression. However, crossing the same flies with the GAL80^{ts}-regulated dsx-GAL4 driver line results in viable progeny. Hence, all the dominant negative lines could be tested using this driver. Although these lines have been successfully used to study the role of EcR isoforms in other contexts (Cherbas et al., 2003; Sharma et al., 2017), a major drawback of using these lines is that they overexpress a mutant form of the isoform without affecting the endogenous EcR isoform levels thereby solely relying on the competition between these mutant and endogenous isoforms. It might be difficult to

determine the true role played by EcR-B2 using this method, but it might help us understand the effects of dysregulated EcR-B2 on SC growth and endoreplication.

Although we know that EcR-B1 is the major isoform expressed in SCs of virgin males, we do not know whether this remains the same in males mated over a six-day period. This would add an important element to our understanding of mating-dependent versus -independent growth. During my DPhil, I have not been successful in being able to use the EcR antibody to stain the AG. I tried different batches of the DSHB pan-EcR antibody (Ag 10.2), but I encountered batch variability issues with either no staining or non-specific staining. I believe that this might be due to some problems with the manufacturing or storage process of the EcR antibody, since no other researchers in the lab, including Aaron Leiblich, who undertook most of the early successful EcR stainings, have been able to reproduce these results recently and there are no recent publications using this antibody. One alternative would be to construct a fluorescently labelled gene trap for EcR to proceed with analysing the expression of various EcR isoforms in the SCs after mating. However, a currently available *EcR* genomic construct marked by a C-terminal GFP (BL 59040) did not express at detectable levels in SCs, suggesting that this strategy may also be challenging.

4.4.5. Modelling the CRPC switch in SCs

Several transcription factors collaborate with the AR to promote prostate cancer progression and induce CRPC. These factors interact with the AR and each other in a complex manner. In this chapter, I tested one such transcription factor, FKH, which appears to affect EcR signalling in SCs in a manner that mirrors the effects of its

homologues on AR signalling. Furthermore, I found evidence that RTK signalling may also be essential for hormone-independent signalling.

Apart from mirroring the switch from hormone-dependence to hormone-independence of the EcR and its interaction with BMP signalling, in Chapter 6, I demonstrate that the SC system also encapsulates the role played by key cell cycle components in prostate cancer progression. Therefore, my data suggest that the SC model system could be further utilised to disentangle the complex network of signalling and transcriptional controls that regulate the transition to CRPC and hormone-independent AR signalling. In Appendix A, I have summarised a possible list of transcription factors that are known to interact with the AR and their corresponding *Drosophila* homologues that could be tested in the first instance. These can then be combined with different manipulations of the EcR, to study their genetic interaction with the EcR, which might shed light on the key regulatory mechanisms and genetic interactions that could then be focussed on in mammalian systems.

Chapter-5:

Regulation of compartment formation and exosome secretion by BMP/EcR signalling axis

5.1. Introduction

The BMP/EcR signalling axis regulates endoreplication-dependent SC growth, which I have shown in Chapter 4 promotes increased biosynthetic activity. I was interested to study the role played by the BMP/EcR pathway in the regulation of biogenesis of various exosome populations and compartments that produce them in SCs. As discussed in Section 1.10, the Wilson research group has previously shown that these exosomes are secreted into the lumen of the accessory gland and have the ability to transfer to females upon mating and reprogramme their behaviour (Corrigan et al., 2014). Furthermore, the exosomes can be marked with a range of fluorescent markers, some of which act as signatures for their endosomal origin (Fan et al., 2020).

5.2. Aims

In this chapter, I assess the importance of the BMP and EcR pathways in regulating SC exosome biogenesis and the identity of the compartments that produce these exosomes. I address the following specific research questions:

- Does the BMP/EcR pathway regulate the formation of compartments marked by the Btl, Rab6 or Rab11?

- Does the BMP/EcR pathway regulate biogenesis of exosomes marked by Btl, Rab6 or Rab11 within the compartments whose limiting membranes are associated with these markers?

5.3. Results

5.3.1. Regulation of Btl-labelled compartment formation and exosome biogenesis by EcR signalling

When *EcR* was either knocked down or overexpressed using the temperature-sensitive *dsx*-GAL4 driver (dsx^{ts}) in a line that co-expresses Btl-GFP under UAS-control (DTBtl), I observed that the total number of Btl-GFP-positive compartments significantly increased. The percentage of these compartments that produced ILVs in an *EcR*-RNAi background was close to 7% as compared to 63% in controls (Fig. 5.1 A, B, D, E). Interestingly, in those exosome-forming compartments, I observed that the ILVs, from which exosomes are formed, were always associated with the limiting membrane of the compartments (Fig. 5.1 B', B'') , unlike controls, where the vesicles were also observed at a distance from the limiting membrane (Fig. 5.1 A'). When EcR-C was overexpressed, it also resulted in a decrease in the proportion of compartments that produced Btl-GFP-positive ILVs, as compared to the controls (Fig. 5.1 C-E). Much like in the controls, the ILVs were associated with or detached from the compartment's limiting membrane (Fig. 5.1 C'). Hence, EcR tightly regulates the production of Btl-containing compartments, but potentially via multiple mechanisms, because both knocking-down and overexpressing *EcR* increases compartment formation. EcR is also necessary for the proper formation of Btl-positive exosomes in SCs.

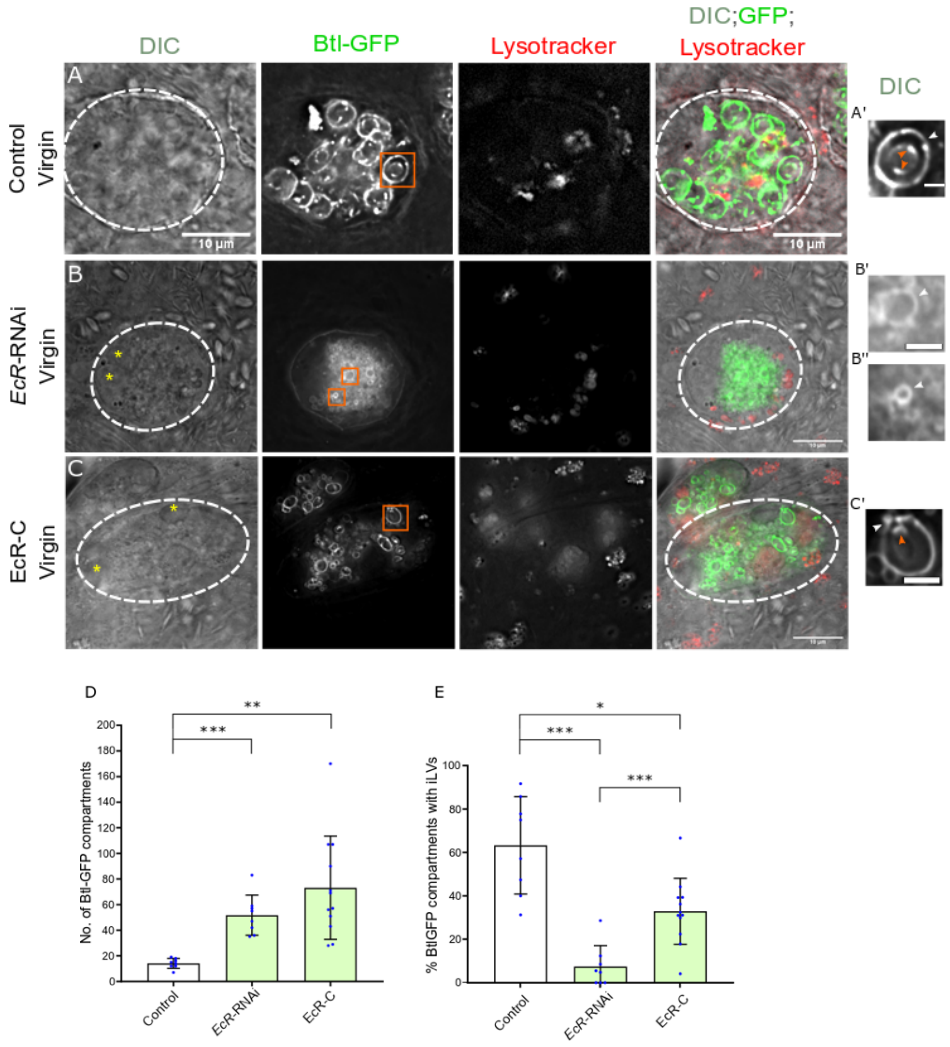

Figure 5.1 Role of EcR in Btl-GFP-labelled compartment formation and exosome synthesis

A-C: Images of SCs from 6-day-old adult virgin males switched to 28.5ºC at eclosion to activate Btl-GFP, *EcR*-RNAi and EcR-C expression in SCs under *dsx*-GAL4 control. Control represents w^{1118} flies expressing only Btl-GFP in SCs. Dashed white ellipses approximately mark the outline of the SCs; yellow stars mark the nuclei when visible in the slice; orange boxes mark the inset in A', B', B'' and C'. Scale bars correspond to 10 µm.

A', B', B'', C': Zoom of representative Btl-GFP compartments when corresponding transgenes are expressed in SCs under *dsx*-GAL4 control. A': In controls, Btl-GFP-positive ILVs (orange arrowheads) are formed and detached from the compartment's limiting membrane (white arrowhead) . B',B'': With *EcR*-RNAi co-expression, most compartments do not contain Btl-GFP-positive ILVs inside the compartment's limiting membrane (white arrowheads). C': With EcR-C co-expression, Btl-GFP-positive ILVs are formed and detach from the compartment's limiting membrane. Scale bar corresponds to 2 µm.

D: Bar chart depicting the mean of the total number of Btl-GFP-positive compartments. The error bars show the standard deviation within the sample. Dysregulation of EcR signalling results in an increase in the number of Btl-GFP-positive compartments. Welch ANOVA test; Games-Howell post-hoc test; $0.01<**p\leq0.001$; $0.0001<***p\leq0.001$ ($n\geq8$ SCs; ≥ 5 males).

E: Bar chart depicting the mean % of Btl-GFP-positive compartments that contain Btl-GFP-positive ILVs. The error bars show the standard deviation within the sample. Dysregulation of EcR signalling results in a decrease in the number Btl-GFP-positive compartments synthesising Btl-GFP-positive ILVs. Welch ANOVA test; Games-Howell post-hoc test; $0.01<*p\leq0.05$; $0.0001<***p\leq0.001$ ($n\geq8$ SCs; ≥5 males).

5.3.2. Regulation of Rab11-compartment maturation by EcR signalling

As discussed in Section 1.10, Rab6-compartments mature to form DCG-containing Rab11-compartments in SCs. In order to determine whether EcR mediates the maturation process, I studied the regulation of Rab6 and Rab11-expressing compartment formation and the synthesis of their respective ILV populations. When *EcR*-RNAi was expressed in SCs using the dsx^{ts} driver in a line that co-expresses CFP-Rab6 under UAS-control, an increase in the total number of Rab6-positive compartments was observed (Fig. 5.2 A, B, D). However, no change was observed in Rab11-compartment number, thereby suggesting that the EcR is necessary for the normal Rab6 to Rab11 maturation process (Fig. 5.3 A, B, D). Knocking down *EcR* significantly reduced the percentage of Rab6-compartments containing ILVs (Fig. 5.2 A, A', B, B', E), but did not have any effect on Rab 11 exosome biogenesis (Fig. 5.3 A, A', B, B', E). Since the Rab6 to Rab11 transition is required for Rab6- and Rab11-ILVs to be formed in SCs (C. Mendes, unpublished data), these data are consistent with a role for EcR in promoting the Rab6 to Rab11 transition. When *EcR* is knocked down, more Rab6-compartments lacking ILVs are therefore formed.

When EcR-C was expressed in SCs, an increase in the total number of Rab6-positive (Fig. 5.2 A, C-D) and Rab11-positive compartments was observed (Fig. 5.3 A, C-D). This result suggests that excess, and potentially functionally neomorphic, EcR potentially increases the production of Rab6-compartments, which can then transition into Rab11-compartments. However, EcR-C overexpression appears to decrease the proportion of Rab6- and Rab11-compartments forming ILVs (Fig. 5.2 A, A', C, C',E; Fig. 5.3 A, A', C, C', E).

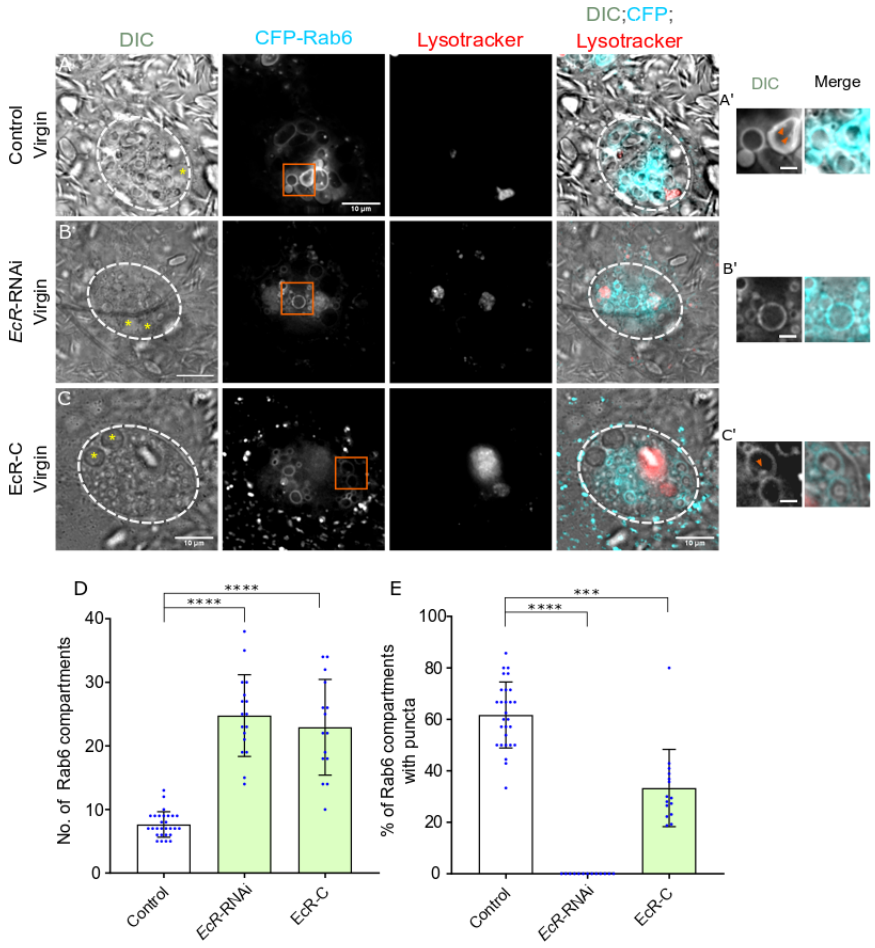

Figure 5.2 Role of EcR in Rab6-labelled compartment formation and exosome synthesis
A-C: Images of SCs from 6-day-old adult virgin males switched to 28.5ºC at eclosion to activate *EcR*-RNAi and EcR-C expression under CFP-Rab6*dsx*-GAL4 control. Control represents w^{1118} flies expressing the *CFP-Rab6* gene trap. Dashed white ellipses approximately mark the outline of the SCs; yellow stars mark the nuclei when seen in the presented Z-slice; orange boxes mark the inset in A', B', B'' and C'. Scale bars correspond to 10 µm.
A'-C': Zoomed representative CFP-Rab6 compartments when corresponding transgene is expressed in SCs under *dsx*-GAL4 control. A': CFP-Rab6 is associated with the limiting membrane of compartments that do not contain a dense core, but it is also observed in the membrane of some compartments which do contain a core, which are thought to be the most immature. CFP-Rab6-positive ILVs inside compartments are marked by orange arrowheads. B': *EcR*-RNAi expression completely suppresses CFP-Rab6-positive ILV formation; the compartments are smaller than controls. C': EcR-C also has smaller compartments, some of which contain CFP-Rab6-positive ILVs. Scale bar corresponds to 2 µm.
D: Bar chart depicting the mean of the total number of CFP-Rab6-positive compartments. The error bars show the standard deviation within the sample. Dysregulation of EcR signalling results in an increase in the number of CFP-Rab6 compartments. Welch ANOVA test; Games-Howell post-hoc test; $0.01<**p\leq0.001$; $0.0001<***p\leq0.001$ ($n\geq8$ SCs; ≥6 males).
E: Bar chart depicting the mean % of CFP-Rab6-positive compartments that contain CFP-Rab6-positive ILVs. The error bars show the standard deviation within the sample. Dysregulation of EcR signalling results in a decrease in the number of CFP-Rab6-positive compartments synthesising CFP-Rab6-positive ILVs. Welch ANOVA test; Games-Howell post-hoc test; $0.01<*p\leq0.05$; $0.0001<***p\leq0.001$ ($n\geq8$ SCs; ≥ 6 males).

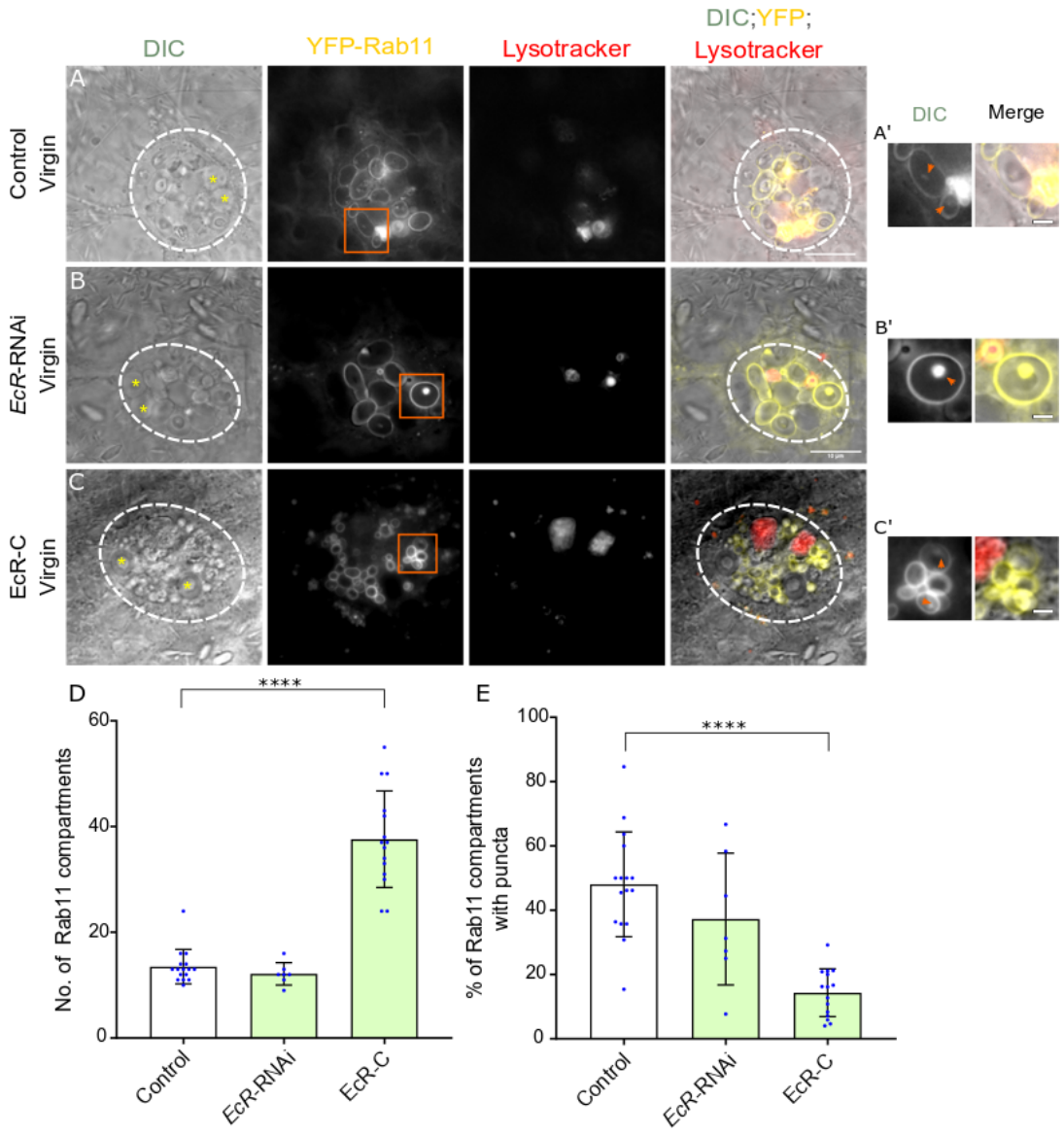

Figure 5.3 Role of EcR in Rab11-labelled compartment formation and exosome synthesis
A-C: Images of SCs from 6-day-old adult virgin males switched to 28.5ºC at eclosion to activate *EcR*-RNAi and EcR-C expression under *dsx*-GAL4 controlYFP-Rab11. Control represents w^{1118} flies expressing only *YFP-Rab11* gene trap. Dashed white ellipses approximately mark the outline of the SCs; yellow stars mark SC nuclei; orange boxes mark the inset in A', B', B'' and C'. Scale bars correspond to 10 µm.
A'-C': Zoomed representative YFP-Rab11-positive compartments when corresponding transgene is expressed in SCs under *dsx*-GAL4 control. A'-B': YFP-Rab11 is associated with the limiting membrane of compartments that contain a dense-core. C': YFP-Rab11 compartments are smaller than controls when EcR-C is overexpressed. Orange arrow heads point to some YFP-Rab11 ILVs. Scale bar corresponds to 2 µm.
D: Bar chart depicting the mean of the total number of YFP-Rab11-positive compartments. The error bars show the standard deviation within the sample. EcR is not essential for Rab11 compartment formation. Kruskal Wallis test; Dunn's post-hoc test; $0.0001<***p\leq0.001$ ($n\geq7$ SCs; ≥ 4 males).
E: Bar chart depicting the mean % of YFP-Rab11 compartments that contain YFP-Rab11 ILVs. The error bars show the standard deviation within the sample. EcR is not essential for YFP-Rab11 ILV formation as well. Kruskal Wallis test; Dunn's post-hoc test; $0.01<*p\leq0.05$; $0.0001<***p\leq0.001$ ($n\geq7$ SCs; ≥ 4 males).

Preliminary results by Cláudia Mendes suggested that some DCG-containing Rab11-compartments in SCs further mature into Rab 19 compartments. It has been speculated that these Rab19-compartments are included in those compartments, which are secreted upon mating. I tested whether EcR-C overexpression might increase the production of these compartments. While there were only an average of two Rab19-compartments in the controls, approximately thirty Rab19-compartments were observed in the EcR-C overexpression background (Fig. 5.4), not greatly different from the number of Rab11-compartments in this genetic background. Therefore, this suggests that EcR-C expression is able to drive the maturation of Rab6-compartments, so that they interact with Rab11 and Rab19, and form DCGs, but the accumulation of Rab19-compartments may reflect a reduction in secretory activity. Also, because the numbers of Rab6-, Rab11- and Rab19-compartments are similar, it is possible that EcR-C overexpression affects the Rab transitions normally associated with maturation, because in wild type cells, Rab6 and Rab19 do not surround the same compartments.

5.3.3. Regulation of Btl-, Rab6- and Rab11-compartment formation by BMP signalling

I modulated the levels of BMP signalling in SCs to test its roles in exosome biogenesis. Reducing BMP signalling by overexpressing Dad in SCs producing Btl-GFP did not have any effects either on the number of Btl-GFP-positive compartments or the percentage of those compartments that synthesised Btl-GFP-positive ILVs (Fig. 5.5 A-B, A'-B', D-E). Similarly, overexpression of Dad did not affect the numbers of Rab6- or Rab11-compartments (Fig. 6.6A,B,D and Fig. 6.7A,B,D). However, very few of these compartments produced Rab-labelled ILVs in contrast to the Btl-GFP analysis (Fig. 6.6E, 7.6E).

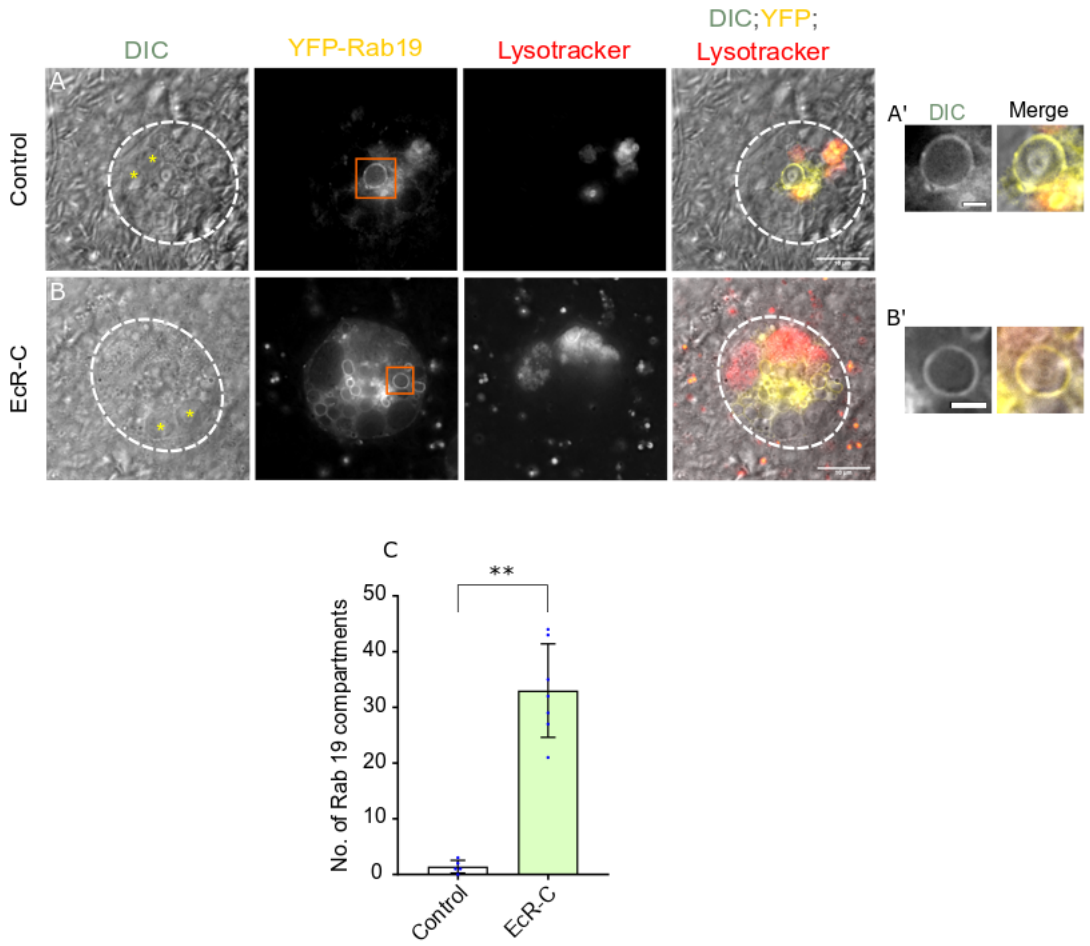

Figure 5.4 Role of EcR in Rab19-labelled compartment formation
A-B: Images of SCs from 6-day-old adult virgin males switched to 28.5ºC at eclosion to activate EcR-C expression under *dsx*-GAL4 control. Control represents w^{1118} flies expressing only *YFP-Rab19* gene trap. Dashed white ellipses approximately mark the outline of the SCs; yellow stars mark the nucleus; dashed orange boxes mark the inset in A', B', B'' and C'. Scale bars correspond to 10 µm.
A'-B': Zoomed representative Rab19-YFP compartments when corresponding transgene is expressed in SCs under DTR19 control. Rab19-YFP is associated with limiting membrane of compartments that contain a dense-core (A'-B'). Scale bar corresponds to 2 µm.
D: Bar chart depicting the mean of the total number of Rab19-YFP-positive compartments. The error bars show the standard deviation within the sample. EcR-C promotes Rab19 compartment formation; Mann-Whitney test; $0.01<**p\leq0.001$ ($n\geq5$ SCs; ≥ 3 males).

Overall, these data suggest that BMP signalling may selectively regulate the formation of Rab-labelled ILVs in SC secretory compartments, which constitute only a subset of ILVs in these compartments (Fan et al., 2020). Upregulation of the BMP signalling by overexpressing Tkv^{act} produced a large number of Btl-GFP compartments, only a few of which contained ILVs (Fig 5.5 A, C, A', C', D-E). The same manipulation also increased the number of Rab6-compartments and suppressed ILV formation in these compartments

(Fig. 6.6C-E). Surprisingly, activating BMP signalling in a *YFP-Rab11* gene trap background did not increase compartment number, but again ILV formation was suppressed (Fig. 6.7C-E). In summary, high levels of BMP signalling may increase the formation of secretory compartments, but maturation of many of these compartments into Rab11-compartments is suppressed, a phenotype that is accompanied by a general suppression in ILV formation.

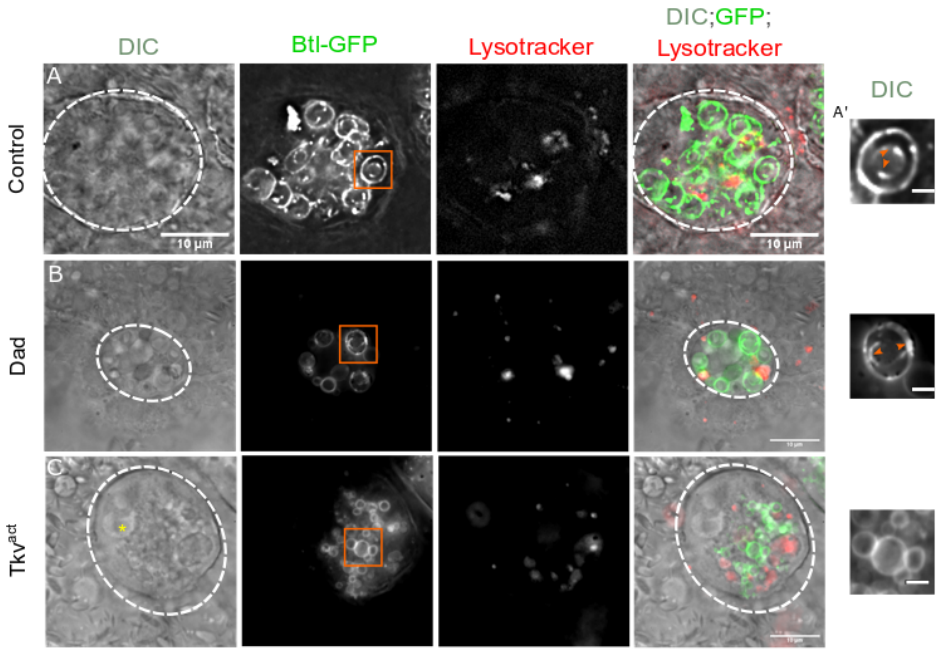

Figure 5.5 Role of BMP signalling in Btl-labelled compartment formation and exosome synthesis

A-C: Images of SCs from 6-day-old adult virgin males switched to 28.5ºC at eclosion to activate Btl-GFP, Dad and Tkv^{act} expression in SCs under *dsx*-GAL4 control. Control represents w^{1118} flies expressing only Btl-GFP in SCs. Dashed white ellipses approximately mark the outline of the SCs; yellow stars mark the nuclei when visible in the slice; orange boxes mark the inset in A', B', B'' and C'. Scale bars correspond to 10 µm.

A', B', C': Zoom of representative Btl-GFP compartments when corresponding transgenes are expressed in SCs under *dsx*-GAL4 control. Both controls and expression of Dad has no effect on Btl-GFP ILV formation (A'-B'). Orange arrow heads point to some representative Btl-GFP ILVs. Scale bar corresponds to 2 µm.

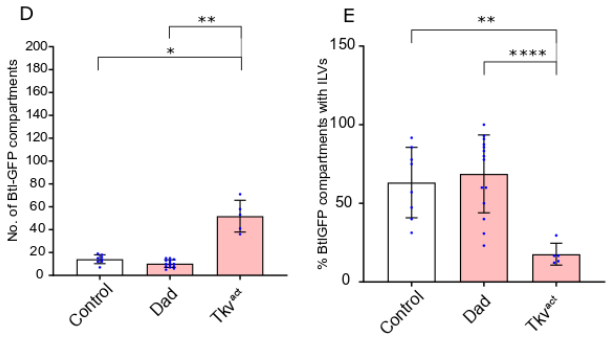

Figure 5.5 Role of BMP signalling in Btl-labelled compartment formation and exosome synthesis

D: Bar chart depicting the mean of the total number of Btl-GFP-positive compartments. The error bars show the standard deviation within the sample. BMP signalling is not essential for Btl-GFP compartment formation. Welch ANOVA test; Games-Howell post-hoc test; $0.01<*p\leq0.05$; $0.01<**p\leq0.001$ ($n\geq5$ SCs; ≥ 3 males).

E: Bar chart depicting the mean % of Btl-GFP compartments that contain Btl-GFP ILVs. The error bars show the standard deviation within the sample. Dysregulation of EcR signalling results in a decrease in the number Btl-GFP compartments synthesising Btl-GFP ILVs. Welch ANOVA test; Games-Howell post-hoc test; $0.001<**p\leq0.01$; $****p\leq0.0001$ ($n\geq5$ SCs; ≥3 males).

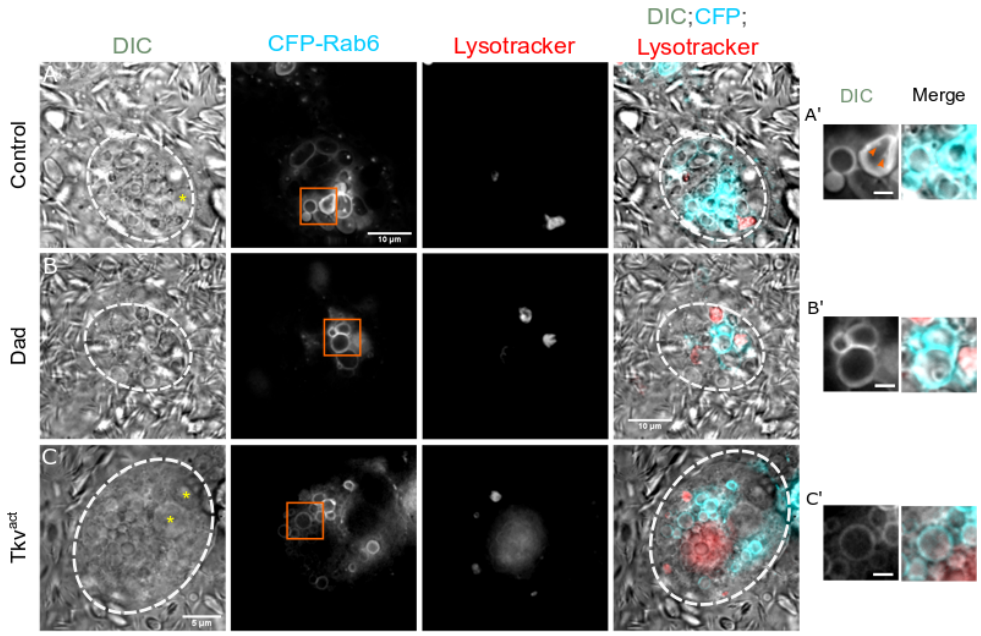

Figure 5.6 Role of BMP signalling in Rab6-labelled compartment formation and exosome synthesis

A-C: Images of SCs from 6-day-old adult virgin males switched to 28.5ºC at eclosion to activate *EcR*-RNAi and EcR-C expression under CFP-Rab6*dsx*-GAL4 control. Control represents w^{1118} flies expressing the *CFP-Rab6* gene trap. Dashed white ellipses approximately mark the outline of the SCs; yellow stars mark the nuclei when seen in the presented Z-slice; orange boxes mark the inset in A', B', B'' and C'. Scale bars correspond to 10 µm.

A'-C': Zoomed representative CFP-Rab6 compartments when corresponding transgene is expressed in SCs under DTR6 control. Dysregulation of BMP signalling forms empty Rab6 compartments. C': Expression of Tkv^{act} has smaller CFP-Rab6 compartments. Orange arrow heads point to some representative CFP-Rab6 ILVs. Scale bar corresponds to 2 µm.

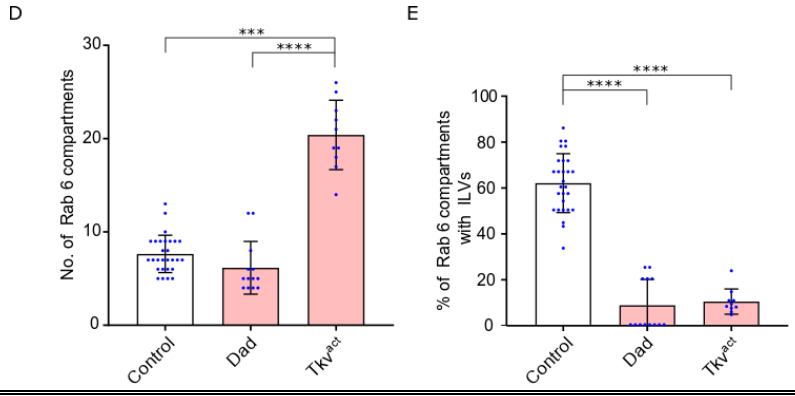

Figure 5.6 Role of BMP signalling in Rab6-labelled compartment formation and exosome synthesis

D: Bar chart depicting the mean of the total number of Btl-GFP-positive compartments. The error bars show the standard deviation within the sample. BMP signalling is not essential for CFP-Rab6 compartment formation. Welch ANOVA test; Games-Howell post-hoc test; $0.01<**p\leq0.001$; $0.0001<***p\leq0.001$ ($n\geq8$ SCs; ≥ 5 males).

E: Bar chart depicting the mean % of CFP-Rab6 compartments that contain CFP-Rab6 ILVs. The error bars show the standard deviation within the sample. Dysregulation of BMP signalling results in a decrease in the number CFP-Rab6 compartments synthesising CFP-Rab6 ILVs. Welch ANOVA test; Games-Howell post-hoc test; $0.01<*p\leq0.05$; $0.0001<***p\leq0.001$ ($n\geq8$ SCs; ≥ 5 males).

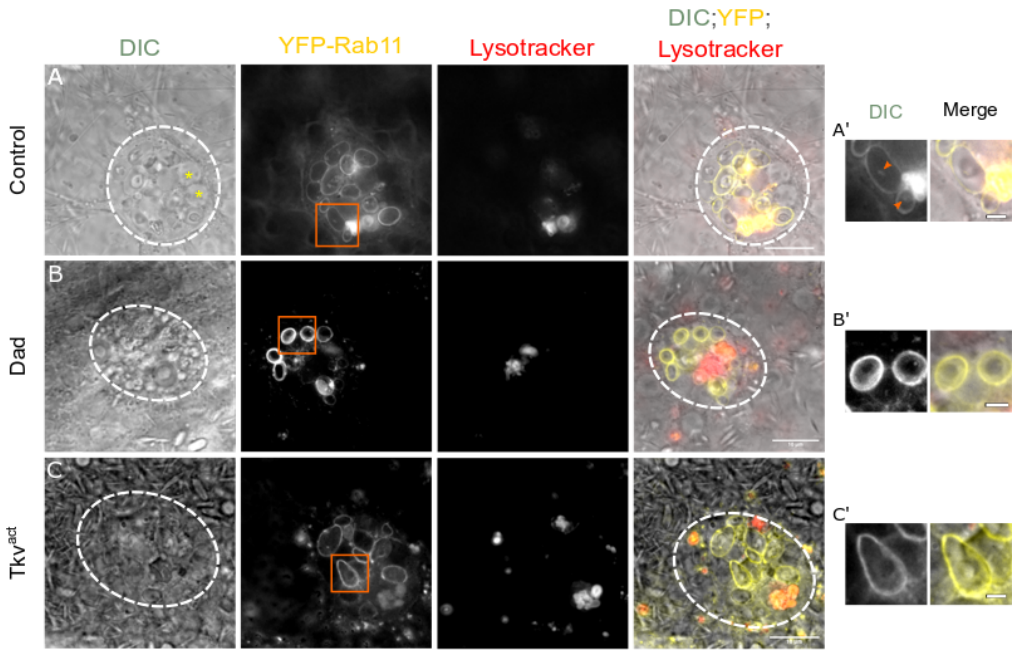

Figure 5.7 Role of BMP signalling in Rab11-labelled compartment formation and exosome synthesis

A-C: Images of SCs from 6-day-old adult virgin males switched to 28.5ºC at eclosion to activate YFP-Rab11 of DTR11 driver. Control represents w^{1118} flies specifically expressing YFP-Rab11 in SCs under dsx^{ts} control. Dashed white ellipses approximately mark the outline of the SCs; yellow stars mark the nucleus when seen in the presented Z-slice; dashed orange boxes mark the inset in A', B', B'' and C'. Scale bars correspond to 10 µm.

A'-C': Zoomed representative YFP-Rab11 compartments when corresponding transgene is expressed in SCs under DTR11 control. Orange arrow heads point to some YFP-Rab11 ILVs. Scale bar corresponds to 2 µm.

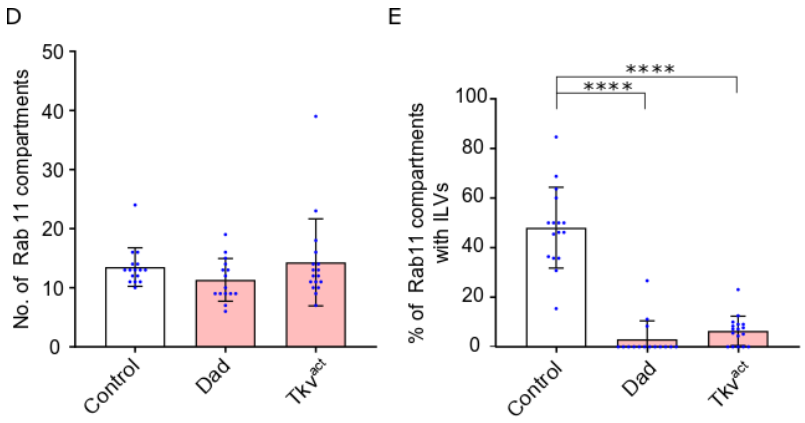

Figure 5.7 Role of BMP signalling in Rab11-labelled compartment formation and exosome synthesis
D: Bar chart depicting the mean of the total number of YFP-Rab11-positive compartments. The error bars show the standard deviation within the sample. BMP signalling has no effect on Rab11 compartment formation. Kruskal Wallis test; Dunn's post-hoc test (n≥7).
E: Bar chart depicting the mean % of YFP-Rab11 compartments that contain YFP-Rab11 ILVs. The error bars show the standard deviation within the sample. Dysregulation of BMP signalling results in a suppression of YFP-RAB11 ILV synthesis. Kruskal Wallis test; Dunn's post-hoc test; ****p≤0.0001 (n≥15 SCs; ≥ 8 males).

5.4. Summary and Discussion

In this chapter, I have clearly demonstrated, using genetic manipulations that increase and decrease signalling activity, that the BMP and EcR signalling pathways play an important role in the regulation of SC compartment maturation and identity, and in exosome biogenesis. Although the activities of these two pathways are functionally linked in the regulation of SC growth, it has previously been shown that their effects are antagonistic in respect to SC migration (Leiblich et al., 2019), which may be connected to some of the differences observed in my secretory analysis, especially since exosomes have been strongly implicated in migratory activity (Che et al., 2019; Luga et al., 2012; Salomon et al., 2013).

Inhibiting EcR and BMP signalling produced different defects in the exosome-generating pathway of SCs. *EcR* knockdown appeared to affect the maturation of Rab6-compartments into Rab11-compartments. This was accompanied by a strong inhibition

of Btl-GFP- and Rab6-positive ILV formation, but not biogenesis of Rab11-exosomes in Rab11-compartments. Since the Rab6 to Rab11 compartment transition appears to be required for exosome formation (C.C. Mendes, unpublished data), this is consistent with a model in which EcR's primary role is to promote this maturation event (Fig. 5.8).

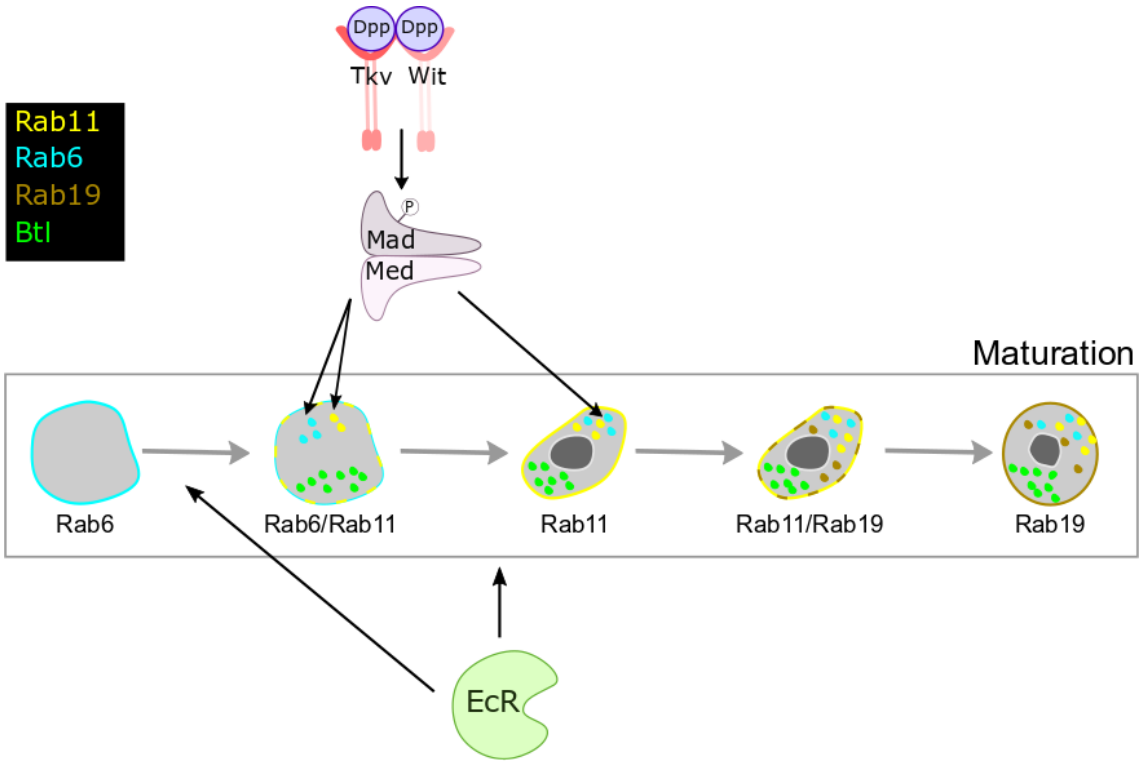

Figure 5.8 Schematic detailing the role of BMP and EcR signalling in the regulation of exosome biogenesis and compartment maturation
The BMP pathway regulates the synthesis of Rab6- and Rab11-exosomes, but not Btl-GFP-labelled exosomes. The most straightforward explanation for the phenotypes generated by *EcR* knockdown is that EcR promotes the formation of Rab11-compartments and so, in its absence, most compartments are Rab11-negative and do not form ILVs, but those compartments that carry Rab11, do form ILVs. The limiting membrane of compartments at all stages shown here can be labelled with Btl-GFP, when it is expressed in SCs, but this is not shown in the diagram for simplicity.

By contrast, suppressing BMP signalling by overexpressing Dad did not appear to affect compartment maturation, suggesting this EcR function is not regulated by BMP signalling. However, BMP signalling is required for the formation of specific Rab-labelled exosomes in these maturing compartments, but not Btl-GFP-marked ILVs,

suggesting that this larger population of vesicles may be regulated differently (Fig. 5.8). Other recent reports from the group (Dar et al., 2020) have suggested that Rab11-marked ILV biogenesis is not controlled in the same way as other vesicles formed in Rab11-compartments, and it appears that BMP signalling may be involved in this.

My observations when EcR-C or Tkv^{act} is overexpressed in SCs were more difficult to interpret, given that they did not appear to have the opposite effect to signalling suppression. In both cases, the overexpressed proteins may lead to hyperactivation or abnormal activation of the EcR and BMP signalling pathways respectively. Although such activation has proved useful and interpretable in my studies of growth and endoreplication, it is difficult to relate my findings to the results from signalling suppression in this chapter. Overexpressing EcR-C appeared to increase the number of secretory compartments in SCs and suppress their exosome-generating activity.

Given that BMP signalling regulates EcR protein levels and interacts with the EcR pathway in SC nuclear growth regulation, it would still be interesting to test if any such BMP/EcR interaction can be identified in exosome and compartment formation. This could be tested using the combination lines Dad+EcR-C and *EcR*-RNAi+Tkv^{act}, which I have already employed in Chapters 3 and 4. In Chapter 6, I show that cell cycle components are also involved in EcR regulation, and it may be informative to determine whether these also affect the secretory functions I have analysed.

In order to follow up some of the findings in this chapter, it will now be necessary to test the proposed effects on compartment maturation rate with specific genetic manipulations, such as *EcR* knockdown. To do this, it will be necessary to follow the maturation process in real-time as Benjamin Kroeger has done for control SCs using the time lapse wide-

field microscopy technique (Kroeger 2017). In this chapter, I have only looked at the formation of exosomes and a next natural step would be to use the exosome secretion assays developed in the lab, which measure the number of exosomes secreted into the lumen, to study the role of the BMP and EcR signalling in the regulation of this process (Fan et al., 2020).

Chapter 6:

Cell cycle regulation of mating-dependent SC growth and genome endoreplication

6.1. Introduction

Since endoreplicating cells utilise a variant of the cell cycle machinery to bring about DNA replication, I decided to determine the molecular mechanisms that regulate the endoreplication switch in SCs. As described in Section 1.5, the loss of Rb and the unchecked activation of E2F in prostate cancer cells promotes the progression to CRPC, at least partly by increasing the transcription levels of the *AR* gene. Previous work by Aaron Leiblich and Dhruv Sharma, as discussed in Section 1.16.2, showed that either knocking down Rbf (*Drosophila* homologue of Rb) or activating E2F1 activity increases EcR protein levels, mirroring the effects observed in prostate cancer. There were also some preliminary data showing that manipulating Rbf or E2F1 expression regulates SC growth. Interestingly, they observed that SCs became mononucleate when a constitutively active form of Rbf was expressed. Therefore, it was imperative for me to assess the dependency of mating-dependent SC growth, endoreplication and nucleation state on the cell cycle components.

In response to mitogenic signals, the G1/S cyclin, CycD, when bound to cdk4, initiates the transition from G- to S- phase by promoting phosphorylation of Rbf. In a hyperphosphorylated state, Rbf is inactivated, thereby allowing E2F1 to undertake its functions. The E2F1 transcription factor is essential for transcribing several genes that are essential for the progression of the S-phase, including CycE. Along with CycD/cdk4, CycE/cdk2 phosphorylates Rbf in order to promote the transition to S-phase. Interestingly, in *Drosophila*

salivary glands, it has been shown that a sustained E2F1/CycE oscillator is required for the progression of endoreplication (Zielke et al., 2011; Zielke, Edgar, and DePamphilis 2013).

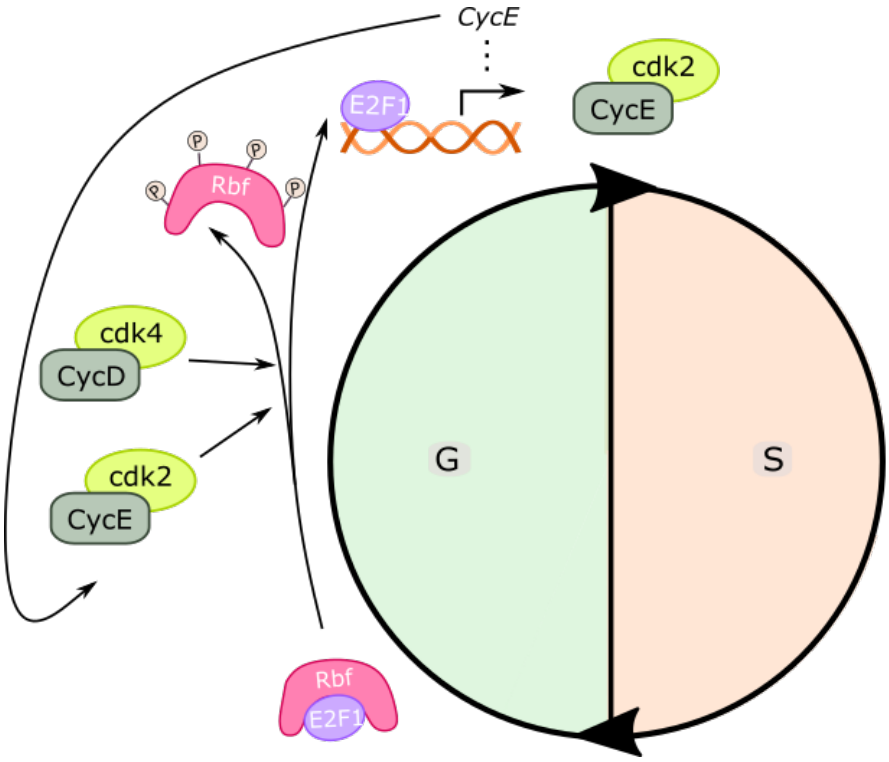

Figure 6.1 Role of cell cycle components in endoreplication

A schematic depicting the role of CycD, CycE, Rbf and E2F1 in endoreplicating cells. G: G phase; S: S-phase; P: Phosphoryl groups.

6.2. Aims

In this chapter, my major focus was to determine the mechanisms through which SC growth and endoreplication are regulated by cell cycle components. The following are the specific research questions that I address in this chapter:

- Do G1 and G1/S cyclins, CycE and CycD respectively, along with Rbf /E2F1 regulate mating-dependent genome endoreplication observed in SCs?

- How do these cell cycle components interact with the BMP/EcR signalling axis to regulate SC growth and endoreplication in virgin and mated males?
- How is SC nucleation state regulated by the Rbf/E2F1 signalling axis?

6.3. Results

6.3.1. EcR signalling regulates SC growth and endoreplication through CycE

Since CycE has been implicated in triggering endoreplication in several *Drosophila* cell types including developmental endoreplication in SCs (Edgar et al., 2014; Taniguchi et al., 2014), I wanted to confirm its role in the induction of mating-dependent endoreplication in SCs. Knocking down *CycE* in SCs, resulted in a decrease in SC growth in both virgins and mated males as compared to the respective controls (Fig. 6.2 C-D, G). Expression of *CycE*-RNAi in SCs also led to a complete suppression of any endoreplication observed after mating (Fig. 6.2 H), thereby proving the necessity of CycE for mating-dependent endoreplication. In the *CycE*-RNAi genetic background, a significant increase in growth was observed in SCs of mated males with respect to virgin males. Therefore, *CycE*-RNAi does not suppress endoreplication-independent SC growth that occurs after mating, which suggests that this mode of mating-dependent growth does not necessarily require CycE. As expected, overexpressing CycE resulted in an increase in SC growth in both virgin and mated males (Fig. 6.2 E-G), but no difference in SC growth was observed between virgin and mated males overexpressing CycE. Furthermore, overexpression of CycE resulted in all SCs undergoing endoreplication in virgin and mated males (Fig. 6.2 H).

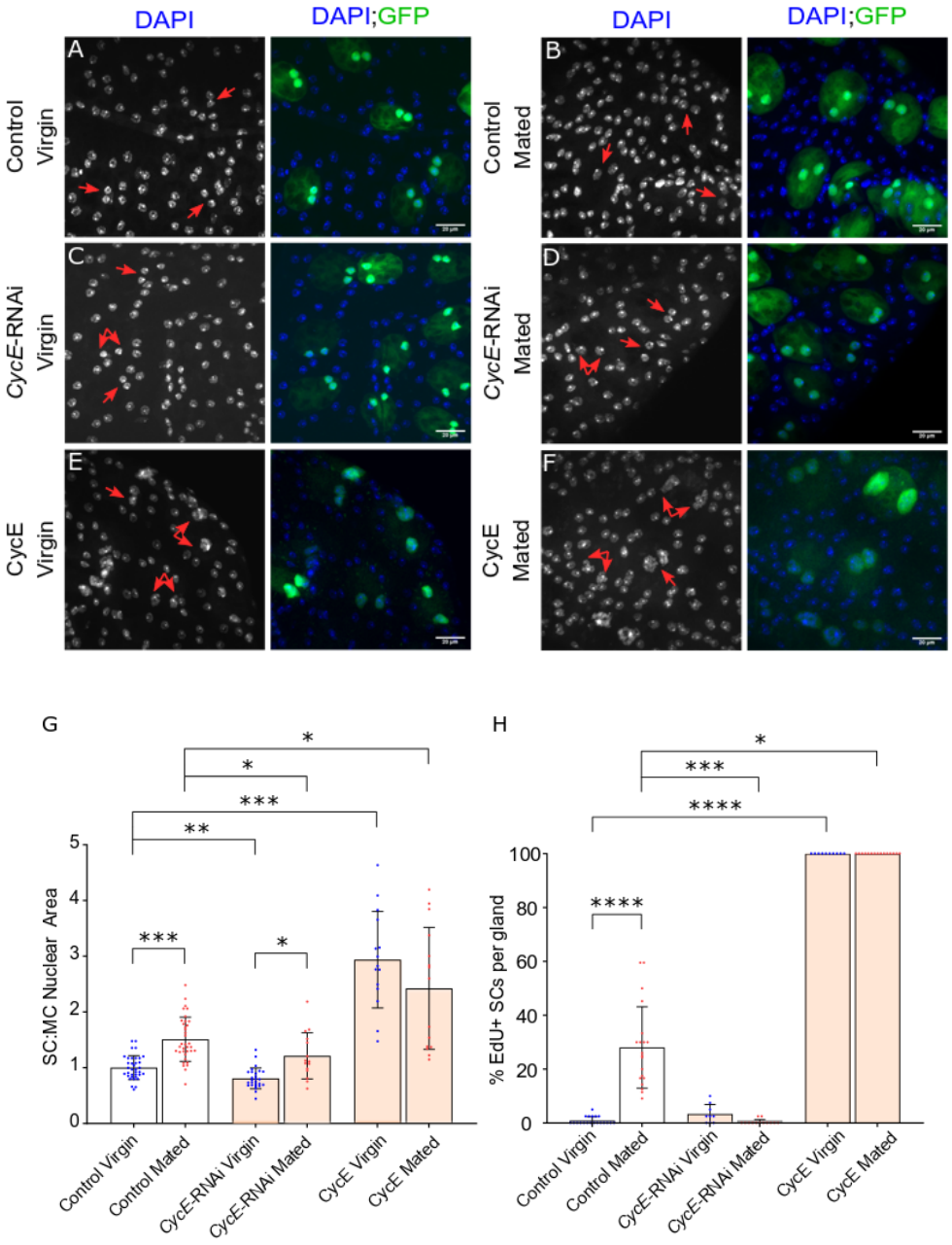

Figure 6.2 Role of CycE in the regulation of SC growth and endoreplication

A-F: Images show distal tip of AGs from 6-day-old adult virgin males expressing the corresponding transgene under the control of the esg^{ts}F/O driver. Control represents w^{1118} flies specifically expressing nuclear GFP (which also stains the cytosol) in SCs. Nuclei are stained with DAPI (blue). Red arrows point to representative SC nuclei for each transgene. Scale bars correspond to 20 µm.
G: Bar chart depicting the mean ratio of the size of SC nuclei relative to neighbouring MC nuclei. Graph includes SC growth assay data of virgin and mated flies expressing no other transgene, *CycE*-RNAi or CycE in SCs. The error bars show the standard deviation within the sample. CycE is necessary and sufficient to promote SC growth. Knocking down *CycE* does not completely inhibit SC growth that occurs after mating. Welch ANOVA; Games-Howell post hoc test; 0.01<*p≤0.05; 0.001<**p≤0.01; 0.0001<***p≤0.001; ****p≤0.0001 (n≥13 SCs; ≥5 males).
H: Bar chart depicting the mean % of EdU+ SCs per gland. Graph includes EdU assay data of virgin and mated flies expressing no other transgene, *CycE*-RNAi or CycE in SCs. The error bars show the standard deviation within the sample. CycE is necessary and sufficient to induce endoreplication in SCs. Kruskal Wallis test; Dunn's post hoc test; 0.01<*p<0.05; 0.0001<***p≤0.001; ****p≤0.0001 (n≥8 males).

Since I had shown in Section 4.3.2 that EcR is necessary and sufficient to induce endoreplication in SCs, I determined how the EcR signal and CycE interact. When *CycE* was co-overexpressed with *EcR*-RNAi in virgin males (Fig. 6.3), no changes in CycE-induced endoreplication or growth were observed. Hence, this shows that EcR is not required for CycE-induced growth and endoreplication in SCs.

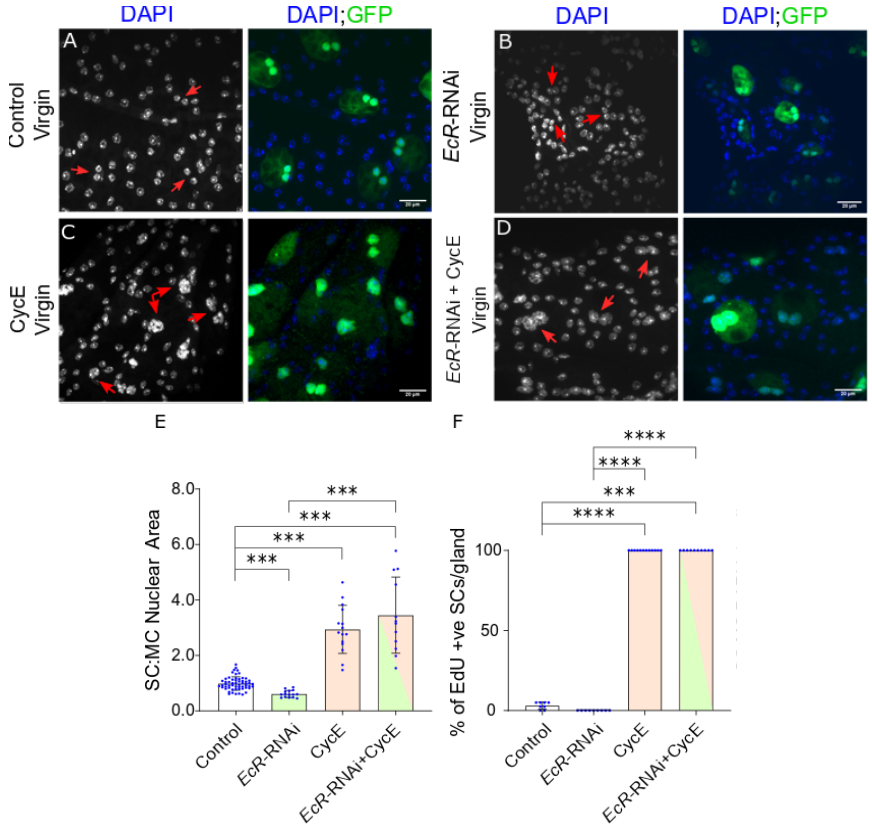

Figure 6.3 EcR is not required for CycE-induced SC growth and endoreplication

A-D: Images show distal tip of AGs from 6-day old adult virgin males expressing the corresponding transgene under the control of the esg^{ts}F/O driver. Control represents w^{1118} flies specifically expressing nuclear GFP (which also stains the cytosol) in SCs. Nuclei are stained with DAPI (blue). Since these experiments were done and analysed with the experiments in Fig. 6.1, I have used the same control image. Red arrows point to representative SC nuclei for each transgene. Scale bars correspond to 20 µm.

E: Bar chart depicting the mean ratio of the size of SC nuclei relative to neighbouring MC. The error bars show the standard deviation within the sample. Graph includes SC growth assay data of virgin flies expressing no other transgene, *EcR*-RNAi, CycE or *EcR*-RNAi + CycE in SCs. Knocking down *EcR* does not affect CycE-mediated SC growth. Welch ANOVA; Games-Howell post hoc test; 0.0001<***p≤0.001 (n≥15 SCs; ≥ 5 males).

F: Bar chart depicting the mean % of EdU+ SCs per gland. The error bars show the standard deviation within the sample. Graph includes EdU assay data of virgin flies expressing no other transgene, *EcR*-RNAi, CycE or *EcR*-RNAi + CycE in SCs. The data from CycE is the same as in Fig 4.1 H as the experiments were done at the same time. Knocking down *EcR* does not have any effect on CycE-mediated SC endoreplication. Kruskal Wallis test; Dunn's post hoc test; 0.0001<***p≤0.001; ****p≤0.0001 (n≥8 males).

6.3.2. CycD is vital for SC growth and endoreplication

In this section I studied the role of CycD, which initiates G/S transition, in the regulation of SC growth and endoreplication. Knocking-down *CycD*, inhibited SC growth and abolished mating-dependent endoreplication (Fig. 6.4 C-D, G-H). However, I observed that expression of *CycD*-RNAi did not affect mating-dependent, endoreplication-independent SC growth (Fig. 6.4 G). For studying the result of increased CycD activity, I overexpressed CycD along with its kinase partner, cdk4, in SCs. All the cells endoreplicated extensively (Fig. 6.4 E-F, G), resulting in polytene-like chromosomes in both virgin and mated males (Fig. 6.4 E'). Taking these results together, it suggests that CycD is necessary for SC growth and endoreplication and it is indeed sufficient to induce growth and endoreplication in SCs.

6.3.3. p53/Rbf/E2F1 regulate nucleation state in adult SCs

In order to constitutively activate Rbf in the SCs, I used the Rbf^{CA} (sometimes referred to as Rbf-280) construct, which has mutations in all of its four phosphorylation sites, thereby making it refractory to regulation by CycE/cdk2 and CycD/cdk4 (Xin et al., 2002). Interestingly, expression of Rbf^{CA} in SCs, resulted in 65% of SCs becoming mononucleate (Fig. 6.5 A, A', G). Knocking down *E2F1* resulted in approximately four mononucleated SCs per gland (Fig. 6.5 D, G). Since mononucleation has never been observed in controls, even if as few as 12% of SCs consistently become mononucleate, it suggests that this phenotype is not occurring by chance.

In order to determine whether nucleation state in MCs is affected by Rbf, I overexpressed Rbf^{CA} in MCs using the temperature-sensitive Acp26Aa-GAL4 MC driver (Chapman et al., 2003; Corrigan et al., 2014). There was no effect on MC nucleation, but interestingly most of the SCs became mononucleated (Fig. 6.5 B, B', H).

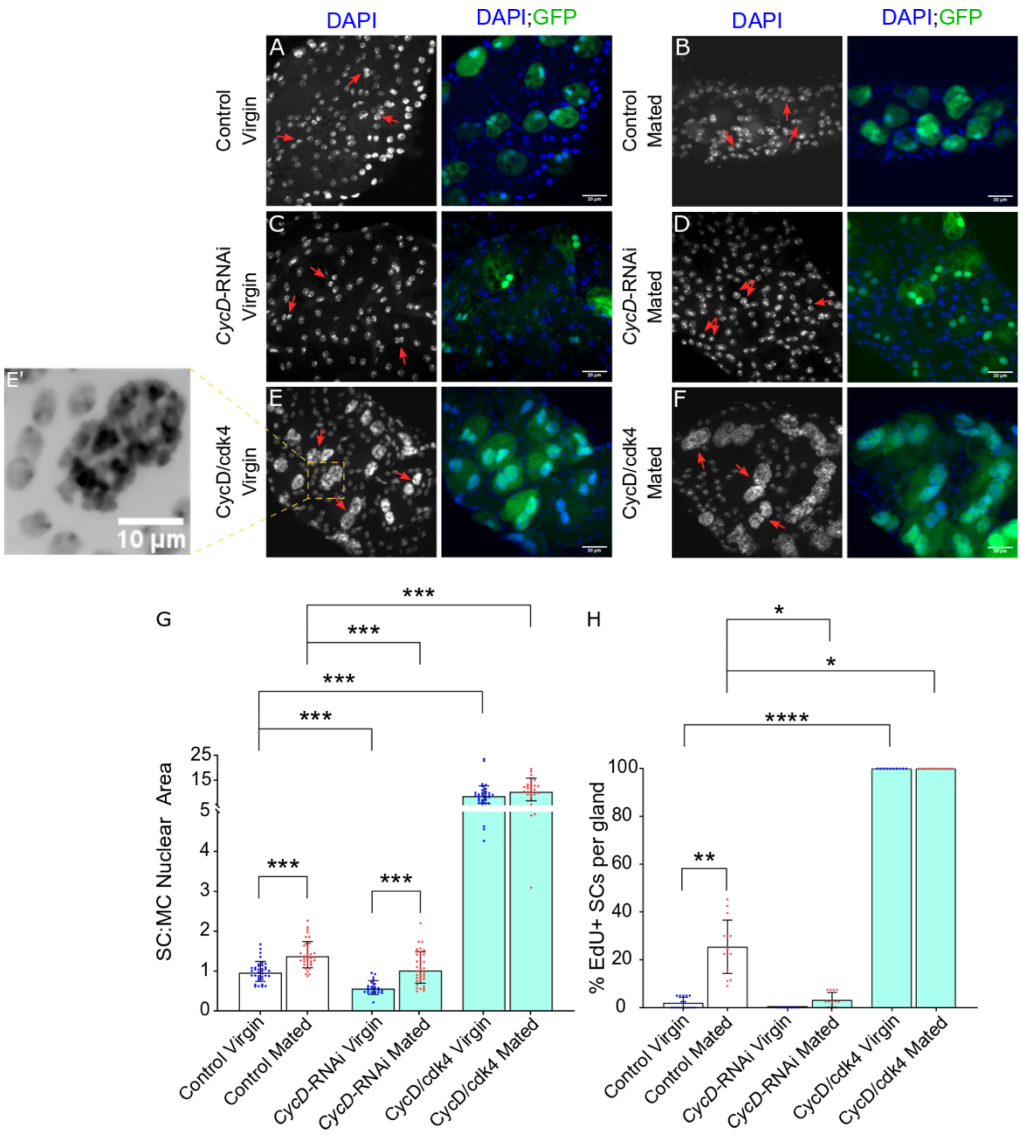

Figure 6.4 Role of CycD in SC growth and endoreplication regulation

A-F: Images show distal tip of AGs from 6-day-old adult virgin and mated males expressing the corresponding transgene under the control of the esg^{ts}F/O driver. Control represents w^{1118} flies specifically expressing nuclear GFP (which also stains the cytosol) in SCs. Nuclei are stained with DAPI (blue). Red arrows point to representative SC nuclei for each transgene. Scale bars correspond to 20 µm.

E': Magnified negative image of yellow dashed square in image C to highlight the polytene-like nuclei in SCs overexpressing CycD/cdk4.

G: Bar chart depicting the geometric mean ratio of the size of SC nuclei relative to neighbouring MC nuclei. The error bars show the geometric standard deviation within the sample. Graph includes SC growth assay data of virgin and mated flies expressing no other transgene, *CycD*-RNAi or CycD/cdk4 in SCs. CycD is necessary and sufficient to promote SC growth. Knocking down *CycD* is unable to completely suppress SC growth between the respective virgin and mated males, which as seen in H, is associated with mating-induced, endoreplication-independent SC growth. Welch ANOVA on log-transformed data; Games-Howell post hoc test; $0.0001<***p\leq0.001$ ($n\geq24$ SCs; ≥8 males).

H: Bar chart depicting the mean % of EdU+ SCs per gland. The error bars show the standard deviation within the sample. Graph includes EdU assay data of virgin and mated flies expressing no other transgene, *CycD*-RNAi or CycD/cdk4 in SCs. CycD is necessary and sufficient to promote SC endoreplication. Kruskal Wallis test; Dunn's post hoc test; $0.01<*p<0.05$; $0.001<**p\leq0.01$; $****p\leq0.0001$ ($n\geq9$ males).

Those SCs that became mononucleate under these conditions were still able to endoreplicate upon mating (Fig. 6.5 C), therefore demonstrating that endoreplication is not affected by the nucleation state of the SC. I was then interested to determine if similar effects were observed when *E2F1*-RNAi was expressed in MCs, but unlike the results observed with Rbf^{CA}, none of the SCs or MCs became mononucleate (Fig. 6.5 E, H). This suggests that the mechanism through which SCs become mononucleate when Rbf^{CA} is overexpressed in SCs and in MCs might be different.

Overexpression in SCs of a putative upstream regulator of Rbf/E2F1 and potential downstream target of Rbf, p53, phenocopied the results observed with expressing *E2F1*-RNAi in SC (Fig.6.5 F, G). Expression of p53 in MCs had major effects on cell structure and the AG epithelium, thereby making it difficult to analyse nucleation state either in SCs or MCs. These results suggest that Rbf employs a dual control on SC nucleation state - autocrine regulation that involves p53 and E2F1 and paracrine regulation whose other regulators are not yet known. I was curious to see whether this regulation of nucleation in the adult involves *Mud*/*Numa*, a gene that mediates AG epithelium binucleation during the pupal stage (Taniguchi et al., 2014). Knocking down *Mud*/*Numa* in either adult SCs or MCs did not result in any change in nucleation state (Fig 6.5 G-H). Therefore, this suggests that the mononucleation phenotype that can be induced in adults involves different machinery to that employed to induce binucleation in development, and that maintenance of the binucleation state in adult SCs does not require *Mud*.

Figure 6.5 Role of p53/Rbf/E2F1 in SC nucleation state regulation

A-B: Images show distal tip of AGs from 6-day-old adult virgin males expressing Rbf^{CA} either under the control of the $esg^{ts}F/O$ driver (A) or the Acp26Aa-GAL4 driver (B) which activates nuclear GFP production (stains cytoplasm in A). Nuclei are stained with DAPI (blue). Dashed red ellipses mark the outline of mononucleate SCs; dashed yellow ellipses mark the outline of binucleate SCs; pink boxes outline the area zoomed in the inset (A',B'). Scale bars correspond to 50 μm.

A'-B': Inset highlighting one mononucleate (red arrow) and one binucleate (yellow arrow) of image A and B.

C: Image shows the distal tip of an AG of a 6-day-old multiply-mated male expressing Rbf^{CA} under the control of the Acp26Aa-GAL4 driver. The AG was stained for EdU, revealing that mononucleate SCs are able to endoreplicate.

D-F: Images show distal tip of AGs from 6-day-old adult virgin males expressing the corresponding transgene either under the control of the $esg^{ts}F/O$ driver (D,F) or the Acp26Aa-GAL4 driver (E), which expresses nuclear GFP (stains cytoplasm in D-F). Nuclei are stained with DAPI (blue). Dashed red ellipses mark the outline of mononucleate SCs (if any); dashed yellow ellipses mark the outline of binucleate SCs. Scale bars correspond to 50 μm.

G: Bar chart depicting the mean % of mononucleate SCs per gland. The error bars show the standard deviation within the sample. Graph includes data from flies expressing no other transgene (w^{1118}), Rbf^{CA}, *E2F1*-RNAi, p53 and *Mud*-RNAi in the SCs using the $esg^{ts}F/O$ driver. Rbf^{CA} promotes SC mononucleation to a much higher extent as compared to *E2F1*-RNAi and p53. No mononucleation is observed when *Mud*-RNAi is expressed in SCs. Student's two-tailed t-test as the means of % of mononucleate SCs per gland of each transgene was only compared with the controls; $0.01<*p<0.05$; $0.0001<***p\leq0.001$; $****p\leq0.0001$ ($n\geq6$ males)

H: Bar chart depicting the mean % of mononucleate SCs per gland. The error bars show the standard deviation within the sample. Graph includes data from flies expressing no other transgene (w^{1118}), Rbf^{CA}, *E2F1*-RNAi and *Mud*-RNAi in the MCs using the Acp26Aa-GAL4 driver. Rbf^{CA} expression in MCs promotes SC mononucleation to a much higher extent as compared to *E2F1*-RNAi. No mononucleation is observed when *Mud*-RNAi is expressed in MCs. Student's two-tailed t-test as the means of % of mononucleate SCs per gland of each transgene was only compared with the controls; All comparisons made with respect to the control and did not have to be corrected for the other comparisons; $****p\leq0.0001$ ($n\geq7$ males).

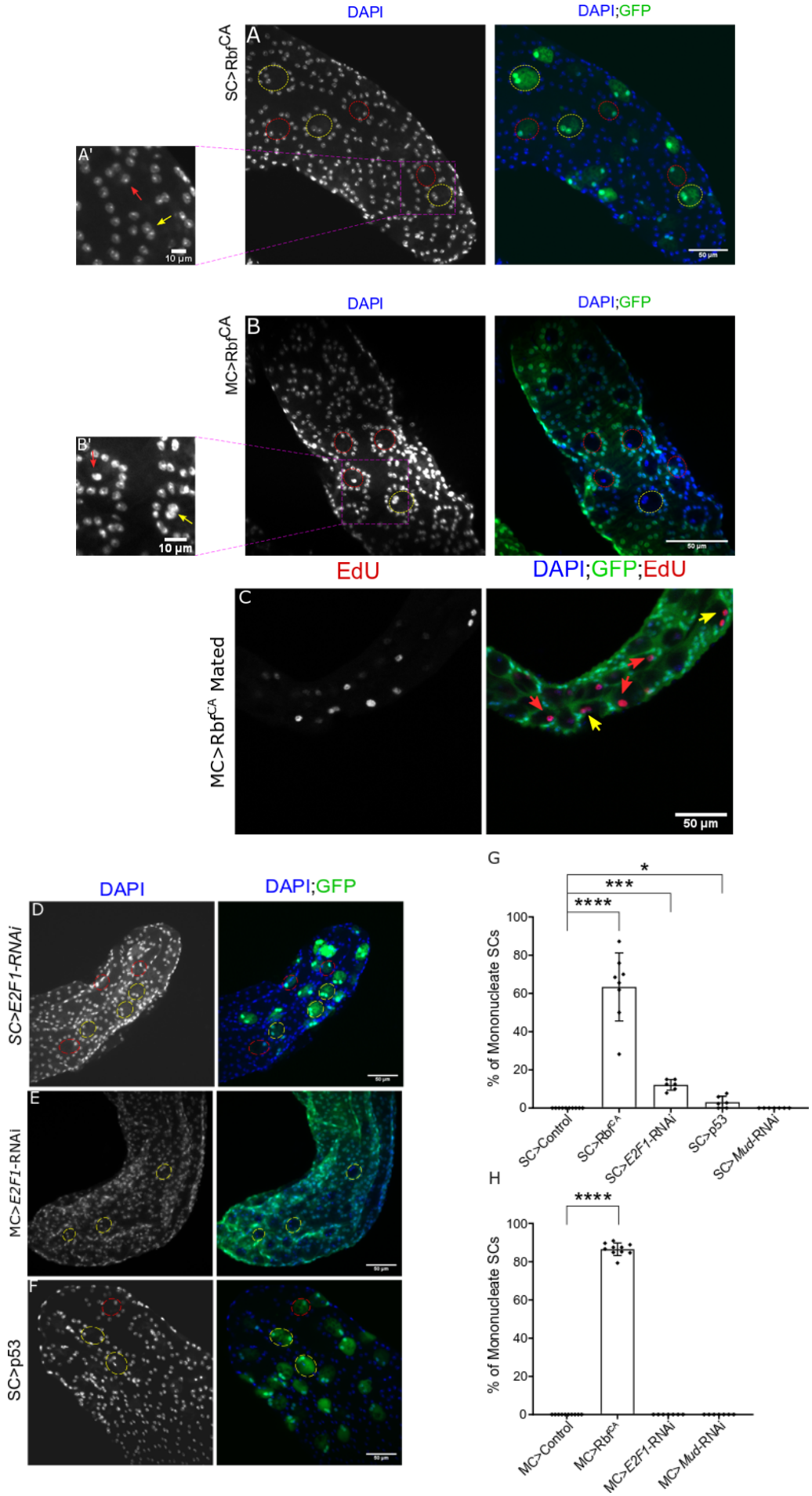
DAPI
DAPI;GFP
SC>RbfCA
A
A'
10 µm
50 µm
DAPI
DAPI;GFP
MC>RbfCA
B
B'
10 µm
50 µm
EdU
DAPI;GFP;EdU
MC>RbfCA Mated
C
50 µm
DAPI
DAPI;GFP
SC>E2F1-RNAi
D
MC>E2F1-RNAi
E
SC>p53
F
G
*
***
****
% of Mononucleate SCs
100
80
60
40
20
0
SC>Control
SC>RbfCA
SC>E2F1-RNAi
SC>p53
SC>Mud-RNAi
H
****
% of Mononucleate SCs
100
80
60
40
20
0
MC>Control
MC>RbfCA
MC>E2F1-RNAi
MC>Mud-RNAi

6.3.4. Rbf negatively regulates SC growth and endoreplication

For mononucleate SCs induced by expression of Rbf^{CA}, the growth assay was quantified by measuring the ratio of the area of the single SC nucleus with respect to the total nuclear area of both the nuclei of the adjacent MC. Overexpressing Rbf^{CA} in the SCs resulted in smaller SC nuclei and no endoreplication in both virgin and mated males (Fig 6.6 C-D, G-H). Additionally, no significant difference in SC growth was observed between virgin and mated males in this genetic background. As discussed in Section 6.3.3, the mononucleation phenotype did not itself hinder the ability of the SCs to endoreplicate, thereby suggesting that the lack of EdU incorporation in Rbf^{CA}-expressing SCs reflects the direct effect of Rbf on the cell cycle. Knocking down *Rbf* resulted in an increase in growth and endoreplication of all SCs in both virgin and mated males (Fig 6.6 E-H). Therefore, this demonstrates that the loss of Rbf is sufficient to induce growth and hormone-independent, steroid receptor-regulated endoreplication in SCs, much like the induction of hormone-independent proliferation in CRPC.

6.3.5. E2F1 is necessary and sufficient to promote SC endoreplication, but is not necessary to drive SC growth

Co-expression of *E2F1* along with its dimerization partner, *Dumpy* (*Dp*), is required to induce increased E2F1 activity. When this construct was expressed in SCs, an increase in SC growth was observed in both virgin and mated males. All the SCs underwent endoreplication in both cases (Fig. 6.7 E-F, I-J). Surprisingly, knocking down *E2F1*, did not have any effect on SC growth in virgin males and an increase in growth was observed in mated males. However, all endoreplication was suppressed after mating. This suggests that E2F1 is not necessary for SC growth in virgin or mated males. After mating, E2F1 appears to favour SC growth involving endoreplication, while suppressing growth that occurs without endoreplication in these cells (Fig. 6.7 C-D, I-J).

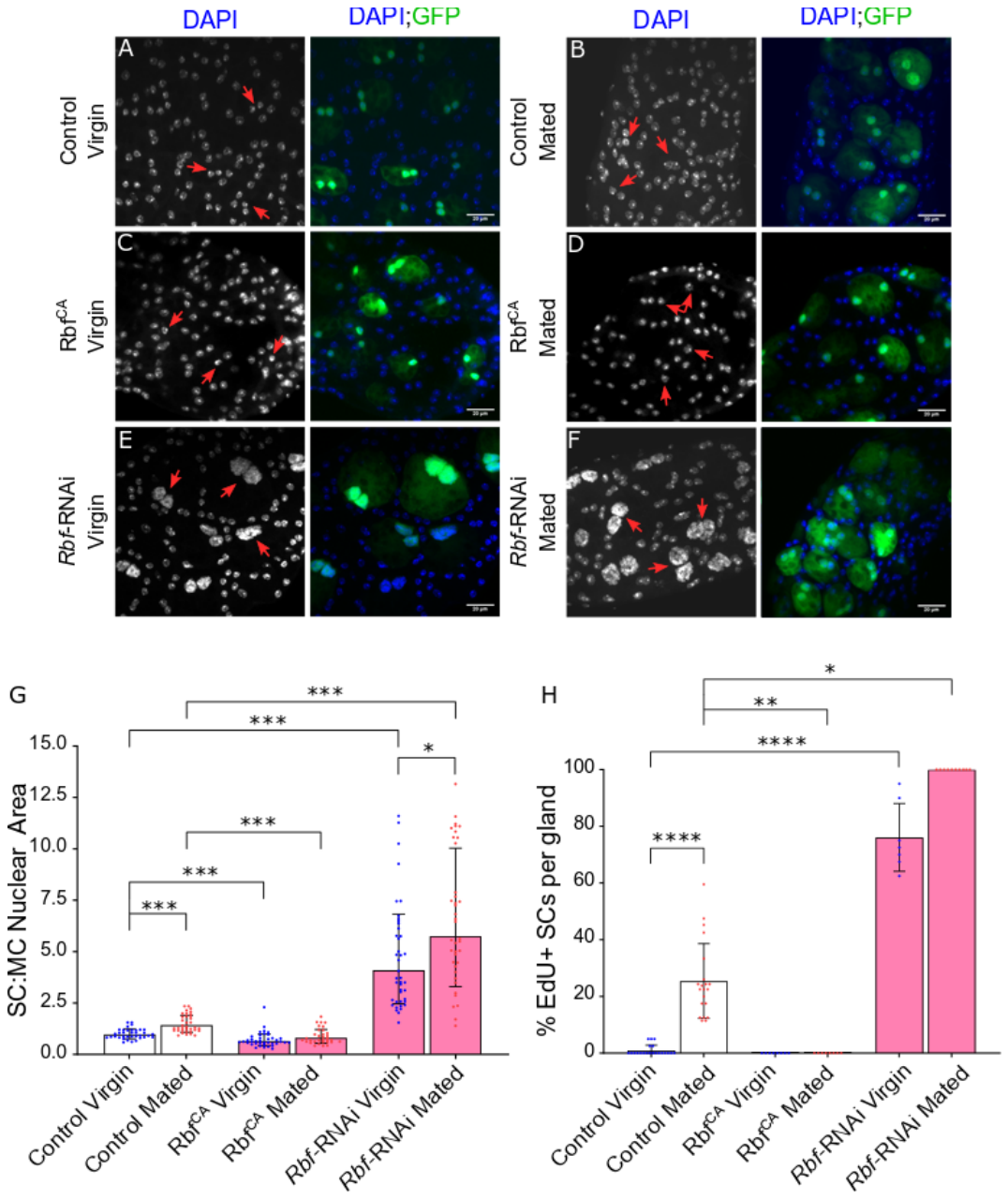

Figure 6.6 Role of Rbf in SC growth and endoreplication regulation

A-F: Images show distal tip of AGs from 6-day-old adult virgin and mated males expressing the corresponding transgene under the control of the esg^{ts}F/O driver. Control represents w^{1118} flies specifically expressing nuclear GFP (which also stains the cytosol) in SCs. Nuclei are stained with DAPI (blue). Red arrows point to representative SC nuclei for each transgene. Scale bars correspond to 20 µm.

G: Bar chart depicting the geometric mean ratio of the size of SC nuclei relative to neighbouring MC nuclei. The error bars show the geometric standard deviation within the sample. Graph includes SC growth assay data of virgin and mated flies expressing no other transgene, Rbf^{CA} or *Rbf*-RNAi in SCs. Rbf^{CA} inhibits SC growth and knocking down *Rbf* promotes SC growth in both virgin and mated males. Welch ANOVA on log-transformed data; Games-Howell post hoc test; 0.01<*p<0.05; 0.0001<***p≤0.001 (n≥33 SCs; ≥11 males).

H: Bar chart depicting the mean % of EdU+ SCs per gland. The error bars show the standard deviation within the sample. Graph includes EdU assay data of virgin and mated flies expressing no other transgene, Rbf^{CA} or *Rbf*-RNAi in SCs. Loss of Rbf promotes SC endoreplication. Kruskal Wallis test; Dunn's post hoc test- 0.01<*p<0.05; 0.001<**p≤0.01; ****p≤0.0001 (n≥7 males).

As discussed above, in *Drosophila* salivary glands, oscillations in E2F1 protein levels are essential for sustaining endocycles. E2F1 induces S-phase via the transcription of *CycE*, which in turn promotes degradation of E2F1 by CRL4^{cdt2} ubiquitin ligase. CRL4^{cdt2} targets E2F1 via the conserved PIP box. When an active and stabilised mutant of E2F1 lacking the PIP box (E2F1.PIP) was expressed in the salivary gland cells, endoreplication was completely blocked (Zielke et al., 2011). The authors also observed that degradation of E2F1 occurs, even when wild type E2F1 was overexpressed, thereby emphasising the importance of the oscillatory E2F1 levels in the regulation of endoreplication. I was interested to determine whether such E2F1 oscillations are required for the induction of mating-dependent SC endoreplication. When the constitutively active form of *E2F1*, *E2F1.PIP*, was expressed in SCs, no change in either the growth or endoreplication levels were observed in either virgin or mated males compared to wild type controls (Figure 6.7 G-J). This suggests that endoreplication that occurs in SCs from mated males does not require the E2F1/CycE oscillator and is consistent with a model in which the cells normally only go through one additional endocycle.

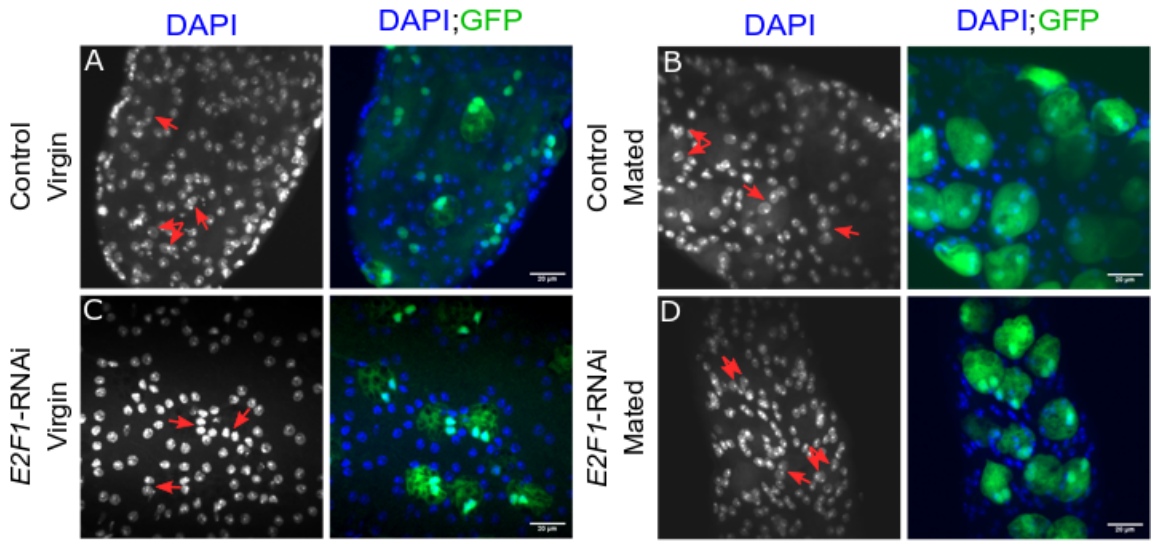

Figure 6.7 Role of E2F1 in SC growth and endoreplication regulation
A-D: Images show distal tip of AGs from 6-day-old adult virgin and mated males expressing the corresponding transgene under the control of the esg^{ts}F/O driver. Control represents w^{1118} flies specifically expressing nuclear GFP (which also stains the cytosol) in SCs. Nuclei are stained with DAPI (blue). Red arrows point to representative SC nuclei for each transgene. Scale bars correspond to 20 µm.

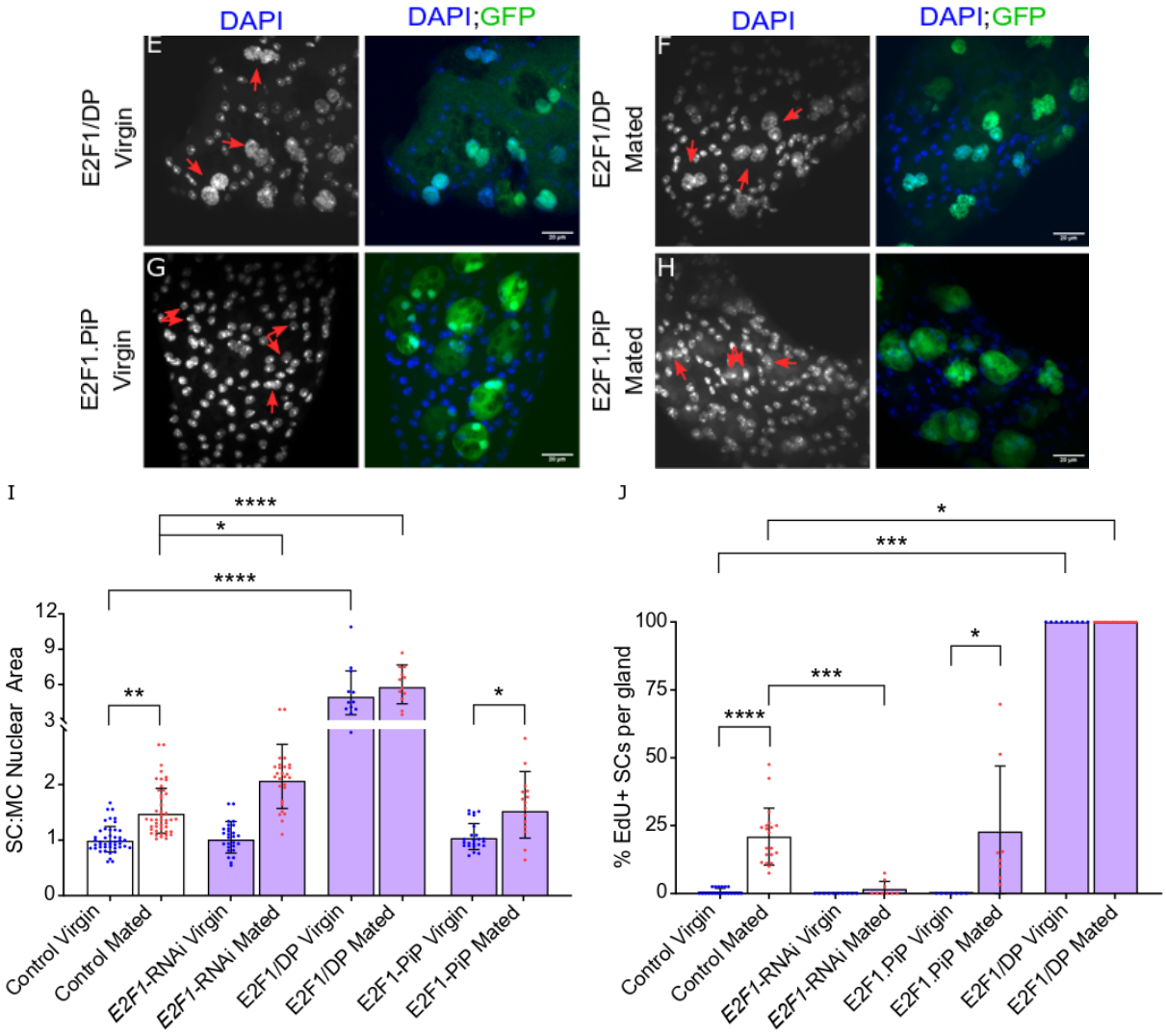

Figure 6.7 Role of E2F1 in SC growth and endoreplication regulation

E-H: Images show distal tip of AGs from 6-day-old adult virgin and mated males expressing the corresponding transgene under the control of the esg^{ts}F/O driver. Control represents w^{1118} flies specifically expressing nuclear GFP (which also stains the cytosol) in SCs. Nuclei are stained with DAPI (blue). Red arrows point to representative SC nuclei for each transgene. Scale bars correspond to 20 µm.

I: Bar chart depicting the geometric mean ratio of the size of SC nuclei relative to neighbouring MC nuclei. The error bars show the geometric standard deviation within the sample. Graph includes SC growth assay data of virgin and mated flies expressing no other transgene, *E2F1*-RNAi, E2F1/DP or E2F1.PiP in SCs. E2F1 is not necessary for SC growth in virgins, but in mated males, it appears that overall it negatively regulates growth, which EdU analysis indicates is endoreplication-independent (J). One-way ANOVA on log-transformed data; Tukey HSD post hoc test; $0.01<*p<0.05$; $0.001<**p\leq0.01$; $****p\leq0.0001$ ($n\geq12$ SCs; ≥ 4 males).

J: Bar chart depicting the mean % of EdU+ SCs per gland. The error bars show the standard deviation within the sample. Graph includes EdU assay data of virgin and mated flies expressing no other transgene, *E2F1*-RNAi, E2F1/DP or E2F1.PiP in SCs. E2F1 is necessary and sufficient to induce endoreplication in SCs. Kruskal Wallis test; Dunn's post hoc test; $0.01<*p<0.05$; $0.0001<***p\leq0.001$; $****p\leq0.0001$ ($n\geq9$ males).

6.3.6. Rbf/E2F1 functions upstream of EcR in a hormone-independent manner to regulate SC growth and endoreplication

Having established that the cell cycle regulators are essential in mediating growth and endoreplication in SCs, I wanted to study the epistatic relationship between these cell cycle components and the BMP/EcR axis. I made combination lines, which included one UAS-regulated transgene that modulates Rbf/E2F1 signalling and another that alters BMP or EcR signalling (refer Section 2.4 for the genetic scheme for making these combinations). One drawback with this method of investigation is that the findings with some of the combinations are not clear-cut, resulting in an intermediate phenotype, which could be explained by insufficient knockdown, competition between transgenes, or the fact that two pathways partly act independently. However, some combinations give very clear outcomes. In this section I focus on the relationship between cell cycle regulators and the EcR pathway.

When Rbf^{CA} was co-expressed with EcR-C, it was observed that 60% of the SCs in virgin males still endoreplicated as compared to no endoreplication in SCs expressing Rbf^{CA} (Fig. 6.8 B-D, H-I). These results suggest that EcR-C is able to induce endoreplication even when the cells express Rbf^{CA}, thereby strongly supporting earlier observations by Leiblich and Sarma that the EcR appears to lie downstream of Rbf, because its expression levels are affected by Rbf/E2F1 signalling. However, co-expressing Rbf^{CA} and EcR-C in SCs of virgins resulted in nuclear growth levels similar to controls. SC growth was greater than SCs expressing Rbf^{CA} and less than SCs that express only EcR-C. When E2F1/DP was co-expressed with *EcR*-RNAi, SC nuclear growth was greater than controls or cells expressing *EcR*-RNAi (Fig. 6.8 E-G, J-K). However, growth was suppressed compared to cells expressing *E2F1/Dp* alone. Interestingly, I observed that *EcR*-RNAi completely suppressed E2F1/DP-induced endoreplication. I conclude that E2F1/DP is able to elicit some SC growth in the absence of EcR. However, somewhat surprisingly, for SC endoreplication, E2F1/DP requires EcR to regulate CycE.

Since endoreplication is a hormone-independent EcR-regulated process, I was interested to determine whether E2F1/DP requires hormone-independent EcR signalling or hormone-dependent EcR signalling to regulate SC endoreplication in virgin males. I co-expressed E2F1/DP with *shd*-RNAi and found that *shd*-RNAi did not have any effect on SC endoreplication induced by E2F1/DP and in fact, resulted in an increase in nuclear growth (Fig. 6.9). Therefore, E2F1/DP-induced SC endoreplication requires hormone-independent EcR signalling and ecdysone may inhibit E2F1/DP-mediated nuclear growth in SCs.

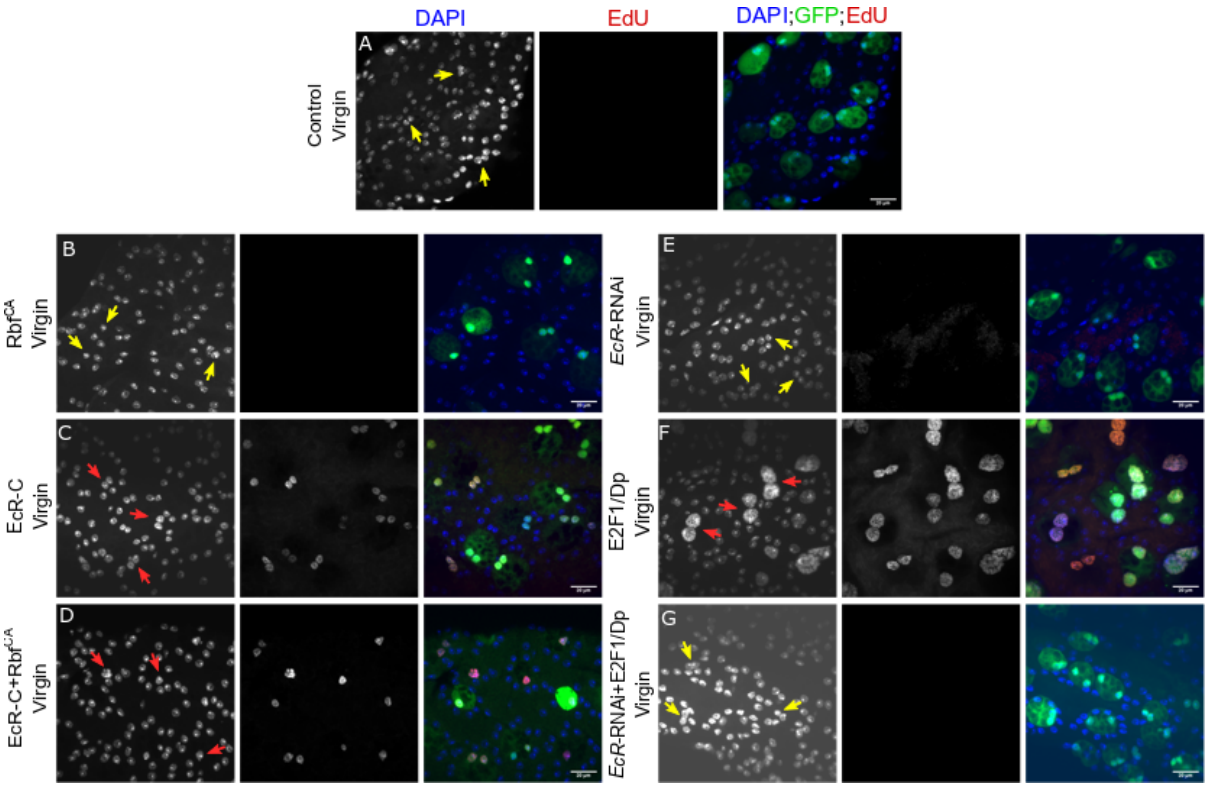

Figure 6.8 Interaction between Rbf/E2F1 and EcR signalling in the regulation of SC growth and endoreplication

A-G: Images show distal tip of AGs from 6-day-old adult virgin males expressing the corresponding transgene under the control of the esg^{ts}F/O driver. Control represents w^{1118} flies specifically expressing nuclear GFP (which also stains the cytosol) in SCs. Nuclei are stained with DAPI (blue). Red arrows point to representative SC nuclei for each transgene. Scale bars correspond to 20 µm.

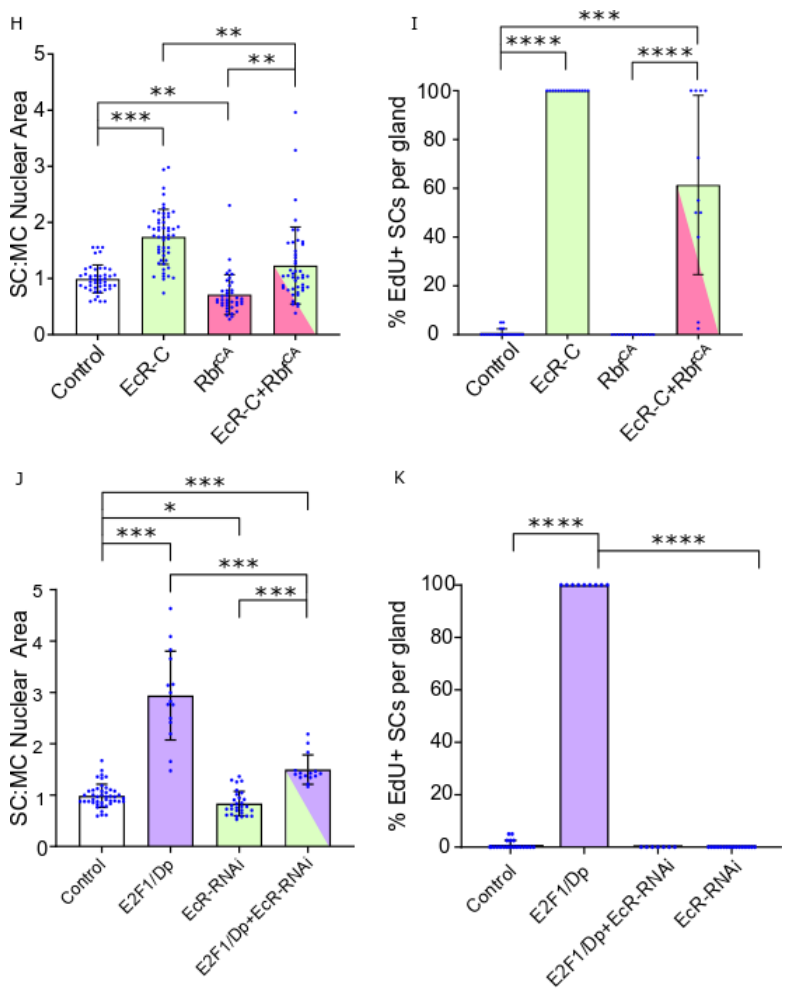

Figure 6.8 Interaction between Rbf/E2F1 and EcR signalling in the regulation of SC growth and endoreplication

H: Bar chart depicting the geometric mean ratio of the size of SC nuclei relative to neighbouring MC nuclei. The error bars show the geometric standard deviation within the sample. Graph includes SC growth assay data of virgin flies expressing no other transgene, Rbf^{CA}, EcR-C and Rbf^{CA}+EcR-C in SCs. Rbf can interact with EcR to regulate growth, but it appears to also act independently. Welch ANOVA on log-transformed data; Games-Howell post hoc test- $0.001<**p\leq0.01$; $0.0001<***p\leq0.001$ ($n\geq38$ SCs; ≥13 males).

I: Bar chart depicting the mean % of EdU+ SCs per gland. The error bars show the standard deviation within the sample. Graph includes EdU assay data of virgin and mated flies expressing no other transgene, Rbf^{CA}, EcR-C and Rbf^{CA}+EcR-C in SCs. EcR can induce endoreplication even when Rbf is constitutively active in SCs. Kruskal Wallis test; Dunn's post hoc test- $****p\leq0.0001$ ($n\geq11$ males).

J: Bar chart depicting the geometric mean ratio of the size of SC nuclei relative to neighbouring MC nuclei. The error bars show the geometric standard deviation within the sample. Graph includes SC growth assay data of virgin flies expressing no other transgene, E2F1/Dp, *EcR*-RNAi and E2F1/Dp+*EcR*-RNAi in SCs. E2F1 can promote some growth in SCs independently of EcR. Welch ANOVA; Games-Howell post hoc test- $0.01<*p\leq0.05$; $0.0001<***p\leq0.001$ ($n\geq15$ SCs; 5 males).

K: Bar chart depicting the mean % of EdU+ SCs per gland. The error bars show the standard deviation within the sample. Graph includes EdU assay data of virgin and mated flies expressing no other transgene, E2F1/Dp, *EcR*-RNAi and E2F1/Dp+*EcR*-RNAi in SCs. *EcR*-RNAi can completely suppress E2F1-mediated endoreplication. Kruskal Wallis test; Dunn's post hoc test- $****p\leq0.0001$ ($n\geq7$ males).

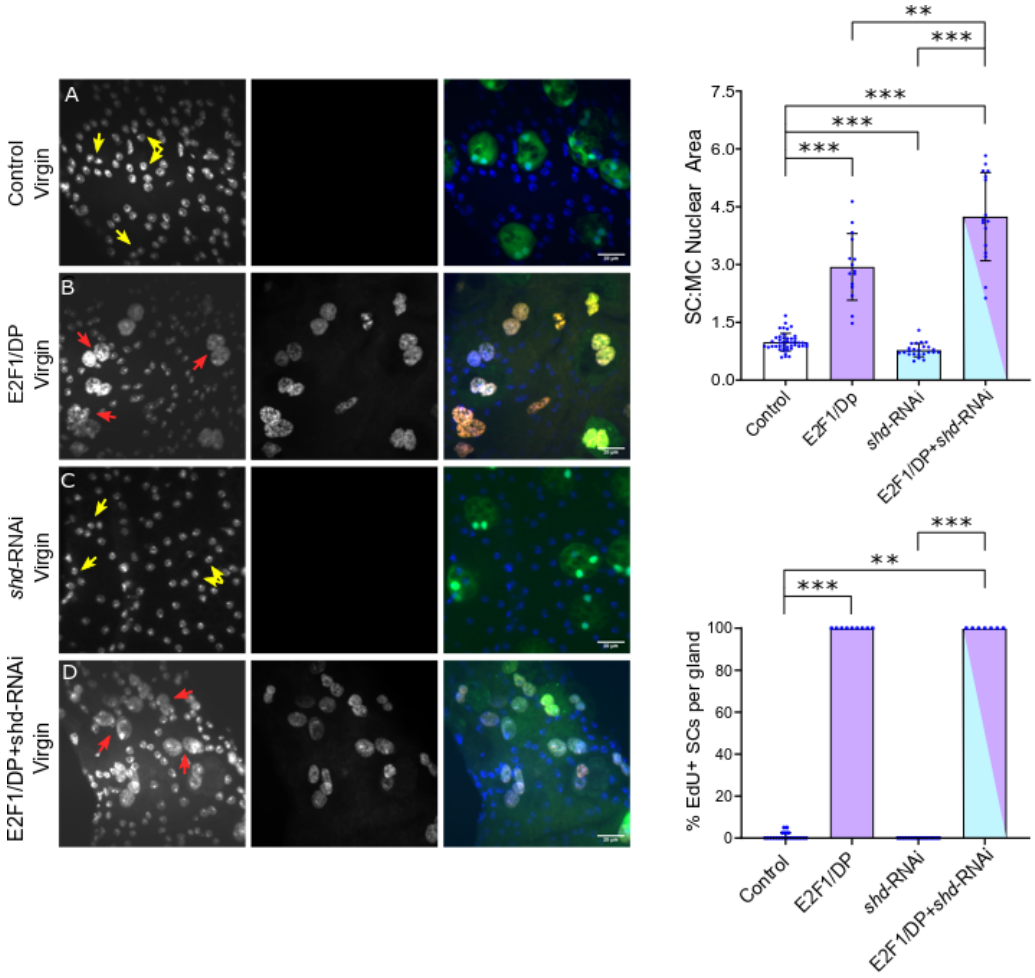

Figure 6.9 E2F1-mediated growth and endoreplication does not require ecdysone

A-D: Images show distal tip of AGs from 6-day-old adult virgin males expressing the corresponding transgene under the control of the esg^{ts}F/O driver. Control represents w^{1118} flies specifically expressing nuclear GFP (which also stains the cytosol) in SCs. Nuclei are stained with DAPI (blue). Red arrows point to EdU+ SC nuclei and yellow arrows point to EdU- SC nuclei for each transgene. Scale bars correspond to 20 µm.

I: Bar chart depicting the mean ratio of the size of SC nuclei relative to neighbouring MC nuclei. The error bars show the standard deviation within the sample. Graph includes SC growth assay data of virgin flies expressing no other transgene, E2F1/Dp, *shd*-RNAi or E2F1/Dp+*shd*-RNAi in SCs. Ecdysone inhibits growth induced by E2F1/Dp. One-way ANOVA; Games-Howell post hoc test- 0.01<**p≤0.001; 0.001<***p≤0.0001 (n≥15 SCs; ≥5 males).

H: Bar chart depicting the mean % of EdU+ SCs per gland. The error bars show the standard deviation within the sample. Graph includes EdU assay data of virgin and mated flies expressing no other transgene, E2F1/Dp, *shd*-RNAi or E2F1/Dp+*shd*-RNAi in SCs. Ecdysone has no effect on endoreplication induced by E2F1/Dp. Kruskal Wallis test; Dunn's post hoc test- 0.01<*p≤0.05; 0.0001≤***p<0.001; ****p≤0.00001 (n≥15 males).

6.3.7. BMP signalling is downstream of CycD/Rbf but upstream of E2F1 in the regulation of SC growth and endoreplication

To study the interaction between the BMP signalling pathway and Rbf/E2F1, I co-expressed E2F1/DP with BMP signalling antagonist Dad in SCs. This resulted in SC nuclear growth which was much higher than the controls and not significantly decreased from cells expressing E2F1/DP alone. Furthermore, all the SCs expressing E2F1/DP + Dad endoreplicated in virgin males (Fig. 6.10 B-D, I, L). Hence, this shows that the BMP signalling is an upstream regulator of E2F1/DP in the regulation of growth and endoreplication. When CycD/cdk4 was co-expressed with Dad, Dad was able to completely suppress any SC nuclear growth that was induced by CycD/cdk4 alone (Fig. 6.10 B, E, J) . Additionally, only 20% of SCs endoreplicated, which might be attributed to Dad expression incompletely suppressing BMP signalling in some SCs (Fig. 6.10 B, E, M). Therefore, CycD acts upstream of BMP signalling's effects on nuclear growth and endoreplication; in turn, BMP signalling is upstream of E2F1/DP. In order to determine how the BMP pathway interacts with Rbf, I co-expressed Rbf^{CA} and Tkv^{act} in SCs, which resulted in nuclear growth similar to controls in virgin males (Fig. 6.10 F-H, K). This growth was much reduced compared to when only Tkv^{act} was expressed and it was significantly different from the growth observed with just expressing Rbf^{CA}, but 80% of the SCs endoreplicated (Fig. 6.10 F-H, N). Overall, it appears that suppressing CycD/cdk4 signalling by Rbf^{CA} overexpression can inhibit the effects of BMP signalling on SC nuclear growth but not endoreplication, suggesting that these two pathways may intersect and both be required upstream of E2F1/DP signalling to control these cellular processes.

Figure 6.10 Interaction between Rbf, E2F1 and BMP signalling in the regulation of SC growth and endoreplication

A-H: Images show distal tip of AGs from 6-day-old adult virgin males expressing the corresponding transgene under the control of the esg^{ts}F/O driver. Control represents w^{1118} flies specifically expressing nuclear GFP (which also stains the cytosol) in SCs. Nuclei are stained with DAPI (blue). Red arrows point to EdU+ SC nuclei and yellow arrows point to EdU- SC nuclei for each transgene. Scale bars correspond to 20 μm.

I: Bar chart depicting the geometric mean ratio of the size of SC nuclei relative to neighbouring MC nuclei. The error bars show the geometric standard deviation within the sample. Graph includes SC growth assay data of virgin flies expressing no other transgene, Dad, E2F1/DP and Dad+E2F1/DP in SCs. Dad is not able to suppress E2F1/DP-mediated SC growth. Welch ANOVA; Games-Howell post hoc test; 0.0001<***p≤0.001 (n≥12 SCs; ≥4 males).

J: Bar chart depicting the geometric mean ratio of the size of SC nuclei relative to neighbouring MC nuclei. The error bars show the geometric standard deviation within the sample. Graph includes SC growth assay data of virgin flies expressing no other transgene, Dad, CycD/cdk4 and CycD/cdk4+Dad in SCs. Dad completely suppresses CycD/cdk4-mediated SC growth. Welch ANOVA; Games-Howell post hoc test; 0.0001<***p≤0.001 (n≥18 SCs; ≥6 males).

K: Bar chart depicting the geometric mean ratio of the size of SC nuclei relative to neighbouring MC nuclei. The error bars show the geometric standard deviation within the sample. Graph includes SC growth assay data of virgin flies expressing no other transgene, Rbf^{CA}, Tkv^{act} and Rbf^{CA}+Tkv^{act} in SCs. Rbf suppresses most of the growth induced by Tkv^{act}. Welch ANOVA; Games-Howell post hoc test; 0.001<**p<0.01; 0.0001<***p≤0.001 (n≥13 SCs; ≥ 5 males).

L: Bar chart depicting the mean % of EdU+ SCs per gland. The error bars show the standard deviation within the sample. Graph includes EdU assay data of virgin and mated flies expressing no other transgene, Dad, E2F1/DP and Dad+E2F1/DP in SCs. Dad has no effect on E2F1/DP-mediated SC endoreplication. Kruskal Wallis test; Dunn's post hoc test; 0.01<*p≤0.05; ****p≤0.0001 (n≥9 males).

M: Bar chart depicting the mean % of EdU+ SCs per gland. The error bars show the standard deviation within the sample. Graph includes EdU assay data of virgin and mated flies expressing no other transgene, Dad, CycD/cdk4 and CycD/cdk4+Dad in SCs. Dad is able to suppress CycD/cdk4-mediated SC endoreplication. Kruskal Wallis test; Dunn's post hoc test; 0.01<*p≤0.05; ****p≤0.0001 (n≥6 males).

N: Bar chart depicting the mean % of EdU+ SCs per gland. The error bars show the standard deviation within the sample. Graph includes EdU assay data of virgin and mated flies expressing no other transgene, Rbf^{CA}, Tkv^{act} and Rbf^{CA}+Tkv^{act} in SCs. Kruskal Wallis test; Dunn's post hoc test-0.0001<***p≤0.001; ****p≤0.0001 (n≥9 males).

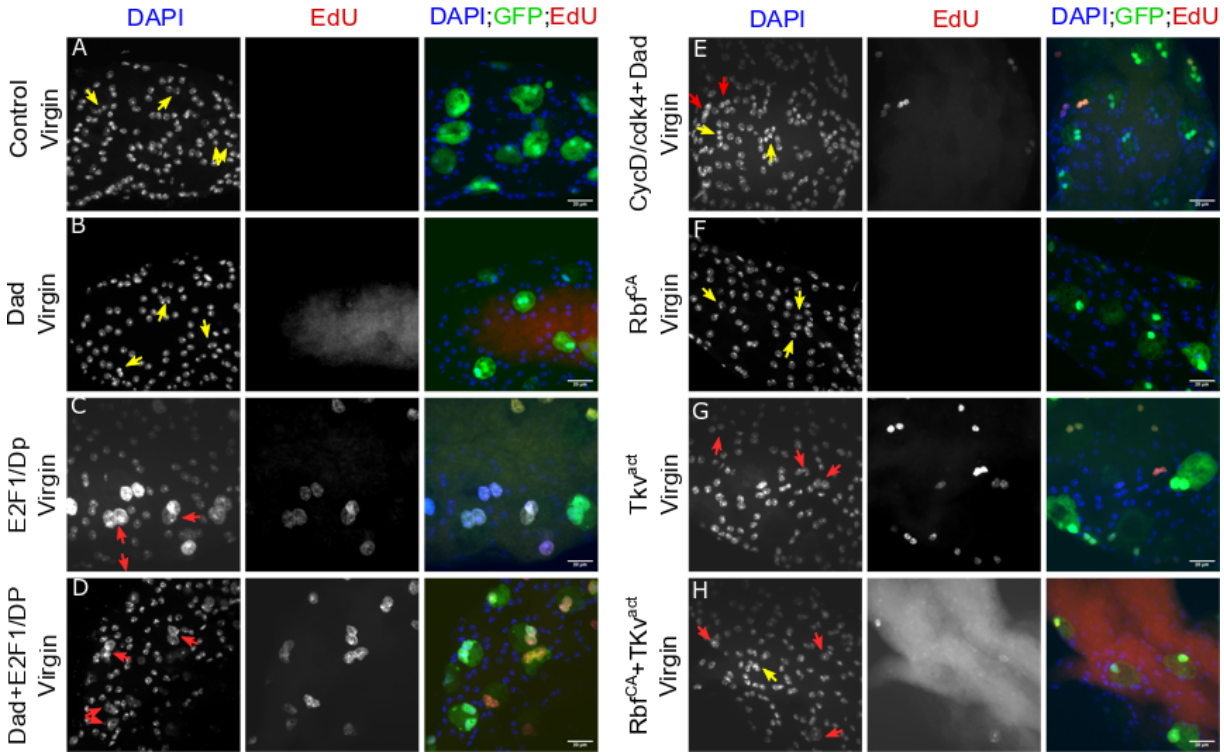
DAPI
EdU
DAPI;GFP;EdU
A
Control Virgin
B
Dad Virgin
C
E2F1/Dp Virgin
D
Dad+E2F1/DP Virgin
E
CycD/cdk4+Dad Virgin
F
RbfCA Virgin
G
TkvAct Virgin
H
RbfCA+TKvAct Virgin

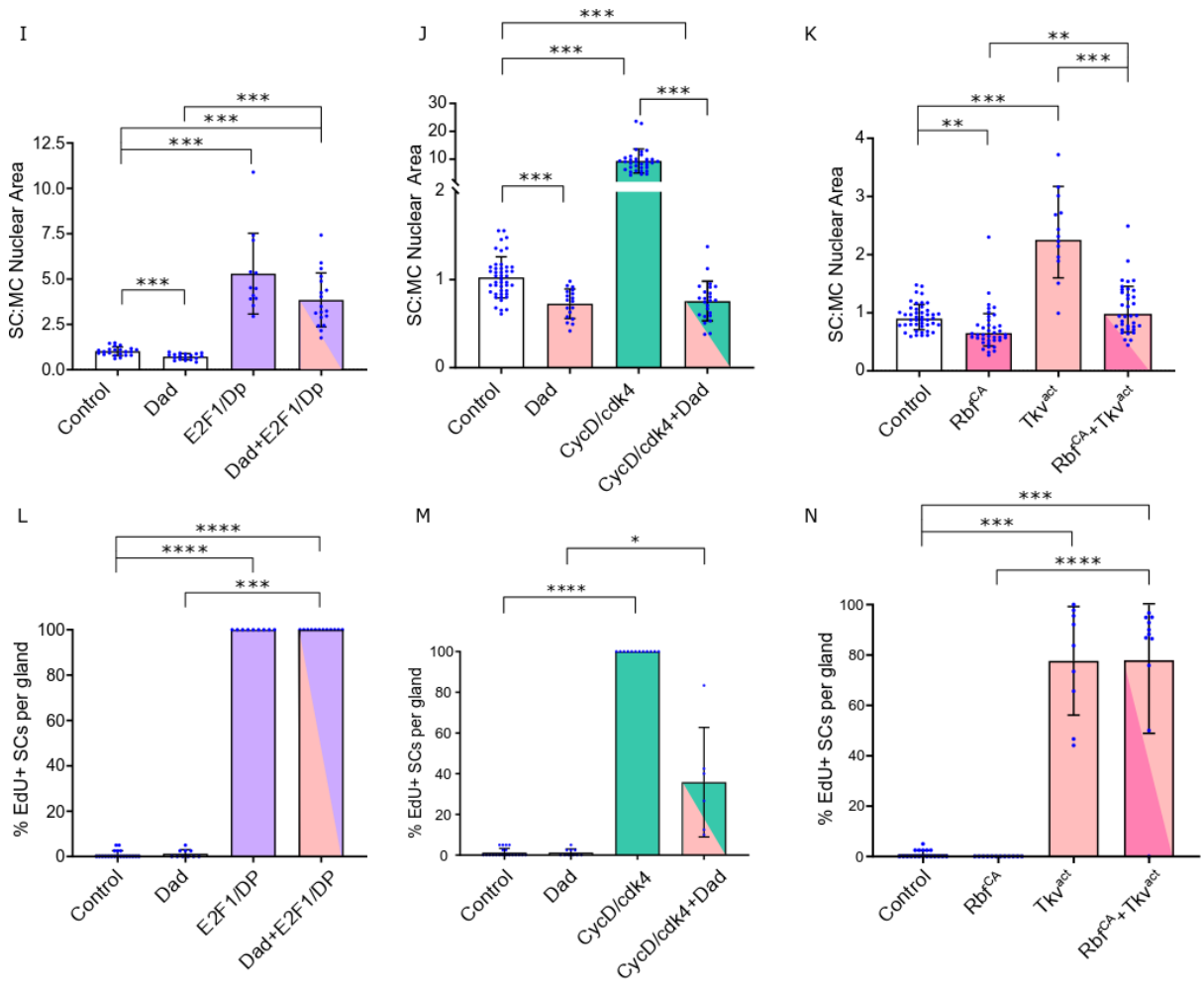
I
SC:MC Nuclear Area
Control
Dad
E2F1/Dp
Dad+E2F1/Dp
J
SC:MC Nuclear Area
Control
Dad
CycD/cdk4
CycD/cdk4+Dad
K
SC:MC Nuclear Area
Control
RbfCA
TkvAct
RbfCA+TkvAct
L
% EdU+ SCs per gland
Control
Dad
E2F1/DP
Dad+E2F1/DP
M
% EdU+ SCs per gland
Control
Dad
CycD/cdk4
CycD/cdk4+Dad
N
% EdU+ SCs per gland
Control
RbfCA
TkvAct
RbfCA+TkvAct

6.4. Summary and Discussion

In this chapter, I have shown that the G1 and G1/S cyclins, CycD and CycE respectively, are necessary and sufficient for the induction of endoreplication in SCs. However, they are not essential for at least some of the SC growth that occurs without endoreplication in mated males. Furthermore, although E2F1 is necessary and sufficient to promote endoreplication in SCs, it is not essential for growth. From the epistasis experiments described here, it appears that BMP signalling intersects the cell cycle regulatory pathway upstream of E2F1 activity and CycE, and downstream of Rbf and CycD. Consistent with previous immunofluorescence data with an anti-EcR antibody, EcR lies downstream of CycD/Rbf/E2F1. Additionally, CycE is placed downstream of EcR in the regulation of endoreplication and growth in SCs. Rbf regulates endoreplication and the various forms of SC growth in virgin and mated males. Apart from its role in growth and endoreplication, Rbf also affects adult SC nucleation state. Expression of Rbf^{CA} in the SCs results in most cells becoming mononucleate, with no effect on MCs. Interestingly, expression of this construct in MCs also results in SC mononucleation, but MCs retain their binucleate nature. Additionally, it appears that the control exercised by Rbf on nucleation state and endoreplication involves different signals, because mating can still induce endoreplication in mononucleate SCs (Fig. 6.11).

Overall, my data lead to five key conclusions.

- The cell cycle regulatory pathway involving CycD/Rbf/E2F1/CycE plays a critical role in controlling SC growth and endoreplication, and based on my previous analysis, these events are important in controlling the biosynthetic activity of these secretory cells in response to mating (Fig. 4.8).
- EcR is surprisingly required for E2F1 to drive endoreplication and growth via CycE, and this requirement is hormone-independent.

- Loss of Rbf in SCs induces hormone-independent, EcR-mediated endoreplication and growth, mirroring observations made in CRPC.
- CycD/Rbf mediates SC growth and endoreplication by regulating BMP signalling, which then regulates E2F1activity.
- Rbf/E2F1 plays an important role in maintaining binucleation in SCs, a finding that may be relevant to binucleate cells in other organisms.

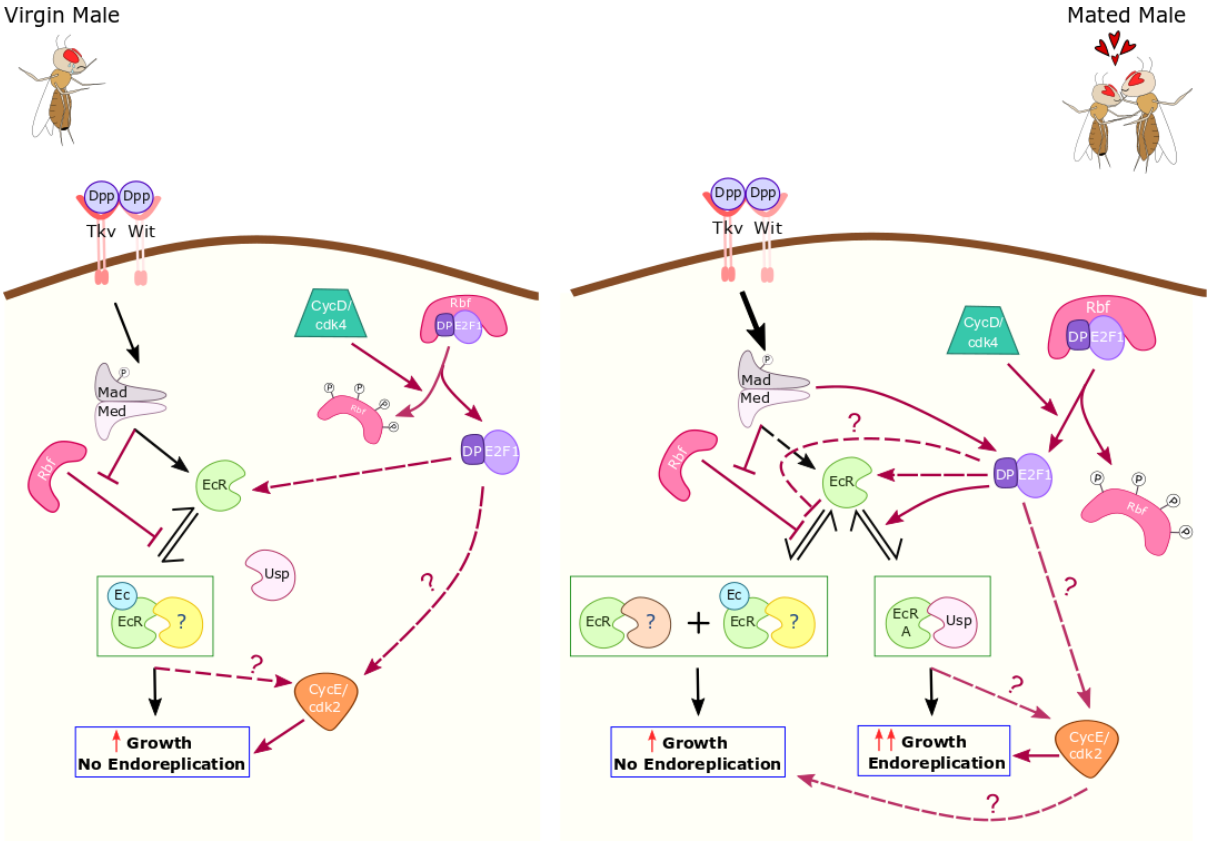

Figure 6.11 Schematic detailing cell cycle regulation of SC growth and genome endoreplication

In virgin males, CycD, Rbf and CycE regulate SC growth, but E2F1 does not play a role in this regulation. In mated males, CycD/Rbf/E2F1/CycE regulates SC growth that occurs through endoreplication. Interestingly, it appears that E2F1 requires EcR to activate endoreplication, but whether either E2F1 or EcR can exert their control through CycE to regulate endoreplication is not known. Rbf can inhibit SC growth that occurs without endoreplication in mated males, but it appears that knocking down CycD or CycE is not able to suppress this growth. Furthermore, CycD/Rbf /E2F1 is an upstream regulator of EcR, while CycE acts downstream of EcR. BMP signalling interacts with the cell cycle regulatory axis downstream of Rbf but upstream of E2F1. Therefore, in SCs, the cell cycle machinery has a distinct role from its cell cycle regulation that involves an important input from the EcR. cdk4/2- cyclin dependent kinase 4/2; CycD- Cyclin D; CycE- Cyclin E; Dp- Dumpy; P- Phosphoryl group; Rbf-Retinoblastoma. Red arrows depict the pathways that regulate SC growth and endoreplication and the dotted arrows show probable signalling interactions.

6.4.1. Activated Rbf reverses the binucleate state in adult SCs independently of its effects on growth and endoreplication

My study has revealed an interesting role for Rbf in controlling the nucleation state in binucleate adult SCs (Fig. 6.12). Rbf^{CA} induces almost all SCs to become mononucleate, with no effect on MC nucleation state. Expression of this construct in the MCs, results in SC mononucleation but MCs retain their binucleate nature. Those SCs which become mononucleate when Rbf^{CA} is expressed in MCs are still able to endoreplicate upon mating. Hence, I propose that an unknown secreted MC signal, which is not Rbf, can direct mononucleation in SCs. Since MCs do not become mononucleated, it seems that unlike SCs, MCs lack the proper machinery to process this mononucleation signal. Furthermore, knocking down E2F1 in SCs results in just a few SCs becoming mononucleate, whereas no effect was observed when E2F1 was knocked down in MCs, potentially suggesting that in MCs, *E2F1*-RNAi does not have the capacity to elicit the mononucleation signal that Rbf^{CA} transmits to SCs. p53, an upstream regulator of Rbf/E2F1, is also able to regulate SC nucleation state. It appears that this switch between binucleation and mononucleation occurs via a mechanism that is different from that used during the development of the AG. I have preliminary results which show that the mononucleation phenotype induced by Rbf^{CA} is reversible, if Rbf^{CA} expression is stopped, but since I have not quantified these data, I have not presented these results here. Interestingly, a recent study has shown that although Rb/E2F does not initiate binucleation in mammalian cardiomyocytes, the binucleate and mononucleate cells have distinct Rb/E2F-mediated transcriptional programmes (Windmueller et al., 2020), thereby emphasising the importance of this pathway in different nucleation states.

Two possible mechanisms can be utilised by Rbf^{CA} to induce mononucleation in SCs - promoting fusion of the two nuclei or destabilising one nucleus. In order to follow up these hypotheses, it would be necessary to capture the binucleation to mononucleation transition in

real-time. An important follow-up of these results would be to try to capture the binucleation to mononucleation transition in real-time. I have stained the nuclei with Hoescht and used the 40X objective lens of the Delta Vision microscope to capture the transition, but as yet, have been unsuccessful. I believe that this might have been more successful if a temperature-controlled microscope stage was used instead, as it is possible that a constant expression of Rbf^{CA} is essential to promote this transition.

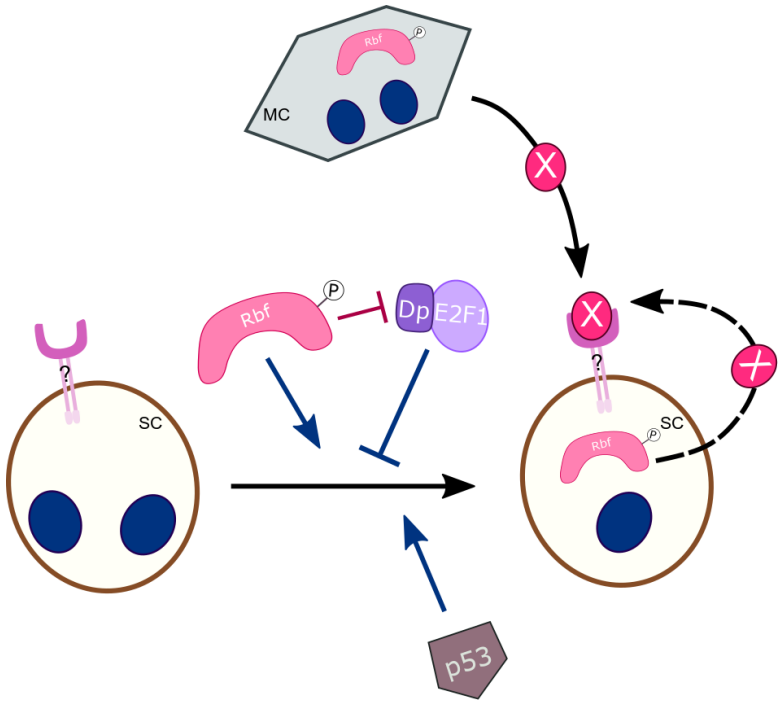

Figure 6.12 Schematic detailing nucleation state regulation in adult SCs
Expression of a constitutively active form of Rbf, Rbf^{CA}, which has mutations in three of its four CDK phosphorylation sites, in SCs is able to induce mononucleation. This phenotype is negatively regulated by E2F1 and positively regulated by p53. Additionally, expression of Rbf^{CA} in MCs is able to activate mononucleation in SCs, presumably by secreting 'X' which could activate an unknown receptor (?) which regulates SC nucleation state. It is possible that Rbf^{CA} when expressed in SCs also promotes mononucleation via this unknown receptor.

In regards to the hypothesis that Rbf^{CA} could destabilise one of the nuclei which results in a mononucleate cell, I observed that when Rbf^{CA} was expressed in the SCs, some binucleate SCs would occasionally have one flat and small nucleus that lost its ability to express nGFP of the $esg^{ts}F/O$ driver (Fig. 6.13). This might suggest that the two nuclei could possibly be independently regulated. This type of regulation is observed in the mammalian myofiber cells

of the skeletal muscle, which can contain up to thousands of post-mitotic nuclei. Each myofiber cell is divided into three regions and the nuclei of these regions have distinct transcriptional activity and protein localisation (Cutler et al., 2018). Similar independence in nuclear regulation is observed in fungal syncytia. In *Ashbya gossypii* syncytia, although they share the same cytoplasm, each nucleus demarcates and compartmentalises a portion of the cytoplasm for its regulation. This is mediated by controlling the spacing of the nuclei via the microtubule networks; the closer the nuclei, the more the synchrony (Anderson et al., 2013; Roberts and Gladfelter 2015). In SCs, we often do observe cells with different nuclear spacings, sometimes close together and sometimes at the two opposite ends of the cell. Therefore, it would be of interest to determine whether the two nuclei of the SCs are regulated and can act independently. Using the available chromosome markers (Le et al., 2006), it would be interesting to determine whether both these nuclei have the same chromosomal copy number and how this is altered when Rbf^{CA} is expressed in SCs. Furthermore, Single molecule Fluorescence *in situ* Hybridization (smFISH) techniques could be employed to quantify if any differences in gene expression levels are observed between the two nuclei. Pasnuri et al., 2018, have developed a modified smFISH method that can be applied to wholemount adult tissues and have demonstrated its use with adult testes. Therefore, there is a high possibility that this technique could be successfully adapted to the adult AGs.

Another interesting experiment that should be undertaken in order to determine other regulators of this mononucleation phenotype would be to sequence the RNA from AGs expressing Rbf^{CA} in the MCs and compare it with the controls. Since there are close to 1000 MCs, unlike the SCs, it is likely that we might be able to pick up any differentially regulated gene products that might be secreted to promote mononucleation in the SCs.

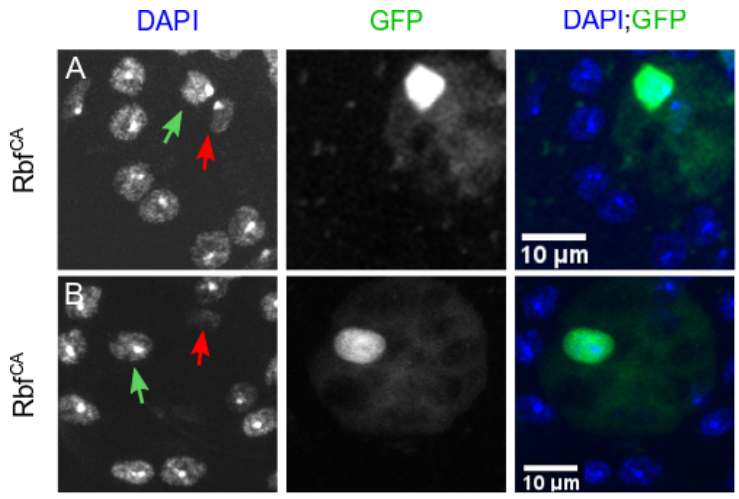

Figure 6.13 Possible nuclear destabilisation upon Rbf^{CA} expression

A-B: Images show a single SC surrounded by a few MCs from 6-day-old adult virgin males expressing Rbf^{CA} under the control of the esg^{ts}F/O driver which expresses nuclear GFP (which also stains the cytosol) in SCs. Nuclei are stained with DAPI (blue). Green arrows point to SC nuclei that express nGFP; red arrows point to SC nucleus that does not express nGFP and is weakly stained with DAPI. Scale bars correspond to 10 µm.

6.4.2. G1 cyclins promote the transition from ligand-dependent to ligand-independent EcR signalling upon mating

I have demonstrated that the G1 cyclin, and upstream EcR regulator, CycD, and the G1/S cyclin, CycE, which acts downstream of EcR, are essential for ecdysone-dependent SC nuclear growth in virgin males, even though no detectable DNA replication occurs in these cells. Perhaps not unexpectedly, in mated males, CycD and CycE are necessary for EcR- and endoreplication-dependent SC nuclear growth, which does not require ecdysone. However, although CycD and CycE are able to regulate endoreplication-independent SC growth in virgin males, knocking down either of these cyclins does not suppress the endoreplication-independent growth that occurs in mated males.

Ligand-dependent and ligand-independent interactions between another steroid nuclear receptor, the oestrogen receptor (ER), and both CycD1 and CycE have been observed in breast cancer cells. In oestrogen-responsive cell lines, it has been shown that the ER activated by estradiol, a major oestrogenic steroid, is able to regulate CycD1 protein levels, phosphorylation

of Rb, and promote CycE activity in these cells (Foster and Wimalasena 1996, 2001). But as with SCs and EcR, overexpression of CycD1/cdk4 can reinitiate ER activation after treatment with anti-oestrogens, thereby promoting hormone-refractory ER signalling and growth (Bindels et al., 2002).

In prostate cancer cells, CycD1, in contrast to its interaction with ER, has been reported to specifically inhibit androgen-dependent activation of the androgen receptor (AR) thereby acting as an AR co-repressor (Petre et al., 2002; Reutens et al., 2001; Schiewer et al., 2009), even though loss of its downstream inhibitory target, Rb, seems to promote hormone-independent AR signalling. Interestingly, it appears that the C-terminal functional domain of CycD1 plays a vital role in a direct interaction with both the ER and AR (Bindels et al., 2002; Petre et al., 2002). In SCs, overexpression of CycD/cdk4 in SCs induces extensive hormone-independent endoreplication, a response that parallels that observed with the ER in breast cancer.

In vitro studies have demonstrated that CycE acts a coactivator of the AR both in the absence and the presence of DHT. Although the exact role played by CycE in prostate cancer is not clear, it has been demonstrated that CycE is expressed at higher levels in mice lacking the *Rb* gene, and this expression of CycE correlates with hyperplastic regions in the *Rb* mutant mice. Furthermore, CycD1 proteins decreased as prostate cancer progressed while CycE levels increased continuously. The authors suggest that this transition from CycD to CycE might be involved in promoting the progression of prostate cancer (Balk and Knudsen 2008; Maddison et al., 2004). Therefore, in the above-mentioned systems, it appears that CycD and CycE regulate hormone-dependent and hormone-independent steroid receptor signalling. I propose that in SCs, CycD and perhaps CycE may be able to mediate a similar switch from ligand-

dependent EcR signalling in virgin males to ligand-independent EcR signalling in mated males via a mechanism that does not require their cell cycle regulatory functions.

6.4.3. Multiple forms of Rbf signalling are involved in the regulation of SC growth and hormone-independent endoreplication

Expression of Rbf^{CA} in SCs of virgin males significantly suppressed SC nuclear growth in virgin males, while knocking-down E2F1 did not have an effect on growth in virgin males. When either *Rbf*-RNAi or E2F1/DP was expressed, a massive increase in SC nuclear growth was observed. In mated males, expression of Rbf^{CA} is able to suppress endoreplication-independent SC growth, unlike expression of *E2F1*-RNAi, which surprisingly appears to over-compensate for the lack of endoreplication-dependent growth with more endoreplication-independent growth. Taking these results together, it appears that Rbf inhibits SC growth in virgins using a novel mechanism that does not require the E2F1 transcription factor. Interestingly, since both Rbf and E2F1 inhibit endoreplication-independent SC growth in mated males, it is possible that both Rbf and E2F1 acts independently of each other to regulate this form of SC growth. There is some evidence pertaining to E2F1 activity independent of Rbf during early embryogenesis (Shibutani et al., 2007)**.** Additionally, Rb functions that occur independently of its E2F transcriptional activity control have been observed in Rb-mediated cell cycle arrest and chromatin stability in mammalian cells (Dick and Rubin, 2013). The E2F1-independent Rbf activity in regulation of chromatin condensation appears to be conserved in *Drosophila* as well (Longworth et al., 2008). However, canonical Rbf/E2F1 signalling is also active in SCs and is required for endoreplication-dependent SC growth in mated males as expression of either Rbf^{CA} or *E2F1*-RNAi completely inhibits this process.

Since Rbf acts upstream of *EcR* and regulates its protein levels, it can be concluded that Rbf at least partly enacts its effect on SC endoreplication and associated growth by manipulating

EcR's concentration, in a process involving E2F1. However, some effects of Rbf in SCs seem less dependent on E2F1 suppression than others, such as its role in endoreplication-independent growth. Determining how these different forms of Rbf signalling mediate their functions will likely require a biochemical analysis of these processes, which is challenging in SCs. However, endoreplication has emerged as one downstream activity in SCs for which the regulatory pathway has been defined by my work.

Loss of Rb, is commonly observed in several cancer types and is considered to be essential for the early development of cancer. However, in prostate cancer, loss of Rb is associated with the progression of prostate cancer and transition to a hormone-independent state (Sharma et al., 2010; Thangavel et al., 2017), rather than its initial development. Similar to the regulation of EcR by Rbf/E2F1 in SCs, Rb/E2F also regulate the expression levels of *AR*. When *Rbf*-RNAi is expressed in SCs of virgin males, all SCs undergo endoreplication, which I have previously shown is under the control of the ecdysone-independent EcR signalling axis, thereby promoting the switch from the hormone-dependent EcR signalling observed in virgin males to hormone-independent EcR signalling. Furthermore, I confirmed that E2F1/DP overexpression induces endoreplication and growth in an ecdysone-independent fashion. This mirrors the effects observed with loss of *Rb* in CRPC, which induces an unsupervised activation of E2F, resulting in an increase in AR protein levels, and promotes the progression of prostate cancer to induce the androgen-refractory form of prostate cancer. Therefore, a physiological process in SCs associated with activating growth and biosynthetic activity in mated males independently of the levels of environmentally regulated ecdysone mirrors a disease process in humans. This raises the question, addressed in the concluding chapter, of whether CRPC in fact reflects the reactivation of a physiological process in the prostate.

Chapter-7: Summary of findings, significance and concluding remarks

7.1. Summary of findings

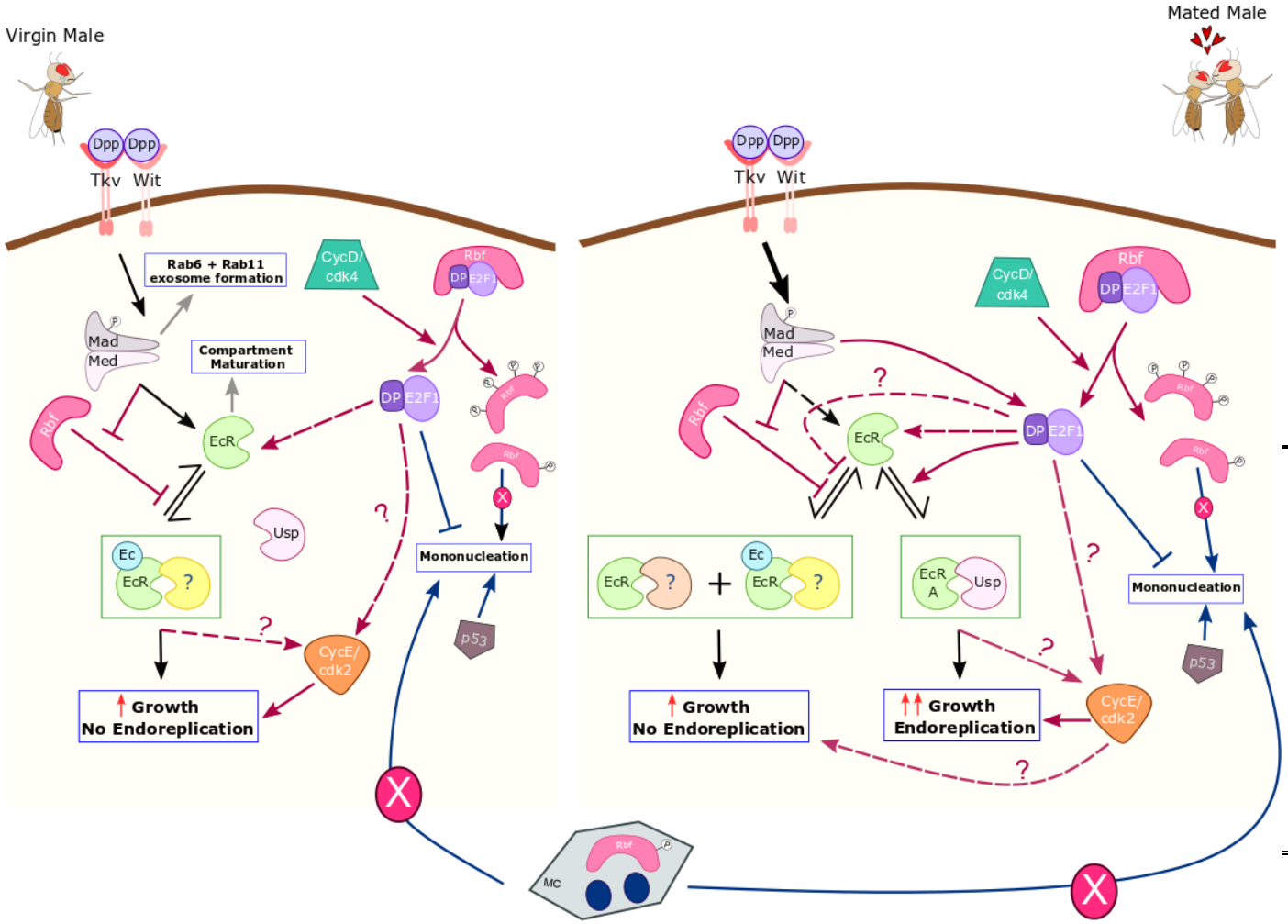

Figure 7.1:
Final schematic depicting key results presented in this thesis

This schematic shows the complex interactions between the EcR signalling, BMP pathway and the CycD/Rbf/E2F1/CycE signalling that are invovled in the regulation of SC growth, endoreplication, compartment formation, exosome biogenesis and nucleation state.

As I have discussed the specific key implications of my results in the previous results chapters, in this chapter I will focus on discussing the broader implications of my work.

7.2. *Drosophila* SCs as an *in vivo* model for studying the role of steroid receptor signalling on secretory activity

My third results chapter is a compilation of preliminary data suggesting that the EcR and BMP signalling pathways are involved in different aspects of secretory regulation in SCs. Additionally, I have shown that in the regulation of exosome biogenesis and compartment formation, the BMP and EcR pathways interact differently from their regulation of growth and endoreplication. Exosomes have been implicated to play a role in prostate cancer progression including metastasis. However, due to the difficulty associated with studying exosome secretion in other systems, there are no conclusive studies that describe the mechanisms through which this occurs. The Wilson lab has pioneered the study exosome synthesis and secretion in *Drosophila* SCs and the lab has developed several tools for the same.

In the case of the role of EcR in regulating exosome biogenesis and compartment identity, the story may be clearer than that for BMP signalling. High EcR signalling activity promotes the compartment maturation process and low EcR signalling activity appears to stall the maturation process at the Rab 6 stage. EcR is required for the proper formation of exosomes, which might be explained by its effects on this maturation process. In the case of exosome regulation by BMP signalling, it will be important to test the role played by the other components of the BMP pathway, as I have looked at only a mutant activated form of the receptor Tkv and Dad, a downstream antagonist, to date. Furthermore, assessing the effects of other manipulations that increase or reduce hormone-independent

EcR signalling, eg. E2F1/DP and *torso*-RNAi expression respectively should start to reveal the specific roles of this form of signalling.

The next line of research would be to determine how BMP and EcR signalling regulate the secretion of exosomes into the lumen, using the established exosome secretory assay developed in the lab (Dar et al., 2020; Fan et al., 2019; Marie et al., 2020). Since it was previously shown that BMP signalling is essential for DCG replenishment after mating, it would definitely be interesting to determine whether and how the EcR and BMP signalling interact to replenish the DCGs. This response is clearly a response to mating in the males and it might possibly be correlated with growth and endoreplication regulation (Redhai et al., 2016). I have helped develop a tool to study DCG formation along with Mark Wainwright and Claudia Mendes. The Mfas protein is specifically present within the DCGs of the SCs, which can be marked by an *mfas-GFP* gene trap driver line. I briefly tested this line with some of the EcR genetic manipulations and it appears that EcR regulates DCG synthesis (Appendix C). However, I did these experiments using the confocal microscope and they need to be repeated using the live wide-field microscope. Much work is indeed necessary to get a complete understanding of how EcR and BMP signalling regulate exosome synthesis, compartment formation and identity, and DCG formation and secretion, however from my initial data it looks like this line of research would definitely yield some very interesting results, and that it may be relevant to similar processes in prostate cancer cells.

7.3. Physiological roles of SC signalling and cell biology

Several studies have focussed on studying the effects of mating on female behaviour and physiology, however there are not many reports on post-mating effects observed in males.

Work presented in my thesis brings to light the regulation of some mating-induced phenomena that specifically occur in the males. I found that genome endoreplication that is observed in SCs after mating, increases SC growth and rate of compartment formation in SCs, which presumably might be necessary for production and eventually secretion of the SC-derived seminal proteins into the lumen. I have shown that although EcR regulation in SCs of virgin males is ecdysone-dependent, this mating-dependent endoreplication process is regulated by an ecdysone-independent EcR signalling mechanism. Endoreplication has also been observed in the AG within 10 hours of eclosion (Box et al., 2019). Although the study suggests that MCs endoreplicate after eclosion, they do not comment on whether SCs endoreplicate during this period. Therefore, it would be interesting to test whether SCs endoreplicate in these early hours after eclosion and to determine its dependency on ecdysone and EcR.

Some socio-sexual cues have been shown to alter ecdysone levels within males, for example in response to mating (Leiblich et al., 2019), courtship behaviour (Ishimoto et al., 2009) and sleep (Ishimoto and Kitamoto, 2010). Behavioural changes may then be associated with the resulting modulation of EcR signalling. As discussed in Section 4.4.2, ecdysone titre levels increase upon mating (Leiblich et al., 2019). An increase in ecdysone levels is also observed when a male has been rejected by a previously mated female and ecdysone levels regulate the formation of courtship-induced long-term memory (Ishimoto et al., 2009). Ecdysone has been shown to have sleep-promoting effects and the EcR has been demonstrated to be involved in controlling the sleep-wakefulness switch (Ishimoto and Kitamoto, 2010). Aaron Leiblich and I tried to replicate the former study to determine if SC growth can be affected by the increased ecdysone levels that are observed after female rejection (Leiblich et al., 2019). We did not observe any change in SC growth,

which might be because rejection induces a short-term change which might be recalibrated over the span of 6-days.

However, the fact that ecdysone levels are regulated by socio-sexual cues highlights the potential importance of the existence of a hormone-independent mechanism in SC growth. For instance, when a virgin male, which has not previously been exposed to females, mates with a female, the hormone-independent endoreplication mechanism might facilitate a faster replenishment of transferred SC products, despite the low ecdysone levels. Furthermore, this kind of rapid, hormone-independent replenishment of luminal products might also be useful when males mate for a longer duration and transfer more seminal fluid proteins in the presence of rivals (Bretman et al., 2009; Wigby et al., 2009). Hence, it would definitely be of interest to determine the effects on SC growth, endoreplication and secretion in response to male competition. One should also test if an increase in the ability of SCs to endoreplicate (such as esg^{ts}F/O>EcR-C and esg^{ts}F/O>CycD/cdk4) can offset the costs associated with phenotypic plasticity such as short life-span and lower number of matings (Bretman et al., 2013).

7.4. *Drosophila* SCs as an *in vivo* model for the transition of prostate cancer to CRPC

My DPhil research, which primarily focussed on studying steroid receptor regulation in SCs, has enabled me to extend the existing parallels between prostate biology and *Drosophila* SC biology. The switch from a hormone-dependent to a hormone-independent steroid receptor signalling, which is key to the transition to CRPC, occurs as a physiological phenomenon in response to the reproductive stress of mating in SCs.

Although growth occurs via hypertrophy in SCs, unlike hyperplasia in prostate cancer, it is interesting to note that similar signalling mechanisms mediate growth in both these cases. Below are some of the important signalling parallels that previous DPhil students and I have established:

- Local synthesis of steroid hormone in both prostate and SCs (this thesis; Stuchbery et al., 2017)
- Different splice variants of the steroid receptor have unique roles in the regulation of hormone-dependent and hormone-independent growth (this thesis; Cao et al., 2016)
- BMP signalling mediates growth via regulating steroid receptor protein levels (this thesis in collaboration with Aaron Leiblich; Lee et al., 2013)
- BMP and EcR signalling regulate cell migration (Aaron Leiblich; Akashi et al., 2006; Darby et al., 2008)
- Autocrine BMP signalling (Siamak Redhai and Josephine Hellberg; Morrissey et al., 2010) regulates hormone-independent hormone receptor signalling (this thesis; G. T. Lee et al., 2014)
- Rb/Rbf and E2F/E2F1 mediate growth by regulating steroid receptor protein levels (Aaron Leiblich and Dhruv Sarma; A. Sharma et al., 2017)
- Cell cycle G1/S cyclins specifically promote hormone-dependent to hormone-independent steroid receptor signalling (this thesis; Petre et al., 2002)
- Loss of Rb/Rbf or overexpression of E2F/E2F1 promotes a switch to hormone-independent steroid receptor signalling (this thesis; A. Sharma et al., 2017)

- The FOXA1/fkh transcription factor specifically regulates a hormone-dependent form of steroid receptor signalling and has no effect on the hormone-independent form of signalling (this thesis; Zhao et al., 2014)
- RTK/torso signalling regulates both hormone-dependent and -independent hormone receptor signalling (this thesis; Brown et al., 2018)

Therefore, I believe that some of the fundamental mechanisms that regulate steroid receptor biology in the SCs and the prostate are conserved. As discussed in Section 1.6, there are several limitations associated with studying prostate cancer in mouse models, which primarily are associated with its different anatomical and morphological structure, and small size. Additionally, the existing mouse and cell-line models are developed from the artificial manipulation of certain oncogenes and tumour-suppressor genes or are derived from a single patient's sample, thereby not capturing the entirety of the various disease modalities. Although many prostate cancer cell lines are being used to study prostate cancer regulation, it is not clear whether most of the them mirror *in vivo* biology and signalling mechanisms. Hence, I propose that the *Drosophila* SC system could be utilised to further understand the fundamental cellular signalling mechanisms that might be involved in the regulation of prostate cancer biology.

Two models have been proposed to describe the development of CRPC - adaptation and selection (Zong and Goldstein 2013). Adaptation refers to the possibility when certain alterations, including mutations, allow the androgen-deprived cells to adapt to the tumour microenvironment. Selection refers to the possibility that multiple populations of cells might already be present, some of which are capable of surviving in a hormone-independent environment, and they could selectively proliferate to lead to the onset of

CRPC (Zong and Goldstein 2013). Since the transition from hormone-dependency to hormone-independency is a naturally occurring phenomenon in *Drosophila* SCs, it is possible that the progression of prostate cancer might not entirely be a pathological condition, but it might be triggered by a physiological response to the lack of androgenic steroids as a result of ADT. The fact that there are many routes by which CRPC can be established (Section 1.3) could be consistent with the idea that many of these routes represent the different physiological signals that control the switch to hormone-independence. I believe that studying this switch *in vivo* using SCs could further enhance our knowledge regarding the signalling cascades that lead to the induction of the hormone-refractory form of growth. Also, it is possible that this physiological switch might be induced during puberty in mammals, and its effects are intensified by persistent activation in CRPC. Perhaps mating might also regulate this hormone-independent signalling. This is a difficult hypothesis to test using humans, but it might be interesting to undertake a set of targeted experiments in this area using rodent models.

Due to the genetically tractable nature of studying molecular processes in *Drosophila*, the SC model can indeed be used to screen for candidate growth regulatory genes and also study the epistatic relationship between a select set of genes that regulate the transition to hormone-independency in mated males. With the recent development of a detailed protocol to isolate this rare population of SCs in order to successfully perform transcriptomics and RNA-seq (Immarigeon et al., 2019), it may be possible to use the *Drosophila* SC model to identify a group of regulatory genes and proteins that promote hormone-independent growth regulation in mated males, as well as some of their downstream targets. The EcR transcriptional target genes that are specifically expressed in SCs derived from multiply-mated males and which are not produced in SCs from virgin

males, could potentially lead us in the direction of determining important downstream targets of hormone-independent hormone receptor signalling. These experiments might not only shed light on genes or proteins that could be inhibited in CRPC therapies, but might also allow us to determine some prognostic biomarkers.

Although the *Drosophila* SC system could prove useful in understanding the cellular signalling events that might be involved in the progression of prostate cancer, this model does have some limitations associated with it. The AR signalling that occurs within the entire prostate gland is modelled within a subset of cells of the *Drosophila* AG. The *Drosophila* SC system can only be used to study some aspects of ethe selection and adaptation hypotheses for CRPC, and cannot easily be employed to resolve which of these mechanisms is important in prostate cancer. Also, cell-cell interaction in the context of prostate cancer and CRPC at a whole tumour level cannot be studied using the *Drosophila* SC model, and the EcR is not sufficiently similar to the AR to be used as a testbed for AR-targeting drugs.

In conclusion, the *Drosophila* SC model appears to offer a simple genetic system which can capture the signalling complexity of the transition of prostate cancer to CRPC. This system could be used as a preliminary model to disentangle the signalling cascades to develop more targeted hypotheses and research aims, both for prostate cancer and normal prostate biology, which could then be tested using prostate cancer cell-lines or mouse models.

7.5. *Drosophila* SCs as an *in vivo* model to study the maintenance of binucleation

A very interesting aspect of SCs is their binucleate nature. There have been a few studies trying to determine the functional significance of the binucleation state of the SCs and the MCs in the AG. As discussed before, there is speculation that binucleated cells result in increased morphological plasticity that is necessary for the shrinkage and expansion of the AG upon mating (Taniguchi et al., 2012, 2018). I have stumbled upon a surprising relationship between Rbf, E2F1 and p53 in the maintenance of binucleation in adult post-mitotic SCs. The effect on binucleation state in adult SCs by Rbf appears to be specifically linked to its phosphorylation status, as evidenced by the strong phenotypes induced when the non-phosphorylatable form is expressed.

A switch from mononucleated to binucleated cells or vice versa has been observed in cardiomyocytes of the heart, hepatocytes of the liver and alveolar epithelial cells of the mammary gland. These cells undergo the transition from mononucleate to binucleate cells upon stress such as developmental or injury-related stress in the case of cardiomyocytes, injury in hepatocytes or physiological changes promoting milk production in alveolar cells (Grizzi and Chiriva-Internati 2007; Rios et al., 2016; Windmueller et al., 2020). As mentioned in Section 6.4.1, Windmueller and colleagues have recently shown that the mononucleate and binucleate cells are transcriptionally distinct and binucleation occurs due to inhibition of E2F target genes. Although the authors suggest that Rb is not necessary for the induction of binucleation, they did not study the effect of the available Rb mutants that have a combination of mutated phosphorylation sites. It would be interesting to test the commercially available set of Rb phosphorylation mutants developed by the Dowdy lab in a cell line which has a mixture of binucleate and

mononucleate cells (Refer Appendix B for a possible list of cell lines that could be used). These latter researchers have developed a series of Rb phosphorylation mutant plasmids that have a single mutated phosphorylation site or multiple combinations of mutated sites (Narasimha et al., 2014). It is important to note that my studies have suggested that some effects of Rbf in SCs are independent of E2F1, and it is possible that these actions also play a role in establishing the mononucleation/binucleation balance.

Another interesting and even more surprising result observed with respect to this phenomenon is that expression of Rbf^{CA} in the MCs did not have any effect on the MCs but promoted SC mononucleation. Furthermore, these mononucleate SCs continue to be able to endoreplicate, thereby ruling out the possibility that Rbf^{CA} is transferred to the SCs where it blocks EcR signalling, and suggesting a role for cell-cell signalling via another pathway. Therefore, in order to better understand the basis of this mononucleation phenotype, it will be necessary to understand the signal that is transmitted to the SCs. It would be interesting to sequence the RNA from AGs expressing Rbf^{CA} in the MCs and compare it with the controls. Since there are close to 1000 MCs, unlike the SCs, it is possible that we would pick up differentially regulated genes that encode secreted proteins that promote mononucleation in the SCs. As mentioned in Section 6.4.1, I have preliminary data which might suggest that this mononucleation phenotype can be reversed when Rbf^{CA} expression is stopped. Since a reversible change between mononucleated and binucleated cells is implicated in tissue regeneration in other tissues of clinical relevance, I believe the *Drosophila* SC model could be used to determine a plausible set of candidate genes that might play a vital role in regulating this process.

7.5 Concluding Remarks

The work presented in this Dissertation tells a story about how I have built upon existing studies and developed the *Drosophila* SC as a model for studying some aspects of the genetic pathway leading to progression of prostate cancer. During this journey I also stumbled upon interesting aspects of SC biology, some of which I have discussed in the main text of the results chapter. In Appendix D, I have included some initial exploratory work that highlights the idiosyncratic nature of these SCs and could inspire potential future studies in SC research. Apart from just developing the SCs as a model for studying prostate cancer or reversible mononucleation, I have also been able to contribute towards understanding basic physiological mechanisms and their functions in the SCs, as well as secretory processes in MCs, such as the recent discovery of Sex Peptide-carrying microcarriers, which may be affected by SC secretion (Wainwright et al., 2020). Although there are many aspects of SC biology that we do not completely understand today, I believe that one day my work and all the other pieces of cell biological information will come together to form an exciting, integrated story, explaining how hormone signalling controls the growth and secretory activity of the entire accessory gland and its complex reproductive signalling functions.

Chapter-8:

Bibliography

Akashi, T., Koizumi, K., Nagakawa, O., Fuse, H., Saiki, I. (2006). Androgen receptor negatively influences the expression of chemokine receptors (CXCR4, CCR1) and ligand-mediated migration in prostate cancer DU-145. *Oncology Reports*, *16*(4), 831–836. https://doi.org/10.3892/or.16.4.831

Anderson, C. A., Eser, U., Korndorf, T., Borsuk, M. E., Skotheim, J. M., Gladfelter, A. S. (2013). Nuclear repulsion enables division autonomy in a single cytoplasm. *Current Biology*, *23*(20), 1999–2010. https://doi.org/10.1016/j.cub.2013.07.076

Ashburner, M. (1990). Puffs, genes, and hormones revisited. *Cell*. Cell Press. https://doi.org/10.1016/0092-8674(90)90205-S

Balk, S. P., Knudsen, K. E. (2008). AR, the cell cycle, and prostate cancer. *Nuclear Receptor Signaling*. SAGE PublicationsSage CA: Los Angeles, CA. https://doi.org/10.1621/nrs.06001

Baumann, H. (1974). The isolation, partial characterization, and biosynthesis of the paragonial substances, PS-1 and PS-2, of Drosophila funebris. *Journal of Insect Physiology*, *20*(11), 2181–2194. https://doi.org/10.1016/0022-1910(74)90043-2

Berni, J., Muldal, A. M., Pulver, S. R. (2010). Using neurogenetics and the warmth-gated ion channel TRPA1 to study the neural basis of behavior in Drosophila. *Journal of Undergraduate Neuroscience Education*, *9*(1), 5–14.

Bertram, M. J., Akerkar, G. A., Ard, R. L., Gonzalez, C., Wolfner, M. F. (1992). Cell type-specific gene expression in the Drosophila melanogaster male accessory gland. *Mechanisms of Development*, *38*(1), 33–40. https://doi.org/10.1016/0925-4773(92)90036-J

Bertram, M. J., Neubaum, D. M., Wolfner, M. F. (1996). Localization of the Drosophila male accessory gland protein Acp36DE in the mated female suggests a role in sperm storage. *Insect Biochemistry and Molecular Biology*, *26*(8–9), 971–980. https://doi.org/10.1016/S0965-1748(96)00064-1

Bindels, E. M. J., Lallemand, F., Balkenende, A., Verwoerd, D., Michalides, R. (2002). Involvement of G1/S cyclins in estrogen-independent proliferation of estrogen receptor-positive breast cancer cells. *Oncogene*, *21*(53), 8158–8165. https://doi.org/10.1038/sj.onc.1206012

Bownes, M., Dübendorfer, A., Smith, T. (1984). Ecdysteroids in adult males and females of Drosophila melanogaster. *Journal of Insect Physiology*, *30*(10), 823–830. https://doi.org/10.1016/0022-1910(84)90019-2

Box, A., Church, S. J., Hayes, D., Nandakumar, S., Taichman, R., Buttitta, L. (2019). Endocycles support tissue growth and regeneration of the adult Drosophila accessory gland. *BioRxiv*, 719013. https://doi.org/10.1101/719013

Bragdon, B., Moseychuk, O., Saldanha, S., King, D., Julian, J., Nohe, A. (2011). Bone Morphogenetic Proteins: A critical review. *Cellular Signalling*. https://doi.org/10.1016/j.cellsig.2010.10.003

Bretman, A., Fricke, C., Chapman, T. (2009). Plastic responses of male Drosophila melanogaster to the level of spermcompetition increase male reproductive fitness. *Proceedings of the Royal Society B: Biological Sciences*, *276*(1662), 1705–1711. https://doi.org/10.1098/rspb.2008.1878

Bretman, A., Westmancoat, J. D., Gage, M. J. G., Chapman, T. (2013). Costs and benefits of lifetime exposure to mating rivals in male drosophila melanogaster. *Evolution*, *67*(8), 2413–2422. https://doi.org/10.1111/evo.12125

Brown, N. E., Paluch, A. M., Nashu, M. A., Komurov, K., Waltz, S. E. (2018). Tumor Cell

Autonomous RON Receptor Expression Promotes Prostate Cancer Growth Under Conditions of Androgen Deprivation. *Neoplasia (United States)*, *20*(9), 917–929. https://doi.org/10.1016/j.neo.2018.07.003

Brummel, T. J., Twombly, V., Marqués, G., Wrana, J. L., Newfeld, S. J., Attisano, L., Massagué, J., O'Connor, M. B., Gelbart, W. M. (1994). Characterization and relationship of dpp receptors encoded by the saxophone and thick veins genes in Drosophila. *Cell*, *78*(2), 251–261. https://doi.org/10.1016/0092-8674(94)90295-X

Calvi, B. R., Lilly, M. A., Spradling, A. C. (1998). Cell cycle control of chorion gene amplification. *Genes and Development*, *12*(5), 734–744. https://doi.org/10.1101/gad.12.5.734

Cao, S., Zhan, Y., Dong, Y. (2016). Emerging data on androgen receptor splice variants in prostate cancer. *Endocrine-Related Cancer*. BioScientifica Ltd. https://doi.org/10.1530/ERC-16-0298

Chandrasekar, T., Yang, J. C., Gao, A. C., Evans, C. P. (2015). Mechanisms of resistance in castration-resistant prostate cancer (CRPC). *Translational Andrology and Urology*, *4*(3), 365–380. https://doi.org/10.3978/j.issn.2223-4683.2015.05.02

Chapman, T., Bangham, J., Vinti, G., Seifried, B., Lung, O., Wolfner, M. F., Smith, K.H., Partridge, L. (2003). The sex peptide of Drosophila melanogaster: Female post-mating responses analyzed by using RNA interference. *Proceedings of the National Academy of Sciences of the United States of America*, *100*(17), 9923–9928. https://doi.org/10.1073/pnas.1631635100

Che, Y., Shi, X., Shi, Y., Jiang, X., Ai, Q., Shi, Y., Fengyan, G., Jiang, W. (2019). Exosomes Derived from miR-143-Overexpressing MSCs Inhibit Cell Migration and Invasion in Human Prostate Cancer by Downregulating TFF3. *Molecular Therapy - Nucleic Acids*, *18*, 232–244. https://doi.org/10.1016/j.omtn.2019.08.010

Chen, S., Wang, S., Xie, T. (2011). Restricting self-renewal signals within the stem cell niche: Multiple levels of control. *Current Opinion in Genetics and Development*. Elsevier Current Trends. https://doi.org/10.1016/j.gde.2011.07.008

Cherbas, L., Hu, X., Zhimulev, I., Belyaeva, E., Cherbas, P. (2003). EcR isoforms in Drosophila: testing tissue-specific requirements by targeted blockade and rescue. *Development*, *130*(2), 271–284. https://doi.org/10.1242/dev.00205

Claudius, A. K., Romani, P., Lamkemeyer, T., Jindra, M., Uhlirova, M. (2014). Unexpected Role of the Steroid-Deficiency Protein Ecdysoneless in Pre-mRNA Splicing. *PLoS Genetics*, *10*(4), e1004287. https://doi.org/10.1371/journal.pgen.1004287

Corrigan, L., Redhai, S., Leiblich, A., Fan, S. J., Perera, S. M. W., Patel, R., Gandy, C., Wainwright, S. M., Morris, J. F., Hamdy, F., Goberdhan, D. C. I., Wilson, C. (2014). BMP-regulated exosomes from Drosophila male reproductive glands reprogram female behavior. *Journal of Cell Biology*, *206*(5), 671–688. https://doi.org/10.1083/jcb.201401072

Costantino, B. F. B., Bricker, D. K., Alexandre, K., Shen, K., Merriam, J. R., Antoniewski, C., Callendar, J. L., Henrich, V. C., Presente, A., Andres, A. J. (2008). A novel ecdysone receptor mediates steroid-regulated developmental events during the mid-third instar of Drosophila. *PLoS Genetics*, *4*(6). https://doi.org/10.1371/journal.pgen.1000102

Costello, L. C., Franklin, R. B. (2016). A comprehensive review of the role of zinc in normal prostate function and metabolism; and its implications in prostate cancer. *Archives of Biochemistry and Biophysics*, *611*, 100–112. https://doi.org/10.1016/j.abb.2016.04.014

Cutler, A. A., Jackson, J. B., Corbett, A. H., Pavlath, G. K. (2018). Non-equivalence of nuclear import among nuclei in multinucleated skeletal muscle cells. *Journal of Cell Science*, *131*(3). https://doi.org/10.1242/jcs.207670

Dai, C., Heemers, H., Sharifi, N. (2017). Androgen signaling in prostate cancer. *Cold*

Spring Harbor Perspectives in Medicine, *7*(9). https://doi.org/10.1101/cshperspect.a030452

Dar, G. H., Mendes, C. C., Kuan, W-L., Conceição, M., El-Andaloussi, S., Mager, I., Roberts, T. C., Barker, R. A., Goberdhan, D. C. I., Wilson, C., Wood, M. J. (2020). GAPDH controls extracellular vesicle biogenesis and enhances therapeutic potential of EVs in silencing the Huntingtin gene in mice via siRNA delivery. *BioRxiv*: 899880. https://doi.org/10.1101/2020.01.09.899880

Darby, S., Cross, S. S., Brown, N. J., Hamdy, F. C., Robson, C. N. (2008). BMP-6 over-expression in prostate cancer is associated with increased Id-1 protein and a more invasive phenotype. *Journal of Pathology*, *214*(3), 394–404. https://doi.org/10.1002/path.2292

Datar, S. A., Jacobs, H. W., De La Cruz, A. F. A., Lehner, C. F., Edgar, B. A. (2000). The Drosophila Cyclin D-Cdk4 complex promotes cellular growth. *EMBO Journal*, *19*(17), 4543–4554. https://doi.org/10.1093/emboj/19.17.4543

de Cuevas, M., Matunis, E. L. (2011). The stem cell niche: Lessons from the Drosophila testis. *Development*, *138*(14), 2861–2869. https://doi.org/10.1242/dev.056242

de Veylder, L., Larkin, J. C., Schnittger, A. (2011). Molecular control and function of endoreplication in development and physiology. *Trends in Plant Science*. Elsevier Current Trends. https://doi.org/10.1016/j.tplants.2011.07.001

Dick, F. A., Rubin, S. M. (2013). Molecular mechanisms underlying RB protein function. *Nature Reviews Molecular Cell Biology*. NIH Public Access. https://doi.org/10.1038/nrm3567

Dikeakos, J. D., Lello, P. Di, Lacombe, M. J., Ghirlando, R., Legault, P., Reudelhuber, T. L., Omichinski, J. G. (2009). Functional and structural characterization of a dense core secretory granule sorting domain from the PC1/3 protease. *Proceedings of the National Academy of Sciences of the United States of America*, *106*(18), 7408–7413. https://doi.org/10.1073/pnas.0809576106

Douglas, T., Anderson, R., Saltz, J. B. (2020). Limits to male reproductive potential across mating bouts in Drosophila melanogaster. *Animal Behaviour*, *160*, 25–33. https://doi.org/10.1016/j.anbehav.2019.11.009

Edgar, B. A., Orr-Weaver, T. L. (2001). Endoreplication cell cycles: More for less. *Cell*. Cell Press. https://doi.org/10.1016/S0092-8674(01)00334-8

Edgar, B. A., Zielke, N., Gutierrez, C. (2014). Endocycles: A recurrent evolutionary innovation for post-mitotic cell growth. *Nature Reviews Molecular Cell Biology*, *15*(3), 197–210. https://doi.org/10.1038/nrm3756

Fan, S., Kroeger, B., Marie, P. P., Bridges, E. M., Mason, J. D., McCormick, K., Zois, C. E., Sheldon, H., Alham, K. H., Johnson, E., Ellis, M., Stefana, M. I., Mendes, C. M., Wainwright, S. M., Cunnigham, C., Hamdy, F. C., Morris, J. F., Harris, A. L., Wilson, C., Goberdhan, D. C. (2020). Glutamine deprivation alters the origin and function of cancer cell exosomes. *The EMBO Journal*. https://doi.org/10.15252/embj.2019103009

Foster, J S, Wimalasena, J. (1996). Estrogen regulates activity of cyclin-dependent kinases and retinoblastoma protein phosphorylation in breast cancer cells. *Molecular Endocrinology*, *10*(5), 488–498. https://doi.org/10.1210/mend.10.5.8732680

Foster, James S., Henley, D. C., Ahamed, S., Wimalasena, J. (2001). Estrogens and cell-cycle regulation in breast cancer. *Trends in Endocrinology and Metabolism*. Elsevier Current Trends. https://doi.org/10.1016/S1043-2760(01)00436-2

Fujita, K., Nonomura, N. (2019). Role of androgen receptor in prostate cancer: A review. *World Journal of Men's Health*. Korean Society for Sexual Medicine and Andrology (KAMJE). https://doi.org/10.5534/wjmh.180040

Gangoda, L., Boukouris, S., Liem, M., Kalra, H., Mathivanan, S. (2015). Extracellular vesicles including exosomes are mediators of signal transduction: Are they protective or pathogenic? *Proteomics*. Wiley-VCH Verlag.

https://doi.org/10.1002/pmic.201400234
Garen, A., Kauvar, L., Lepesant, J-A. (1977). Roles of ecdysone in Drosophila development (steroid hormone/temperature-sensitive mutants). *Genetics*, *74*(11), 5099–5103. https://doi.org/10.1073/pnas.74.11.5099
Giacinti, C., Giordano, A. (2006). RB and cell cycle progression. *Oncogene*, *25*(38), 5220. https://doi.org/10.1038/sj.onc.1209615
Gligorov, D., Sitnik, J. L., Maeda, R. K., Wolfner, M. F., Karch, F. (2013). A Novel Function for the Hox Gene Abd-B in the Male Accessory Gland Regulates the Long-Term Female Post-Mating Response in Drosophila. *PLoS Genetics*, *9*(3). https://doi.org/10.1371/journal.pgen.1003395
Grabowska, M. M., Degraff, D. J., Yu, X., Jin, R. J., Chen, Z., Borowsky, A. D., Matusik, R. J. (2014). Mouse models of prostate cancer: Picking the best model for the question. *Cancer and Metastasis Reviews*. Kluwer Academic Publishers. https://doi.org/10.1007/s10555-013-9487-8
Gradilla, A. C., Mansilla, A., Ferrús, A. (2011). Isoform-specific regulation of a steroid hormone nuclear receptor by an E3 ubiquitin ligase in Drosophila melanogaster. *Genetics*, *189*(3), 871–883. https://doi.org/10.1534/genetics.111.132191
Grizzi, F., Chiriva-Internati, M. (2007). Human binucleate hepatocytes: Are they a defence during chronic liver diseases? *Medical Hypotheses*, *69*(2), 258–261. https://doi.org/10.1016/j.mehy.2006.12.029
Hamaratoglu, F., Affolter, M., Pyrowolakis, G. (2014). Dpp/BMP signaling in flies: From molecules to biology. *Seminars in Cell and Developmental Biology*. Elsevier Ltd. https://doi.org/10.1016/j.semcdb.2014.04.036
Hamdy, F. C., Autzen, P., Robinson, M. C., Horne, C. H., Neal, D. E., Robson, C. N. (1997). Immunolocalization and messenger RNA expression of bone morphogenetic protein-6 in human benign and malignant prostatic tissue. *Cancer Research*, *57*(19), 4427–4431. Retrieved from http://www.ncbi.nlm.nih.gov/pubmed/9331107
Harbour, J. W., Dean, D. C. (2000). The Rb/E2F pathway: Expanding roles and emerging paradigms. *Genes and Development*. Cold Spring Harbor Laboratory Press. https://doi.org/10.1101/gad.813200
Hazelrigg, T., Levis, R., Rubin, G. M. (1984). Transformation of white locus DNA in Drosophila: Dosage compensation, zeste interaction, and position effects. *Cell*, *36*(2), 469–481. https://doi.org/10.1016/0092-8674(84)90240-X
Heinlein, C. A., Chang, C. (2004). Androgen Receptor in Prostate Cancer. *Endocrine Reviews*, *25*(2), 276–308. Retrieved from http://dx.doi.org/10.1210/er.2002-0032
Hellberg, J. E. E. U. (2018). *Sex, signalling, and steroids: regulation of nuclear size and intracellular trafficking in secondary cells in the D. melanogaster male accessory gland*. University of Oxford.
Henry, G. H., Malewska, A., Joseph, D. B., Malladi, V. S., Lee, J., Torrealba, J., Muak, J. R., Gahan, J. C., Raj, G. V., Roehrborn, C. G., Hon, G. C., MacConmara, M. P., Reese, J. C., Hutchinson, R. C., Vezina, C. M., Strand, D. W. (2018). A Cellular Anatomy of the Normal Adult Human Prostate and Prostatic Urethra. *Cell Reports*, *25*(12), 3530-3542.e5. https://doi.org/10.1016/j.celrep.2018.11.086
Hentze, J. L., Moeller, M. E., Jørgensen, A. F., Bengtsson, M. S., Bordoy, A. M., Warren, J. T., Gilbert, L. I., Anderson, O., Rewitz, K. F. (2013). Accessory Gland as a Site for Prothoracicotropic Hormone Controlled Ecdysone Synthesis in Adult Male Insects. *PLoS ONE*, *8*(2). https://doi.org/10.1371/journal.pone.0055131
Herndon, L. A., Chapman, T., Kalb, J. M., Lewin, S., Partridge, L., Wolfner, M. F. (1997). Mating and hormonal triggers regulate accessory gland gene expression in male Drosophila. *Journal of Insect Physiology*, *43*(12), 1117–1123. https://doi.org/10.1016/S0022-1910(97)00062-0
Hill, S. M. (1998,). Receptor crosstalk: Communication through cell signaling pathways.

Anatomical Record. John Wiley Sons, Ltd. https://doi.org/10.1002/(SICI)1097-0185(199804)253:2<42::AID-AR7>3.0.CO;2-G
Hopkins, B. R., Sepil, I., Bonham, S., Miller, T., Charles, P. D., Fischer, R., Kessler, B. M., Wilson, C., Wigby, S. (2019). BMP signaling inhibition in Drosophila secondary cells remodels the seminal proteome and self and rival ejaculate functions. *Proceedings of the National Academy of Sciences of the United States of America*, *116*(49), 24719–24728. https://doi.org/10.1073/pnas.1914491116
Huang, Y., Jiang, X., Liang, X., Jiang, G. (2018). Molecular and cellular mechanisms of castration resistant prostate cancer. *Oncology Letters*. Spandidos Publications. https://doi.org/10.3892/ol.2018.8123
Hübner, A., Mulholland, D. J., Standen, C. L., Karasarides, M., Cavanagh-Kyros, J., Barrett, T., Chi, H., Greiner, D. L., Tournier, C., Sawyers, C. L., Flavell, R. A., Wu, H., Davis, R. J. (2012). JNK and PTEN cooperatively control the development of invasive adenocarcinoma of the prostate. *Proceedings of the National Academy of Sciences of the United States of America*, *109*(30), 12046–12051. https://doi.org/10.1073/pnas.1209660109
Huggins, C., Hodges, C. V. (1941). Studies on Prostatic Cancer. I. The Effect of Castration, of Estrogen and of Androgen Injection on Serum Phosphatases in Metastatic Carcinoma of the Prostate. *Cancer Research*, *1*(4), 293 LP – 297. Retrieved from http://cancerres.aacrjournals.org/content/1/4/293.abstract
Immarigeon, C., Karch, F., Maeda, R. K. (2019). A FACS-based protocol to isolate RNA from the secondary cells of drosophila male accessory glands. *Journal of Visualized Experiments*, *2019*(151), e60218. https://doi.org/10.3791/60218
Ishimoto, H., Kitamoto, T. (2010). The steroid molting hormone ecdysone regulates sleep in adult Drosophila melanogaster. *Genetics*, *185*(1), 269–281. https://doi.org/10.1534/genetics.110.114587
Ishimoto, H., Sakai, T., Kitamoto, T. (2009). Ecdysone signaling regulates the formation of long-term courtship memory in adult Drosophila melanogaster. *Proceedings of the National Academy of Sciences of the United States of America*, *106*(15), 6381–6386. https://doi.org/10.1073/pnas.0810213106
Jiang, H., Patel, P. H., Kohlmaier, A., Grenley, M. O., McEwen, D. G., Edgar, B. A. (2009). Cytokine/Jak/Stat Signaling Mediates Regeneration and Homeostasis in the Drosophila Midgut. *Cell*, *137*(7), 1343–1355. https://doi.org/10.1016/j.cell.2009.05.014
King-Jones, K., Thummel, C. S. (2005). Nuclear receptors - A perspective from Drosophila. *Nature Reviews Genetics*, *6*(4), 311–323. https://doi.org/10.1038/nrg1581
Kishigami, S., Mishina, Y. (2005). BMP signaling and early embryonic patterning. *Cytokine and Growth Factor Reviews*, *16*(3 SPEC. ISS.), 265–278. https://doi.org/10.1016/j.cytogfr.2005.04.002
Koryakina, Y., Ta, H. Q., Gioeli, D. (2014). Androgen receptor phosphorylation: Biological context and functional consequences. *Endocrine-Related Cancer*. BioScientifica Ltd. https://doi.org/10.1530/ERC-13-0472
Kroeger, B. R. (2017). *The genetic regulation and subcellular dynamics of secretory and endolysosomal organelles of Drosophila secondary cells.* University of Oxford.
Kumar, V. L., Majumder, P. K. (1995). Prostate gland: Structure, functions and regulation. *International Urology and Nephrology*, *27*(3), 231–243. https://doi.org/10.1007/BF02564756
Lanzi, C., Cassinelli, G., Cuccuru, G., Supino, R., Zuco, V., Ferlini, C., Scambia, G., Zunino, F. (2001). Cell cycle checkpoint efficiency and cellular response to paclitaxel in prostate cancer cells. *The Prostate*, *48*(4), 254–264. https://doi.org/10.1002/pros.1105
Le, T., Liang, Z., Patel, H., Yu, M. H., Sivasubramaniam, G., Slovitt, M., Tanetzapf, G.,

Mohanty, N., Paul, S. M., Wu, V. M., Beitel, G. J. (2006). A new family of Drosophila balancer chromosomes with a w- dfd-GMR yellow fluorescent protein marker. *Genetics*, *174*(4), 2255–2257. https://doi.org/10.1534/genetics.106.063461

Lee, G. T., Kang, D. I., Ha, Y. S., Jung, Y. S., Chung, J., Min, K., Kim, T. H., Moon, K. H., Chung, J. M., Lee, D. H., Kim, W-J., Kim, I. Y. (2014). Prostate cancer bone metastases acquire resistance to androgen deprivation via WNT5A-mediated BMP-6 induction. *British Journal of Cancer*, *110*(6), 1634–1644. https://doi.org/10.1038/bjc.2014.23

Lee, Geun Taek, Jung, Y. S., Ha, Y. S., Kim, J. H., Kim, W. J., Kim, I. Y. (2013). Bone morphogenetic protein-6 induces castration resistance in prostate cancer cells through tumor infiltrating macrophages. *Cancer Science*, *104*(8), 1027–1032. https://doi.org/10.1111/cas.12206

Leiblich, A. (2015). *Cell biology and genetic regulation of secondary cells in the Drosophila accessory gland*. University of Oxford.

Leiblich, A., Hellberg, J. E. E. U., Sekar, A., Gandy, C., Mendes, C. C., Redhai, S., Mason, J., Waiwright, M., Marie, P., Goberdhan, D. C. I., Wilson, C. (2019). Mating induces switch from hormone-dependent to hormone-independent steroid receptor–mediated growth in Drosophila secondary cells. *PLoS Biology*, *17*(10), e3000145. https://doi.org/10.1371/journal.pbio.3000145

Leiblich, A., Marsden, L., Gandy, C., Corrigan, L., Jenkins, R., Hamdy, F., Wilson, C. (2012). Bone morphogenetic protein- and mating-dependent secretory cell growth and migration in the Drosophila accessory gland. *PNAS*, *109*(47), 19292–19297. https://doi.org/10.1073/pnas.1214517109.

Lezzi, M., Bergman, T., Mouillet, J. F., Henrich, V. C. (1999). The ecdysone receptor puzzle. *Archives of Insect Biochemistry and Physiology*, *41*(2), 99–106. https://doi.org/10.1002/(SICI)1520-6327(1999)41:2<99::AID-ARCH6>3.0.CO;2-W

Li, Hao, Harrison, D., Jones, G., Jones, D., Cooper, R. L. (2001). Alterations in development, behavior, and physiology in Drosophila larva that have reduced ecdysone production. *Journal of Neurophysiology*, *85*(1), 98–104. https://doi.org/10.1152/jn.2001.85.1.98

Li, Hongjie, Qi, Y., Jasper, H. (2013). Dpp Signaling Determines Regional Stem Cell Identity in the Regenerating Adult Drosophila Gastrointestinal Tract. *Cell Reports*, *4*(1), 10–18. https://doi.org/10.1016/j.celrep.2013.05.040

Liu, H., Kubli, E. (2003). Sex-peptide is the molecular basis of the sperm effect in Drosophila melanogaster. *Proceedings of the National Academy of Sciences of the United States of America*, *100*(17), 9929–9933. https://doi.org/10.1073/pnas.1631700100

Longworth, M. S., Herr, A., Ji, J. Y., Dyson, N. J. (2008). RBF1 promotes chromatin condensation through a conserved interaction with the Condensin II protein dCAP-D3. *Genes and Development*, *22*(8), 1011–1024. https://doi.org/10.1101/gad.1631508

Lorenzo, P. I., Saatcioglu, F. (2008). Inhibition of apoptosis in prostate cancer cells by androgens is mediated through downregulation of c-Jun N-terminal kinase activation. *Neoplasia*, *10*(5), 418–428. https://doi.org/10.1593/neo.07985

Luga, V., Zhang, L., Viloria-Petit, A. M., Ogunjimi, A. A., Inanlou, M. R., Chiu, E., Buchanan, M., Hosein, A. N., Basik, M., Wrana, J. L. (2012). Exosomes mediate stromal mobilization of autocrine Wnt-PCP signaling in breast cancer cell migration. *Cell*, *151*(7), 1542–1556. https://doi.org/10.1016/j.cell.2012.11.024

Lynch, J. A., Roth, S. (2011). The evolution of dorsal-ventral patterning mechanisms in insects. *Genes and Development*. Cold Spring Harbor Laboratory Press. https://doi.org/10.1101/gad.2010711

Maddison, L. A., Sutherland, B. W., Barrios, R. J., Greenberg, N. M. (2004). Conditional deletion of Rb causes early stage prostate cancer. *Cancer Research*, *64*(17), 6018–

6025. https://doi.org/10.1158/0008-5472.CAN-03-2509
Mansilla, A., Martín, F. A., Martín, D., Ferrús, A. (2016). Ligand-independent requirements of steroid receptors EcR and USP for cell survival. *Cell Death Differentiation*, *23*(3), 405–416. https://doi.org/10.1038/cdd.2015.108
Marie, P. P., Fan, S.-J., Mendes, C. C., Wainwright, S. M., Harris, A. L., Goberdhan, D. C. I., Wilson, C. (2020). Accessory proteins selectively regulate Rab11-exosome biogenesis in Drosophila secondary cells. *BioRxiv*. https://doi.org/10.1101/2020.06.18.158725
Mittal, K., Donthamsetty, S., Kaur, R., Yang, C., Gupta, M. V., Reid, M. D., Choi, D. H., Rida, P. C. G., Aneja, R. (2017). Multinucleated polyploidy drives resistance to Docetaxel chemotherapy in prostate cancer. *British Journal of Cancer*, *116*(9), 1186–1194. https://doi.org/10.1038/bjc.2017.78
Moon, D. O., Choi, Y. H., Kim, G. Y. (2011). Role of p21 in SP600125-induced cell cycle arrest, endoreduplication, and apoptosis. *Cellular and Molecular Life Sciences*, *68*(19), 3249–3260. https://doi.org/10.1007/s00018-011-0626-5
Morrissey, C., Brown, L. G., Pitts, T. E. M., Vessella, R. L., Corey, E. (2010). Bone morphogenetic protein 7 is expressed in prostate cancer metastases and its effects on prostate tumor cells depend on cell phenotype and the tumor microenvironment. *Neoplasia*, *12*(2), 192–205. https://doi.org/10.1593/neo.91836
Mouillet, J. F., Henrich, V. C., Lezzi, M., Vögtli, M. (2001). Differential control of gene activity by isoforms A, B1 and B2 of the Drosophila ecdysone receptor. *European Journal of Biochemistry*, *268*(6), 1811–1819. https://doi.org/10.1046/j.1432-1327.2001.02051.x
Mykles, D. L. (2011). Ecdysteroid metabolism in crustaceans. *Journal of Steroid Biochemistry and Molecular Biology*. Pergamon. https://doi.org/10.1016/j.jsbmb.2010.09.001
Namekawa, T., Ikeda, K., Horie-Inoue, K., Inoue, S. (2019). Application of Prostate Cancer Models for Preclinical Study: Advantages and Limitations of Cell Lines, Patient-Derived Xenografts, and Three-Dimensional Culture of Patient-Derived Cells. *Cells*, *8*(1), 74. https://doi.org/10.3390/cells8010074
Narasimha, A. M., Kaulich, M., Shapiro, G. S., Choi, Y. J., Sicinski, P., Dowdy, S. F. (2014). Cyclin D activates the Rb tumor suppressor by mono-phosphorylation. *ELife*, *2014*(3). https://doi.org/10.7554/eLife.02872.001
Nellen, D., Burke, R., Struhl, G., Basler, K. (1996). Direct and long-range action of a DPP morphogen gradient. *Cell*, *85*(3), 357–368. https://doi.org/10.1016/S0092-8674(00)81114-9
Niwa, R., Niwa, Y. S. (2014). Enzymes for ecdysteroid biosynthesis: Their biological functions in insects and beyond. *Bioscience, Biotechnology and Biochemistry*. Japan Society for Bioscience Biotechnology and Agrochemistry. https://doi.org/10.1080/09168451.2014.942250
Orr-Weaver, T. L. (2015). When bigger is better: The role of polyploidy in organogenesis. *Trends in Genetics*, *31*(6), 307–315. https://doi.org/10.1016/j.tig.2015.03.011
Pankotai, T., Popescu, C., Martin, D., Grau, B., Zsindely, N., Bodai, L., … Boros, I. (2010). Genes of the Ecdysone Biosynthesis Pathway Are Regulated by the dATAC Histone Acetyltransferase Complex in Drosophila. *Molecular and Cellular Biology*, *30*(17), 4254–4266. https://doi.org/10.1128/mcb.00142-10
Pasnuri, N., Khuntia, P., Mazumder, A. (2018). Single transcript imaging to assay gene expression in wholemount Drosophila melanogaster tissues. *Mechanisms of Development*, *153*, 10–16. https://doi.org/10.1016/j.mod.2018.08.006
Petre, C. E., Wetherill, Y. B., Danielsen, M., Knudsen, K. E. (2002). Cyclin D1: Mechanism and consequence of androgen receptor co-repressor activity. *Journal of Biological Chemistry*, *277*(3), 2207–2215. https://doi.org/10.1074/jbc.M106399200

Pippione, A. C., Boschi, D., Pors, K., Oliaro-Bosso, S., Lolli, M. L. (2017). Androgen-AR axis in primary and metastatic prostate cancer: chasing steroidogenic enzymes for therapeutic intervention. *Journal of Cancer Metastasis and Treatment*, *3*(12), 328. https://doi.org/10.20517/2394-4722.2017.44

Prince, E., Kroeger, B., Gligorov, D., Wilson, C., Eaton, S., Karch, F., Brankatschk, M., Maeda, R. K. (2019). Rab-mediated trafficking in the secondary cells of Drosophila male accessory glands and its role in fecundity. *Traffic*, *20*(2), 137–151. https://doi.org/10.1111/tra.12622

Prostasomes as Diagnostic Tool for Prostate Cancer Detection. (2018). https://clinicaltrials.gov/ct2/show/study/NCT03694483

Raftery, L. A., Umulis, D. M. (2012). Regulation of BMP activity and range in Drosophila wing development. *Current Opinion in Cell Biology*. NIH Public Access. https://doi.org/10.1016/j.ceb.2011.11.004

Ravi Ram, K., Wolfner, M. F. (2007). Seminal influences: Drosophila Acps and the molecular interplay between males and females during reproduction. *Integrative and Comparative Biology*, *47*(3), 427–445. https://doi.org/10.1093/icb/icm046

Ravi Ram, K., Wolfner, M. F. (2009). A network of interactions among seminal proteins underlies the long-term postmating response in Drosophila. *Proceedings of the National Academy of Sciences of the United States of America*, *106*(36), 15384–15389. https://doi.org/10.1073/pnas.0902923106

Rea, D., Vecchio, V. del, Palma, G., Barbieri, A., Falco, M., Luciano, A., Biase, D. D., Perdonà, S., Facchini, G., Arra, C. (2016). Mouse Models in Prostate Cancer Translational Research: From Xenograft to PDX. *BioMed Research International*, *2016*. https://doi.org/10.1155/2016/9750795

Redfern, C. P., Bownes, M. (1983). Pleiotropic effects of the "ecdysoneless-1" mutation of Drosophila melanogaster. *MGG Molecular General Genetics*, *189*(3), 432–440. https://doi.org/10.1007/BF00325905

Redhai, S., Hellberg, J. E. E. U., Wainwright, M., Perera, S. W., Castellanos, F., Kroeger, B., Gandy, C., Leiblich, A., Corrigan, L., Hilton, T., Patel, B., Fan, S-J., Hamdy, F., Goberdhan, D. C. I., Wilson, C. (2016). Regulation of Dense-Core Granule Replenishment by Autocrine BMP Signalling in Drosophila Secondary Cells. *PLoS Genetics*, *12*(10), 1–32. https://doi.org/10.1371/journal.pgen.1006366

Reutens, A. T., Fu, M., Wang, C., Albanese, C., McPhaul, M. J., Sun, Z., Balk, S. P., Jänne, O. A. Palvimo, J. J., Pestell, R. G. (2001). Cyclin D1 binds the androgen receptor and regulates hormone-dependent signaling in a p300/CBP-associated factor (P/CAF)-dependent manner. *Molecular Endocrinology*, *15*(5), 797–811. https://doi.org/10.1210/mend.15.5.0641

Rios, A. C., Fu, N. Y., Jamieson, P. R., Pal, B., Whitehead, L., Nicholas, K. R., Lindeman, G. J., Visvader, J. E. (2016). Essential role for a novel population of binucleated mammary epithelial cells in lactation. *Nature Communications*, *7*(1), 1–12. https://doi.org/10.1038/ncomms11400

Roberts, S. E., Gladfelter, A. S. (2015). Nuclear autonomy in multinucleate fungi. *Current Opinion in Microbiology*. Elsevier Ltd. https://doi.org/10.1016/j.mib.2015.08.009

Rudrapatna, V. A., Cagan, R. L., Das, T. K. (2012). Drosophila cancer models. *Developmental Dynamics*. John Wiley Sons, Ltd. https://doi.org/10.1002/dvdy.22771

Ruhmann, H., Wensing, K. U., Neuhalfen, N., Specker, J.-H., Fricke, C. (2016). Early reproductive success in Drosophila males is dependent on maturity of the accessory gland. *Behavioral Ecology*, *27*(6), 1859-1868. https://doi.org/10.1093/beheco/arw123

Rylett, C. M., Walker, M. J., Howell, G. J., Shirras, A. D., Isaac, R. E. (2007). Male accessory glands of Drosophila melanogaster make a secreted angiotensin I-converting enzyme (ANCE), suggesting a role for the peptide-processing enzyme in seminal fluid. *Journal of Experimental Biology*, *210*(20), 3601–3606.

https://doi.org/10.1242/jeb.009035
Salomon, C., Ryan, J., Sobrevia, L., Kobayashi, M., Ashman, K., Mitchell, M., Rice, G. E. (2013). Exosomal Signaling during Hypoxia Mediates Microvascular Endothelial Cell Migration and Vasculogenesis. *PLoS ONE*, *8*(7), e68451. https://doi.org/10.1371/journal.pone.0068451
Schiewer, M. J., Morey, L. M., Burd, C. J., Liu, Y., Merry, D. E., Ho, S. M., Knudsen, K. E. (2009). Cyclin D1 repressor domain mediates proliferation and survival in prostate cancer. *Oncogene*, *28*(7), 1016–1027. https://doi.org/10.1038/onc.2008.446
Schubiger, M., Tomita, S., Sung, C., Robinow, S., Truman, J. W. (2003). Isoform specific control of gene activity in vivo by the Drosophila ecdysone receptor. *Mechanisms of Development*, *120*(8), 909–918. https://doi.org/10.1016/S0925-4773(03)00134-5
Schwedes, C. C., Carney, G. E. (2012). Ecdysone signaling in adult Drosophila melanogaster. *Journal of Insect Physiology*, *58*(3), 293–302. https://doi.org/10.1016/j.jinsphys.2012.01.013
Sharma, A., Yeow, W. S. W., Ertel, A., Coleman, I., Clegg, N., Thangavel, C., Morrissey, C., Zhang, X., Comstock, C. E. S., Witkiewicz, A. K., Gomella, L., Knudsen, E. S., Nelson, P. S., Knudsen, K. E. (2010). The retinoblastoma tumor suppressor controls androgen signaling and human prostate cancer progression. *Journal of Clinical Investigation*, *120*(12), 4478–4492. https://doi.org/10.1172/JCI44239
Sharma, V., Pandey, A. K., Kumar, A., Misra, S., Gupta, H. P. K., Gupta, S., Singh, A., Buehner, N. A., Ravi Ram, K. (2017). Functional male accessory glands and fertility in Drosophila require novel ecdysone receptor. *PLoS Genetics*, *13*(5), e1006788. https://doi.org/10.1371/journal.pgen.1006788
Shibutani, S., Swanhart, L. M., Duronio, R. J. (2007). Rbf1-independent termination of E2f1-target gene expression during early Drosophila embryogenesis. *Development*, *134*(3), 467–478. https://doi.org/10.1242/dev.02738
Shu, Z., Row, S., Deng, W. M. (2018). Endoreplication: The Good, the Bad, and the Ugly. *Trends in Cell Biology*. Elsevier Ltd. https://doi.org/10.1016/j.tcb.2018.02.006
Sitnik, J., Gligorov, D., Maeda, R., Karch, F., Wolfner, M. F. (2016). The female post-mating response requires genes expressed in the secondary cells of the male accessory gland in Drosophila melanogaster. *Genetics*, *202*(3), 1029–1041. https://doi.org/10.1534/genetics.115.181644
Sonoshita, M., Cagan, R. L. (2017). Modeling Human Cancers in Drosophila. In *Current Topics in Developmental Biology*, *121*, 287–309. https://doi.org/10.1016/bs.ctdb.2016.07.008
Stenmark, H. (2009). Rab GTPases as coordinators of vesicle traffic. *Nature Reviews Molecular Cell Biology*. Nature Publishing Group. https://doi.org/10.1038/nrm2728
Stuchbery, R., McCoy, P. J., Hovens, C. M., Corcoran, N. M. (2017). Androgen synthesis in prostate cancer: Do all roads lead to Rome? *Nature Reviews Urology*. Nature Publishing Group. https://doi.org/10.1038/nrurol.2016.221
Talbot, W. S., Swyryd, E. A., Hogness, D. S. (1993). Drosophila tissues with different metamorphic responses to ecdysone express different ecdysone receptor isoforms. *Cell*, *73*(7), 1323–1337. https://doi.org/10.1016/0092-8674(93)90359-X
Tan, M. E., Li, J., Xu, H. E., Melcher, K., Yong, E. L. (2015). Androgen receptor: Structure, role in prostate cancer and drug discovery. *Acta Pharmacologica Sinica*. Nature Publishing Group. https://doi.org/10.1038/aps.2014.18
Taniguchi, K., Kokuryo, A., Imano, T., Minami, R., Nakagoshi, H., Adachi-yamada, T. (2012). Binucleation of Drosophila Adult Male Accessory Gland Cells Increases Plasticity of Organ Size for Effective Reproduction. *Biological Systems : Open Access*, *1*(1), 1–5. https://doi.org/10.4172/bso.1000e101
Taniguchi, K., Kokuryo, A., Imano, T., Minami, R., Nakagoshi, H., Adachi-Yamada, T. (2014). Isoform-specific functions of Mud/NuMA mediate binucleation of Drosophila

male accessory gland cells. *BMC Developmental Biology*, *14*(1), 1–18. https://doi.org/10.1186/s12861-014-0046-5

Taniguchi, K., Kokuryo, A., Imano, T., Nakagoshi, H., Adachi-Yamada, T. (2018). Binucleation of Accessory Gland Lobe Contributes to Effective Ejection of Seminal Fluid in Drosophila melanogaster. *Zoological Science*, *35*(5), 446. https://doi.org/10.2108/zs170188

Tayler, T. D., Pacheco, D. A., Hergarden, A. C., Murthy, M., Anderson, D. J. (2012). A neuropeptide circuit that coordinates sperm transfer and copulation duration in Drosophila. *Proceedings of the National Academy of Sciences of the United States of America*, *109*(50), 20697–20702. https://doi.org/10.1073/pnas.1218246109

Thangavel, C., Boopathi, E., Liu, Y., Haber, A., Ertel, A., Bhardwaj, A., Addya, S., Williams, N., Ciment, S. J., Cotzia, P., Dean, J. L., Snook, A., McNair Chris., Price, M., Hernandez, J. R., Zhao., S. G., Birbe, R., McCarthy, J. B., Turley, E. A., Pienta, K. J., Feng, F. Y., Dicker, A. P., Knudsen, K. E., Den, R. B. (2017). RB loss promotes prostate cancer metastasis. *Cancer Research*, *77*(4), 982–995. https://doi.org/10.1158/0008-5472.CAN-16-1589

Tilki, D., Schaeffer, E. M., Evans, C. P. (2016). Understanding Mechanisms of Resistance in Metastatic Castration-resistant Prostate Cancer: The Role of the Androgen Receptor. *European Urology Focus*. Elsevier B.V. https://doi.org/10.1016/j.euf.2016.11.013

Truman, J. W. (1996). Steroid receptors and nervous system metamorphosis in insects. *Developmental Neuroscience*, *18*(1–2), 87–101. https://doi.org/10.1159/000111398

Tsuneizumi, K., Nakayama, T., Kamoshida, Y., Kornberg, T. B., Christian, J. L., Tabata, T. (1997). Daughters against dpp modulates dpp organizing activity in Drosophila wing development. *Nature*, *389*(6651), 627–631. https://doi.org/10.1038/39362

Upadhyay, A., Moss-Taylor, L., Kim, M. J., Ghosh, A. C., O'Connor, M. B. (2017). TGF-β family signaling in drosophila. *Cold Spring Harbor Perspectives in Biology*, *9*(9). https://doi.org/10.1101/cshperspect.a022152

Uryu, O., Ameku, T., Niwa, R. (2015). Recent progress in understanding the role of ecdysteroids in adult insects: Germline development and circadian clock in the fruit fly Drosophila melanogaster. *Zoological Letters*, *1*(1), 32. https://doi.org/10.1186/s40851-015-0031-2

Vlaeminck-Guillem, V. (2018). Extracellular vesicles in prostate cancer carcinogenesis, diagnosis, and management. *Frontiers in Oncology*. https://doi.org/10.3389/fonc.2018.00222

Wigby, S., Sirot, L. K., Linklater, J. R., Buehner, N., Calboli, F. C. F., Bretman, A., Wolfner, M. F., Chapman, T. (2009). Seminal Fluid Protein Allocation and Male Reproductive Success. *Current Biology*, *19*(9), 751–757. https://doi.org/10.1016/j.cub.2009.03.036

Wilson, C., Leiblich, A., Goberdhan, D. C. I., Hamdy, F. (2017). The Drosophila Accessory Gland as a Model for Prostate Cancer and Other Pathologies. In *Current topics in developmental biology*,*121*,339–375). https://doi.org/10.1016/bs.ctdb.2016.06.001

Windmueller, R., Leach, J. P., Babu, A., Zhou, S., Morley, M. P., Wakabayashi, A., Petrenko, N. B., Viatour, P., Morrisey, E. E. (2020). Direct Comparison of Mononucleated and Binucleated Cardiomyocytes Reveals Molecular Mechanisms Underlying Distinct Proliferative Competencies. *Cell Reports*, *30*(9), 3105-3116.e4. https://doi.org/10.1016/j.celrep.2020.02.034

Wolfner, M. F. (1997). Tokens of love: Functions and regulation of Drosophila male accessory gland products. *Insect Biochemistry and Molecular Biology*. https://doi.org/10.1016/S0965-1748(96)00084-7

Wu, M., Pastor-Pareja, J. C., Xu, T. (2010). Interaction between RasV12 and scribbled clones induces tumour growth and invasion. *Nature*, *463*(7280), 545–548.

https://doi.org/10.1038/nature08702
Xiang, J., Bandura, J., Zhang, P., Jin, Y., Reuter, H., Edgar, B. A. (2017). EGFR-dependent TOR-independent endocycles support Drosophila gut epithelial regeneration. *Nature Communications*, *8*(1), 1–13. https://doi.org/10.1038/ncomms15125
Xie, T., Spradling, A. C. (1998). decapentaplegic is essential for the maintenance and division of germline stem cells in the Drosophila ovary. *Cell*, *94*(2), 251–260. https://doi.org/10.1016/S0092-8674(00)81424-5
Xin, S., Weng, L., Xu, J., Du, W. (2002). The role of RBF in developmentally regulated cell proliferation in the eye disc and in Cyclin D/Cdk4 induced cellular growth. *Development*, *129*(6), 1345–1356.
Xu, R., Hu, J. (2020). The role of JNK in prostate cancer progression and therapeutic strategies. *Biomedicine and Pharmacotherapy*. https://doi.org/10.1016/j.biopha.2019.109679
Xu, T., Jiang, X., Denton, D., Kumar, S. (2020). Ecdysone controlled cell and tissue deletion. *Cell Death and Differentiation*. https://doi.org/10.1038/s41418-019-0456-9
Yamanaka, N., Marqués, G., O'Connor, M. B. (2015). Vesicle-Mediated Steroid Hormone Secretion in Drosophila melanogaster. *Cell*, *163*(4), 907–919. https://doi.org/10.1016/j.cell.2015.10.022
Yamanaka, N., Rewitz, K. F., O'Connor, M. B. (2013). Ecdysone Control of Developmental Transitions: Lessons from Drosophila Research. *Annual Review of Entomology*, *58*(1), 497–516. https://doi.org/10.1146/annurev-ento-120811-153608
Ye, L., Lewis-Russell, J. M., Kyanaston, H. G., Jiang, W. G. (2007). Bone morphogenetic proteins and their receptor signaling in prostate cancer. *Histology and Histopathology*. https://doi.org/10.14670/HH-22.1129
Zekri, A., Ghaffari, S. H., Ghanizadeh-Vesali, S., Yaghmaie, M., Salmaninejad, A., Alimoghaddam, K., Modarressi, M. H., Ghavamzadeh, A. (2015). AZD1152-HQPA induces growth arrest and apoptosis in androgen-dependent prostate cancer cell line (LNCaP) via producing aneugenic micronuclei and polyploidy. *Tumor Biology*, *36*(2), 623–632. https://doi.org/10.1007/s13277-014-2664-8
Zhao, Y., Tindall, D. J., Huang, H. (2014). Modulation of androgen receptor by FOXA1 and FOXO1 factors in prostate cancer. *International Journal of Biological Sciences*, *10*(6), 614–619. https://doi.org/10.7150/ijbs.8389
Zielke, N., Edgar, B. A., DePamphilis, M. L. (2013). Endoreplication. *Cold Spring Harbor Perspectives in Biology*. https://doi.org/10.1101/cshperspect.a012948
Zielke, N., Kim, K. J., Tran, V., Shibutani, S. T., Bravo, M. J., Nagarajan, S., Straaten, M. V., Woods, B., Dassow, G. V., Rottig, C., Lehner, C. F., Grewal, S. S., Duronio, R. J., Edgar, B. A. (2011). Control of Drosophila endocycles by E2F and CRL4 CDT2. *Nature*, *480*(7375), 123–127. https://doi.org/10.1038/nature10579
Zijlstra, C., Stoorvogel, W. (2016). Prostasomes as a source of diagnostic biomarkers for prostate cancer. *Journal of Clinical Investigation*. American Society for Clinical Investigation. https://doi.org/10.1172/JCI81128
Zong, Y., Goldstein, A. S. (2013). Adaptation or selection - Mechanisms of castration-resistant prostate cancer. *Nature Reviews Urology*, *10*(2), 90–98. https://doi.org/10.1038/nrurol.2012.237

Appendix A: AR interacting transcription factors

As discussed in Chapter 4, certain homologues of transcription factors that are known to interact with the AR also interact with the EcR in the SCs to regulate growth and endoreplication. In this appendix, I have compiled a list of AR collaborators that have been implicated in prostate cancer and CRPC (Obinata et al., 2017) and their corresponding homologues. The roles played by these transcription factors in the regulation of growth and endoreplication in these SCs should be testes. Furthermore, combinations with different manipulations of EcR or other transcription factors could also be made to understand how these transcription factors interact with each other and the EcR.

Transcription factors	***Drosophila* homologues**
GATA2	serpent
OCT1	nubbin
ETS1	pointed
ERG	seizure (erg/derg)
NKX3-1	bagpipe
C/EBPs	slow border cell
NFI	Nf1
RUNX1	runt
FOXP1	foxp
MYC	myc
STAT3	stat92E

Appendix B: Mammalian cell lines to study Rb regulation of nucleation state

This appendix consists of a list of multinucleate mammalian cell lines that could possibly be used to investigate whether Rbf phosphorylation mutants can regulate nucleation state. Transfecting some of the Rb phosphorylation mutant plasmids from the Dowdy lab (Narasimha et al., 2014) into these cell lines and monitoring the percentage of mononucleate and multinucleate cells using flow cytometry analysis might help understand whether the effect observed with Rbf^{CA} expression in SCs, is a conserved phenomenon.

Cell Line	Description	Reference
HepG2 : Human hepatocellular carcinoma	65-70% of cells are binucleate and 20% are multinucleate	(Machado et al., 2019; Zhou, Jiang, Geng, Cao, Zhong, 2009; Zou et al., 2009)
HUVEC: Human umblical vein endothelial cells (Vascular endothelial cells)	50% of cells are binucleate. Use the specific culture protocol in reference.	(Machado et al., 2019)
SNU-449: Human grade II-III/IV, hepatocellular carcinoma	18% binucleate cells.Percentage of binucleate cells increases to 50% when treated with KIF14 siRNA;KIF14 is a mitotic kinesin that promotes completion of cytokinesis.	(Xu et al., 2014)
B16-F10: Mouse cell line derived from melanoma cells	24hr in suspension media: 15-20% binucleation and 4% multinucleate 48hr in suspension media: 27% binucleation and 10% multinucleate 72hr in suspension media: 50% multinucleate	(Ben-Ze'ev Raz, 1981)
H9c2 Cell Line: Derived from the embryonic rat heart	Culturing in 10%-serum media cells grow as mononucleate cells. Treatment with 1 μM retinoic acid results in 75% of cells to become binucleate.	(Shin et al., 2018)
NIH-3T3: Mouse fibroblast line	20% of cells are binucleate when cultured in suspension media	(Ben-Ze'ev Raz, 1981)

Appendix C: Probable regulation of DCG formation by EcR

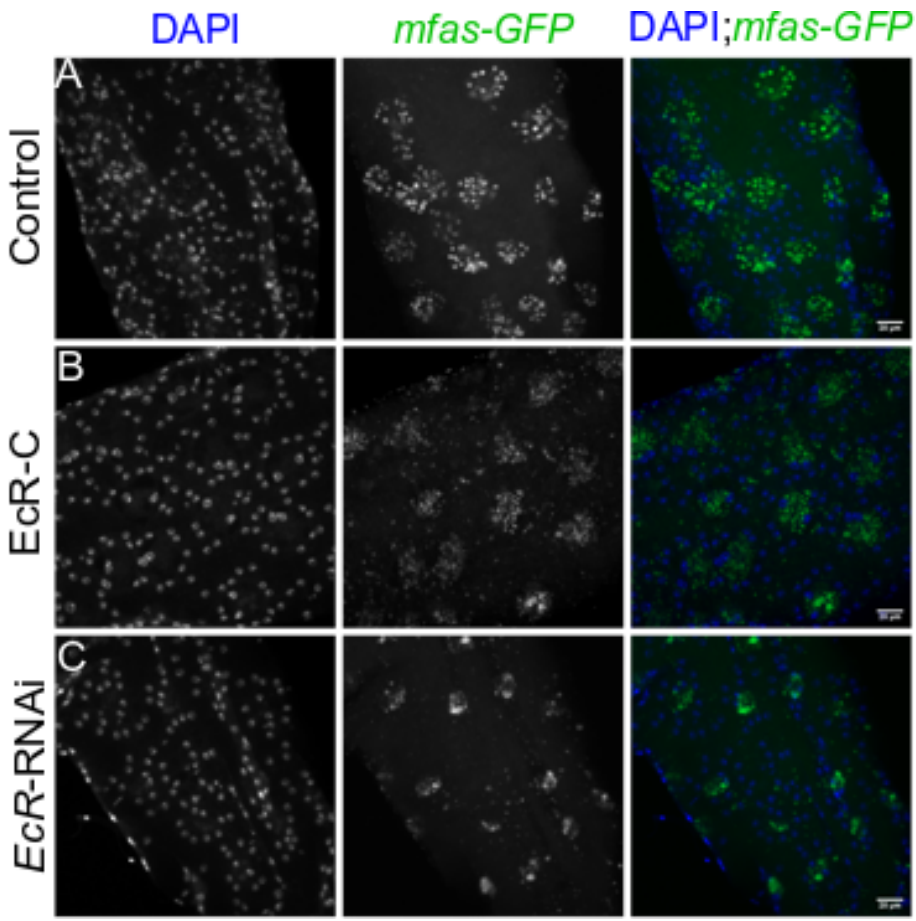

Figure C.1: Dysregulation of EcR appears to have an effect on DCG formation
A-C: Images show distal tip of AGs from 6-day-old adult virgin males expressing no transgene, EcR-C or *EcR*-RNAi under the control of the temperature-sensitive dsx-GAL4 driver and the *mfas*-GFP gene trap (BL 63204). Control represents w^{1118} flies specifically expressing mfas-GFP (which is a DCG-specific protein) in SCs. Nuclei are stained with DAPI (blue). EcR-C expression results in an increase in the number of DCGs and these DCGs appear to be smaller in size than those of controls. Expression of *EcR*-RNAi results in smaller number of DCGs of varying sizes. Scale bars correspond to 20 µm.

When Dad was expressed using the *mfas*-GFP gene trap line, I did not observe any GFP expression in the SCs, which might suggest a possible role for Dad in the regulation of DCG synthesis. These experiments should be repeated using the wide-field DeltaVision microscope.

Appendix D: Miscellaneous exploratory experiments

D.1. Diffused expression of Asterless (Asl) in SCs

When testing for appropriate nuclei markers to observe the live transition from binucleation to mononucleation in adult SCs with the expression of Rbf^{CA}, I came across the *Asl*-GFP gene trap. Asterless is a component of the centriole and is required for proper centrosome function. In a mononucleate cell not undergoing mitosis, two Asl-GFP dots corresponding to the two centrioles should be visible. These Asl-GFP dots are visible in MCs, but interestingly specifically in SCs, they appear to be diffused. Older mated males from the stock were imaged. Therefore, it would be interesting to test the expression of *Asl-GFP* with respect to mating status and age.

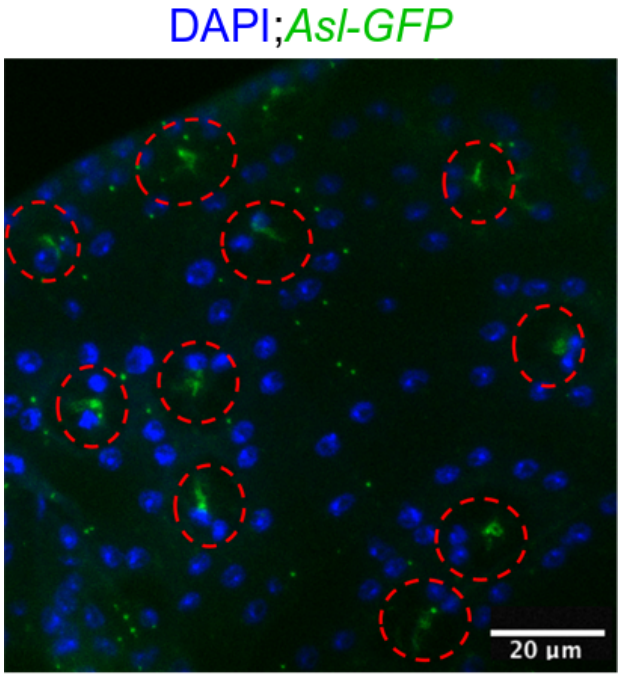

Figure D.1: Asl expression in SCs of old mated males
Image shows distal tip of AG from an old mated male expressing the *Asl-GFP* gene trap (Courtesy of the Raff lab). Dashed red ellipses mark the SCs. Scale bars correspond to 20 µm.

D.2. Mating decreases Putative Achaete Scute Target 1 (PAST1) expression

PAST1 associates predominantly with the plasma membrane and genetically interacts with Notch signalling. It is also implicated to play a role in endocytosis, male sterility, temperature sensitivity and life span (Olswang-Kutz et al., 2009). It appears that PAST1 might play a role in the regulation of SCs after mating.

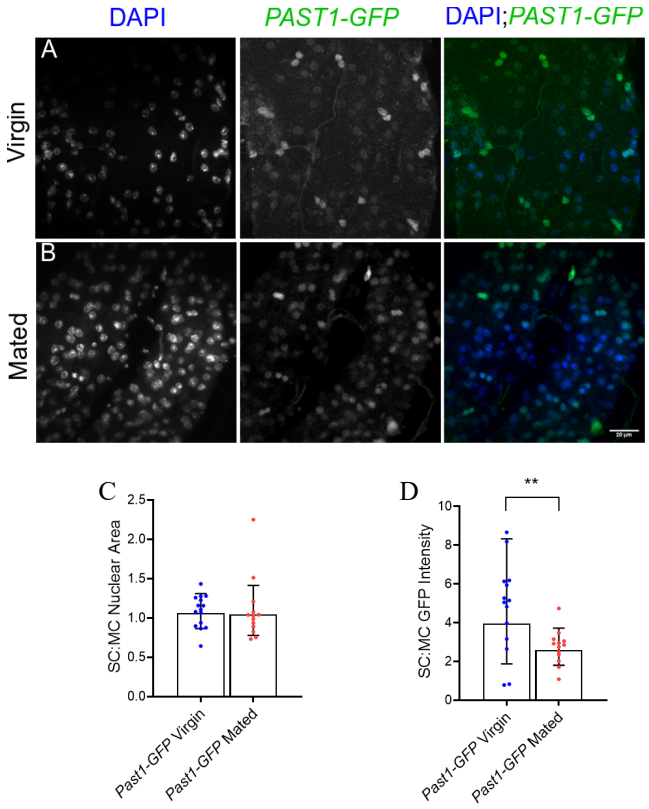

Figure D.2: PAST1 expression decreases upon mating
A-B: Images show distal tip of AGs from 6-day-old adult virgin males expressing no transgene (w^{1118}) under the control of *PAST1-GFP* under UAS control (BL 80068; w-; UAS-Past1.B.GFP). Nuclei are stained with DAPI (blue). Scale bars correspond to 20 µm.
C: Scatterplot graph depicts SC growth assay for *PAST1-GFP* expressing virgin and mated males. No growth is induced upon mating. Two-tailed Mann-Whitney test.
D: Scatterplot graph depicts the ratio of SC to MC total GFP intensity for *PAST1-GFP* expressing virgin and mated males. It appears that a decrease in PAST1 expression occurs after mating. Two-tailed Mann-Whitney test; **p=0.0078

D.3. *Tdc2* is specifically expressed in SCs

Tdc2 gene encodes for TDC, which is an enzyme required for octopamine synthesis from tyrosine in the neurons. *Tdc2*-GaL4 is generally used to label octapaminergic (OA) neurons and interestingly, it appears these OA neurons specifically innervate the SCs of the AG (Burke et al., 2012). These neurons are associated with the reward signal and it might be interesting to see if any changes are observed upon mating.

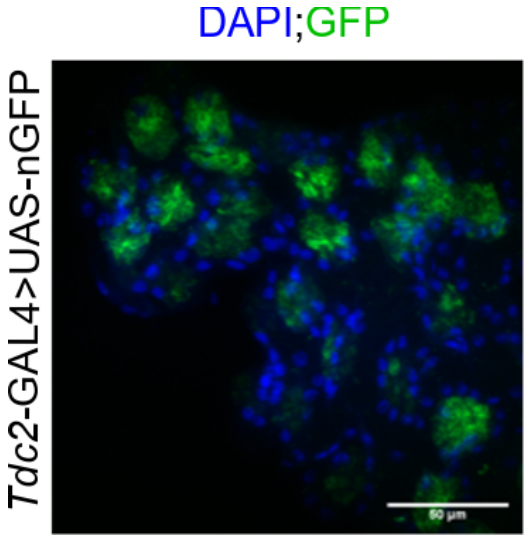

Figure D.3: Octopaminergic neurons innervate the SCs
Image shows distal tip of AG from 6-day-old adult virgin males expressing *Tdc2*-GAL4 (Courtesy of Goodwin Lab) under the UAS-nGFP control. Nuclei are stained with DAPI (blue). Scale bars correspond to 50 µm.

D.4. Calcium reporter signalling increases after mating

When a calcium reporter protein, GCaMP3, which is under the UAS control (Weislogel et al., 2013), is specifically expressed in SCs, using the temperature-sensitive *dsx*-GAL4 line, an increase in calcium reporter signalling is observed upon mating.

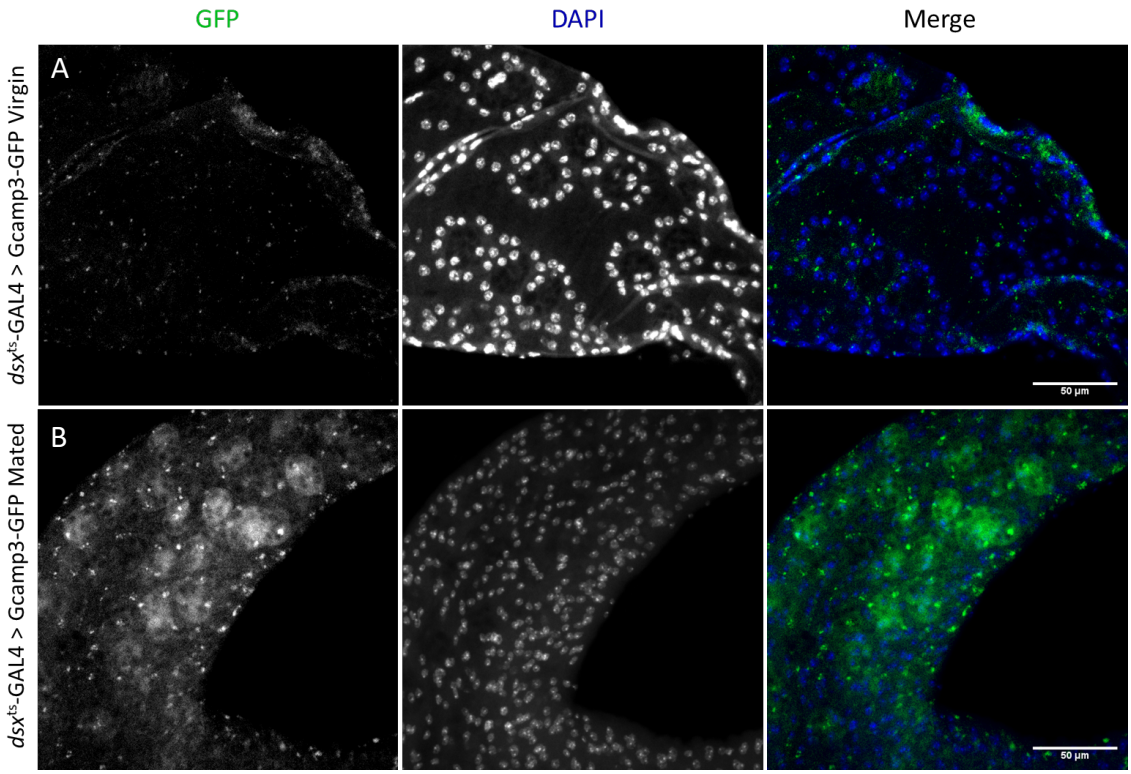

Figure D.4: GCaMP3-GFP expression increases after mating
A-B: Images show distal tip of AGs from 6-day-old adult virgin and mated males expressing GCaMP3-GFP under UAS control (BL 32116; w[1118]; P{y[+t7.7] w[+mC]=UAS-GCaMP3.T}attP40) using the SC-specific *dsx*^{ts}-GAL4 driver. Nuclei are stained with DAPI (blue). Scale bars correspond to 50 µm.

Appendix E: Python Statistics Programme Code

```
import numpy as np
import pandas as pd
from scipy import stats
import pingouin as pg
import matplotlib.pyplot as pp
from statsmodels.stats.multicomp import pairwise_tukeyhsd
import scikit_posthocs as sp


class DataRetrieve:

    def __init__(self, file_path, file_name):

        self.file_path = file_path
        self.file_name = file_name
        self.Data = pd.read_csv(file_path + '\\' + file_name + '.csv')
        self.u = list(self.Data.columns)
        self.toPlot = []
        self.toPlotLog = []
        self.file = None
        self.df = pd.DataFrame(columns=['Genotype', 'Size'])
        for i in range(len(self.u)):
            tpt = self.toPlotf()
            for j in range(len(tpt[i])):
                self.df = self.df.append({'Genotype': self.u[i], 'Size': tpt[i][j]},
                                         ignore_index=True)

    def fopen(self):
        self.file = open((self.file_path + '\\' +
                          self.file_name + '_Statistical_Analysis.csv'),
                         'a')
        return self.file

    def fclose(self):
        return self.file.close()

    def toPlotf(self):

        for x in self.u:
            temp = self.Data[self.Data[x] >= 0][x]
            self.toPlot.append(temp)
        return self.toPlot

    def toPlotLogf(self):

        for x in self.u:
            temp = self.Data[self.Data[x] >= 0][x]
            self.toPlotLog.append(np.log(temp))
        return self.toPlotLog


class NormalityVarianceTests:

    def __init__(self, dr,
                 lg=''):  # dr--> Data_Retrieve object which has
        # already created toPlot and toPlotLog arrays***

        self.lg = lg
        self.dr = dr
        if lg is '':
            self.toPlot = self.dr.toPlotf()
            self.SW_counter = -1
            self.DP_counter = -1

        else:
            self.toPlot = self.dr.toPlotLogf()
            self.SW_counter = 0
            self.DP_counter = 0

    def normality_plots(self):

        fig, ax = pp.subplots(len(self.dr.u), 2, figsize=(15, 15))

        for x in range(len(self.dr.u)):
            ax[x][0].hist(self.toPlot[x], histtype='step', density=True)
            self.toPlot[x].plot.density(bw_method=0.5, ax=ax[x][0])
            ax[x][0].set_xlabel(self.lg + 'SC:MC Nuclear Area')
            ax[x][0].set_ylabel('Frequency')
            ax[x][0].set_title(self.dr.u[x] + '-' + self.lg +
                               'SC:MC Nuclear Area_Frequency Distribution')

            # Inverse Normal Plot
            stats.probplot(self.toPlot[x], dist='norm', rvalue=True, plot=ax[x][1])
            ax[x][1].set_title(self.dr.u[x] + ' ' + self.lg +
                               ' SC:MC Nuclear Area_Inverse Normal Plot')

        pp.subplots_adjust(left=None, bottom=None, right=None,
```

```
                            top=None, wspace=0.5, hspace=0.8)
        if self.lg=='':
            fig.savefig(self.dr.file_path + '\\' +'_Graphs_' + self.dr.file_name + '.↘
                png')
        else:
            fig.savefig(self.dr.file_path + '\\' +
                        'Log Transformation_Graphs_' + self.dr.file_name + '.png')

    def shapiro_wilk(self):
        # Shapiro-Wilk Normality Test

        swtest = list()
        swtest_result = list()
        for x in range(len(self.dr.u)):
            shapiro_wilk = stats.shapiro(self.toPlot[x])
            swtest.append(shapiro_wilk[1])
            if shapiro_wilk[1] < 0.01:
                swtest_result.append('Not Gaussian')
                self.SW_counter += 1
            else:
                swtest_result.append('Possibly Gaussian')

        toprint_sw = np.column_stack(tup=(self.dr.u, swtest, swtest_result))

        file = self.dr.fopen()

        file.write('\n' + self.lg + '-  Shapiro-Wilk Normality Test:\n')

        s = [[str(e) for e in row] for row in toprint_sw]
        lens = [max(map(len, col)) for col in zip(*s)]
        fmt = '\t'.join('{{:{}}}'.format(toprint_sw) for toprint_sw in lens)
        table = [fmt.format(*row) for row in s]
        file.write('\n'.join(table))

        file.write('\n')

        self.dr.fclose()


    def d_augostino_pearson(self):

        dptest = list()
        dptest_result = list()

        for x in range(len(self.dr.u)):
            augostino_pearson = stats.normaltest(self.toPlot[x])
            dptest.append(augostino_pearson[1])
            if augostino_pearson[1] < 0.01:
                dptest_result.append('Not Gaussian')
                self.DP_counter += 1
            else:
                dptest_result.append('Possibly Gaussian')

        toprint_dw = np.column_stack(tup=(self.dr.u, dptest, dptest_result))

        file = self.dr.fopen()

        file.write('\n' + self.lg + '-  D\'Augostino and Pearson\'s Normality Test:\n')

        s = [[str(e) for e in row] for row in toprint_dw]
        lens = [max(map(len, col)) for col in zip(*s)]
        fmt = '\t'.join('{{:{}}}'.format(toprint_dw) for toprint_dw in lens)
        table = [fmt.format(*row) for row in s]
        file.write('\n'.join(table))

        file.write('\n')

        self.dr.fclose()


    def distribution_metrics(self):

        genotype = []
        mean = []
        stdev = []

        file = self.dr.fopen()

        file.write('\n' + self.lg + ' Data Parameters' + '\n')
        for i in range(len(self.dr.u)):
            genotype.append(self.dr.u[i])
            mean.append(np.mean(self.toPlot[i]))
            stdev.append(np.std(self.toPlot[i]))

        dm = pd.DataFrame({'Genotype': genotype, 'Mean': mean,
                           'Standard Deviation': stdev})

```

```
174             dm.to_csv(file, sep=';', line_terminator='\n', index=None, mode='a')
175
176             self.dr.fclose()
177             return dm
178
179
180         def bartlett_test(self):
181
182             bt = stats.bartlett(*[list(self.toPlot[i]) for i in range(len(self.dr.u))])[1]
183             file = self.dr.fopen()
184             if bt > 0.01:
185                 file.write(
186                     "\n{} - Normal Data_Bartlett Test: Variance of groups are similar.\n"
187                         .format(self.lg))
188             else:
189                 file.write(
190                     "\n{} - Normal Data_Bartlett Test: Variance of groups are dissimilar."
191                         .format(self.lg))
192             self.dr.fclose()
193
194             return bt
195
196         def brown_forsythe(self):
197
198             lv = stats.levene(*[list(self.toPlot[i]) for i in range(len(self.dr.u))], ↘
                    center='mean')[1]
199             # Brown Forscythe variance test   (Levene--> median; Brown forsythe --> mean)
200             file = self.dr.fopen()
201             if lv > 0.01:
202                 file.write('\n'+self.lg +
203                     "- Non-Normal Data_Brown Forsythe Test: Variance of groups are similar↘
                            .\n")
204             else:
205                 file.write('\n'+self.lg + "- Non-Normal Data_Brown Forsythe Test:"
206                                           "Variance of groups are dissimilar\n")
207             self.dr.fclose()
208
209             return lv
210
211         def levene_test(self):
212
213             lv = stats.levene(*[list(self.toPlot[i]) for i in range(len(self.dr.u))], ↘
                    center='median')[1]
214             # Brown Forscythe variance test   (Levene--> median; Brown forsythe --> mean)
215             file = self.dr.fopen()
216             if lv > 0.01:
217                 file.write('\n'+self.lg + "- Non-Normal Data_Levene Test: "
218                                           "Variance of groups are similar.\n")
219             else:
220
221                 file.write('\n'+self.lg + "- Non-Normal Data_Levene Test :"
222                                           "Variance of groups are dissimilar\n")
223
224             self.dr.fclose()
225
226             return lv
227
228
229     class PosthocTests:
230
231         def __init__(self, dr,
232                      lg=''):
233             # dr--> Data_Retrieve object which has already
234             # created toPlot and toPlotLog arrays***
235
236             self.dr = dr
237             self.lg = lg
238
239             if self.lg is None:
240                 self.toPlot = dr.toPlot()
241
242             else:
243                 self.toPlot = dr.toPlotLogf()
244
245         def anova(self):
246
247             anova_var = stats.f_oneway(*[list(self.dr.toPlot[i]) for i in range(len(self.dr
                    .u))])
248             if anova_var[1] < 0.05:
249                 file = self.dr.fopen()
250                 file.write('\n'+self.lg + '- ANOVA: Significant difference between groups \r
                        ')
251                 self.dr.fclose()
252             else:
253                 file = self.dr.fopen()
254                 file.write('\n'+self.lg + '- ANOVA:No significant difference '
255                                           'between any pair of groups \n')
```

```
256             self.dr.fclose()
257         return anova_var[1]
258
259     def tukey_hsd(self):
260
261         file = self.dr.fopen()
262         file.write('\n'+self.lg + '- Tukey HSD post hoc test: \n')
263         self.dr.fclose()
264
265         melt_data = self.dr.Data.melt(value_vars=self.dr.u)
266         data_melted = melt_data.dropna(0, 'any')
267         grp = list(data_melted['variable'])
268         nums = list(data_melted['value'])
269         T = pairwise_tukeyhsd(nums, grp, alpha=0.05)
270         res = pd.DataFrame(data=T._results_table.data[1:], columns=T._results_table.↘
                data[0])
271         posthoc = res[['group1', 'group2', 'p-adj']]\
272             .rename(columns={'group1': 'A', 'group2': 'B', 'p-adj': 'pval'})
273         posthoc['sign'] = posthoc.pval.apply(lambda x: '****' if x <= 0.0001 else (
274             '***' if x <= 0.001 else
275             ('**' if x <= 0.01 else ('*' if x <= 0.05 else 'n.s.'))))
276
277         file = self.dr.fopen()
278         posthoc.to_csv(file, sep=';', line_terminator='\n', index=None, mode='a')
279         self.dr.fclose()
280
281     def welch_anova(self):
282         welch_var = pg.welch_anova(dv='Size', between='Genotype', data=self.dr.df)['p-↘
                unc']\
283             .values
284         file = self.dr.fopen()
285
286         if welch_var < 0.05:
287             file.write( '\n'+self.lg +
288                 ' -Welch_ANOVA: Significant difference between groups.' + '\n')
289         else:
290             file.write('\n'+self.lg + ' -Welch_ANOVA:No significant difference '
291                                       'between any pair of groups \n')
292
293         self.dr.fclose()
294         return welch_var
295
296     def games_howell(self):
297
298         file = self.dr.fopen()
299         file.write('\n'+self.lg +' -Games-Howell post hoc test:\n')
300         self.dr.fclose()
301
302         ph = pg.pairwise_gameshowell(data=self.dr.df, dv='Size', between='Genotype')
303         posthoc = ph[['A', 'B', 'pval']]
304         posthoc['sign'] = posthoc.pval.apply(lambda x: '****' if x <= 0.0001 else (
305             '***' if x <= 0.001 else ('**' if x <= 0.01
306                                       else ('*' if x <= 0.05 else 'n.s.'))))
307
308         file = self.dr.fopen()
309         posthoc.to_csv(file, sep=';', line_terminator='\n', index=None, mode='a')
310         self.dr.fclose()
311
312     def kruskal_wallis(self):
313         kruskal_wallis_var = stats.kruskal(*[list(self.dr.toPlot[i])
314                                              for i in range(len(self.dr.u))])
315         file = self.dr.fopen()
316
317         if kruskal_wallis_var[1] < 0.05:
318             file.write('\n'+ self.lg + ' -Kruskal-Wallis Test: '
319                                        'Significant difference between groups.\n')
320         else:
321             file.write('\n'+ self.lg + ' -Kruskal-Wallis Test: '
322                                        'No significant difference \n')
323         self.dr.fclose()
324         return kruskal_wallis_var[1]
325
326     def dunn(self):
327
328         t = sp.posthoc_dunn(self.dr.df, 'Size', 'Genotype')
329
330         h = pd.DataFrame(columns=['A', 'B', 'pval'])
331         k = len(t.columns)
332         for i in range(len(t.columns)):
333             for j in range(i + 1, (len(t.columns))):
334                 h = h.append({'A': list(t.columns)[i], 'B': list(t.columns)[j],
335                               'pval': t[t.columns[i]][j]},
336                              ignore_index=True)
337
338         h['sign'] = h.pval.apply(lambda x: '****' if x < 0.0001 else (
339             '***' if x < 0.001 else ('**' if x < 0.01 else ('*' if x < 0.05 else 'n.s.'↘
                ))))
```

```
340
341         file = self.dr.fopen()
342         file.write('\n'+ self.lg + ':-Dunn post-hoc test')
343         h.to_csv(file, sep=';', line_terminator='\n', index=None, mode='a')
344         self.dr.fclose()
345
346
347 class pipeline:
348
349     def __init__(self, file_path, file_name):
350
351         self.dr = DataRetrieve(file_path, file_name)
352         self.nvt = NormalityVarianceTests(self.dr)
353         self.pht = PosthocTests(self.dr)
354
355         self.nvt.normality_plots()
356         self.nvt.shapiro_wilk()
357         self.nvt.d_augostino_pearson()
358         var = self.nvt.distribution_metrics()
359
360         if self.nvt.SW_counter == -1 or self.nvt.DP_counter == -1:
361             self.normal_data_analysis()
362
363
364         else:
365             self.nvtl = NormalityVarianceTests(self.dr, 'Log Transformation:')
366             self.phtl = PosthocTests(self.dr, 'Log Transformation:')
367
368             self.nvtl.normality_plots()
369             self.nvtl.shapiro_wilk()
370             self.nvtl.d_augostino_pearson()
371             varl = self.nvtl.distribution_metrics()
372
373             if self.nvtl.SW_counter == 0 or self.nvtl.DP_counter == 0:
374                 self.normal_data_analysis('Log Transformation:')
375
376             else:
377                 if self.pht.kruskal_wallis() < 0.05:
378                     if self.nvt.brown_forsythe() > 0.02:
379                         self.pht.dunn()
380
381                     elif var['Standard Deviation'].max() <= 4*var['Standard Deviation'↘
                         ].min():
382                         file = self.dr.fopen()
383                         file.write('Homoscedasticity by Rule of Thumb '
384                                    '(Max. Variance < 4*Min. Variance \n')
385                         self.dr.fclose()
386                         self.pht.dunn()
387
388
389                     else:
390                         file = self.dr.fopen()
391                         file.write('\n Non-normal Data; '
392                                    'No Transformation works; Heteroscedastic Data  \n')
393
394     def normal_data_analysis(self, lg=''):
395
396         if lg is '':
397             a1 = self.nvt
398             a2 = self.pht
399         else:
400             a1 = self.nvtl
401             a2 = self.phtl
402
403         if a1.bartlett_test() > 0.02:
404             if a2.anova() < 0.05:
405                 a2.tukey_hsd()
406         else:
407             if a2.welch_anova() < 0.05:
408                 a2.games_howell()
409
410
411 class pipeline_edu:
412
413     def __init__(self, file_path, file_name):
414
415         self.dr = DataRetrieve(file_path, file_name)
416         self.nvt = NormalityVarianceTests(self.dr)
417         self.pht = PosthocTests(self.dr)
418
419
420         var = self.nvt.distribution_metrics()
421
422         if self.pht.kruskal_wallis() < 0.05:
423                 if self.nvt.brown_forsythe() > 0.02:
424                     self.pht.dunn()
425
```

Appendix F: Data curation

All microscopy images have been arranged into folders describing the experiment type, transgene and driver and have been stored in CW-001 Desktop with a copy in the Wilson Group USB-2 hard-disk. Each image has been labelled in the following format 'Transgene_Lab Stock Number_Driver_Channels Imaged_Antibodies Used_Date'. Four integrated excel files have all the SC growth assay and EdU assay data pertaining to EcR manipulations, BMP manipulations, Cell cycle manipulations and EcR, BMP and, Cell cycle combinations and recombinations respectively. One integrated excel sheet has all the data pertaining to the mononucleation project and another excel sheet incorporate the compartment and ILV biogenesis data. The first sheet of each of these integrated excel sheets detail the experimental conditions including transgene and driver lines with lab stock numbers.

Appendix References

Ben-Ze'ev, A., Raz, A. (1981). Multinucleation and inhibition of cytokinesis in suspended cells: Reversal upon reattachment to a substrate. *Cell*. https://doi.org/10.1016/0092-8674(81)90038-6

Burke, C. J., Huetteroth, W., Owald, D., Perisse, E., Krashes, M. J., Das, G., … Waddell, S. (2012). Layered reward signalling through octopamine and dopamine in Drosophila. *Nature*, *492*(7429), 433–437. https://doi.org/10.1038/nature11614

Machado, A. R. T., Aissa, A. F., Ribeiro, D. L., Costa, T. R., Ferreira, R. S., Sampaio, S. V., Antunes, L. M. G. (2019). Cytotoxic, genotoxic, and oxidative stress-inducing effect of an L-amino acid oxidase isolated from Bothrops jararacussu venom in a co-culture model of HepG2 and HUVEC cells. *International Journal of Biological Macromolecules*, *127*, 425–432. https://doi.org/10.1016/j.ijbiomac.2019.01.059

Narasimha, A. M., Kaulich, M., Shapiro, G. S., Choi, Y. J., Sicinski, P., Dowdy, S. F. (2014). Cyclin D activates the Rb tumor suppressor by mono-phosphorylation. *ELife*, *2014*(3). https://doi.org/10.7554/eLife.02872.001

Obinata, D., Takayama, K., Takahashi, S., Inoue, S. (2017). Crosstalk of the Androgen Receptor with Transcriptional Collaborators: Potential Therapeutic Targets for Castration-Resistant Prostate Cancer. *Cancers*, *9*(12), 22. https://doi.org/10.3390/cancers9030022

Olswang-Kutz, Y., Gertel, Y., Benjamin, S., Sela, O., Pekar, O., Arama, E., … Segal, D. (2009). Drosophila Past1 is involved in endocytosis and is required for germline development and survival of the adult fly. *Journal of Cell Science*, *122*(4), 471–480. https://doi.org/10.1242/jcs.038521

Shin, A. N., Han, L., Dasgupta, C., Huang, L., Yang, S., Zhang, L. (2018). SIRT1 increases cardiomyocyte binucleation in the heart development. *Oncotarget*, *9*(8), 7996–8010. https://doi.org/10.18632/oncotarget.23847

Weislogel, J. M., Bengtson, C. P., Müller, M. K., Hörtzsch, J. N., Bujard, M., Schuster, C. M., Bading, H. (2013). Requirement for nuclear calcium signaling in drosophila long-term memory. *Science Signaling*, *6*(274), ra33–ra33. https://doi.org/10.1126/scisignal.2003598

Xu, H., Choe, C., Shin, S. H., Park, S. W., Kim, H. S., Jung, S. H., Yim, S. H., Kim, T. M., Chung, Y. J. (2014). Silencing of KIF14 interferes with cell cycle progression and cytokinesis by blocking the p27Kip1 ubiquitination pathway in hepatocellular carcinoma. *Experimental and Molecular Medicine*, *46*(5). https://doi.org/10.1038/emm.2014.23

Zhou, S. M, Jiang, L. P, Geng, C. Y, Cao, J., Zhong, L. F. (2009). Patulin-induced genotoxicity and modulation of glutathione in HepG2 cells. *Toxicon*, *53*(5), 584–586. https://doi.org/10.1016/j.toxicon.2009.01.030

Zou, J., Chen, Q., Tang, S., Jin, X., Chen, K., Zhang, T., Xiao, X. (2009). Olaquindox-induced genotoxicity and oxidative DNA damage in human hepatoma G2 (HepG2) cells. *Mutation Research - Genetic Toxicology and Environmental Mutagenesis*, *676*(1), 27–33. https://doi.org/10.1016/j.mrgentox.2009.03.001

PLOS BIOLOGY

RESEARCH ARTICLE

Mating induces switch from hormone-dependent to hormone-independent steroid receptor–mediated growth in *Drosophila* secondary cells

Aaron Leiblich[1,2☯], Josephine E. E. U. Hellberg[1☯], Aashika Sekar[1☯], Carina Gandy[1], Claudia C. Mendes[1], Siamak Redhai[1], John Mason[1], Mark Wainwright[1], Pauline Marie[1], Deborah C. I. Goberdhan[1], Freddie C. Hamdy[2], Clive Wilson[1]*

1 Department of Physiology, Anatomy and Genetics, University of Oxford, Oxford, United Kingdom,
2 Nuffield Department of Surgical Sciences, University of Oxford, Oxford, United Kingdom

☯ These authors contributed equally to this work.
* clive.wilson@dpag.ox.ac.uk

Check for updates

OPEN ACCESS

Citation: Leiblich A, Hellberg JEEU, Sekar A, Gandy C, Mendes CC, Redhai S, et al. (2019) Mating induces switch from hormone-dependent to hormone-independent steroid receptor–mediated growth in *Drosophila* secondary cells. PLoS Biol 17 (10): e3000145. https://doi.org/10.1371/journal.pbio.3000145

Academic Editor: Mariana Federica Wolfner, Cornell University, UNITED STATES

Received: January 14, 2019

Accepted: September 16, 2019

Published: October 7, 2019

Copyright: © 2019 Leiblich et al. This is an open access article distributed under the terms of the Creative Commons Attribution License, which permits unrestricted use, distribution, and reproduction in any medium, provided the original author and source are credited.

Data Availability Statement: All relevant data are within the paper and its Supporting Information files.

Funding: We acknowledge the Biotechnology and Biological Sciences Research Council (BBSRC; https://bbsrc.ukri.org/; BB/K017462/1, BB/L007096/1, BB/N016300/1, BB/R004862/1 to CG, CCM, MW, DCIG, CW), Cancer Research UK (https://www.cancerresearchuk.org/; C19591/A19076 to PM, DCIG, CW), the Cancer Research

Abstract

Male reproductive glands like the mammalian prostate and the paired *Drosophila melanogaster* accessory glands secrete seminal fluid components that enhance fecundity. In humans, the prostate, stimulated by environmentally regulated endocrine and local androgens, grows throughout adult life. We previously showed that in fly accessory glands, secondary cells (SCs) and their nuclei also grow in adults, a process enhanced by mating and controlled by bone morphogenetic protein (BMP) signalling. Here, we demonstrate that BMP-mediated SC growth is dependent on the receptor for the developmental steroid ecdysone, whose concentration is reported to reflect sociosexual experience in adults. BMP signalling appears to regulate ecdysone receptor (EcR) levels via one or more mechanisms involving the EcR's N terminus or the RNA sequence that encodes it. Nuclear growth in virgin males is dependent on ecdysone, some of which is synthesised in SCs. However, mating induces additional BMP-mediated nuclear growth via a cell type–specific form of hormone-independent EcR signalling, which drives genome endoreplication in a subset of adult SCs. Switching to hormone-independent endoreplication after mating allows growth and secretion to be hyperactivated independently of ecdysone levels in SCs, permitting more rapid replenishment of the accessory gland luminal contents. Our data suggest mechanistic parallels between this physiological, behaviour-induced signalling switch and altered pathological signalling associated with prostate cancer progression.

Introduction

In all higher organisms in which fertilisation takes place in the female reproductive tract, males not only deliver sperm to females but also transfer seminal fluid containing a cocktail of molecules that optimise fecundity. For example, secretions from the mammalian prostate and

UK Oxford Centre Development Fund (C38302/A12278 to DCIG, FCH,CW), the John Fell Fund, Oxford (141/063 to FCH, CW), the Medical Research Council (MRC; https://mrc.ukri.org/; #1530147 and #1252459 to SR and JEEUH), the Urology Foundation (https://www.theurologyfoundation.org/; to AL), and the Wellcome Trust (https://wellcome.ac.uk/; Strategic Awards #091911, #107457; MICRON imaging facility) for grants, studentships and scholarships supporting this work. The funders had no role in study design, data collection and analysis, decision to publish, or preparation of the manuscript.

Competing interests: The authors have declared that no competing interests exist.

Abbreviations: 20-HE, 20-hydroxyecdysone; *Abd-B*, *Abdominal B*; Acp, AG protein; AF1, activation function 1; AG, accessory gland; AR, androgen receptor; BMP, bone morphogenetic protein; BrdU, bromodeoxyuridine; CHO, Chinese hamster ovary; CycE, Cyclin E; Dad, Daughters against Decapentaplegic; Dpp, Decapentaplegic; *ecd*, *ecdysoneless*; EcR, ecdysone receptor; EdU, 5-ethynyl-2′-deoxyuridine; *Eip74EF*, *Ecdysone-induced protein 74EF*; *esg*, *escargot*; esg^{ts}F/O, the yeast transcription factor GAL4 expressed under the control of the promoter of the gene *esg* in a temperature-dependent fashion; Fas3, Fasciclin3; GFP, green fluorescent protein; MC, main cell; *Med*, *Medea*; NTD, N-terminal domain; P-Mad, phosphorylated Mothers against Decapentaplegic; PTTH, prothoracicotropic hormone; RNAi, RNA interference; RT-PCR, reverse-transcription PCR; *ry*, *rosy*; SC, secondary cell; *shd*, *shade*; *spo*, *spook*; TGF-β, transforming growth factor β; Tkv, Thick veins; tub-GAL80^{ts}, a temperature-sensitive form of the GAL4 inhibitor GAL80 expressed under the control of the *tubulin* gene promoter; USP, Ultraspiracle; Wit, Wishful thinking.

seminal vesicles contribute most of the seminal fluid volume, activate sperm [1], and promote embryo implantation [2]. The paired accessory glands (AGs) in the fruit fly, *Drosophila melanogaster*, perform related functions and can also substantially alter female behaviour after mating, increasing egg laying, promoting sperm storage, and reducing female receptivity to subsequent mating attempts [3–6]. Most of the key AG proteins (Acps) involved, such as Sex Peptide, which plays a central role in driving female postmating responses, are secreted by about 1,000 so-called main cells (MCs) found in the monolayered AG epithelium [7,8]. However, secondary cells (SCs), a small population of about 40 epithelial cells at the distal tip of each AG (Fig 1A), also play an essential role [9–11].

As humans age, the prostate epithelium frequently becomes hyperplastic. Indeed, many males over the age of 65 develop symptomatic benign prostatic hyperplasia [12]. SCs are not proliferative, but they also grow in adults, unlike other cells in the AG [9]. Mating enhances this growth, which is most easily assayed by measuring nuclear size. Interestingly, we have found that autocrine bone morphogenetic protein (BMP) signalling is crucial for the normal, age-dependent growth of SCs both in virgin and mated males [9]. Growth of SCs involves elevated synthesis of macromolecules including secreted proteins. Inhibition of BMP signalling specifically in adult SCs reduces the ability of males to suppress female remating. Furthermore, BMP signalling promotes secretion of the contents of large compartments that contain so-called dense-core granules at their centre [13] and exosomes, nanovesicles formed inside endosomal compartments that are released by fusion of these compartments to the plasma membrane [14]. These exosomes appear to be involved in female behavioural reprogramming, providing at least part of the explanation for SCs' BMP-dependent effects on females.

Although BMP signalling is implicated in mammalian prostate development [15] and cancer growth and metastasis [16,17], steroid signalling through the androgen receptor (AR) is thought to be the central regulator of these processes and prostate hyperplasia [18,19]. Aberrations in steroid signalling are implicated in both benign and malignant disease of this organ [20,21]. Because androgen levels are modulated by factors such as developmental stage [18], nutrition [22], and sexual activity [23], this endocrine input potentially allows males to adapt prostate function during development and in response to the environment and reproductive demands. In advanced cancer, hormone deprivation therapy effectively blocks tumour growth, but typically within 2 years, hormone-independent cells emerge, which frequently still require the AR for growth and will lead to the death of the patient [24].

Flies employ a more limited range of steroid hormones than mammals, with the major characterised steroid hormone, 20-hydroxyecdysone (usually called 20-HE or ecdysone), primarily involved in developmental transitions, particularly during metamorphosis [25,26]. However, ecdysone levels also fluctuate in adult males in response to sociosexual interactions [27]. Ecdysone regulates male courtship behaviour [28–30] and affects the male germ line [31,32]. Ecdysteroids can also induce expression of multiple Acps in AGs [33], and the ecdysone receptor (EcR) is required for normal AG development [34]. However, the cells and molecular mechanisms involved in these processes, as well as the physiological functions of the EcR in adult AGs, remain unclear. We hypothesised that ecdysone signalling might affect adult SC function, potentially providing a sociosexual environmental input, which complements mating-dependent growth of SCs.

Here, we show that the EcR is specifically expressed in SCs within the adult AG epithelium and that EcR signalling in these cells is critical for normal growth. BMP signalling promotes growth by regulating levels of the EcR protein. Whereas nuclear growth in virgin males is BMP, EcR, and ecdysone dependent, some EcR-mediated nuclear growth observed after mating is hormone independent and specifically drives endoreplication in a subset of SCs, increasing their secretory activity. We propose that this novel form of steroid receptor control in flies

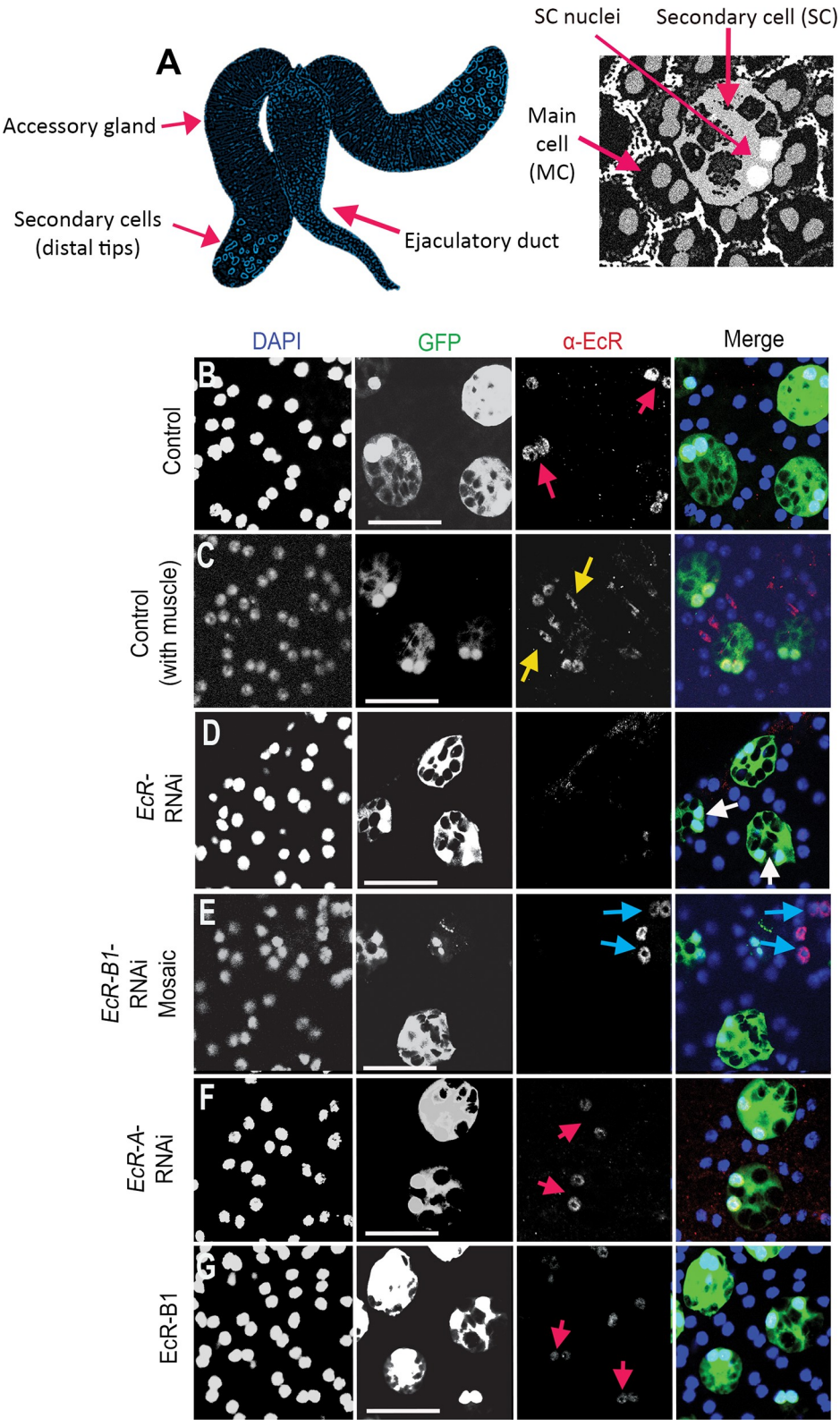

Fig 1. The EcR-B1 isoform of the EcR is the predominant isoform expressed in SC nuclei. (A) Schematic of *Drosophila* male AGs and binucleate SCs and MCs within their monolayer epithelium. (B-G) Images show distal tips of AGs dissected from 6-day-old males (except for mosaic in [E]). SCs (nuclei marked by red arrows) express nuclear

GFP (which also labels SC cytosol) and other transgenes under esg^{ts}F/O control. Nuclei are stained with DAPI (blue). (B, C) Immunostaining with an antibody that cross-reacts with all EcR isoforms reveals expression in SC nuclei ([B]; red arrows) and in muscle cell nuclei ([C]; yellow arrows) but not in MCs (non-GFP-positive nuclei in [B]) in 6-day-old males. (D-F) Whereas expression of an RNAi targeting the EcR-A transcript does not affect EcR expression (F), mosaic expression of an RNAi targeting *EcR-B1* transcripts ([E], green cells) or expression of an RNAi targeting all isoforms (D) strongly reduces nuclear EcR staining in SCs. In mosaics, staining is still present in non-RNAi-expressing SCs, which are not labelled with GFP ([E]; blue arrows). (G) esg^{ts}F/O-driven expression of the EcR-B1 isoform has no detectable effect on nuclear EcR levels in SCs. Scale bars, 50 μm. AG, accessory gland; EcR, ecdysone receptor; *esg*, *escargot*; esg^{ts}F/O, the yeast transcription factor GAL4 expressed under the control of the promoter of the gene *esg* in a temperature-dependent fashion; GFP, green fluorescent protein; MC, main cell; RNAi, RNA interference; SC, secondary cell.

https://doi.org/10.1371/journal.pbio.3000145.g001

permits SC activity to be flexibly regulated following mating to ensure that resources are employed according to demand.

Results

EcR-B1 is the predominant isoform expressed by SCs in the adult AG epithelium

In order to mark and genetically manipulate SCs, we used the SC-specific esg^{ts}F/O GAL4 system [35], in which the yeast transcription factor GAL4 can be expressed in SCs under the control of the promoter of the gene *escargot* (*esg*) in a temperature-dependent fashion. Expression can be activated exclusively in adults through inactivation of a ubiquitously expressed, temperature-sensitive form of the GAL4 inhibitor GAL80 (tub-GAL80^{ts}) by a temperature shift to 28.5˚C at eclosion [9,35]. Staining AGs with a pan-EcR antibody that cross-reacts with all three characterised EcR isoforms [36] revealed EcR expression in the nuclei of muscle cells and SCs, which (like MCs) are binucleate (Fig 1B and 1C). This staining was lost in SCs expressing a previously characterised RNA interference (RNAi) construct targeting transcripts for all EcR isoforms (Fig 1D) [37].

We were unable to detect a robust signal in the AG with isoform-specific EcR-A and EcR-B1 antibodies. However, in an alternative approach, we expressed isoform-specific RNAi constructs [38] in SCs under esg^{ts}F/O control, either throughout adulthood or by using a temperature shift in 3-day-old males. The latter approach leads to maintained RNAi expression in only a subset of SCs [9]. *EcR-A*-RNAi did not affect EcR levels (Fig 1F), but little, if any, EcR protein was detected in SCs expressing an *EcR-B1*-RNAi construct, demonstrating that EcR-B1 is the predominant isoform produced by these cells (Fig 1E).

At least two EcR isoforms promote hormone-dependent SC nuclear growth in virgin males

To test the roles of the EcR in adult SC growth, the pan-*EcR*-RNAi construct was expressed in these cells posteclosion. As described previously, we assessed growth by measuring SC nuclear size in adult virgin males after 6 days relative to nuclear size in adjacent MCs, which do not grow with age or in response to mating, because this controls for nuclear size changes produced by flattening AGs upon mounting [9].

The growth of SC nuclei was inhibited by expression of *EcR*-RNAi (Fig 2A, 2B and 2K, S1 Data) but not by expression of a control RNAi targeting the *rosy* (*ry*) gene (S1H and S1I Fig, S1 Data). Surprisingly, not only did the isoform-specific *EcR-B1*-RNAi inhibit nuclear SC growth, but so did *EcR-A*-RNAi (Fig 2C–2E and 2L, S1 Data), suggesting that *EcR-A* is involved in this process despite its low levels of protein expression in SCs relative to EcR-B1. Because the EcR-B2 isoform only has a short unique N-terminal domain (NTD), there is no EcR-B2-

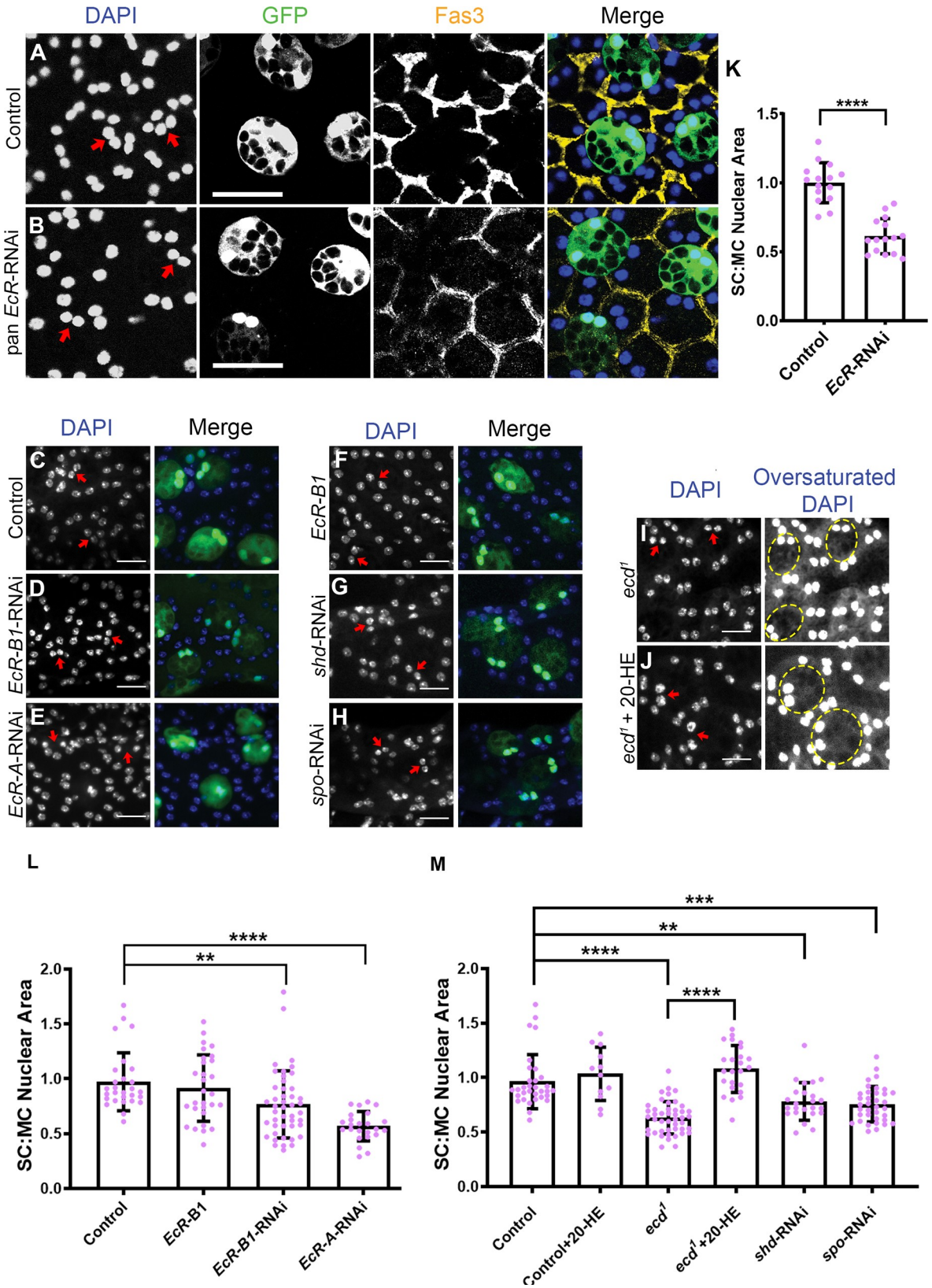

Fig 2. Ecdysone and the EcR are required to promote SC nuclear growth in virgin males. (A-J) Dissected AGs from 6-day-old virgin males were stained with DAPI (blue nuclei) and, in some cases (A and B), with an antibody against Fas3 to label the apical outlines of SCs

and neighbouring MCs (yellow). Selected SC nuclei are marked with red arrows, and in (A-H), express GFP and other transgenes under esg^{ts}F/O control. In *ecd*^{1} flies, SCs are recognised by their characteristic vacuolar morphology; selected SCs are highlighted by dashed circles (I and J). (A-E) RNAi knockdown of *EcR* expression in SCs with a pan-*EcR*-RNAi (B), *EcR-B1*-RNAi (D), or *EcR-A*-RNAi (E) significantly restricts growth of SC nuclei compared with control glands expressing GFP only (A and C). (F) Overexpression of EcR-B1 in SCs has no effect on SC nuclear size. (G, H) SCs expressing RNAis targeting the ecdysone synthesis genes *shd* (G) and *spo* (H) have smaller nuclei. (I, J) The SC nuclei of the temperature-sensitive *ecd*^{1} mutant are significantly smaller than control glands when adult virgin males are maintained at 28.5˚C (I), which blocks *ecd* function, but not when these flies are fed with 20-HE (J). (K-M) Histograms showing size of SC nuclei relative to MC nuclei in AGs in which SCs express different transgenes and in *ecd*^{1} mutant males. Significance was assessed by an unpaired *t* test (K), Kruskal-Wallis test with Dunn's multiple-comparison test (L), or one-way ANOVA with Sidak's multiple-comparison test (M). $^{*}p < 0.05$, $^{**}p < 0.01$, $^{***}p < 0.001$, $^{****}p < 0.0001$, $n = 15$ (K), $n \geq 24$ (L, M). Scale bars, 50 μm (A, B), 20 μm (C-J). Underlying data for this figure can be found in S1 Data. 20-HE, 20-hydroxyecdysone; AG, accessory gland; *ecd*, *ecdysoneless*; EcR, ecdysone receptor; *esg*, *escargot*; esg^{ts}F/O, the yeast transcription factor GAL4 expressed under the control of the promoter of the gene *esg* in a temperature-dependent fashion; Fas3, Fasciclin3; GFP, green fluorescent protein; MC, main cell; RNAi, RNA interference; SC, secondary cell; *shd*, *shade*; *spo*, *spook*.

https://doi.org/10.1371/journal.pbio.3000145.g002

specific RNAi available. EcR-B2's function was tested by overexpressing a dominant negative form of the receptor that cannot bind ligand (EcR-B2-ΔC655.W650A) [49]; it did not affect SC nuclear growth (S1J Fig, S1 Data).

Steroid receptors typically modulate gene expression in the presence of their ligands, but in some contexts, it has been proposed that the unliganded EcR is repressive, and this repression is released by the hormone [39]. To test whether ecdysone is required to induce EcR-dependent growth in SCs or inhibit it, we initially employed a temperature-sensitive allele of *ecdysoneless* (*ecd*), *ecd*^{1} [25], a gene with pleiotropic effects on processes required for ecdysone synthesis and signalling in flies [40]. When males were shifted to the nonpermissive temperature (28.5˚C) directly after eclosion, SCs and their nuclei failed to grow (Fig 2I and 2M, S1 Data), mirroring the phenotype of *EcR* knockdown. This growth suppression was rescued by feeding exogenous 20-HE to adult virgin *ecd*^{1} males (Fig 2J and 2M, S1 Data), confirming that reduced ecdysone levels in *ecd*^{1} flies are responsible for the phenotype.

Insect adult AGs can produce ecdysone, and SCs have previously been proposed to be sites of ecdysone synthesis in *Drosophila* [41] because they express Torso, the receptor for prothoracicotropic hormone (PTTH), which stimulates ecdysone biosynthesis in the larval ring gland. We knocked down in SCs two genes in the ecdysone synthesis pathway: *shade* (*shd*), which is involved the final step in the pathway, and *spook* (*spo*), which encodes a cytochrome P450 enzyme that appears to function in nonlarval stages [42]. Adult SC growth was inhibited after both treatments (Fig 2G, 2H and 2M, S1 Data). These experiments strongly support the hypothesis that ecdysone synthesised in SCs is required for normal EcR-dependent SC growth in virgin males.

In several other cell types, the EcR functions as a heterodimer with the nuclear receptor Ultraspiracle (USP) [43,44]. USP can promote nuclear localisation of EcR in Chinese hamster ovary (CHO) cells [45]. Staining with an antibody that recognises USP [46] revealed that this protein is expressed in SC nuclei (S2H Fig). However, *Usp*-RNAi knockdown in SCs had no effect on cell growth (S1A, S1B and S1I Fig, S1 Data) or EcR localisation and expression (S2A and S2B Fig) in SCs, even though it strongly reduced USP levels (S2I Fig), suggesting that conventional EcR/USP-mediated transcriptional regulation does not drive SC growth in virgin males.

The EcR promotes hormone-independent SC nuclear growth in mated males

To test whether EcR and ecdysone signalling are also required for the additional growth of SC nuclei observed in multiply-mated males [9], we cultured individual newly eclosed males with 7–10 virgin females for 6 days and then analysed nuclear size. Pan-*EcR* knockdown strongly

suppressed nuclear growth under these conditions, mirroring the effects of blocking BMP signalling by expressing the transcriptional repressor Daughters against Decapentaplegic (Dad) (Fig 3A–3D and 3I, S1 Data) [13]. Whereas expression of *EcR-B1*-RNAi in mated males did not inhibit SC nuclear growth, *EcR-A*-RNAi did (Fig 3I, S1 Data), suggesting that it plays a more important role than *EcR-B1* after mating. Knockdown of *Usp* also had no effect on SC nuclear growth (Fig 3I, S1 Data). These experiments again suggest that a USP-independent form of EcR signalling controls SC nuclear growth in mated males, but unlike in virgins, EcR-B1 is not required.

Surprisingly, when we analysed temperature-shifted ecd^1 males, they exhibited higher levels of SC growth after mating than mated controls (Fig 3G, 3H and 3J, S1 Data). Feeding with 20-HE did not affect this overgrowth phenotype (Fig 3J, S1 Data). To further confirm that EcR-associated SC nuclear growth in mated males is ecdysone-independent, the effects of *shd* and *spo* knockdown in SCs were also examined. Again SC nuclear growth was not suppressed by these treatments (Fig 3E, 3F and 3J, S1 Data). This suggests that, unlike in virgin males, EcR-mediated nuclear growth in response to mating is primarily hormone independent.

One possible explanation for this switch to hormone-independent growth is that it allows SCs to rapidly increase their biosynthetic capacity after mating independently of ecdysone levels. Ecdysone is thought to fluctuate in adult males according to sociosexual experience, so SC growth in virgins could vary in response to this. For example, work by Ishimoto and colleagues [27] has previously shown that ecdysteroid synthesis is increased in males immediately after they have been rejected by females over a 7-hour period.

We therefore tested whether SC growth is enhanced in rejected virgin males. However, because males must age for 6 days in order to observe sizeable increases in SC nuclear growth, we exposed males to repeated daily rejection over a 6-day period (see Materials and methods). We did not detect any difference in SC growth in adult males subjected to this 'rejection regime' when compared with males cultured in the absence of females (S3A Fig, S1 Data). However, we were also unable to detect any change in 20-HE concentrations in the former males (S3B Fig, S1 Data), providing an explanation for this finding. By contrast, 20-HE levels were significantly elevated in multiply-mated males compared with virgins (S3B Fig, S1 Data), suggesting that our assay could detect physiological changes in 20-HE concentration. We conclude from our mutant and knockdown analysis that in virgin males, but not in mated males, ecdysone levels can affect SC growth, but using the rejection assay, we were unable to detect long-term changes in 20-HE of sufficient magnitude to test the physiological implications of this regulation in virgins.

EcR protein levels are controlled by BMP signalling to regulate growth

Because EcR-B1 is the major isoform expressed by SCs, we examined the effect of overexpressing it in these cells under esg^{ts}F/O control. Unexpectedly, SC nuclear size was not affected by this treatment (Fig 2F and 2L, S1 Data) or by overexpression of EcR-A or EcR-B2 (S1D, S1F and S1I Fig, S1 Data). However, when we analysed EcR protein levels in these backgrounds, they appeared unchanged compared with controls (Fig 1G, S2A, S2D and S2F Fig), even though these constructs increase EcR levels when expressed in adjacent MCs (S4A, S4C, S4E and S4G Fig). Because many other UAS-coupled transgenes can be overexpressed in SCs under esg^{ts}F/O control [9,13,14], our data suggest that EcR levels are tightly controlled by a mechanism that acts after the initiation of transcription in these cells so that increased *EcR* transcription has no obvious effect on receptor levels or growth.

Previous work has shown that SC growth is positively regulated by BMP signalling [9]. Because EcR signalling also promotes growth, we investigated the effect of BMP signalling on

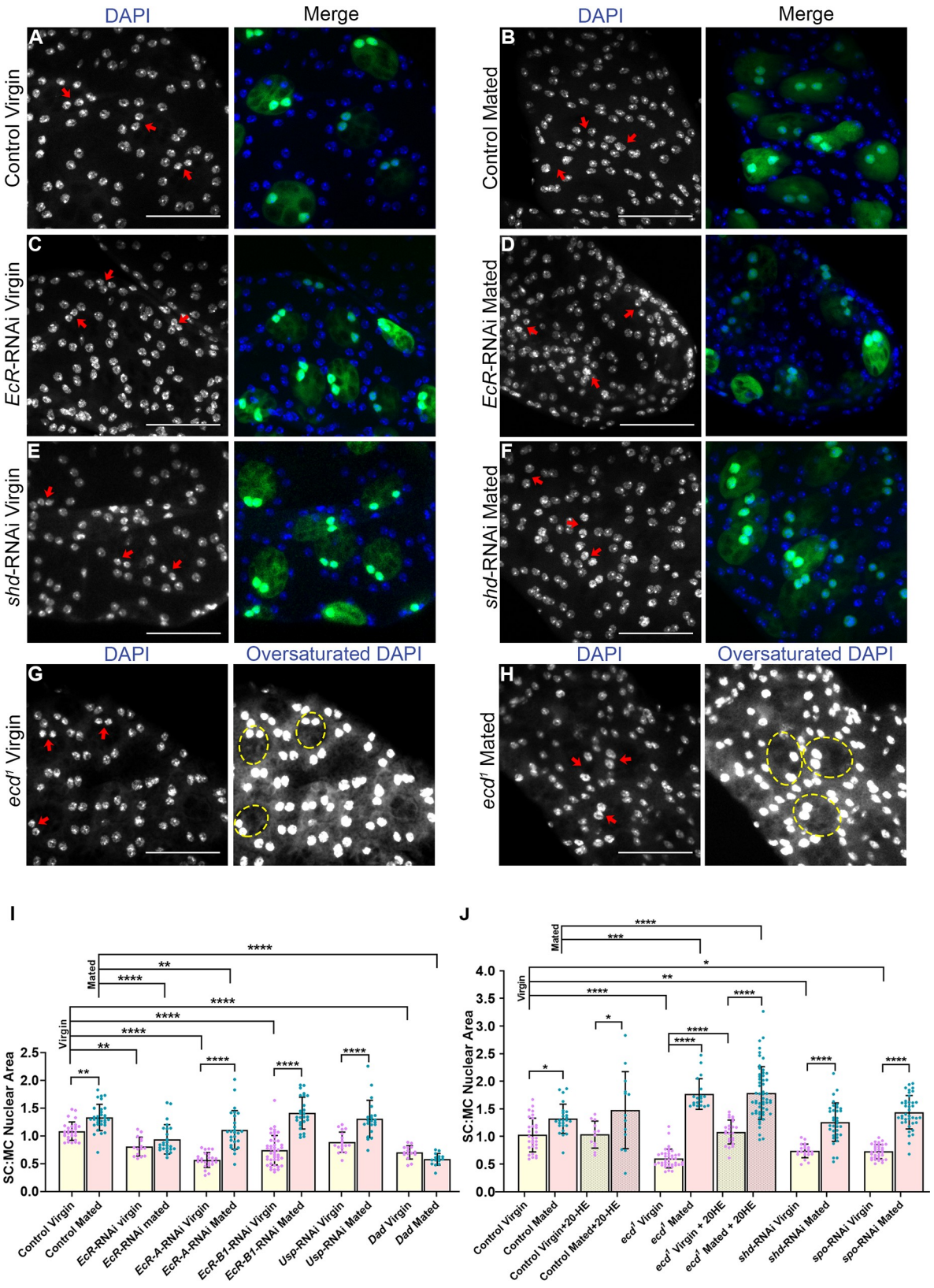

Fig 3. Mating induces hormone-independent, EcR-regulated SC nuclear growth. (A-H) SCs from glands of 6-day-old males were identified by GFP expression or their characteristic vacuolar morphology in *ecd*^{1} flies. In the latter, the approximate outlines of selected SCs

are marked by a dashed circle. (A-D) SC nuclei (marked by red arrows; stained with DAPI) following pan-*EcR* knockdown are smaller than controls in virgin ([C] versus [A]) and mated ([D] versus [B]) males. (E, F) Knockdown of *shd* in SCs only suppresses nuclear growth in virgin males. (G, H) In ecd^1 virgin males (G), nuclei are much smaller than controls, but they are enlarged compared with controls after mating (H). (I, J) Histograms showing SC nuclear size relative to adjacent MC nuclei in 6-day-old males for control glands, glands expressing different transgenes in SCs under esg^{ts}F/O control, and ecd^1 mutant glands (with and without 20-HE in the diet). Mating induces nuclear growth in control glands (B), which is suppressed when EcR and BMP signalling is reduced (I). Nuclear size is unaffected by 20-HE feeding in mated control and ecd^1 mutant males (J). Data in (I) and (J) were analysed using one-way ANOVA and Sidak's multiple-comparisons test; $^{*}p < 0.05$, $^{**}p < 0.01$, $^{***}p < 0.001$, $^{****}p < 0.0001$. $n \geq 15$. Scale bars, 50 μm. Underlying data for this figure can be found in S1 Data. 20-HE, 20-hydroxyecdysone; BMP, bone morphogenetic protein; Dad, Daughters against Decapentaplegic; *ecd*, *ecdysoneless*; EcR, ecdysone receptor; *esg*, *escargot*; esg^{ts}F/O, the yeast transcription factor GAL4 expressed under the control of the promoter of the gene *esg* in a temperature-dependent fashion; GFP, green fluorescent protein; MC, main cell; RNAi, RNA interference; SC, secondary cell; *shd*, *shade*; *spo*, *spook*; USP, Ultraspiracle.

https://doi.org/10.1371/journal.pbio.3000145.g003

EcR protein expression. SC-specific expression of a constitutively active form of the type I BMP receptor Thick veins (Tkv^{Q199D} or Tkv^{ACT}) [47] induced increased levels of EcR protein, which was primarily localised in the nucleus (Fig 4A and 4B). When BMP signalling was reduced in SC mosaics by inducing SC-specific knockdown of *Medea* (*Med*), encoding a downstream co-Smad transcription factor in the BMP signalling pathway, virtually no EcR protein was observed in knockdown cells (Fig 4C). A similar BMP-dependent effect on EcR levels was not observed in MCs, and MC growth was also unaffected by Tkv^{ACT}, EcR, or combined Tkv^{ACT}/EcR expression (S4 Fig). Taken together, these data indicate that BMP signalling is a key regulator of EcR protein levels specifically in SCs.

To interrogate the interaction between BMP and EcR signalling further, we next tested whether overexpressing EcR when BMP signalling is hyperactivated might further increase EcR protein levels and promote growth. Co-overexpression of Tkv^{ACT} and EcR-B1 in SCs resulted in a strong synergistic enhancement of growth (Fig 5A, 5B and 5D–5F, S1 Data). Similar synergistic growth effects were observed with both EcR-A and EcR-B2, even though overexpressing either EcR isoform in the absence of Tkv^{ACT} had no effect on nuclear size (S1A, S1C–S1G and S1I Fig, S1 Data).

In addition to these dramatic growth effects, very high levels of EcR expression were observed in SCs coexpressing Tkv^{ACT} and any of the EcR isoforms (Fig 6, S2A and S2D–S2G Fig). The highest EcR levels were observed in nuclei, but all coexpressing cells also had detectable cytosolic EcR, which was highly elevated in some cells (Fig 6D, S2E and S2G Fig).

The increased expression in response to elevated BMP signalling could either result from greater transcript levels, posttranslational regulation, or both. When EcR isoforms were overexpressed in SCs, it was not possible to detect any increase in *EcR* transcripts using quantitative reverse-transcription PCR (RT-PCR) of AG mRNA. However, because muscle cells in the gland also express the *EcR*, this expression might mask the GAL4-induced increase in *EcR* transcripts in the small number of SCs in each gland, so we cannot conclude that transcript levels are unaffected by overexpression.

In light of the strong dependence of growth-regulatory EcR protein levels on BMP signalling, we tested whether BMP-dependent growth in SCs is mediated through EcR signalling by coexpressing Tkv^{ACT} with pan-*EcR*-RNAi. Tkv^{ACT}-induced growth was strongly suppressed, and the resulting SC nuclei were not significantly different in size from wild-type controls (Fig 5A–5C and 5F, S1 Data), indicating that BMP-dependent SC growth requires the presence of the EcR.

Sequences associated with the unique activation function 1–containing NTDs of each EcR isoform appear to be involved in SC-specific regulation of EcR levels by BMP signalling

Previous in vitro studies have revealed that when the *Drosophila* EcR-A and EcR-B1 isoforms are expressed in CHO cells, the different NTDs of these proteins, which include the activation

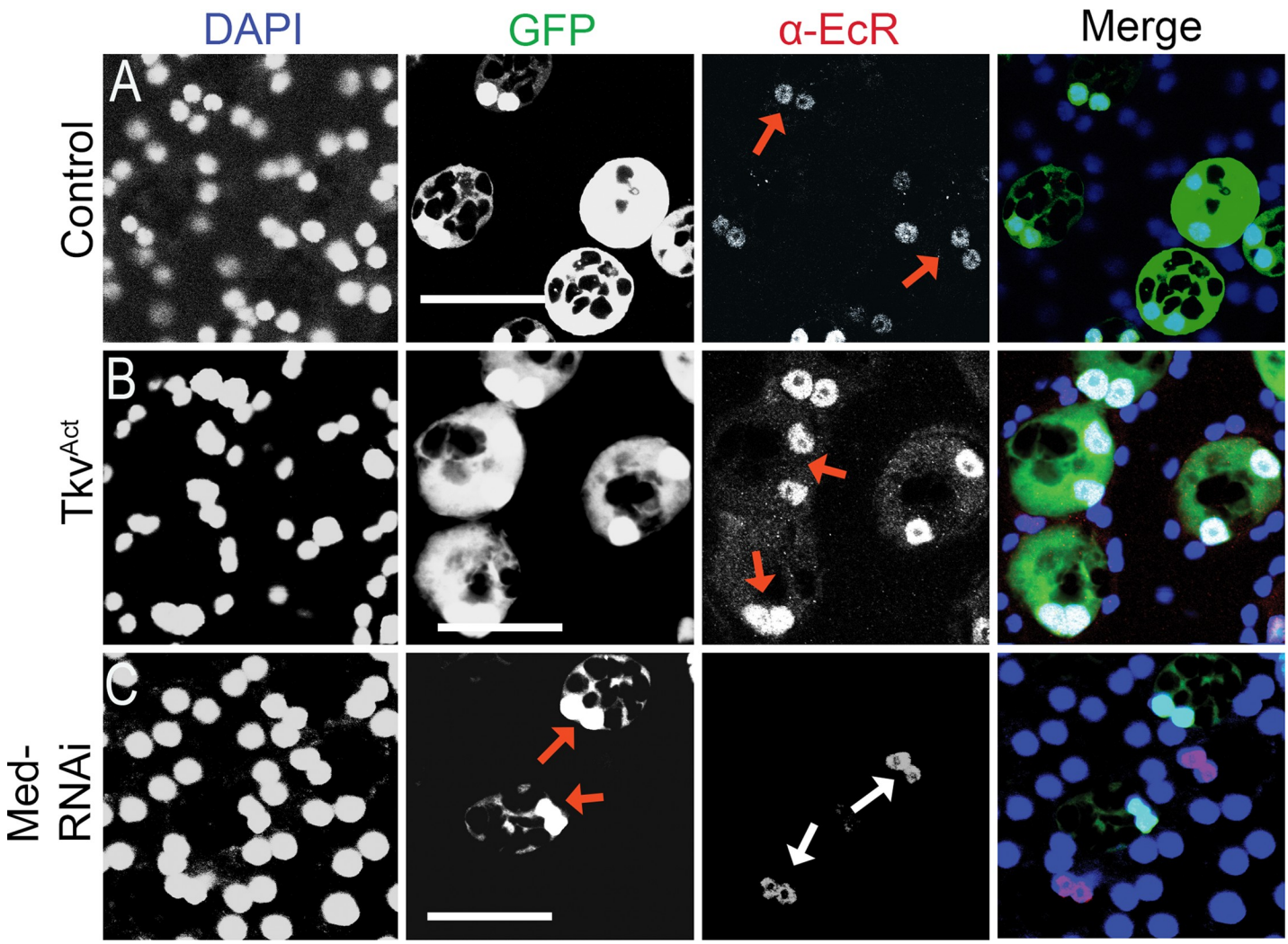

Fig 4. BMP signalling regulates levels of the EcR protein in SCs. Images show the AG epithelium dissected from 6-day-old virgin males expressing GFP and other transgenes under esg^{ts}F/O control and stained with a pan-EcR antibody. (A, B) Up-regulation of BMP signalling by SC-specific Tkv^{ACT} overexpression in adults results in increased expression of EcR (B) compared with control (A), with an enhanced nuclear signal (red arrows) and some cytosolic expression. (C) RNAi knockdown of Med in only some SCs by activating the esg^{ts}F/O driver system in 3-day-old adults reduces BMP signalling in these cells and leads to a marked reduction in SC-specific EcR expression (nuclei marked with red arrows) after a further 6 days. EcR expression in SCs that do not express the RNAi construct is normal (white arrows). Scale bars, 50 μm. AG, accessory gland; BMP, bone morphogenetic protein; EcR, ecdysone receptor; *esg*, *escargot*; esg^{ts}F/O, the yeast transcription factor GAL4 expressed under the control of the promoter of the gene *esg* in a temperature-dependent fashion; GFP, green fluorescent protein; Med, Medea; RNAi, RNA interference; SC, secondary cell; Tkv, Thick veins.

https://doi.org/10.1371/journal.pbio.3000145.g004

function 1 (AF1) domain, one of the two transcriptional activation domains in these receptors, partially destabilise the proteins through a ubiquitination-dependent mechanism [48]. Although these experiments were performed in a heterologous system and did not reveal similar regulation for the EcR-B2 isoform, which has a much shorter AF1 domain, we tested whether the NTD plays a role in SC-specific, BMP-dependent control of EcR protein levels. We expressed EcR-C, an artificial isoform of the protein in which the NTD sequence has been deleted, in SCs. This protein only contains sequences common to all isoforms [49], and in other cell types, it usually has reduced activity compared with native forms of EcR when overexpressed.

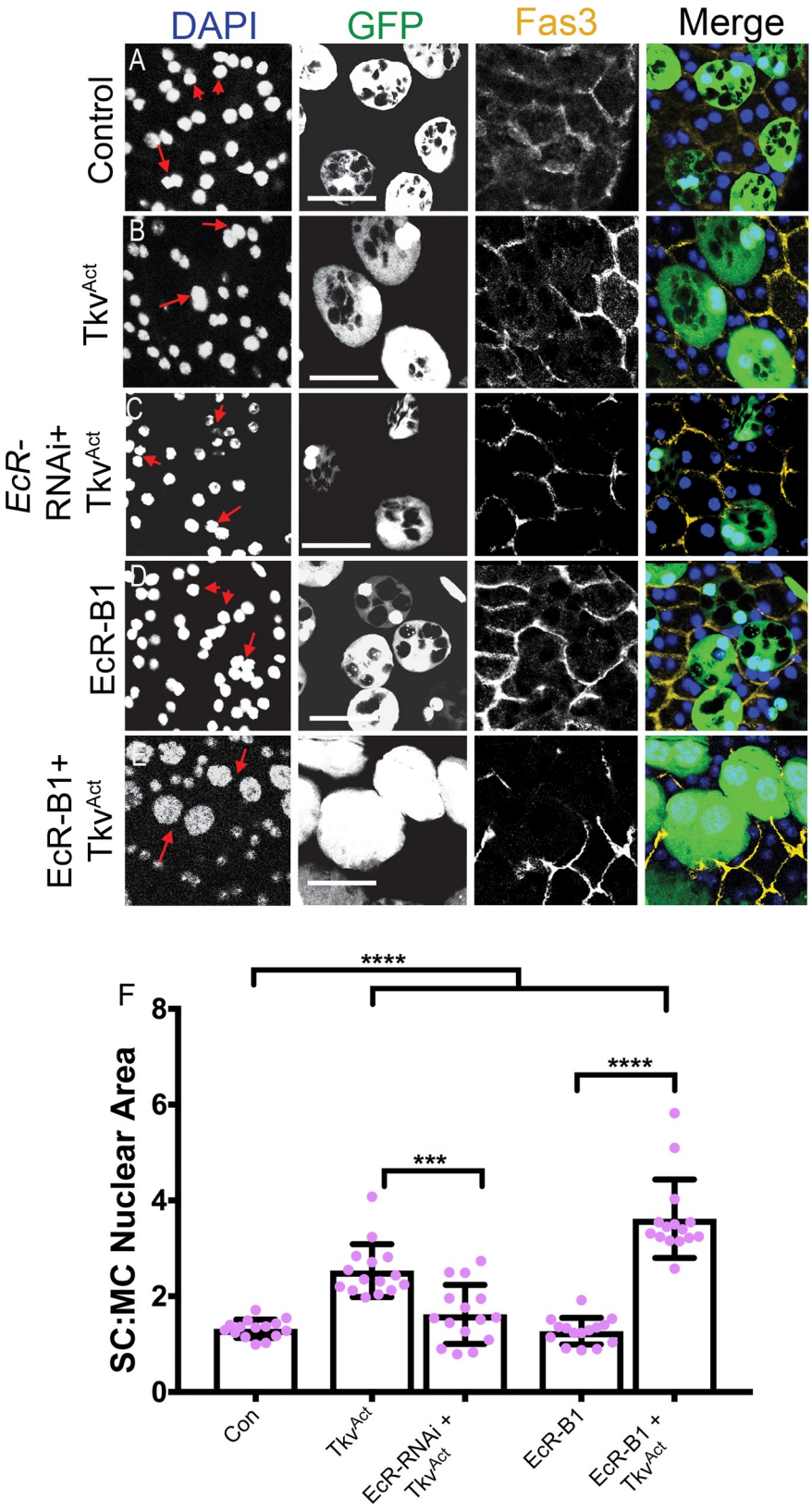

Fig 5. BMP signalling and the EcR synergise to regulate SC growth. Dissected AGs from 6-day-old virgin males expressing GFP and other transgenes under esg^{ts}F/O control were stained with an antibody against Fas3 to mark the

apical outlines of SCs and neighbouring MCs (yellow) and DAPI (blue nuclei). (A-C) The nuclear growth induced by SC-specific expression of Tkv^{ACT} (B) is completely suppressed by coexpression of pan-*EcR*-RNAi (C) to levels comparable with controls (A). (D, E) Coexpression of Tkv^{ACT} (to up-regulate BMP signalling) and EcR-B1 (E) produces a synergistic enhancement of nuclear (and cell) growth in 6-day-old adults relative to the effects of Tkv^{ACT} (B) or EcR-B1 (D) alone. Note that some MCs are compressed between the giant coexpressing SCs. (F) Histogram showing size of SC nuclei relative to MC nuclei in AGs in which SCs are expressing *Tkv* and *EcR* transgenes. Selected SC nuclei are marked with red arrows. Data were analysed using one-way ANOVA and Tukey's multiple-comparisons test. $^{*}p < 0.02$, $^{***}p < 0.0001$. $n = 15$. Scale bars, 50 μm. Underlying data for this figure can be found in S1 Data. AG, accessory gland; BMP, bone morphogenetic protein; Con, control; EcR, ecdysone receptor; *esg*, *escargot*; $esg^{ts}F/O$, the yeast transcription factor GAL4 expressed under the control of the promoter of the gene *esg* in a temperature-dependent fashion; Fas3, Fasciclin3; GFP, green fluorescent protein; MC, main cell; RNAi, RNA interference; SC, secondary cell; Tkv, Thick veins.

https://doi.org/10.1371/journal.pbio.3000145.g005

Unlike the endogenously expressed isoforms of EcR, overexpression of EcR-C promoted growth of SCs (Fig 7A, 7C and 7E, S1 Data) and produced high levels of EcR protein in the nuclei and cytosol of SCs when expressed alone (Fig 7F and 7H). A simple explanation of our data, given the known role of EcR NTD sequences in protein stability [48], is that BMP signalling activity regulates levels of different EcR isoforms via a genetic interaction with each of their unique NTDs. Alternatively, BMP signalling may affect transcript levels specifically via the sequences encoding each NTD, which are absent in the *EcR-C* transcript. The growth effects of EcR-C were further enhanced by coexpression with Tkv^{ACT} in virgin males (Fig 7C–7E), indicating that BMP signalling affects EcR activity via more than one mechanism. Indeed, relative levels of nuclear versus cytosolic EcR-C appeared to be increased by Tkv^{ACT} overexpression in many, but not all, SCs, suggesting that BMP signalling might also regulate the nuclear trafficking of EcR (Fig 7G–7I).

Regulation of the EcR by BMP signalling that is independent of transcription initiation has not previously been reported in *Drosophila*. It was not observed in MCs (S4I and S4J Fig). We conclude that BMP signalling controls EcR levels and EcR signalling in SCs via a cell type–specific interaction that appears to partly involve the NTD of each EcR isoform or the transcript sequences encoding these NTDs.

BMP and EcR signalling function antagonistically to regulate SC migration

We have previously shown that BMP signalling promotes not only SC growth [9] and secretion [14] but also migratory activity of SCs. A small subset of SCs delaminates apically from the AG epithelium after multiple matings and migrates to the proximal end of the gland [9], where the cells can be transferred to females following further mating. Activating BMP signalling in adult SCs by expressing Tkv^{ACT} induces a similar phenotype in virgin males. We sought to test whether EcR plays a role in this migration. Whereas increased BMP signalling activity promoted spontaneous delamination and migration of SCs in virgin males (S5A, S5B, and S5H Fig, S1 Data), coexpression with EcR isoforms markedly reduced the number of migrating cells (S5D–S5H Fig). In fact, knocking down *EcR* transcripts in virgin males also appeared to promote low levels of SC migration (S5C and S5H Fig, S1 Data). This suggests that, in contrast to growth regulation, the EcR acts antagonistically to BMP signalling in migration control.

Mating drives synthesis of new DNA in SCs, which is regulated by BMP-dependent, but hormone-independent, EcR signalling

In *Drosophila*, increased nuclear and cell size is often associated with endoreplication, which increases gene expression through elevated gene copy number [50]. At eclosion, both SCs and MCs have two large nuclei, each estimated to be tetraploid, because of endoreplication during pupal development [51]. Previously we were unable to detect additional endoreplication in

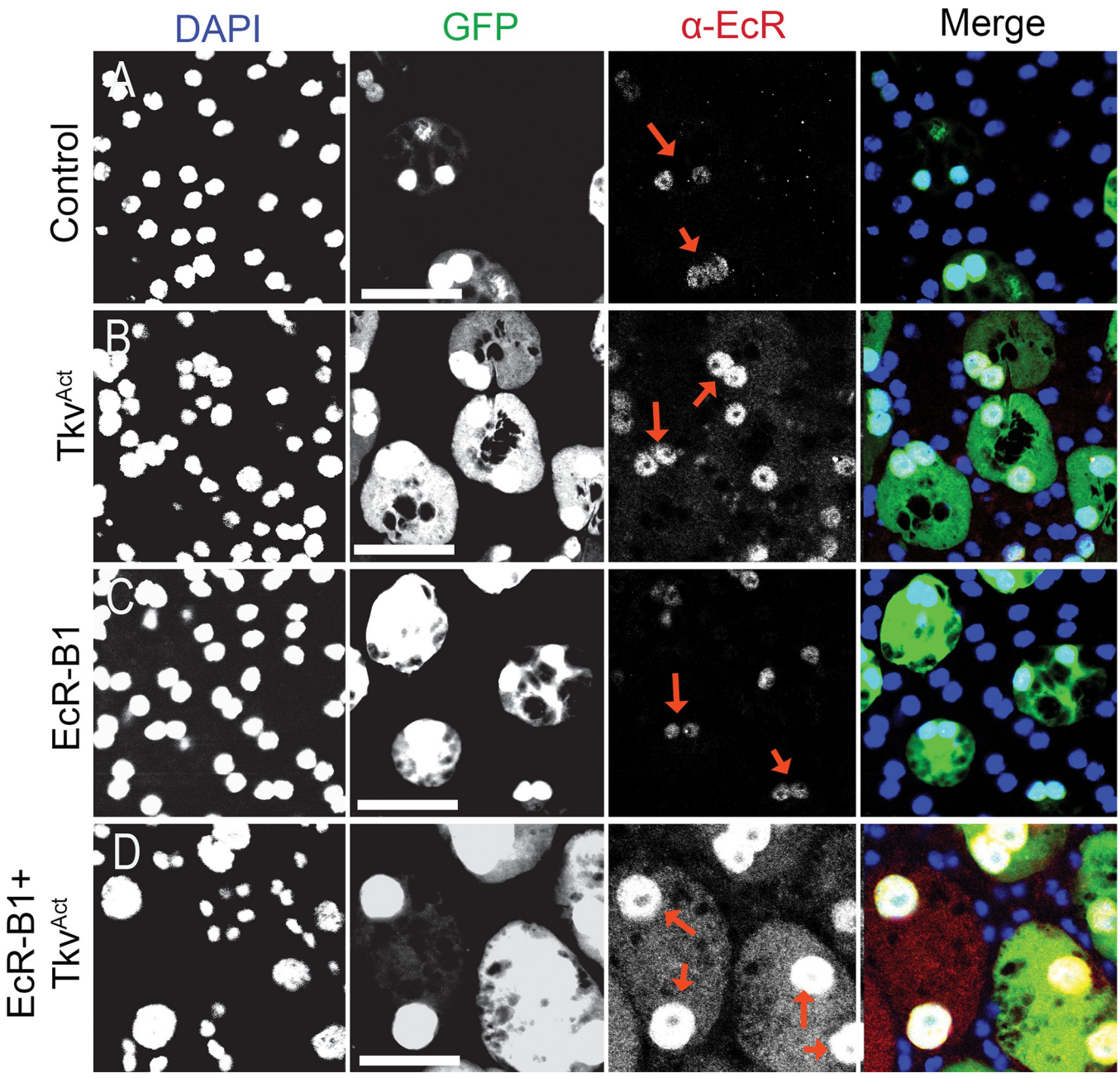

Fig 6. BMP signalling regulates EcR levels in SCs. Dissected AGs from 6-day-old virgin males expressing GFP and other transgenes under esg^{ts}F/O control were stained with a pan-EcR antibody (red arrows) and DAPI (blue nuclei). (A, B) Nuclear EcR levels in SCs are elevated when BMP signalling is increased upon expression of Tkv^{ACT} (B) compared with controls (A). (C, D) Nuclear EcR levels are unaffected by overexpression of EcR-B1 alone (C), but levels of nuclear protein are highly up-regulated when coexpressed with Tkv^{ACT} (D). Some cytosolic EcR is also present. Scale bars, 50 μm. AG, accessory gland; BMP, bone morphogenetic protein; EcR, ecdysone receptor; *esg*, *escargot*; esg^{ts}F/O, the yeast transcription factor GAL4 expressed under the control of the promoter of the gene *esg* in a temperature-dependent fashion; GFP, green fluorescent protein; SC, secondary cell; Tkv, Thick veins.

https://doi.org/10.1371/journal.pbio.3000145.g006

adult SCs of mated flies fed with the nucleotide analogue bromodeoxyuridine (BrdU) [9]. However, we reasoned that this might be explained by poor penetration of the anti-BrdU antibody in AGs, and we therefore repeated these experiments by feeding males during adulthood with 5-ethynyl-2′-deoxyuridine (EdU), which can be detected chemically. Although EdU

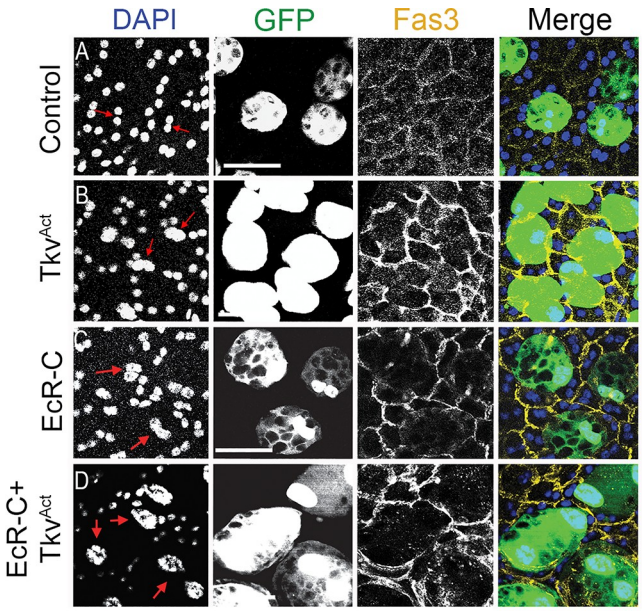
DAPI
GFP
Fas3
Merge
A
Control
B
TkvAct
C
EcR-C
D
EcR-C+ TkvAct

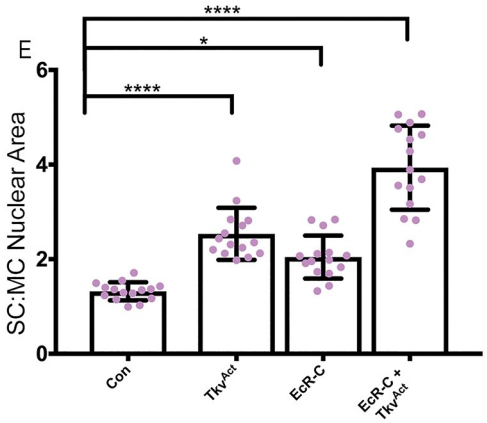
E
SC:MC Nuclear Area
0
2
4
6
****
*
****
Con
TkvAct
EcR-C
EcR-C + TkvAct

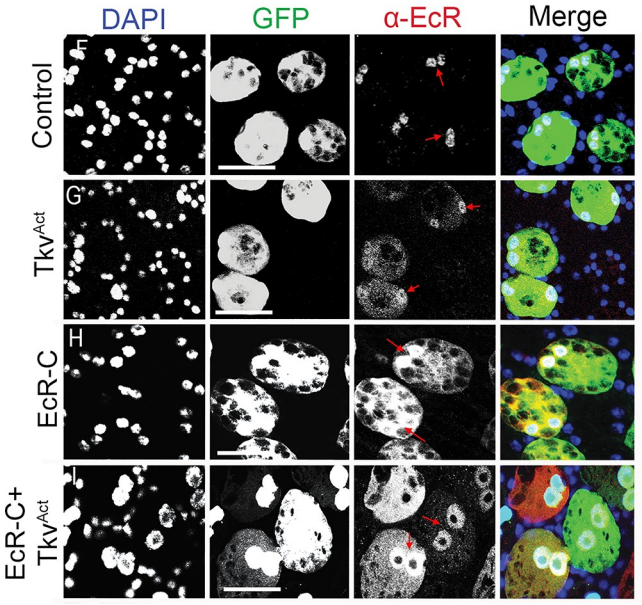
DAPI
GFP
α-EcR
Merge
F
Control
G
TkvAct
H
EcR-C
I
EcR-C+ TkvAct

Fig 7. Sequences associated with the AF1-containing N-terminal domain of different EcR isoforms are involved in BMP-dependent regulation. Dissected AGs from 6-day-old virgin males expressing GFP and other transgenes under esg^{ts}F/O control were stained either with an antibody against Fas3 to mark the apical outlines of SCs and neighbouring MCs (yellow; [A-D]) or with a pan-EcR antibody (red arrows; [F-I]) and DAPI (blue nuclei). (A-D) EcR-C overexpression promotes SC nuclear growth (C) relative to controls (A). Combining EcR-C overexpression with elevated BMP signalling induced by Tkv^{ACT} synergistically drives further SC nuclear growth (D) significantly greater than Tkv^{ACT} alone (B). (E) Histogram showing the size of SC nuclei relative to MC nuclei in AGs in which SCs express different transgenes. (F-I) Overexpression of the N-terminally truncated EcR protein, EcR-C, leads to accumulation of nuclear and cytosolic EcR (H) compared with controls (F). Coexpression with Tkv^{ACT} appears to increase the ratio of nuclear to cytosolic EcR in some cells (I) and lead to much higher levels of EcR protein in SCs than with Tkv^{ACT} alone (G). Significance was assessed by one-way ANOVA and Tukey's multiple-comparisons test. $^{*}p < 0.05$, $^{****}p < 0.0001$, $n \geq 15$. Scale bars, 50 μm. Underlying data for this figure can be found in S1 Data. AF1, activation function 1; AG, accessory gland; BMP, bone morphogenetic protein; Con, control; EcR, ecdysone receptor; *esg*, *escargot*; esg^{ts}F/O, the yeast transcription factor GAL4 expressed under the control of the promoter of the gene *esg* in a temperature-dependent fashion; Fas3, Fasciclin3; GFP, green fluorescent protein; MC, main cell; SC, secondary cell; Tkv, Thick veins.

https://doi.org/10.1371/journal.pbio.3000145.g007

uptake was rarely observed in SCs of 6-day-old virgin males, approximately 30%–40% of SCs from multiply-mated males incorporated EdU, indicating that new DNA synthesis was occurring in a subset of these adult cells (Fig 8A, 8B and 8K, S1 Data). No new DNA synthesis was observed in the MCs of either virgin or mated glands (Fig 8A and 8B).

Interestingly, SC nuclei that take up EdU in mated glands were larger than EdU-negative nuclei (Fig 9A, S1 Data), indicating that part of the increase in SC nuclear size is a consequence of new DNA synthesis. Furthermore, EdU incorporation was distributed across all parts of the nucleus (Fig 8B′), suggesting that it is not the result of focal gene amplification, as is seen for chorion genes in ovarian follicle cell nuclei [52].

We have previously shown that SC secretion of exosomes is under BMP control [14] and that mating induces increased secretory activity in SCs [13]. To test whether endoreplication in adult SCs drives enhanced biosynthetic activity in the secretory system compared with other SCs, we expressed a green fluorescent protein (GFP)-tagged form of the human exosome marker CD63-GFP in a 24-hour pulse in multiply-mated males [14]. This protein labels all large secretory compartments in SCs, and therefore, the number of GFP-positive compartments produced during the pulse of expression provides a measure of the rate of compartment biogenesis, which is approximately one compartment per 4 or 5 hours in virgin males [13,14]. There were significantly more labelled compartments in SCs that had undergone endoreplication than those that had not (Fig 9B and 9C, S1 Data), consistent with the hypothesis that a key role for endoreplication in adults is to increase secretory biosynthetic capacity.

To further assess whether genome endoreplication is responsible for mating-dependent growth, we tested the effect of overexpressing and knocking down the G1/S cyclin, Cyclin E (CycE), in adult SCs. CycE is required for endoreplication in other *Drosophila* cell types [50]. Although knockdown of *CycE* had no significant effect on nuclear growth in virgin males, it inhibited endoreplication and additional SC nuclear growth in mated males (Fig 8J–8L). Furthermore, overexpression of *CycE* in virgin males stimulated nuclear growth and endoreplication in all adult SCs, but this growth was not enhanced further by mating (Fig 8I, 8K and 8L, S1 Data). Consistent with these findings, studies of endoreplication in the salivary gland have suggested that constant overexpression of CycE can drive one cycle of endoreplication but does not permit further rounds [53].

Because both BMP and EcR signalling modulate SC nuclear growth in mated males, we tested whether these pathways regulate DNA synthesis in adult SCs. In complete contrast to controls, the majority of SCs expressing Tkv^{ACT} in adult virgin males typically incorporated EdU over 6 days (Fig 8F and 8K, S1 Data). Furthermore, all SCs expressing the EcR-C construct contained nuclear EdU (Fig 8H and 8K, S1 Data). EdU uptake was significantly

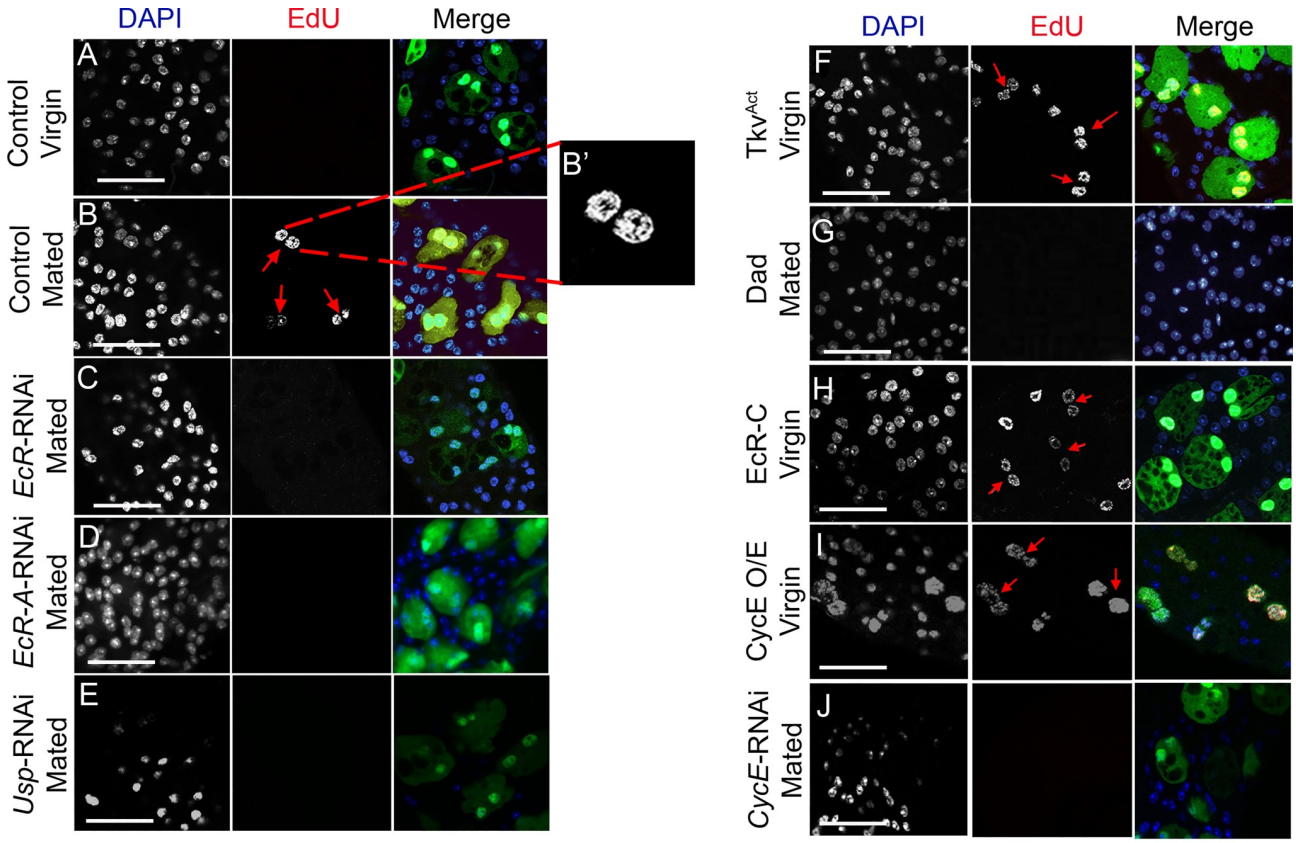
DAPI
EdU
Merge
A
Control Virgin
B
Control Mated
B'
C
EcR-RNAi Mated
D
EcR-A-RNAi Mated
E
Usp-RNAi Mated
F
TkvAct Virgin
G
Dad Mated
H
EcR-C Virgin
I
CycE O/E Virgin
J
CycE-RNAi Mated

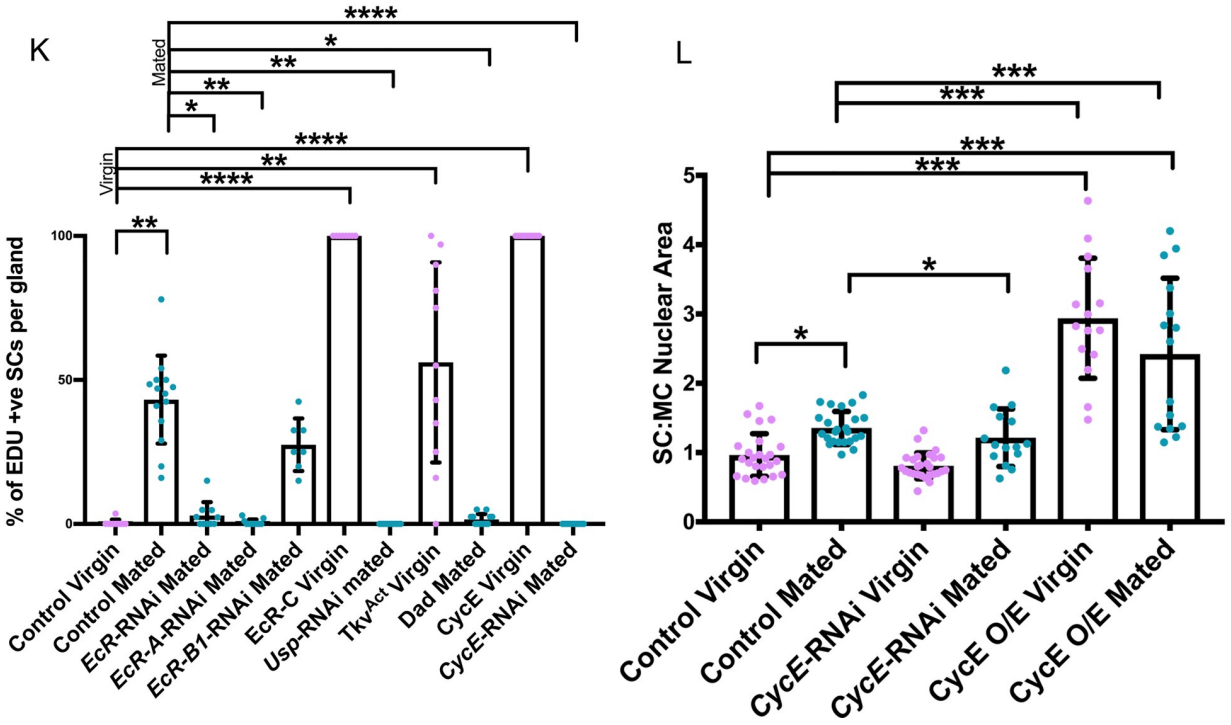
K
Mated
Virgin
% of EDU +ve SCs per gland
Control Virgin
Control Mated
EcR-RNAi Mated
EcR-A-RNAi Mated
EcR-B1-RNAi Mated
EcR-C Virgin
Usp-RNAi mated
TkvAct Virgin
Dad Mated
CycE Virgin
CycE-RNAi Mated
L
SC:MC Nuclear Area
Control Virgin
Control Mated
CycE-RNAi Virgin
CycE-RNAi Mated
CycE O/E Virgin
CycE O/E Mated

Fig 8. EcR-mediated endoreplication of SC DNA is stimulated by mating. Males expressing GFP and other transgenes under esg^{ts}F/O control were cultured on EdU-containing food posteclosion and dissected at 6 days, and their AGs were probed for EdU uptake to assess adult DNA replication and stained with DAPI. (A, B) EdU is incorporated in about 30%–40% of adult SCs after mating ([B]; arrows depict SCs with EdU uptake) but not in virgins (A). Enlargement in (B′) shows a high-magnification view of a single SC. (C-E) SC-specific expression of *EcR*-RNAi (C), *EcR-A*-RNAi (D), and *Usp*-RNAi (E) blocks EdU incorporation in mated males. (F-H) Expression of Tkv^{ACT} (F) or EcR-C (H) in SCs promotes EdU incorporation in SCs from virgin males, whereas Dad-expressing SCs do not incorporate EdU after mating ([G]; note that weak GFP expression in these cells is masked following the EdU staining procedure). (I, J) Overexpression of *CycE* in SCs of virgin males induces endoreplication (I), whereas knockdown of *CycE* in mated males suppresses it (J). (K) Histogram showing EdU incorporation into SC nuclei in different genetic backgrounds with and without mating. (L) Histogram showing SC nuclear size relative to adjacent MC nuclei in 6-day-old males for control glands and glands expressing different transgenes affecting CycE levels in SCs under esg^{ts}F/O control. Data were analysed by the Kruskal-Wallis test with Dunn's multiple-comparison test (K) or by one-way ANOVA with Dunnett's multiple-comparisons test (L). $^{*}p < 0.05$, $^{**}p < 0.01$, $^{***}p < 0.001$, $^{****}p < 0.0001$, $n \geq 10$ (K), $n \geq 15$ (L). Scale bars, 70 μm. Underlying data for this figure can be found in S1 Data. +ve, positive; AG, accessory gland; *CycE*, Cyclin E; Dad, Daughters against Decapentaplegic; EcR, ecdysone receptor; EdU, 5-ethynyl-2′-deoxyuridine; *esg*, *escargot*; esg^{ts}F/O, the yeast transcription factor GAL4 expressed under the control of the promoter of the gene *esg* in a temperature-dependent fashion; GFP, green fluorescent protein; O/E, overexpression; RNAi, RNA interference; SC, secondary cell; Tkv, Thick veins; *Usp*, Ultraspiracle.

https://doi.org/10.1371/journal.pbio.3000145.g008

suppressed in glands from multiply-mated males expressing EcR-RNAi or the BMP antagonist Dad in SCs (Fig 8C, 8G and 8K, S1 Data). Consistent with their effects on SC nuclear growth after mating, *EcR-A*-RNAi, but not *EcR-B1*-RNAi, completely suppressed endoreplication (Fig 8D and 8K, S1 Data), demonstrating that EcR-A plays the critical role in this process.

Given the surprising finding that mating-dependent, EcR-mediated growth is hormone independent, we explored whether blocking ecdysone synthesis had any effect on endoreplication. The number of SCs incorporating EdU in *ecd*^{1} males shifted to the nonpermissive temperature after eclosion was assessed in virgin and mated males. In contrast to virgins, in which no endoreplication was observed, incorporation in multiply-mated males was increased compared with controls, with positive staining in virtually all SCs, suggesting that mating-induced, EcR-mediated endoreplication is not hormone dependent (Fig 10A, 10B and 10E, S1 Data). However, levels of endoreplication were also elevated when mated *ecd*^{1} males were fed with 20-HE (Fig 10C and 10E, S1 Data), indicating that the increase in endoreplication in this mutant, when mated, might not be due to changes in 20-HE. Importantly, though, in support of a hormone-independent control of endoreplication, knockdown of either *spo* or *shd* in SCs also had no effect on the proportion of endoreplicating SCs after mating (Fig 10D and 10E, S1 Data). Taken together, these data indicate that both BMP and EcR signalling cooperate in SCs of mated males to promote synthesis of new DNA. Endoreplication explains much of the additional nuclear growth in a subset of SCs after mating (Fig 9A, S1 Data), but unlike growth in virgin males, this process is ecdysone independent.

Because the form of EcR signalling that controls mating-dependent growth differs from virgins, we tested whether it might involve USP, the well-characterised transcriptional partner of EcR. SC-specific *Usp* knockdown in mated males blocked endoreplication (Fig 8E and 8K, S1 Data), mirroring *EcR-A* knockdown, demonstrating that this aspect of hormone-independent growth is likely to be controlled by an EcR-A/USP heterodimer. However, *Usp* knockdown did not suppress the additional growth in SCs associated with mating (Fig 3I, S1 Data), suggesting that mating-dependent, endoreplication-independent growth does not require USP and, indeed, that it may be up-regulated in the absence of this molecule.

Discussion

Secretory cells in both the mammalian prostate and the fly AG have unusual growth properties in adults. Androgens play a central role in regulating growth and proliferation in the prostate, potentially linking nutrition and sexual activity to adult glandular function [22,23], as well as driving maturation during puberty. In advanced prostate cancer, when tumour cells can

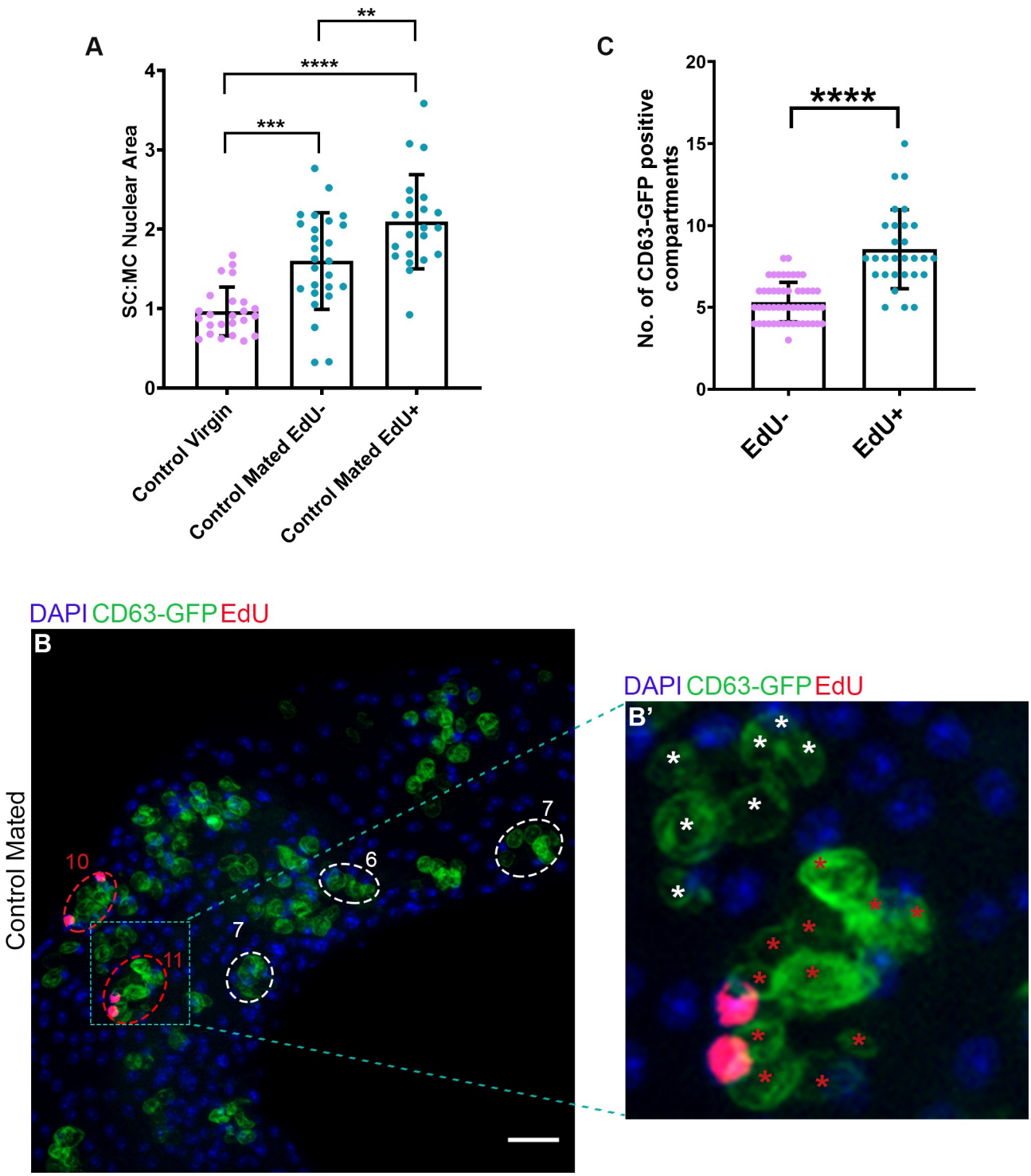

Fig 9. Endoreplicating SCs have larger nuclei and greater biosynthetic secretory activity than other SCs. (A) Histogram showing SC:MC nuclear size ratio for EdU-positive and EdU-negative SCs from esg^{ts}F/O control mated males versus virgins. (B) Confocal microscopy image of males after a 24-hour pulse of CD63-GFP expression in SCs directly after multiple matings. Some SCs are marked by dashed circles (red for SCs with adult endoreplication, white for those without; number of CD63-GFP-marked compartments is given in each case). Not all labelled compartments can be seen in this single z-plane. Magnified maximum projection image shows examples of one EdU-positive and one EdU-negative SC, with each labelled compartment marked with a red or white asterisk, respectively. (C) Histogram showing number of CD63-GFP-positive compartments per cell in EdU-positive and EdU-negative SCs from multiply-mated males, following a 24-hour pulse of CD63-GFP expression. Data analysed by one-way ANOVA with Sidak's multiple-comparisons test (A) or a two-tailed Mann-Whitney test (C). $^{**}p < 0.01$, $^{***}p < 0.001$, $^{****}p < 0.0001$, n ≥ 21 (A), n ≥ 29 (C).

Scale bars, 20 μm. Underlying data for this figure can be found in S1 Data. EdU, 5-ethynyl-2′-deoxyuridine; *esg*, *escargot*; esg^{ts}F/O, the yeast transcription factor GAL4 expressed under the control of the promoter of the gene *esg* in a temperature-dependent fashion; GFP, green fluorescent protein; MC, main cell; No., number; SC, secondary cell.

https://doi.org/10.1371/journal.pbio.3000145.g009

become resistant to antiandrogen treatment, they frequently grow via a hormone-independent, AR-driven process that remains incompletely understood [24].

Here, we demonstrate that SC nuclear growth in virgin male flies also involves hormone-dependent steroid receptor activity. This activity is modulated by local autocrine BMP signals via a novel mechanism. After mating, EcR-dependent nuclear growth becomes partially hormone independent and requires CycE-driven endoreplication. As we discuss below, these regulatory mechanisms drive increased SC growth and secretion after mating, independently of ecdysone concentration, so that SC products that have been transferred to females can be rapidly replenished in males.

BMP signalling tightly regulates EcR levels to control SC growth

Our findings that BMP signalling is required in SCs for them to express detectable levels of the EcR and that knocking down EcR expression blocks BMP-stimulated growth strongly indicate that EcR signalling is a primary mediator of BMP-dependent growth-regulatory effects in these cells. The most abundant EcR isoform, EcR-B1, plays an important in this process in virgin males, but as in the developing AG [34], it is clear that EcR-A is also involved in SC growth and can be regulated by BMP signalling (S1 and S2 Figs), despite being expressed at lower levels.

The BMP/EcR interaction, which does not involve transcriptional control of *EcR* expression, appears highly cell type specific in flies. It cannot be induced in MCs of the AG and has not been reported in multiple tissue types during *Drosophila* development. Signalling by Activins, members of another class of transforming growth factor β (TGF-β) ligands, is required for EcR-B1 expression during neuronal remodelling of the fly brain at metamorphosis [54]. However, the effects of losing the type I Activin receptor Baboon can be overcome by GAL4/UAS-driven expression of EcR-B1, suggesting a direct transcriptional mechanism [54]. Regulation of EcR-B1 expression by TGF-β/BMP signalling has also been reported in larval motoneurons as they dismantle during metamorphosis, but the detailed mechanisms involved have not been characterised [55].

Each of the three normal isoforms of EcR has a unique NTD, which includes a so-called AF1 transcriptional activation domain. The EcR-C protein lacks an NTD, and it can partially evade control by BMP signalling. The transcript sequences encoding the normal EcR isoforms and EcR-C are all identical, except in the 5′ regions that encode the isoform-specific NTDs. Either these different 5′ sequences are all independently targeted by a mechanism that mediates BMP-dependent control of EcR protein levels or the regulation is posttranslational. The latter appears more likely because the NTDs of both EcR-A and EcR-B1 are involved in degradative mechanisms that control EcR protein levels [48]. However, because we have not been able to assess *EcR* transcript levels in SCs in different genetic backgrounds, we cannot exclude a transcript-specific regulatory mechanism.

Multiple forms of noncanonical EcR signalling in SCs control growth in virgin and mated males

Not only is the EcR regulated via a unique BMP-dependent mechanism in SCs, it also has an unusual and complex mode of action and target specificity (Fig 10F). Although USP, the well-

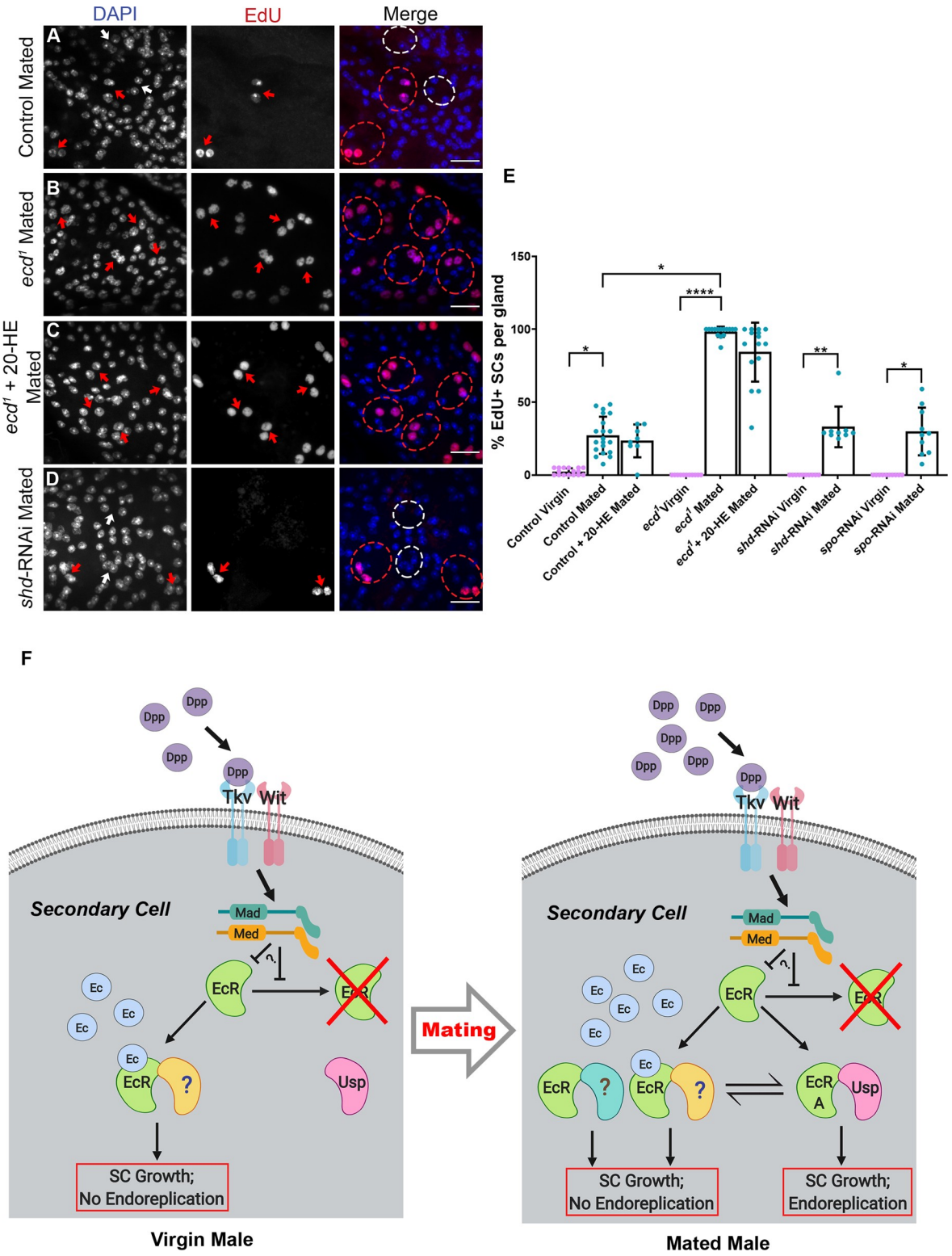

Fig 10. Hormone-independent, EcR-mediated endoreplication of SC DNA is stimulated by mating. Males expressing GFP and other transgenes under esg^{ts}F/O control or *ecd*^{1} mutants were cultured on EdU-containing food posteclosion and dissected at 6 days, and their AGs were probed for EdU uptake to assess DNA replication and stained with DAPI. SCs were recognised by GFP expression or by their characteristic vacuolar morphology in *ecd*^{1} mutants; selected cells are highlighted by dashed circles (red for EdU-positive, white for EdU-negative). (A) EdU is incorporated in about 30%–40% of SCs after mating (red arrows depict SCs with EdU uptake, white arrows mark

those without EdU). (B, C) Almost all SCs in ecd^1 males contain EdU in their nuclei after mating (B), and this is unaffected by 20-HE feeding (C). (D) SC-specific expression of *shd*-RNAi has no effect on the number of SCs containing EdU in mated males. (E) Histogram showing EdU incorporation into SC nuclei in different genetic backgrounds. (F) Proposed model explaining the different forms of hormone-dependent and hormone-independent, EcR-mediated SC growth in virgin and mated males. Our data reveal that EcR-dependent growth of SCs is differentially modulated by the presence of Ec according to mating status. An Ec-EcR complex, which requires a dimerisation partner other than USP (marked ?; this could be an EcR dimer, for example) is necessary for normal SC nuclear growth observed in virgin males. In mated males, SC growth is enhanced, at least in part due to new DNA synthesis driven by a hormone-independent EcR-A/USP complex. This complex must either repress or activate a subset of genes that are not EcR targets in virgin males, hence inducing cell cycle regulators like *CycE* either directly or indirectly. In mated males, EcR complexes that do not involve USP can also drive non-endoreplication-mediated growth, potentially via hormone-dependent and hormone-independent mechanisms, which may be coordinately regulated with endoreplication (e.g., this growth appears to increase following *Usp* knockdown). EcR levels and signalling are stimulated by elevated BMP signalling induced by autocrine BMP ligand Dpp through the heterodimeric Tkv/Wit receptor [13]. Data were analysed by the Kruskal-Wallis test with Dunn's multiple-comparisons test. $^{*}p < 0.05$, $^{**}p < 0.01$, $^{****}p < 0.0001$, $n \geq 8$. Scale bars, 20 μm. Underlying data for this figure can be found in S1 Data. 20-HE, 20-hydroxyecdysone; AG, accessory gland; BMP, bone morphogenetic protein; *CycE*, *Cyclin E*; Dpp, Decapentaplegic; Ec, ecdysone; EcR, Ec receptor; *ecd*, *ecdysoneless*; EdU, 5-ethynyl-2′-deoxyuridine; *esg*, *escargot*; esg^{ts}F/O, the yeast transcription factor GAL4 expressed under the control of the promoter of the gene *esg* in a temperature-dependent fashion; GFP, green fluorescent protein; Med, Medea; RNAi, RNA interference; SC, secondary cell; *shd*, *shade*; *spo*, *spook*; Tkv, Thick veins; USP, Ultraspiracle, Wit, Wishful thinking.

https://doi.org/10.1371/journal.pbio.3000145.g010

characterised binding partner of EcR during development, is expressed selectively in the nuclei of SCs, *Usp* knockdown does not alter SC nuclear size in either virgin or mated males. In virgin males, knockdown of either *EcR-B1*, which is abundantly expressed in SCs, or *EcR-A* suppresses SC nuclear growth. We were unable to detect any role for EcR-B2 using a dominant negative construct.

USP-independent EcR signalling has been reported previously in one developmental scenario in larvae [56]; the mechanisms involved have not been characterised, although the authors propose that the EcR may act as a homodimer or bind with an alternative partner. Furthermore, recent work has shown that expression of multiple EcR isoforms is functionally important in development of the adult AG epithelium but that USP is not required [34]. These authors did not identify the cells involved or the precise cellular defects.

We have screened for expression of several of the known target genes of EcR in development, such as *Broad* and *Ecdysone-induced protein 74EF* (*Eip74EF*), using well-characterised antibodies [57] and specific gene traps but have not been able to identify any downstream targets of the EcR in SCs. Cell type–specific analysis of genomic EcR binding sites or the SC transcriptome will be required to unravel the genetic programme controlled by the specialised EcR signalling taking place in these cells.

Whereas EcR signalling in SCs of virgin males is potentially mediated by a single hormone-dependent mechanism, multiple mechanisms are involved in mated males (Fig 10F). One of these mechanisms appears to involve an EcR-A/USP heterodimer and produces a mating-specific and hormone-independent downstream effect, endoreplication. All three genetic manipulations that reduce ecdysone levels and inhibit SC nuclear growth in virgin animals (the ecd^1 mutation and *shd*/*spo* knockdown) did not suppress growth or endoreplication in mated males. In fact, in the ecd^1 mutant, endoreplication occurred in almost all SCs, although this might be the result of an ecdysone-unrelated effect of the mutant [40] because it was not suppressed by 20-HE feeding.

Epithelial cells in the AG endoreplicate during pupal development [51], and this process is essential for normal growth of the gland [58]. However, in adults, we find that endoreplication is normally only seen upon mating (Fig 8) and is responsible for much of the additional SC growth seen after mating (Fig 9A, S1 Data). Indeed, *CycE* knockdown specifically suppresses mating-dependent growth. Endoreplication and increased growth can be phenocopied in virgin males by activation of BMP signalling or overexpression of EcR-C in SCs. Expressing any EcR isoform in SCs with elevated BMP signalling induces excessive levels of nuclear growth

(Fig 5 and S1 Fig). However, it remains unclear whether these effects mirror the normal EcR-dependent mechanism controlling endoreplication after mating or a novel form of regulation induced by the artificially high EcR levels in these genetic backgrounds.

Hyperactivated BMP signalling may be an important trigger for endoreplication after mating. We have previously shown that only about 30% of SCs increase BMP signalling detectably following multiple matings [13], mirroring the proportion of endoreplicating cells under these conditions. However, we have yet to develop a robust protocol with which we can codetect EdU and the BMP transcriptional target, phosphorylated Mothers against Decapentaplegic (P-Mad), to confirm that these two populations are the same. Furthermore, because genetically activating BMP signalling in SCs does not induce endoreplication in all cells, there is probably a second as-yet-unidentified mechanism that modulates the number of endoreplicating cells.

Because SCs in mated males, which have not endoreplicated, are larger than in virgin males (Fig 9A, S1 Data), the EcR must also regulate other forms of mating-dependent nuclear growth that are not linked to endoreplication. We have not characterised these in detail (Fig 10F). However, as in virgin males, this growth potentially reflects greater decondensation of chromatin. Interestingly, SC-specific *Usp* knockdown blocks endoreplication but not mating-dependent growth (Figs 8E, 8K and 3I, S1 Data), suggesting that endoreplication-independent growth mechanisms can sometimes compensate when endoreplication-dependent growth is inhibited. Because mating-dependent growth does not appear to be suppressed by genetic manipulations that reduce ecdysone levels (Fig 3J, S1 Data), it seems likely that the endoreplication-independent form of this EcR-mediated growth is at least partly hormone-independent. However, we cannot exclude the possibility that hormone-dependent growth is also involved and that the balance of hormone and EcR isoform dependency varies depending on ecdysone levels and genetic background.

Finally, although BMP and EcR signalling cooperate in controlling growth, in both virgin and adult males, their effects appear to be antagonistic in the regulation of cell migration. Presumably BMP's promigratory functions are mediated via non-EcR-dependent pathways, which are typically dominant to the EcR in those SCs that normally delaminate from the AG epithelium after multiple matings [9].

Functional consequences of mating-dependent, hormone-independent endoreplication

As well as promoting SC growth, we found that adult endoreplication increases the rate of secretory compartment formation in mated males (Fig 9). Endoreplication is employed to promote high levels of transcriptional activity and secretion in a range of organisms from mammals to plants [50]; for example, in the salivary glands and follicle cells of the egg chamber in *Drosophila*. In SCs, up-regulation of gene expression following genomic duplication and increased secretory activity presumably facilitates the rapid replenishment of secreted SC products that are extruded from the AG as a result of mating.

So why might adult SC endoreplication and other EcR-mediated, mating-induced growth be hormone-independent? Other studies have shown that whole-animal 20-HE titres increase in male flies exposed to previously mated females [27] and that EcR signalling activity in the fly brain is required for normal courtship behaviours [27,29]. The functional significance of reducing ecdysone levels and SC growth in virgin males, particularly in the absence of females, is likely to involve the conservation of resources. A hormone-independent endoreplication mechanism allows such female-deprived flies to rapidly up-regulate SC activity following mating using the EcR.

Unfortunately, the experimental conditions under which 20-HE has been shown to be altered in response to female rejection [27] and sleep deprivation [59] involve short-term changes, which are very unlikely to affect SC nuclear growth over the 6-day period that we study. When we extended the 'rejection regime' for 6 days, we were unable to detect significant changes in 20-HE levels and consequently saw no effects on SC nuclear size. Other treatments that induce long-term physiological changes in endogenous 20-HE levels will need to be defined in virgin males before we are able to test the hypothesis that EcR-regulated growth plays an important role in conserving resources under different social or environmental conditions.

Could the ecdysone-dependent control of SC activity have physiological functions outside of SCs? Application of topical 20-HE to males exposed to females, which have an experimentally sealed ovipositor that prevents mating, rescues the reduction in AG secretory activity exhibited by these animals [33], strongly suggesting that the overall activity of the gland can be influenced by this hormone. We propose that direct effects of ecdysone on SCs, cells which have an important role in AG reproductive function [9–11] and can affect the normal processing of MC products like Ovulin [11], provide one route by which this hormone can alter the activity of the entire gland. Indeed, Sitnik and colleagues [60] have presented evidence that blocking the normal development of SCs in a specific *Abdominal B* (*Abd-B*) mutant may have indirect effects on the transcriptional programme of MCs, further supporting the idea that SCs can coordinate functions of both epithelial cell types in the AG.

Growth in both prostate cells and fly SCs is regulated by BMPs and different forms of steroid receptor signalling

Previous work has suggested several similarities between mammalian prostate cells and *Drosophila* SCs, including cell growth in adults [9] and the secretion of exosomes that can fuse with sperm when transferred to females during mating [14]. We initially tested the function of EcR signalling in SCs because of the critical role of androgens and AR signalling in normal and tumorigenic prostate epithelial growth. This has uncovered further potential similarities between humans and flies: the receptor for a steroid hormone, which is regulated by sociosexual experience and environment, is involved in controlling growth of secretory cells in both male glands and can function by hormone-dependent and hormone-independent mechanisms. In flies, the switch to hormone independence plays a physiological role, whereas in the prostate, it has only been observed to date in cancer. Furthermore, in both organisms, cells make active steroid hormone locally, promoting an autocrine form of hormone-dependent growth signalling.

Of course, there are also significant differences between these steroid receptor–regulated forms of growth in humans and flies. The human prostate grows by hyperplasia, whereas SCs are hypertrophic postmitotic cells. Nevertheless, the existence of hormone-independent steroid receptor signalling in advanced prostate cancer cells and in SCs is a surprising finding given that hormone-independent EcR signalling has not been observed in any other *Drosophila* cell type. Furthermore, this form of EcR signalling partly acts through the control of cell cycle genes, though this is not coupled to nuclear and cellular division as it is in the prostate. Inevitably, there will be some genetic changes associated with the development of prostate cancer that are not involved in normal SC biology. However, it will be interesting to test whether other cell cycle regulators, which are specifically associated with castration-resistant prostate cancer [61,62], also play a role in hormone-independent signalling in SCs.

Like steroids, BMP signalling has been implicated in prostate growth and metastasis [15–17]. However, its effects are complex because different BMP ligands, which signal through

alternative pathways, can have opposite effects. In prostate cancer, BMP signalling has been implicated in the androgen-independent AR signalling associated with castration resistance [63–65], though its mode of action remains unclear. Our findings suggest links between BMPs and steroid receptors in the male reproductive system of the fly that switch the EcR to a hormone-independent mode under physiological conditions. The mechanisms involved now require further investigation in both flies and humans, with particular focus on defining the cellular conditions under which BMP-induced, hormone-independent signalling is activated.

Materials and methods

Fly strains and culture

The following fly strains (obtained from the Bloomington Stock Centre, except where noted) were employed: esg^{ts}F/O (*w; esg-GAL4, UAS-GFPnls; act>CD2>GAL4, UAS-FLP*; gift from B. Edgar) [35], *UAS-EcR-RNAi* (TRiP.JF02538) [66], *UAS-EcR-B1*, *UAS-EcR-A*, *UAS-EcR-B2*, *UAS-EcR-C*, *UAS-EcR-B2-ΔC655.W650A* [49,67], *UAS-EcR-B1-RNAi*, *UAS-EcR-A-RNAi* [38], *UAS-Tkv^{Q199D}* [47], *UAS-Med-RNAi* [68], *UAS-Usp-RNAi* (TRiP.JF02546), *UAS-ry-RNAi* (TRiP.44106), *UAS-CycE-RNAi* (TRiP.GL00511), *UAS-CycE* [69], *UAS-CD63-GFP* [14] (gift from S. Eaton), *dsx-GAL4* [14], and *Acp26Aa-GAL4* (gifts from S. Goodwin) [70]. TRiP UAS-RNAi lines are described in [71]. Flies were fed on standard cornmeal agar medium. No dried yeast was added to the vials. 20-HE-containing food was prepared by mixing standard medium with a 10 mM 20-HE (Selleckchem/Cambridge Biosciences) stock solution to a final concentration of 0.1 mM with or without 0.2 mM EdU (see below). Flies were cultured on this food from eclosion until analysis at 6 days.

Fly genetics

To express UAS-transgenes in adult SCs under esg^{ts}F/O control [9], fly crosses were initially cultured at a nonpermissive temperature, 18˚C or 25˚C (*w^{1118}* and *UAS-ry-RNAi* flies were used in control crosses with the esg^{ts}F/O strain). Newly eclosed virgin males of the appropriate genotype were selected, separated from females, and transferred to 28.5˚C immediately. All SCs that induce FLP-mediated recombination of the *act>CD2>GAL4* construct continue to express GFP. Mosaic experiments were performed by delaying the temperature shift until day 3 of adult life, with dissection of adults at approximately 9 days posteclosion [9]. Expression of *esg-GAL4* is gradually lost in some adult SCs, so delaying the temperature shift results in *act>CD2>GAL4* recombination in a subset of SCs. Combining the dominant negative EcR constructs with the esg^{ts}F/O line produced very few adults of the appropriate genotype, presumably due to leaky expression during development. For the EcR-B2 dominant negative experiment, SC-specific *dsx-GAL4* under GAL80^{ts} regulation [14] was therefore employed as an alternative driver. For nuclear size measurements and growth analysis, males were typically dissected at 6 days.

Male rejection regime

Virgin males were isolated in vials shortly after eclosion. Each male was placed overnight with a white-eyed premated female, and this was repeated daily until day 6. Premated females had been mated the previous day by incubating with three virgin white-eyed males; the vials were observed to ensure mating occurred. Virgin females were kept after mating, and progeny were checked for eye colour to ensure the 'rejected' males (which were all red eyed) had not successfully mated. At 6 days, the rejected males were dissected and prepared for immunostaining or used for 20-HE measurements.

Measurement of whole-body 20-HE

Ecdysteroid levels were measured using an enzyme immunoassay (EIA) 20-HE EIA SPI-Bio kit (A05120; Cayman Chemicals); 20-HE and 20-E acetylcholinesterase were used as the standard and enzymatic tracer, respectively [27]. For sample preparation, 10 flies per condition were homogenised in ice-cold PBS and centrifuged at 10,000*g* for 15 minutes. To extract 20-HE, the precipitates were resuspended in 1 ml methanol and centrifuged at 10,000*g* for 10 minutes. The supernatants were then evaporated to dryness and resuspended in 100 μl of EIA buffer. Ellman's reagent was used for the chromogenic reaction, and absorbance was read at 415 nm using a Victor3 multilabel plate reader (Perkin Elmer). All assays were performed in triplicate.

Immunohistochemistry and imaging

This followed previously published methods [9,14]. Flies were anaesthetised using CO_2 and dissected with fine forceps in 4% paraformaldehyde dissolved in PBS. Dissected AGs were transferred to Eppendorf tubes, fixed for 20 min at 22˚C, and then washed 6 × 10 minutes in 1 ml PBST (1× PBS, 0.3% Triton X-100 [Sigma-Aldrich]). Anti-Fas3 [72], anti-pan-EcR, anti-EcR-A, and anti-EcR-B1 [36] antibodies were all obtained as supernatants from the Developmental Studies Hybridoma Bank, Iowa, and diluted 1 in 10 in PBSTG (PBST, 10% goat serum). Mouse anti-USP antibody (1:100 dilution) was a kind gift from the Kafatos laboratory [46], and the rabbit anti-ANCE antibody (1 in 200) was kindly provided by E. Isaac [73]. Glands were incubated overnight at 4˚C in primary antibody. They were then washed for 6 × 10 minutes in PBST before incubation with either Cy3- or Cy5-conjugated donkey anti-mouse secondary antibody (Jackson Laboratories) used at a dilution of 1 in 400 for 2 hours at room temperature. Glands were further washed in PBST for 6 × 10 min before mounting on slides using DAPI-containing Vectashield (Vector Laboratories). Imaging of glands was performed using a Zeiss Axioplan 2 scanning confocal microscope with an LSM510 laser module or a Zeiss 880 Airyscan system. Nuclear areas were measured using Axiovision freeware (Zeiss) as previously described [9].

SC migration assay

The AGs of 16-day-old adult virgin males were dissected and fixed as described earlier. Glands were incubated in TRITC-phalloidin (Sigma-Aldrich; diluted 1:400 from a 1-mg/ml stock) for 1 hour and then washed three times for 5 minutes in PBST before mounting in DAPI-containing medium (Vectashield; Vector Laboratories). Glands were then examined by confocal microscopy as described earlier, and the number of proximally located SCs was counted.

Analysis of SC secretion

CD63-GFP [14] was used instead of GFP-GPI [13] for the compartment pulse-labelling experiment because GFP-GPI fluorescence is poorly preserved after paraformaldehyde fixation, which is required for EdU detection. Males expressing CD63-GFP under temperature-inducible *dsx-GAL4* control [14] were multiply mated for 6 days at 25˚C with 10 w^{1118} females on EdU-containing food. On day 7, the males were mated with five new w^{1118} females on EdU-containing food for 24 hours at 25˚C. The males were isolated, and then a pulse of CD63-GFP expression was induced at 29˚C for 24 hours on normal food. The AGs were then dissected and stained for EdU using the Click-iT Plus EdU kit. The number of CD63-GFP-labelled large compartments in each SC was counted in endoreplicated and nonendoreplicated cells.

Detection of DNA replication using EdU

To detect DNA replication using the thymidine analogue EdU, either the Click-iT EdU imaging kit or the Click-iT Plus EdU imaging kit (Invitrogen) was used [74]. Adult flies were maintained on medium containing 0.2 mM EdU (ThermoFisher) from eclosion until dissection at 6 days. The EdU-containing medium was prepared by mixing standard cornmeal agar medium with a 10 mM stock solution (diluted in PBS per the manufacturer's instruction). To detect EdU incorporation, dissected AGs were fixed in paraformaldehyde and processed as they were for immunohistochemistry. The Click-iT EdU reaction mix was prepared following the manufacturer's instructions using a 1:400 dilution of a 2 mM stock of azide-fluor 555 (Sigma-Aldrich) dissolved in DMSO (this preparation was not required for the Click-iT Plus EdU kit). To label EdU-containing DNA in the sample, 200 μl of the reaction mix was added to the vials and left to incubate away from light for 30 minutes at 20˚C. Glands were washed three times in 200 μl PBST and then resuspended in 200 μl PBS before mounting on coverslips using DAPI-containing mounting medium (Vectorshield; Vector Laboratories).

Statistical analyses

We compared the mean SC:MC nuclear area across genotypes and controls. Having confirmed that the data were normally distributed by the Shapiro-Wilk test, we used one-way ANOVA and either Tukey's or Sidak's multiple-comparison posttest to identify significant changes. For nonparametric data, a Kruskal-Wallis test was performed with Dunn's multiple-comparison test. Differences were deemed significant at a p-value < 0.05. Statistical analyses were performed using GraphPad Prism 7.0 or 8.0, (GraphPad Software, www.graphpad.com). Similar statistical analyses were performed to compare the mean proportion of SCs incorporating EdU across genotypes with control glands, whereas a two-tailed Mann-Whitney test was employed for the secretion data involving compartment counts.

Supporting information

S1 Fig. BMP signalling and the EcR synergise to regulate SC growth. Dissected AGs from 6-day-old males were stained with an antibody against Fasciclin3 to mark the apical outlines of SCs and neighbouring MCs (yellow) and with DAPI (blue nuclei). Selected SC nuclei are marked with red arrows and express GFP and other transgenes under esg^{ts}F/O control. (A, B) RNAi-mediated knockdown of *Usp* has no effect on SC nuclear growth (B) compared with control (A). (D-G) Overexpression of the -A (D) and -B2 (F) isoforms of EcR has no effect on SC nuclear growth, but coexpression of these isoforms with Tkv^{ACT} synergistically promotes growth (E, G). (H) RNAi-mediated knockdown of a control gene, *ry*, had no effect on growth. (I, J) Histograms showing size of SC nuclei relative to MC nuclei in AGs in which SCs express different transgenes as above. Note that the EcR-B2-ΔC655.W650A construct was expressed in SCs using a temperature-inducible *dsx-GAL4* driver (see Materials and methods). Significance was assessed by one-way ANOVA with Tukey's multiple-comparisons test. $^{***}p < 0.001$, $n \geq 9$ (I), $n \geq 29$ (J). Scale bars, 60 μm. Underlying data for this figure can be found in S1 Data. AG, accessory gland; BMP, bone morphogenetic protein; *dsx-GAL4*, *doublesex-GAL4*; EcR, ecdysone receptor; *esg*, *escargot*; esg^{ts}F/O, the yeast transcription factor GAL4 expressed under the control of the promoter of the gene *esg* in a temperature-dependent fashion; GFP, green fluorescent protein; MC, main cell; RNAi, RNA interference; *ry*, *rosy*; SC, secondary cell; Tkv, Thick veins; *Usp*, Ultraspiracle.
(TIF)

S2 Fig. BMP signalling, but not USP, regulates levels of the EcR protein in SCs. Images show the AG epithelium dissected from 6-day-old virgin males expressing nuclear GFP and other transgenes under esg^{ts}F/O control and stained with a pan-EcR antibody (A-G) or anti-USP antibody (H,I). Nuclei are stained with DAPI (blue). Selected SC nuclei are marked with red arrows. (A, B) *Usp* knockdown (B) has no effect on EcR expression compared with control (A). (C-G) Overexpression of EcR-A (D) or EcR-B2 (F) does not appear to significantly alter EcR expression compared with controls (A). Coexpression of these isoforms with Tkv^{ACT} in SCs ([E] and [G], respectively) increases EcR expression in SCs compared with controls (A) and SCs expressing Tkv^{ACT} alone (C). (H,I) Immunostaining with an antibody that recognises USP reveals expression in the nuclei of control SCs (H), but absence of expression in the nuclei of SCs expressing an RNAi targeting *Usp* (I). Scale bars, 60 μm (A-G), 120 μm (H, I). AG, accessory gland; BMP, bone morphogenetic protein; EcR, ecdysone receptor; *esg*, *escargot*; esg^{ts}F/O, the yeast transcription factor GAL4 expressed under the control of the promoter of the gene *esg* in a temperature-dependent fashion; GFP, green fluorescent protein; RNAi, RNA interference; SC, secondary cell; Tkv, Thick veins; USP, Ultraspiracle.
(TIF)

S3 Fig. Repeated rejection of males by females does not affect SC nuclear size or 20-HE levels. (A) Histogram showing SC nuclear size in control virgin males and males rejected daily over a period of 6 days prior to isolation and analysis of accessory glands. (B) Histogram showing whole-animal titres of 20-HE in virgin and mated males and in males subjected to a female-rejection regime. Titres were significantly elevated in mated 6-day-old males compared with virgin controls but not after rejection. Significance was assessed by unpaired *t* test ([A]; $n > 10$) and by one-way ANOVA with Dunnett's multiple-comparisons test (B). $^{**}p < 0.01$, $n \geq 36$ (A), $n = 3$ (B). Underlying data for this figure can be found in S1 Data. 20-HE, 20-hydroxyecdysone; SC, secondary cell.
(TIF)

S4 Fig. BMP signalling does not regulate levels of the EcR protein in main cells. Images show the AG epithelium dissected from 6-day-old virgin males expressing nuclear GFP and other transgenes in main cells under Acp26Aa-GAL4 control and stained with a pan-EcR antibody. Note that GFP is also observed in the main cell cytoplasm when expressed at high levels in these cells. Nuclei are stained with DAPI (blue). Merge does not include DAPI channel for increased clarity. (A, B) Expression of Tkv^{ACT} in main cells (B), which do not normally express EcR (see control cells in [A]), does not affect EcR levels. (C-J) Expression of EcR-B1 (C), -B2 (E), -A (G), and -C (I) in main cells leads to accumulation of EcR in these cells, in contrast to SCs. Coexpression with Tkv^{ACT} does not appear to alter either the levels or subcellular localisation of EcR (D, F, H, J). Scale bars, 100 μm. Acp, AG protein; AG, accessory gland; BMP, bone morphogenetic protein; EcR, ecdysone receptor; GFP, green fluorescent protein; SC, secondary cell; Tkv, Thick veins.
(TIF)

S5 Fig. BMP and EcR signalling function antagonistically to regulate SC migration. (A-G) Confocal images of whole accessory glands expressing nuclear GFP and other transgenes under esg^{ts}F/O control. Panels show a single z-plane and therefore do not include all SCs in each gland; also, not all migrated SCs express GFP at sufficiently high levels to be detected at this magnification. In 16-day-old virgin males, an average of 11 ± 3 SCs expressing Tkv^{ACT} (B) and 4 ± 1 SCs expressing *EcR*-RNAi (C) migrate to the proximal end of the accessory gland (marked with white arrows), whereas no cells migrate from the distal tip (red arrows) in controls (A). Overexpression of EcR-B1 (D) or EcR-C (F) has no effect on SC migration. However,

coexpression of EcR-B1 with Tkv^{ACT} (E) strongly suppresses cell migration, as does coexpression of Tkv^{ACT} with EcR-C (G). (H) Data analysed using the Kruskal-Wallis test with Dunn's multiple-comparisons test. $^{****}p < 0.0001$, $n = 15$. Underlying data for this figure can be found in S1 Data. BMP, bone morphogenetic protein; EcR, ecdysone receptor; *esg*, *escargot*; esg^{ts}F/O, the yeast transcription factor GAL4 expressed under the control of the promoter of the gene *esg* in a temperature-dependent fashion; GFP, green fluorescent protein; RNAi, RNA interference; SC, secondary cell; Tkv, Thick veins.
(TIF)

S1 Data. Excel spreadsheet containing, in separate sheets, the underlying numerical data for panels in Figs 2, 3, 5 and 7–10 and S1, S3 and S5 Figs.
(XLSX)

Acknowledgments

We thank Elwyn Isaac, Fotis Kefatos, Bruce Edgar, Suzanne Eaton, and Stephen Goodwin for stocks and reagents; we are grateful to the Bloomington *Drosophila* Stock Center and Vienna Drosophila Stock Center for flies and to the Developmental Studies Hybridoma Bank (DSHB), Iowa, for antibodies. Some microscopy was undertaken in the Micron Oxford Advanced Bioimaging Unit.

Author Contributions

Conceptualization: Aaron Leiblich, Josephine E. E. U. Hellberg, Aashika Sekar, Claudia C. Mendes, Siamak Redhai, John Mason, Pauline Marie, Deborah C. I. Goberdhan, Freddie C. Hamdy, Clive Wilson.

Data curation: Aaron Leiblich, Josephine E. E. U. Hellberg, Aashika Sekar, Claudia C. Mendes, Siamak Redhai, Pauline Marie.

Formal analysis: Aaron Leiblich, Josephine E. E. U. Hellberg, Aashika Sekar, Clive Wilson.

Funding acquisition: Aaron Leiblich, Deborah C. I. Goberdhan, Clive Wilson.

Investigation: Aaron Leiblich, Josephine E. E. U. Hellberg, Aashika Sekar, Carina Gandy, Siamak Redhai, Mark Wainwright.

Methodology: Aaron Leiblich, Josephine E. E. U. Hellberg, Aashika Sekar, Claudia C. Mendes, John Mason.

Project administration: Aaron Leiblich, Clive Wilson.

Resources: Clive Wilson.

Supervision: Aaron Leiblich, Claudia C. Mendes, Pauline Marie, Deborah C. I. Goberdhan, Clive Wilson.

Validation: Aaron Leiblich, Josephine E. E. U. Hellberg, Aashika Sekar.

Visualization: Aaron Leiblich, Josephine E. E. U. Hellberg, Aashika Sekar, Siamak Redhai, Mark Wainwright, Pauline Marie, Deborah C. I. Goberdhan, Freddie C. Hamdy, Clive Wilson.

Writing – original draft: Aaron Leiblich, Clive Wilson.

Writing – review & editing: Aaron Leiblich, Josephine E. E. U. Hellberg, Aashika Sekar, Carina Gandy, Claudia C. Mendes, Siamak Redhai, John Mason, Mark Wainwright, Pauline Marie, Deborah C. I. Goberdhan, Freddie C. Hamdy, Clive Wilson.

References

1. Mann T, Lutwak-Mann C. Secretory function of male accessory organs of reproduction in mammals. Physiological Reviews. 1951; 31:27–55. https://doi.org/10.1152/physrev.1951.31.1.27 PMID: 14807716
2. Robertson SA, Sharkey DJ. Seminal fluid and fertility in women. Fertility and Sterility. 2016; 106:511–9. https://doi.org/10.1016/j.fertnstert.2016.07.1101 PMID: 27485480
3. Chapman T, Liddle LF, Kalb JM, Wolfner MF, Partridge L. Cost of mating in *Drosophila melanogaster* females is mediated by male accessory gland products. Nature. 1995; 373:241–4. https://doi.org/10.1038/373241a0 PMID: 7816137
4. Wolfner MF. Tokens of love: functions and regulation of *Drosophila* male accessory gland products. Insect Biochem Molec. 1997; 27:179–92.
5. Wolfner MF. "S.P.E.R.M." (seminal proteins (are) essential reproductive modulators): the view from *Drosophila*. Society of Reproduction and Fertility supplement. 2007; 65:183–99. PMID: 17644962
6. Wilson C, Leiblich A, Goberdhan DC, Hamdy F. The *Drosophila* accessory gland as a model for prostate cancer and other pathologies. Current Topics Dev Biol. 2017; 121:339–375.
7. Kubli E. Sex-peptides: seminal peptides of the *Drosophila* male. Cell Mol Life Sci. 2003; 60:1689–704. https://doi.org/10.1007/s00018-003-3052 PMID: 14504657
8. Sirot LK, LaFlamme BA, Sitnik JL, Rubinstein CD, Avila FW, Chow CY, et al. Molecular social interactions: *Drosophila melanogaster* seminal fluid proteins as a case study. Advances in genetics. 2009; 68:23–56. https://doi.org/10.1016/S0065-2660(09)68002-0 PMID: 20109658
9. Leiblich A, Marsden L, Gandy C, Corrigan L, Jenkins R, Hamdy F, et al. Bone morphogenetic protein-and mating-dependent secretory cell growth and migration in the *Drosophila* accessory gland. Proc Natl Acad Sci U S A. 2012; 109:19292–7. https://doi.org/10.1073/pnas.1214517109 PMID: 23129615
10. Minami R, Wakabayashi M, Sugimori S, Taniguchi K, Kokuryo A, Imano T, et al. The homeodomain protein defective proventriculus is essential for male accessory gland development to enhance fecundity in Drosophila. PLoS ONE. 2012; 7:e32302. https://doi.org/10.1371/journal.pone.0032302 PMID: 22427829
11. Gligorov D, Sitnik JL, Maeda RK, Wolfner MF, Karch F. A novel function for the Hox gene *Abd-B* in the male accessory gland regulates the long-term female post-mating response in *Drosophila*. PLoS Genet. 2013; 9:e1003395. https://doi.org/10.1371/journal.pgen.1003395 PMID: 23555301
12. Timms BG, Hofkamp LE. Prostate development and growth in benign prostatic hyperplasia. Differentiation. 2011; 82:173–83. https://doi.org/10.1016/j.diff.2011.08.002 PMID: 21939815
13. Redhai S, Hellberg JE, Wainwright M, Perera SW, Castellanos F, Kroeger B, et al. Regulation of dense-core granule replenishment by autocrine BMP signalling in *Drosophila* secondary cells. PLoS Genet. 2016; 12:e1006366. https://doi.org/10.1371/journal.pgen.1006366 PMID: 27727275
14. Corrigan L, Redhai S, Leiblich A, Fan SJ, Perera SM, Patel R, et al. BMP-regulated exosomes from *Drosophila* male reproductive glands reprogram female behavior. J Cell Biol. 2014; 206:671–88. https://doi.org/10.1083/jcb.201401072 PMID: 25154396
15. Mehta V, Schmitz CT, Keil KP, Joshi PS, Abler LL, Lin TM, et al. Beta-catenin (CTNNB1) induces BMP expression in urogenital sinus epithelium and participates in prostatic bud initiation and patterning. Dev Biol. 2013; 376:125–35. https://doi.org/10.1016/j.ydbio.2013.01.034 PMID: 23396188
16. Dai J, Keller J, Zhang J, Lu Y, Yao Z, Keller ET. Bone morphogenetic protein-6 promotes osteoblastic prostate cancer bone metastases through a dual mechanism. Cancer Res. 2005; 65:8274–85. https://doi.org/10.1158/0008-5472.CAN-05-1891 PMID: 16166304
17. Lee YC, Cheng CJ, Bilen MA, Lu JF, Satcher RL, Yu-Lee LY, et al. BMP4 promotes prostate tumor growth in bone through osteogenesis. Cancer Res. 2001; 71:5194–203.
18. Cunha GR, Ricke W, Thomson A, Marker PC, Risbridger G, Hayward SW, et al. Hormonal, cellular, and molecular regulation of normal and neoplastic prostatic development. Journal Steroid Biochem Mol Biol. 2004; 92:221–36.
19. Wen S, Chang HC, Tian J, Shang Z, Niu Y, Chang C. Stromal androgen receptor roles in the development of normal prostate, benign prostate hyperplasia, and prostate cancer. Am J Pathol. 2015; 185:293–301. https://doi.org/10.1016/j.ajpath.2014.10.012 PMID: 25432062

20. La Vignera S, Condorelli RA, Russo GI, Morgia G, Calogero AE. Endocrine control of benign prostatic hyperplasia. Andrology. 2016; 4:404–11. https://doi.org/10.1111/andr.12186 PMID: 27089546

21. Zhou Y, Bolton EC, Jones JO. Androgens and androgen receptor signaling in prostate tumorigenesis. J Mol Endocrinol. 2015; 54:R15–29. https://doi.org/10.1530/JME-14-0203 PMID: 25351819

22. Alvarado LC. Do evolutionary life-history trade-offs influence prostate cancer risk? a review of population variation in testosterone levels and prostate cancer disparities. Evol Appl. 2013; 6:117–33. https://doi.org/10.1111/eva.12036 PMID: 23396824

23. Jannini EA, Fisher WA, Bitzer J, McMahon CG. Is sex just fun? How sexual activity improves health. J Sex Med. 2009; 6:2640–8. https://doi.org/10.1111/j.1743-6109.2009.01477.x PMID: 19817979

24. Tilki D, Schaeffer EM, Evans CP. Understanding mechanisms of resistance in metastatic castration-resistant prostate cancer: the role of the androgen receptor. Eur Urol Focus. 2016; 2:499–505. https://doi.org/10.1016/j.euf.2016.11.013 PMID: 28723515

25. Garen A, Kauvar L, Lepesant JA. Roles of ecdysone in *Drosophila* development. Proc Natl Acad Sci U S A. 1977; 74:5099–103. https://doi.org/10.1073/pnas.74.11.5099 PMID: 16592466

26. Yamanaka N, Rewitz KF, O'Connor MB. Ecdysone control of developmental transitions: lessons from *Drosophila* research. Ann Rev Entomol. 2013; 58:497–516.

27. Ishimoto H, Sakai T, Kitamoto T. Ecdysone signaling regulates the formation of long-term courtship memory in adult *Drosophila melanogaster*. Proc Natl Acad Sci U S A. 2009; 106:6381–6. https://doi.org/10.1073/pnas.0810213106 PMID: 19342482

28. Ganter GK, Desilets JB, Davis-Knowlton JA, Panaitiu AE, Sweezy M, Sungail J, et al. *Drosophila* female precopulatory behavior is modulated by ecdysteroids. J Insect Physiol. 2012; 58:413–9. https://doi.org/10.1016/j.jinsphys.2012.01.004 PMID: 22265929

29. Ganter GK, Panaitiu AE, Desilets JB, Davis-Heim JA, Fisher EA, Tan LC, et al. *Drosophila* male courtship behavior is modulated by ecdysteroids. J Insect Physiol. 2011; 57:1179–84. https://doi.org/10.1016/j.jinsphys.2011.05.007 PMID: 21704633

30. Ganter GK, Walton KL, Merriman JO, Salmon MV, Brooks KM, Maddula S, et al. Increased male-male courtship in ecdysone receptor deficient adult flies. Behav Genet. 2007; 37:507–12. https://doi.org/10.1007/s10519-006-9140-1 PMID: 17238001

31. Li Y, Ma Q, Cherry CM, Matunis EL. Steroid signaling promotes stem cell maintenance in the *Drosophila* testis. Devl Biol. 2014; 394:129–41.

32. Qian Y, Dominado N, Zoller R, Ng C, Kudyba K, Siddall NA, et al. Ecdysone signaling opposes epidermal growth factor signaling in regulating cyst differentiation in the male gonad of *Drosophila melanogaster*. Dev Biol. 2014; 394:217–27. https://doi.org/10.1016/j.ydbio.2014.08.019 PMID: 25169192

33. Wolfner MF, Partridge L, Lewin S, Kalb JM, Chapman T, Herndon LA. Mating and hormonal triggers regulate accessory gland gene expression in male *Drosophila*. J Insect Physiol. 1997; 43:1117–1123. https://doi.org/10.1016/s0022-1910(97)00062-0 PMID: 12770484

34. Sharma V, Pandey AK, Kumar A, Misra S, Gupta HPK, Gupta S, et al. Functional male accessory glands and fertility in *Drosophila* require novel ecdysone receptor. PLoS Genet. 2017; 13:e1006788. https://doi.org/10.1371/journal.pgen.1006788 PMID: 28493870

35. Jiang H, Patel PH, Kohlmaier A, Grenley MO, McEwen DG, Edgar BA. Cytokine/Jak/Stat signaling mediates regeneration and homeostasis in the *Drosophila* midgut. Cell. 2009; 137:1343–55. https://doi.org/10.1016/j.cell.2009.05.014 PMID: 19563763

36. Talbot WS, Swyryd EA, Hogness DS. *Drosophila* tissues with different metamorphic responses to ecdysone express different ecdysone receptor isoforms. Cell. 1993; 73:1323–37. https://doi.org/10.1016/0092-8674(93)90359-x PMID: 8324824

37. Koelle MR, Talbot WS, Segraves WA, Bender MT, Cherbas P, Hogness DS. The *Drosophila EcR* gene encodes an ecdysone receptor, a new member of the steroid receptor superfamily. Cell. 1991; 67:59–77. https://doi.org/10.1016/0092-8674(91)90572-g PMID: 1913820

38. Bernardi F, Romani P, Tzertzinis G, Gargiulo G, Cavaliere V. EcR-B1 and Usp nuclear hormone receptors regulate expression of the VM32E eggshell gene during *Drosophila* oogenesis. Dev Biol. 2009; 328:541–51. https://doi.org/10.1016/j.ydbio.2009.01.013 PMID: 19389369

39. Schubiger M, Carre C, Antoniewski C, Truman JW. Ligand-dependent de-repression via EcR/USP acts as a gate to coordinate the differentiation of sensory neurons in the *Drosophila* wing. Development. 2005; 132:5239–48. https://doi.org/10.1242/dev.02093 PMID: 16267093

40. Claudius AK, Romani P, Lamkemeyer T, Jindra M, Uhlirova M. Unexpected role of the steroid-deficiency protein ecdysoneless in pre-mRNA splicing. PLoS Genet. 2014; 10:e1004287. https://doi.org/10.1371/journal.pgen.1004287 PMID: 24722212

41. Hentze JL, Moeller ME, Jørgensen AF, Bengtsson MS, Bordoy AM, Warren JT, et al. Accessory gland as a site for prothoracicotropic hormone controlled ecdysone synthesis in adult male insects. PLoS ONE. 2013; 8:e55131. https://doi.org/10.1371/journal.pone.0055131 PMID: 23383307

42. Ono H, Rewitz KF, Shinoda T, Itoyama K, Petryk A, Rybczynski R, et al. Spook and Spookier code for stage-specific components of the ecdysone biosynthetic pathway in Diptera. Dev Biol. 2006; 298:555–70. https://doi.org/10.1016/j.ydbio.2006.07.023 PMID: 16949568

43. Buszczak M, Segraves WA. *Drosophila* metamorphosis: the only way is USP? Curr Biol. 1998; 8:R879–82. https://doi.org/10.1016/s0960-9822(07)00550-7 PMID: 9843674

44. Yao TP, Segraves WA, Oro AE, McKeown M, Evans RM. *Drosophila* ultraspiracle modulates ecdysone receptor function via heterodimer formation. Cell. 1992; 71:63–72. https://doi.org/10.1016/0092-8674(92)90266-f PMID: 1327536

45. Cronauer MV, Braun S, Tremmel Ch, Kröncke KD, Spindler-Barth M. Nuclear localization and DNA binding of ecdysone receptor and ultraspiracle. Arch Insect Biochem Physiol. 2007; 65:125–33. https://doi.org/10.1002/arch.20184 PMID: 17570142

46. Christianson AM, King DL, Hatzivassiliou E, Casas JE, Hallenbeck PL, Nikodem VM, et al. DNA binding and heteromerization of the *Drosophila* transcription factor chorion factor 1/ultraspiracle. Proc Natl Acad Sci U S A. 1992; 89:11503–7. https://doi.org/10.1073/pnas.89.23.11503 PMID: 1280827

47. Hoodless PA, Haerry T, Abdollah S, Stapleton M, O'Connor MB, Attisano L, et al. MADR1, a MAD-related protein that functions in BMP2 signaling pathways. Cell. 1996; 85:489–500. https://doi.org/10.1016/s0092-8674(00)81250-7 PMID: 8653785

48. Schauer S, Burster T, Spindler-Barth M. N- and C-terminal degradation of ecdysteroid receptor isoforms, when transiently expressed in mammalian CHO cells, is regulated by the proteasome and cysteine and threonine proteases. Insect Mol Biol. 2012; 21:383–94 https://doi.org/10.1111/j.1365-2583.2012.01144.x PMID: 22568680

49. Cherbas L, Hu X, Zhimulev I, Belyaeva E, Cherbas P. EcR isoforms in *Drosophila*: testing tissue-specific requirements by targeted blockade and rescue. Development. 2003; 130:271–84. https://doi.org/10.1242/dev.00205 PMID: 12466195

50. Edgar BA, Zielke N, Gutierrez C. Endocycles: a recurrent evolutionary innovation for post-mitotic cell growth. Nat Rev Mol Cell Biol. 2014; 15:197–210. https://doi.org/10.1038/nrm3756 PMID: 24556841

51. Taniguchi K, Kokuryo A, Imano T, Minami R, Nakagoshi H, Adachi-Yamada T. Isoform-specific functions of Mud/NuMA mediate binucleation of Drosophila male accessory gland cells. BMC Dev Biol. 2014; 14:46. https://doi.org/10.1186/s12861-014-0046-5 PMID: 25527079

52. Calvi BR, Lilly MA, Spradling AC. Cell cycle control of chorion gene amplification. Genes Dev. 1998; 12:734–44. https://doi.org/10.1101/gad.12.5.734 PMID: 9499407

53. Weiss A, Herzig A, Jacobs H, Lehner CF. Continuous Cyclin E expression inhibits progression through endoreduplication cycles in *Drosophila*. Curr Biol. 1998; 8:239–42. https://doi.org/10.1016/s0960-9822(98)70090-9 PMID: 9501988

54. Zheng X, Wang J, Haerry TE, Wu AY, Martin J, O'Connor MB, et al. TGF-beta signaling activates steroid hormone receptor expression during neuronal remodeling in the *Drosophila* brain. Cell. 2003; 112:303–15. https://doi.org/10.1016/s0092-8674(03)00072-2 PMID: 12581521

55. Boulanger A, Farge M, Ramanoudjame C, Wharton K, Dura JM. *Drosophila* motor neuron retraction during metamorphosis is mediated by inputs from TGF-beta/BMP signaling and orphan nuclear receptors. PLoS ONE. 2012; 7:e40255. https://doi.org/10.1371/journal.pone.0040255 PMID: 22792255

56. Costantino BF, Bricker DK, Alexandre K, Shen K, Merriam JR, Antoniewski C, et al. A novel ecdysone receptor mediates steroid-regulated developmental events during the mid-third instar of *Drosophila*. PLoS Genet. 2008; 4:e1000102. https://doi.org/10.1371/journal.pgen.1000102 PMID: 18566664

57. Caceres L, Nilson LA. Production of gurken in the nurse cells is sufficient for axis determination in the *Drosophila* oocyte. Development. 2005; 132:2345–53. https://doi.org/10.1242/dev.01820 PMID: 15829517

58. Xue L, Noll M. Dual role of the *Pax* gene paired in accessory gland development of *Drosophila*. Development. 2002; 129:339–46. PMID: 11807027

59. Ishimoto H, Kitamoto T. The steroid molting hormone Ecdysone regulates sleep in adult *Drosophila melanogaster*. Genetics. 2010; 185:269–81. https://doi.org/10.1534/genetics.110.114587 PMID: 20215472

60. Sitnik JL, Gligorov D, Maeda RK, Karch F, Wolfner MF. The female post-mating response requires genes expressed in the secondary cells of the male accessory gland in *Drosophila melanogaster*. Genetics. 2016; 202:1029–41. https://doi.org/10.1534/genetics.115.181644 PMID: 26746709

61. Sharma A, Yeow WS, Ertel A, Coleman I, Clegg N, Thangavel C, et al. The retinoblastoma tumor suppressor controls androgen signaling and human prostate cancer progression. J Clin Invest. 2010; 120:4478–92. https://doi.org/10.1172/JCI44239 PMID: 21099110

62. Xu H, Xu K, He HH, Zang C, Chen CH, Chen Y, et al. Integrative Analysis Reveals the Transcriptional Collaboration between EZH2 and E2F1 in the Regulation of Cancer-Related Gene Expression. Mol Cancer Res. 2016; 14:163–72. https://doi.org/10.1158/1541-7786.MCR-15-0313 PMID: 26659825

63. Kwon SJ, Lee GT, Lee JH, Iwakura Y, Kim WJ, Kim IY. Mechanism of pro-tumorigenic effect of BMP-6: neovascularization involving tumor-associated macrophages and IL-1a. Prostate. 2014; 74:121–33. https://doi.org/10.1002/pros.22734 PMID: 24185914

64. Lee GT, Jung YS, Ha YS, Kim JH, Kim WJ, Kim IY. Bone morphogenetic protein-6 induces castration resistance in prostate cancer cells through tumor infiltrating macrophages. Cancer Sci. 2013; 104:1027–32. https://doi.org/10.1111/cas.12206 PMID: 23710822

65. Lee GT, Kang DI, Ha YS, Jung YS, Chung J, Min K, et al. Prostate cancer bone metastases acquire resistance to androgen deprivation via WNT5A-mediated BMP-6 induction. Br J Cancer. 2014; 110:1634–44. https://doi.org/10.1038/bjc.2014.23 PMID: 24518599

66. Colombani J, Bianchini L, Layalle S, Pondeville E, Dauphin-Villemant C, Antoniewski C, et al. Antagonistic actions of ecdysone and insulins determine final size in *Drosophila*. Science. 2005; 310:667–70. https://doi.org/10.1126/science.1119432 PMID: 16179433

67. Lee T, Marticke S, Sung C, Robinow S, Luo L. Cell-autonomous requirement of the USP/EcR-B ecdysone receptor for mushroom body neuronal remodeling in *Drosophila*. Neuron. 2000; 28:807–18. https://doi.org/10.1016/s0896-6273(00)00155-0 PMID: 11163268

68. Sander V, Eivers E, Choi RH, De Robertis EM. *Drosophila* Smad2 opposes Mad signaling during wing vein development. PLoS ONE. 2010; 5:e10383. https://doi.org/10.1371/journal.pone.0010383 PMID: 20442782

69. Richardson H, O'Keefe LV, Marty T, Saint R. Ectopic *cyclin E* expression induces premature entry into S phase and disrupts pattern formation in the *Drosophila* eye imaginal disc. Development. 1995; 121:3371–3379. PMID: 7588070

70. Chapman T, Bangham J, Vinti G, Seifried B, Lung O, Wolfner MF, et al. The sex peptide of *Drosophila melanogaster*: female post-mating responses analyzed by using RNA interference. Proc Natl Acad Sci U S A. 2003; 100:9923–8. https://doi.org/10.1073/pnas.1631635100 PMID: 12893873

71. Perkins LA, Holderbaum L, Tao R, Hu Y, Sopko R, McCall K, et al. The Transgenic RNAi Project at Harvard Medical School: Resources and Validation. Genetics. 2015; 201:843–52. https://doi.org/10.1534/genetics.115.180208 PMID: 26320097

72. Patel NH, Snow PM, Goodman CS. Characterization and cloning of fasciclin III: a glycoprotein expressed on a subset of neurons and axon pathways in *Drosophila*. Cell. 1987; 48:975–88. https://doi.org/10.1016/0092-8674(87)90706-9 PMID: 3548998

73. Rylett CM, Walker MJ, Howell GJ, Shirras AD, Isaac RE. Male accessory glands of *Drosophila melanogaster* make a secreted angiotensin I-converting enzyme (ANCE), suggesting a role for the peptide-processing enzyme in seminal fluid. Journal Exp Biol. 2007; 210:3601–6.

74. Daul AL, Komori H, Lee CY. EdU (5-ethynyl-2'-deoxyuridine) labeling of *Drosophila* mitotic neuroblasts. Cold Spring Harb Protoc. 2010: pdb.prot5461.